Selbsterneuerung *versus* Differenzierung von hämatopoietischen Stamm- und Vorläuferzellen

Habilitationsschrift zur Erlangung der Venia legendi für das Fach *Molekulare Medizin* des Fachbereiches Humanmedizin der Heinrich-Heine-Universität Düsseldorf

2007

vorgelegt von

Dr. rer. nat. Bernd Giebel

aus Köln

Inhaltsverzeichnis

1 Einleitung

1.1 Definition des Stammzellbegriffs

In einem multizellulären Organismus gehen ständig verschiedenste Arten von Zellen aufgrund von traumatischen, Krankheits- oder Alterungs-bedingten Ereignissen verloren, wie z.B die Blut-, Haar- und Hautzellen. Diese Zellen müssen zur Aufrechterhaltung des Organismus ständig erneuert bzw. ersetzt werden. Es zeigte sich hierbei, dass Stammzellen für diese Regeneration verantwortlich sind. Stammzellen sind undifferenzierte Zellen, die sich über einen langen Zeitraum hinweg sowohl selbst erneuern als auch differenzierte Zellen hervorbringen können. Reduziert sich der Gehalt an Stammzellen bzw. die Stammzellaktivität innerhalb eines Gewebes, z.B. während der Alterung, verringert sich die Regenerationsfähigkeit und kann im Extremfall, wie in Abbildung 1 schematisch dargestellt, zur Degeneration des Gewebes führen (Anversa et al., 2005; Kamminga and de Haan, 2006; Taupin and Gage, 2002; Wagers and Conboy, 2005). Ähnlich problematisch ist die unkontrollierte Expansion von Stammzellen (Abbildung 1); gerade in letzter Zeit mehren sich die Hinweise, dass verschiedene Krebserkrankungen auf die unkontrollierte Expansion von Stammzell-artigen Zellen, den so genannten Tumorstammzellen, zurückzuführen sind (Al-Hajj, 2007; Beachy et al., 2004; Reya et al., 2001). Somit ist es ersichtlich, dass die Mechanismen, die entscheiden, wann und wie häufig sich Stammzellen teilen und wie das weitere Zellschicksal entstehender Tochterzellen spezifiziert wird, eine zentrale Rolle in der Stammzellbiologie spielen. Die Aufklärung solcher Mechanismen sollte daher nicht nur wesentlich zum allgemeinen Verständnis der Stammzellbiologie beitragen, sondern auch eine essentielle Grundlage für die Konzeption neuer klinischer Forschungsansätze in der Regenerativen- und Tumormedizin darstellen.

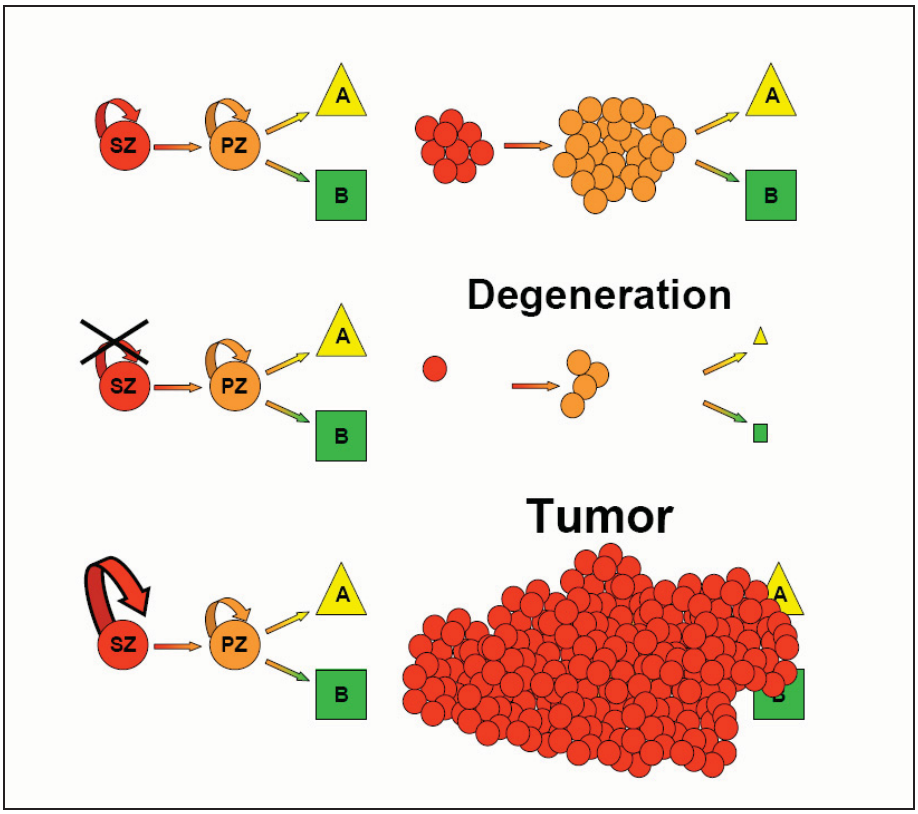

Abbildung 1 *Die Entscheidung Selbsterneuerung versus Differenzierung von Stammzellen (SZ) muss hoch kontrolliert sein. Eine zu geringe Selbsterneuerungsrate kann zur Degeneration betroffener Gewebe führen und eine zu hohe zur Tumorentstehung. PZ: Progenitorzelle, A, B: differenzierte Zelle.*

1.2 Selbsterneuerung *versus* Differenzierung von Stammzellen

Prinzipiell gibt es unterschiedliche Strategien, die zur Entscheidung Selbsterneuerung *versus* Differenzierung führen. So könnten Stammzellen durch invariante asymmetrische Zellteilungen Tochterzellen hervorbringen, die von vornherein unterschiedlich sind und von denen eine weiter spezifiziert ist, während die andere die Stammzelleigenschaften beibehält. Solche Teilungsmechanismen würden ausschließlich durch intrinsische Faktoren gesteuert. Andererseits könnten sich alle Stammzellen symmetrisch teilen; die Entscheidung, ob die Tochterzellen als Stammzellen erhalten bleiben oder sich zu weiter spezifizierten Vorläuferzellen entwickeln, hinge

ausschließlich von äußeren regulativen Faktoren ab, die in bestimmten, für den Stammzellerhalt erforderlichen Kombinationen räumlich auf bestimmte Orte begrenzt sind, den Stammzellnischen.

1.3 Hämatopoietische Stammzellen

Während der Ontogenese wird die Bildung von hämatopoietischen Stammzellen (HSZ) im Dottersack, in der Aorta-Gonad-Mesenephros (AGM)-Region und in der Plazenta initiiert (Dzierzak, 2005; Mikkola et al., 2005). Von dort aus besiedeln HSZ die fötale Leber, die bis zur Entdeckung der Hämatopoiese in der Plazenta als Hauptorgan der frühen fötalen Hämatopoiese angesehen wurde. Kurz vor der Geburt besiedeln sie schließlich das Knochenmark, den Ort der Hämatopoiese im Kindes- und Erwachsenenalter (Dzierzak, 2005; Mikkola et al., 2005). HSZ lassen sich aus der fötalen Leber, aus Nabelschnurrestblut und aus Knochenmark anreichern. Des Weiteren verlassen vereinzelte HSZ das Knochenmark und wandern kurzzeitig ins periphere Blut ein, ein Prozess der sich durch den *Granulozyten Kolonie-stimulierenden* Faktor (G-CSF) in hohem Maße steigern lässt (Nervi et al., 2006). Alle vier HSZ-Quellen eignen sich für den klinische Einsatz und können das hämatopoietische System von Patienten, das durch myeloablative Therapie zerstört wurde, rekonstituieren (Korbling and Anderlini, 2001).

Hieraus wird ersichtlich, dass HSZ die Fähigkeit besitzen, sämtliche Zellen des hämatopoietischen Systems zu bilden. Des Weiteren können sie *in vivo* expandieren, wie besonders durch sequenzielle Transplantationsexperimente an letal bestrahlten Mäusen gezeigt wurde (Iscove and Nawa, 1997). Da sich entsprechende Versuche am Menschen verbieten, werden zur Beurteilung des primitiven Zustands früher menschlicher hämatopoietischer Zellen verschiedene Tiermodelle eingesetzt, die von

immun-defizienten Mäusen bis hin zu fötalen Schafen reichen. Nach xenogener Transplantation wird hierbei die Fähigkeit von menschlichen hämatopoietischen Zellfraktionen beurteilt, Aspekte eines humanen hämatopoietischen Systems in diesen Tieren auszubilden (Kamel-Reid and Dick, 1988; Lapidot et al., 1992; Larochelle et al., 1996; Zanjani et al., 1992).

Die meisten hämatopoietischen Zellen, die sich in solchen xenogenen Tierversuchen ins Knochenmark dieser Tiere einnisten und menschliche Blutzellen hervorbringen können, gehören der Fraktion der $CD34^+$ Zellen an, genauer der Fraktion der $CD34^+$ Zellen, die keine Blutlinien-spezifischen Oberflächenmarker exprimieren (*lineage negativ*; lin^-) und die negativ oder nur geringfügig positiv für den Marker CD38 sind, die also der $lin^-CD34^+CD38^{low/-}$ Fraktion angehören (Bhatia et al., 1997b; Civin et al., 1996). Eine Population von Zellen mit entsprechenden Eigenschaften findet sich auch in der sehr kleinen Fraktion der $lin^-CD34^-CD38^-$ Zellen (Bhatia et al., 1998; Zanjani et al., 1998), von denen zumindest die aus Nabelschnurrestblut isolierten Zellen den Stammzellmarker CD133, nicht aber den lymphoiden Vorläufermarker CD7 exprimieren (Gallacher et al., 2000). Auch wenn es sich bei diesen Zellfraktionen um sehr kleine Zellpopulationen handelt, soll nicht unerwähnt bleiben, dass diese Fraktionen dennoch heterogene Gruppen von Zellen repräsentieren, in denen vermutlich nur wenige Zellen ein humanes HSZ-Potential besitzen. Mit anderen Worten, es ist bislang nicht möglich, humane HSZ zu isolieren. Entsprechend wird im Folgenden meist nicht von HSZ, sondern von primitiven hämatopoietischen Zellen oder von HSZ/hämatopoietischen Vorläuferzellen (HVZ) die Rede sein.

1.4 Hämatopoietische Stammzellnischen und der Notch-Signalweg

Aufgrund der bereits erwähnten Tatsache, dass HSZ *in vivo* expandieren können, wurden vielfältige Versuche unternommen, HSZ bzw. primitive hämatopoietische Zellen in Kultur zu vermehren. Hierbei zeigte sich jedoch, dass der primitive Zustand dieser Zellen in Stromazell-freien Kulturen nach einer anfänglichen, geringfügigen Expansion verloren geht (Bhatia et al., 1997a; Conneally et al., 1997; Shimizu et al., 1998). Im Unterschied hierzu kann ihr primitiver Zustand in Gegenwart bestimmter Stromazellen über einen längeren Zeitraum hinweg erhalten werden (Moore et al., 1997; Nolta et al., 2002; Punzel et al., 1999a; Shih et al., 1999). Diese Befunde verdeutlichen, dass die Umgebung und somit bestimmte äußere, d.h. extrinsische Signale darüber entscheiden, ob primitive hämatopoietische Zellen als solche erhalten bleiben oder ob sie zu weiterentwickelten Zellen heranreifen. Die für den HSZ-Erhalt erforderlichen Signale werden allem Anschein nach räumlich begrenzt in HSZ-Nischen bereitgestellt, die bereits 1978 von Raymond Schofield postuliert wurden (Schofield, 1978). HSZ-Nischen wurden sowohl im Endosteum des Knochenmarks als auch in der Umgebung sinusoidaler Endothelzellen in der Milz und im Knochenmark nachgewiesen (Calvi et al., 2003; Kiel et al., 2005; Zhang et al., 2003). Es zeigte sich, dass neben der Aktivierung der Rezeptortyrosin-Kinase Tie2 durch das von Osteoblasten gebildete Angiopoietin-1, eine wesentliche Funktion der HSZ-Nischen darin besteht, den Notch-Signalweg in HSZ zu aktivieren (Arai et al., 2004; Calvi et al., 2003).

Auf eine Beteiligung des Notch-Signalwegs an der Aufrechterhaltung primitiver hämatopoietischer Zellschicksale deutete bereits zuvor eine Reihe verschiedener Experimente (Chiba, 2006; Kojika and Griffin, 2001; Milner and Bigas, 1999; Suzuki and Chiba, 2005). Es konnte gezeigt werden, dass humane $CD34^+$ Zellen den Transmembranrezeptor Notch1 exprimieren (Milner et al., 1994) und generierte,

lösliche Formen der Notch Liganden Jagged-1 und Delta-1 dazu beitragen, primitive hämatopoietische Zellen kurzfristig in Stroma-freien Kultur zu erhalten bzw. leicht zu expandieren (Karanu et al., 2000; Karanu et al., 2001; Lauret et al., 2004; Ohishi et al., 2002; Suzuki et al., 2006). In Mäusen inhibieren konstitutiv aktivierte Formen von Notch sowohl eine HSZ-Differenzierung *in vitro* als auch *in vivo* und bewirken eine Expansion von Zellen, die sich in sekundäre Empfänger transplantieren lassen (Stier et al., 2002; Varnum-Finney et al., 2000).

1.5 Hinweise auf asymmetrische Zellteilungen im primitiven hämatopoietischen Zellkompartiment

Neben Befunden, welche die Existenz von HSZ-Nischen untermauern, deuten verschiedene Beobachtungen darauf hin, dass sich primitive hämatopoietische Zellen asymmetrisch teilen können.

Die Gruppe um Makio Ogawa konnte in den 1980er Jahren zeigen, dass Tochterzellen von HVZ nach Trennung durch Mikromanipulation teilweise Kolonien hervorbringen, die sich in ihrer Größe und ihrer Linienzusammensetzung erheblich unterscheiden, was als Folge stochastischer Entscheidungsprozeße interpretiert wurde (Leary et al., 1985; Suda et al., 1984a; Suda et al., 1984b). Ähnliche Beobachtungen wurden 1993 von Mayani et al. beschrieben, die Tochterzellen von $CD34^{+}CD45RA^{low}CD71^{low}$ Zellen trennten und sie entweder unter identischen oder unterschiedlichen Bedingungen kultivierten. Da sich in diesen Experimenten 3-17% der Tochterzellpaare unabhängig von den zugesetzten Zytokinen unterschiedlich entwickelten, vermuteten die Autoren, dass es sich um Folgen stochastisch gesteuerter, asymmetrischer Zellteilungen handelte (Mayani et al., 1993).

Nachdem gezeigt werden konnte, dass nur 20% bzw. 50% der humanen $CD34^{+}CD38^{-}$ Zellen aus Knochenmark bzw. Nabelschnurrestblut in der Lage sind, nach 5 wöchiger Co-Kultur mit bestrahlten Stromazellen Kolonien zu bilden (Conneally et al., 1997; Petzer et al., 1996), untersuchten Brümmendorf und Kollegen das Koloniebildungspotential von aus fötaler Leber isolierten $CD34^{+}CD38^{-}$ $CD71^{low}CD45RA^{low}$ Zellen. Neben Unterschieden in der Proliferationskinetik fanden sie, dass langsam teilende Zellen ein primitiveres Schicksal aufweisen als sich schneller teilende Zellen und dass sich Nachkommen einer einzelnen $CD34^{+}CD38^{-}$ Zelle in Bezug auf diese Eigenschaften ebenfalls voneinander unterscheiden (Brummendorf et al., 1998). Da in diesen Versuchen die Kulturbedingungen konstant gehalten wurden, vermuteten die Autoren, dass solche Unterschiede ähnlich wie bei asymmetrischen Zellteilungen in Modellorganismen (z.B. *Drosophila melanogaster*) auf die unterschiedliche Verteilung von intrinsichen Determinanten zurück zu führen ist (Brummendorf et al., 1998).

Unter Verwendung des Membranfarbstoffs PKH2, der in die Plasmamembran von Zellen interkaliert und gleichmäßig auf entstehende Tochterzellen verteilt wird, führten Huang et al. weitere Analysen zur Proliferationskinetik von $CD34^{+}CD38^{-}$ Zellen durch, die sowohl aus fötaler Leber, Nabelschnurrestblut als auch aus Knochenmark isoliert wurden. In Abhängigkeit der verwendeten Zytokine variierte der Zeitpunkt der 1. Zellteilung zwischen 36 und 38 bzw. zwischen 48 und 50 Stunden. Der Anteil der Zellen, die sich asynchron teilende Tochterzellen hervorbrachte, wurde in Abhängigkeit der einzelnen Quellen mit 20%-40% beziffert. Auch hier wurde vermutet, dass solche asynchronen Zellteilungen auf asymmetrische Zellteilungen zurückzuführen sind, bei denen intrinsische Determinanten ungleich auf entstehende Tochterzellen verteilt werden (Huang et al., 1999). In Fortführung dieser Arbeiten fanden Michael Punzel und

seine Kollegen, dass sich primitivere HVZ in der Tat langsamer und zu einem höheren Anteil asynchron teilen als etwas reifere HVZ (Punzel et al., 2002). Wie im folgenden Abschnitt etwas genauer beschrieben wird, konnten wir in Zusammenarbeit mit der Gruppe um Michael Punzel tatsächlich nachweisen, dass die primitivsten *in vitro* detektierbaren hämatopoietischen Zellen, die sowohl ein myeloisches als auch ein lymphatisches Entwicklungspotential aufweisen zu über 80% unterschiedlich spezifizierte Tochterzellen hervorbringen (Giebel et al., 2006). Von diesen als *myeloisch-lymphatisch initiierende Zellen* (ML-IC) bezeichnet Zellen (Punzel et al., 1999b; Punzel et al., 2002) übernahm scheinbar eine Tochterzelle das gesamte und die andere nur einen Teil des ursprünglichen Entwicklungspotentials (Giebel et al., 2006).

2 Ergebnisse

2.1 Unterschiedliche Entwicklung primitiver hämatopoietischer Tochterzellen (Giebel et al., 2006)

Humane Zellen, die nach xenogener Transplantation Anteile eines humanen hämatopoietischen Systems in Tieren ausbilden können, sind in der heterogenen Fraktion der $lin^{-}CD34^{+}CD38^{low/-}$ Zellen stark angereichert (Bhatia et al., 1997b; Civin et al., 1996). Da sich Zellen dieser Fraktion hinsichtlich ihrer Proliferationskinetiken voneinander unterscheiden (Brummendorf et al., 1998; Huang et al., 1999; Punzel et al., 2002), haben wir zunächst den Einfluss unterschiedlicher Zytokinkombinationen auf das Proliferationsverhalten primitiver hämatopoietischer Zellen analysiert. Hierzu haben wir aus Nabelschnurrestblut angereicherte $CD34^{+}$ Zellen mit dem Membranfarbstoff PKH2 markiert und in Gegenwart von früh (SCF, TPO, FLT3L) oder spät wirksamen Zytokinen (IL-3 IL-6, GM-CSF, bFGF, ILGF, Epo, SCF) über mehrere Tage hinweg kultiviert. Durch Messung des PKH2 Gehaltes haben wir ab Kulturtag 3 ermittelt, wie häufig sich Zellen der $CD34^{+}$ Fraktion in Kultur geteilt haben. Da mehr als 90% aller frisch isolierten $CD34^{+}$ Zellen auch den Stammzellmarker CD133 exprimieren, haben wir zusätzlich den CD133- und CD34-Zelloberflächengehalt dieser Zellen bestimmt. Es zeigte sich hierbei, dass sich ab Kulturtag 3 unter beiden Bedingungen die Population der $CD34^{+}CD133^{+}$ Zellen in eine $CD34^{+}CD133^{+}$ und eine $CD34^{+}CD133^{low/-}$ Population unterteilen lässt und der Anteil der $CD34^{+}CD133^{low/-}$ Zellen mit steigender Kulturdauer größer wird (Beckmann et al., 2007; Giebel et al., 2006). Während sich alle $CD34^{+}$ Zellen in Gegenwart von früh wirksamen Zytokinen annähernd gleich häufig teilen, fanden wir, dass sich unter Einfluss von spät wirksamen Zytokinen reifere $CD34^{+}CD133^{low/-}$Zellen öfter teilen als primitivere $CD34^{+}CD133^{+}$ Zellen (Giebel et al.,

2006). Somit lassen sich durch Kultivierung in Gegenwart von spät wirksamen Zytokinen primitivere und reifere HVZ schon alleine durch ihr Proliferationsverhalten voneinander unterscheiden.

Aufgrund dieser Beobachtungen und mit dem Ziel, das Tochterzellschicksal von sehr primitiven hämatopoietischen Zellen individuell zu analysieren, wurden $CD34^{+}CD38^{-}$ Zellen als einzelne Zellen in 96 *Well* Platten abgelegt und in Gegenwart von spät wirksamen Zytokinen analysiert. Zellen, die sich innerhalb der ersten fünf Kulturtage geteilt haben, wurden als *reifer* eingestuft und nicht weiter berücksichtigt. Zellen, die sich zwischen dem 5. und 10. Kulturtag erstmals teilten, wurden als *primitiv* angesehen und weiter analysiert (Giebel et al., 2006). Sobald erkannt wurde, dass sich diese Zellen geteilt haben, wurden die Tochterzellen durch Mikromanipulation voneinander getrennt und einzeln auf bestrahlten murinen Stromazellen (AFT024) weiter kultiviert (Punzel et al., 1999b). Nach 2 wöchiger Kultur wurde die Nachkommenschaft dieser Tochterzellen geteilt und ihr Entwicklungspotential in unterschiedlichen Auswertesystemen bestimmt. Zur Ermittlung des lymphatischen Entwicklungspotentials wurde ihre Fähigkeit zur Natürlichen Killerzell-Entwicklung in so genannten *Natrual Killer cell initiating cell* (NK-IC) Ansätzen getestet, und das myeloische Entwicklungspotential in myeloischen Langzeitkulturansätzen bestimmt, in so genannten *long term culture initiating cell* (LTC-IC) Kulturen (Giebel et al., 2006; Punzel et al., 1999b).

Nach Auswertung konnte retrospektiv das Entwicklungspotential der ursprünglich vereinzelten Tochterzellen und folglich auch das ihrer einzeln abgelegten Mutterzellen ermittelt werden. Hierbei fanden wir heraus, dass mindestens eine der Tochterzellen das Zellschicksal der primär abgelegten Ausgangszellen übernahm. Wir fanden keine Tochterzellpaare, in denen z.B. die eine Tochterzelle ein lymphatisches und die andere Tochterzelle ein myeloisches Schicksal realisierte (Giebel et al., 2006).

Bemerkenswerterweise entwickelten sich Tochterzellen von ursprünglich abgelegten Zellen mit nachgewiesenem myeloischen und lymphatischen Entwicklungspotential, dem ML-IC Potential (Punzel et al., 2002), in über 80% der Fälle unterschiedlich, während *reifere* Zellen oftmals sich gleich entwickelnde Tochterzellen hervorbrachten (Giebel et al., 2006). Dies deutet darauf hin, dass es Mechanismen gibt, die bewirken, dass Tochterzellen von primitiveren Zellen unter den angewendeten Bedingungen mit einer höheren Wahrscheinlichkeit unterschiedliche Zellschicksale annehmen als reifere HVZ. Als mögliche Erklärung lässt sich hier das Modell der asymmetrischen Zellteilung anführen, nach dem intrinsische Zellschicksalsdeterminanten ungleich auf die entstehenden Tochterzellen verteilt werden und sich hierdurch bedingt ungleiche Entwicklungspotentiale manifestieren.

Im Rahmen der Studie konnten wir als einen weiteren neuen Aspekt Zellen identifizieren, die neben NK Zellen auch Makrophagen, jedoch keine weiteren myeloischen Zellen hervorbrachten. Da Makrophagen zu den myeloischen Zellen zählen und dem klassischen Modell der Hämatopoiese zur Folge alle myeloischen Zellen von einer gemeinsamen Vorläuferzelle, dem *common myeloid progenitor* (CMP), und alle lymphatischen Zellen von einem *common lymphocyte progenitor* (CLP) abstammen (Reya et al., 2001), haben wir eine Art von Zellen beschrieben, die nach diesem Modell nicht existieren sollte. Wir haben sie daher als *macrophage Natural Killer cell initiating cell* (M-NK-IC) bezeichnet (Giebel et al., 2006). In diesem Zusammenhang soll angemerkt werden, dass unlängst auch in der Maus Zellen beschrieben worden sind, die das gesamte lymphatische und nur Teile des myeloischen Entwicklungspotentials aufweisen, so dass das klassische Modell in seiner bisherigen Form wohl nicht aufrecht erhalten werden kann (Adolfsson et al., 2005; Buza-Vidas et al., 2007; Iwasaki and Akashi, 2007).

2.2 Asymmetrische Zellteilung *versus* post-mitotischer Zellschicksals-spezifizierung und der Notch-Signalweg in *Drosophila melanogaster* (Giebel 1999)

Unsere Beobachtungen, dass primitive hämatopoietische Zellen oftmals Tochterzellen hervorbringen, die unterschiedliche Zellschicksale realisieren, lassen sich wie im letzten Abschnitt erwähnt und in Abbildung 2 dargestellt, mit dem Modell der asymmetrischen Zellteilung erklären, nach dem bei der Zellteilung bestimmte Zellschicksalsdeterminanten ungleich auf die entstehenden Tochterzellen verteilt werden. Andererseits lassen sich aber sowohl unsere Beobachtungen (Giebel et al., 2006) als auch die der anderen Gruppen (Brummendorf et al., 1998; Huang et al., 1999; Leary et al., 1985; Mayani et al., 1993; Punzel et al., 2002; Suda et al., 1984a; Suda et al., 1984b) durch ein anderes Modell erklären. Theoretisch könnten entstandene Tochterzellen zunächst identische Entwicklungskapazitäten besitzen. Durch Kommunikation der beiden Zellen in dem Zeitraum zwischen Abschluss der Mitose und der experimentellen Separation könnten sie dann gegenseitig ihr weiteres Zellschicksal beeinflussen und somit unterschiedlich werden (Beckmann et al., 2007; Giebel et al., 2006). Ein hierfür prädestinierter Signalweg ist der wie im Folgenden genauer am Beispiel der frühen Neurogenese und Myogenese von *Drosophila melanogaster* beschrieben Notch-Signalweg, der wie bereits diskutiert (1.4) an der Aufrechterhaltung primitiver hämatopoietischer Zellschicksale beteiligt ist.

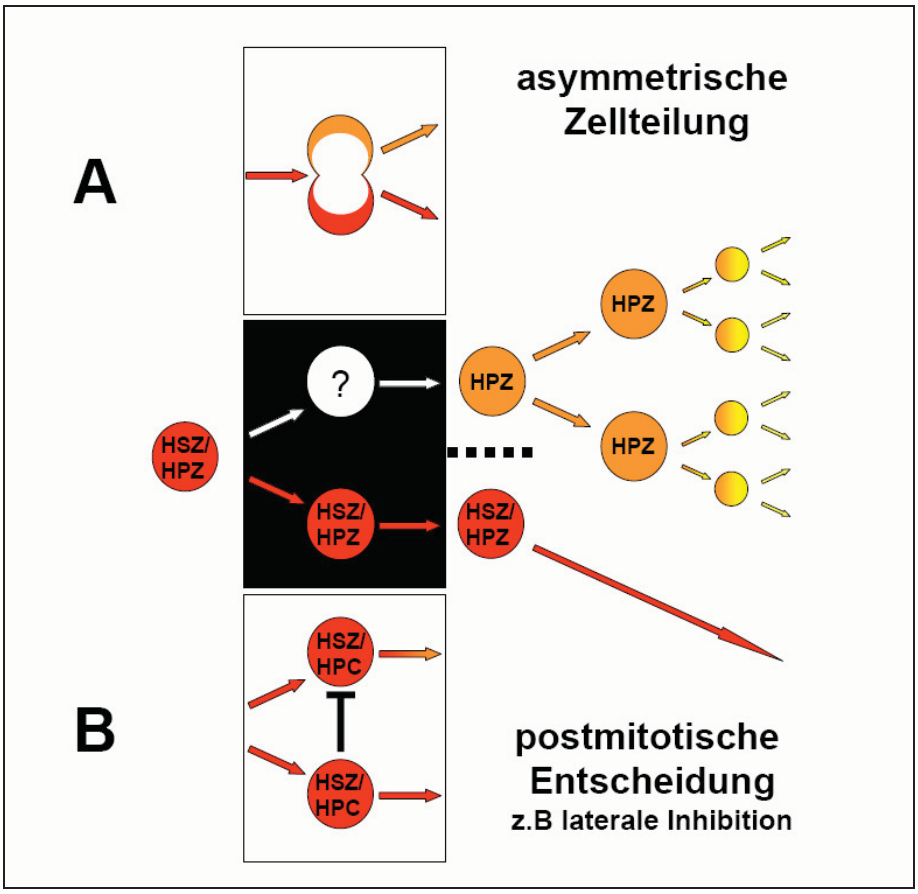

Abbildung 2 *Die Tatsache, dass primitive hämatopoietische Zellen (HSZ/HPZ) oftmals unterschiedlich spezifizierte Tochterzellen hervorbringen, lässt sich zum einen durch das Model der asymmetrischen Zellteilung erklären, nach dem durch die ungleiche Verteilung von Zellschicksalsdeterminanten entstehende Tochterzellen unmittelbar unterschiedlich spezifiziert werden (A). Andererseits könnten Tochterzellen zunächst identische Entwicklungskapazitäten besitzen und ihr weiteres Schicksal nach Vollendung der Mitose gegenseitig beeinflussen, so dass sie erst postmitotisch unterschiedlich werden (B). HPZ: hämatopoietische Stammzelle, HPZ hämatopoietische Vorläuferzelle.*

Der Notch-Signalweg in *Drosophila*

Während der embryonalen Entwicklung von *Drosophila* entstehen durch die Funktion so genannter proneuraler Gene, die Transkriptionsfaktoren der bHLH-Familie kodieren, in verschiedenen Geweben Gruppen von Zellen, die zunächst alle identische

Entwicklungsmöglichkeiten besitzen, dennoch aber unterschiedliche Entwicklungswege ein schlagen: Im so genannten Neuroektoderm, der Region, aus der das ventrale zentrale Nervensystem und die ventrale Epidermis hervorgehen, entwickeln sich aus solchen als *proneurale Cluster* bezeichneten Äquivalenzgruppen sowohl die Stammzellen des ventralen Nervensystems, die Neuroblasten, als auch die der Epidermis, die Epidermoblasten (Cabrera et al., 1987; Romani et al., 1987; Skeath and Carroll, 1992).

Es zeigte sich, dass an der Aufspaltung in beide Entwicklungslinien der Notch-Signalweg zentral beteiligt ist. Bedingt durch die Aktivität der proneuralen Gene wird in allen Zellen einer Äquivalenzgruppe der Notch-Ligand DELTA exprimiert, über den die Zellen mit ihren Nachbarzellen in Kontakt treten. DELTA bindet an NOTCH, das hierdurch bedingt gespalten und aktiviert wird; die intrazelluläre, aktivierte Domäne von Notch wandert in den Kern der Signal-empfangenden Zellen und aktiviert dort zusammen mit dem Transkriptionsfaktor SUPPRESSOR OF HAIRLESS Gene des ENHANCER OF SPLIT-Komplexes, einer Familie von so genannten *neurogenen* Transkriptionsfaktoren, die antagonistisch zu den proneuralen Genen wirken (Artavanis-Tsakonas et al., 1999; Martinez Arias et al., 2002; Portin, 2002). Durch die wechselseitige Signalübertragung, in denen die Zellen versuchen sich gegenseitig zu hemmen und die als laterale Inhibition bezeichnet wird, etablieren sich schließlich Zellen mit hoher proneuraler und andere mit hoher neurogener Genaktivität. Während erstere sich hierdurch bedingt zu Neuroblasten entwickeln, werden letztere zu Epidermoblasten spezifiziert (Cabrera et al., 1987; Romani et al., 1987; Skeath and Carroll, 1992).

In Analogie zum Neuroektoderm ist dieser Mechanismus erforderlich, um im Mesoderm einzelne Zellen entsprechender Äquivalenzgruppen zu Muskelgründerzellen zu spezifizieren, die sämtliche Informationen für die Entwicklung spezieller Muskeln

enthalten. Die übrigen Zellen der Äquivalenzgruppe, in denen der Notch-Signalweg transduziert wird, entwickeln sich hingegen zu fusionskompetenten Myoblasten, die mit den Muskelgründerzellen fusionieren und den Muskeln Volumen verleihen (Bate, 1990; Bate et al., 1993; Carmena et al., 1995; Corbin et al., 1991; Giebel, 1999).

Durch Überexpression verschiedener Mediatoren des Notch-Signalwegs konnte ich bestehende Parallelen zwischen der Neurogenese und der Myogenese experimentell darstellen. So unterdrückte die Überexpression von konstitutiv aktivem Notch sowohl im Neuroektoderm die Spezifizierung der Neuroblasten als auch im Mesoderm die der Muskelgründerzellen, und resultierte in der Entwicklung aneuraler und amuskulärer Embryonen. Wurde der Notch-Signalweg jedoch durch Überexpression eines Notch-Antagonisten abgeschwächt, entwickelten sich zusätzliche neurale Zellen und mehr Muskeln als in wildtypischen Embryonen (Giebel, 1999).

Laterale Inhibition in der frühen Hämatopoiese

Der Notch Signalweg wurde in der Evolution konserviert, und es konnte gezeigt werden, dass in primitiven humanen hämatopoietische Zellen der $CD34^+$ Fraktion sowohl Notch-1 und Notch-2 als auch die Notch Liganden Delta-1 and Delta-4 exprimiert werden, die beide die Entwicklung primitiver hämatopoietischer Zellen beeinflussen können (Karanu et al., 2001; Milner et al., 1994; Ohishi et al., 2000). Prinzipiell ist es daher möglich, dass entstehende Geschwisterzellen über diesen Signalweg miteinander in Kontakt treten und wechselseitig ihr weiteres Entwicklungspotential beeinflussen (Beckmann et al., 2007; Giebel et al., 2006). Voraussetzung für eine solche Interaktion ist, dass die entstehenden Tochterzellen nach der Mitose benachbart bleiben. Eine solch enge Nachbarschaft zwischen zwei Tochterzellen konnten wir oftmals nach der Mitose beobachten. Somit ist auch diese Voraussetzung für eine postmitotische Interaktion erfüllt. Ob eine solche Interaktion

aber tatsächlich stattfindet, ist derzeit noch unklar und soll durch die Verwendung von Reportergenen, die durch transduziertes Notch-Signal aktiviert werden, in nächster Zeit ermittelt werden.

Asymmetrische Zellteilungen im frühen hämatopoietischen System

Mit dem Modell der asymmetrischen Zellteilung können somit zwar die Ergebnisse der Tochterzellseparationsexperimente erklärt werden, aber es gibt auch andere plausibel erscheinende Modelle, die zur Erklärung unserer Beobachtungen herangezogen werden können. Vor diesem Hintergrund setzten wir es uns zum Ziel, eindeutige Hinweise für die Existenz von asymmetrischen Zellteilungen im frühen humanen hämatopoietischen System zu suchen.

Asymmetrische Zellteilungen sind bislang am Besten in den Modellorganismen *Drosophila melanogaster* und *Caenorhabditis elegans* beschrieben worden. In *Drosophila* teilen sich die bereits erwähnten Neuroblasten asymmetrisch und bringen jeweils eine größere Tochterzelle hervor, die als Neuroblast erhalten bleibt, und eine kleinere, als Ganglionmutterzelle (GMC) bezeichnete Tochterzelle, die nach einer weiteren Teilung postmitotisch wird. Es zeigte sich, dass in Abhängigkeit der Aktivität verschiedener Zellpolaritäts-organisierender Proteine u.a. der Transkriptionsfaktor PROSPERO als auch dessen kodierende mRNA an dem basalen Pol der Neuroblasten deponiert werden und bedingt durch eine Rotation der mitotischen Spindel um 90° überwiegend in die sich zu GMC entwickelnden Tochterzellen segregieren. Dort ist PROSPERO entscheidend an der Zellschicksalsspezifizierung der GMC beteiligt; es aktiviert die Transkription GMC spezifischer und reprimiert Neuroblasten-spezifische Gene (Wodarz and Huttner, 2003).

In Analogie hierzu teilen sich sowohl die Zygote als auch resultierende Blastomeren von *C. elegans* asymmetrisch. Hier wird ebenfalls in Abhängigkeit von Zellpolaritäts-organisierenden Proteinen, die zu denen von *Drosophila* homolog sind, die so genannte P-Granula an den posterioren Pol der Zygote lokalisiert, die nach einer Spindelrotation ausschließlich in die posterior zu liegen kommende Tochterzelle segregiert. Da diese P-Granula unter anderem Determinanten der Keimbahn enthält, wird dass Potential zur Keimbahnentwicklung nur an die posterioren Blastomeren vererbt (Kemphues et al., 1988; Watts et al., 1996).

Vor dem Hintergrund dieser Befunde postulierten wir, dass im Falle einer asymmetrischen Zellteilung im frühen hämatopoietischen System, HSZ/HVZ während der Mitose polarisiert sein sollten. Da zu Beginn dieser Arbeiten nicht viel über die Zellpolarität von frühen hämatopoietischen Zellen bekannt war, untersuchten wir, inwieweit diese Zellen überhaupt eine Zellpolarität besitzen.

2.3 Zellpolarität humaner HSZ/HVZ (Giebel et al., 2004)

Frisch isolierte $CD34^+$ Zellen sind kleine runde Zellen, die keine Anzeichen einer Polaritätsachse aufweisen (Abbildung 3 A, C). Mit unseren Arbeiten konnten wir zeigen, dass diese anfänglich nicht-polaren Zellen in Kultur ihre Morphologie verändern und eine polare Form annehmen, die dem Migrationsphänotypen von immunoreaktiven Leukozyten entspricht und essenziell für die Wanderung dieser Zellen ist (Abbildung 3 B, D). Die kultivierten $CD34^+$ Zellen bilden am vorderen Ende eine Leitfront aus, die so genannte *leading edge*, und am Hinterende einen Ausläufer, der als Uropod bezeichnet wird (Giebel et al., 2004). Neben der morphologischen Veränderung kommt es bei dieser Polarisierung zur Umverteilung verschiedener Oberflächenmarker. So konnten wir zeigen, dass neben den aus immunoreaktiven Leukozyten bekannten

Uropodmarkern CD43, CD44, CD50 und CD54 auch der Stammzellmarker CD133 (Prominin-1) nach Polarisierung der $CD34^+$ Zellen spezifisch im Uropod lokalisiert wird (Abbildung 3 B). Andere Marker wie der Chemokin-Rezeptor CXCR4 oder das Gangliosid GM3 werden - ebenfalls immunoreaktiven Leukozyten entsprechend - stark in der *leading edge* angereichert. Mit CD34 und CD45 fanden wir Beispiele für Moleküle, die in kultivierten $CD34^+$ Zellen nicht polarisiert, sondern gleichmäßig auf der gesamten Zelloberfläche verteilt vorliegen (Giebel et al., 2004).

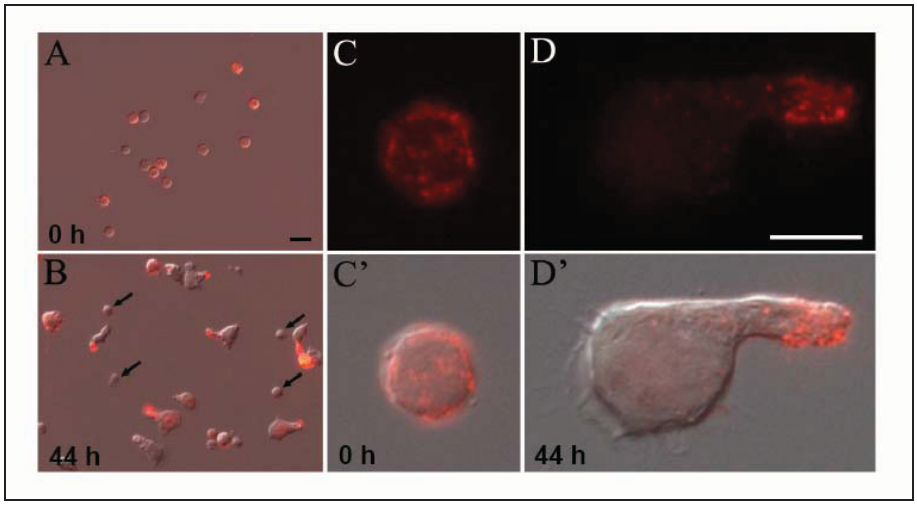

Abbildung 3 *Frisch isolierte $CD34^+$ Zellen sind klein und rund und weisen keine Anzeichen einer Zellpolarität auf (A, C). In Kultur werden sie größer und erlangen eine polarisierte Morphologie. Einhergehend mit dieser morphologischen Polarisierung werden verschiedene Zelloberflächenantigene, wie hier am Beispiel des Stammzellmarkers CD133 gezeigt (rote Färbung) umverteilt (entnommen aus Giebel et al., 2004).*

2.4 Polaritätsmarker in mitotischen HSZ/HVZ (Beckmann et al., 2006)

In weiterführenden Arbeiten untersuchten wir die Verteilung der identifizierten Polaritätsmarker in sich teilenden Zellen und fanden, dass CD43, CD44, CD50 und CD54 wie auch CD133 in der Teilungsfurche und später in der zytoplasmatischen

Verbindung der beiden entstehenden Tochterzellen, dem so genannten *Midbody*, angereichert werden (Beckmann et al., 2007). Den Chemokin-Reszeptor CXCR4 fanden wir hingegen im Cortex der Zellen angereichert. Auch wenn diese Daten belegen, dass sich teilende $CD34^+$ Zellen polarisiert sind, fanden wir in den untersuchten mitotischen $CD34^+$ Zellen keine Hinweise, die auf eine asymmetrische Verteilung eines dieser Markerproteine hindeuteten. Wir folgerten, dass sich $CD34^+$ Zellen zumindest unter den von uns verwendeten Bedingungen nicht asymmetrisch teilen oder andere Proteine existieren, die asymmetrisch verteilt werden (Beckmann et al., 2007).

Wie bereits unter 2.1 beschrieben spaltet sich die Population frisch isolierter $CD34^+CD133^+$ Zellen nach Einsetzen der Zellteilungsaktivität in eine $CD34^+CD133^+$ und eine $CD34^+CD133^{low/-}$ Population auf, wobei der Anteil der $CD34^+CD133^{low/-}$ Zellen mit steigender Kulturdauer immer größer wird (Beckmann et al., 2007; Giebel et al., 2006). Prinzipiell passt diese Kinetik zu einem Modell, nach dem sich 20-30% aller $CD34^+CD133^+$ Zellen asymmetrisch teilen und eine der beiden jeweils entstehenden Tochterzellen CD133 dauerhaft verliert, während die andere Tochterzelle und ihre Nachkommen zumindest bis zur nächsten asymmetrischen Zellteilung CD133 positiv bleiben. Auch wenn CD133 selbst nicht asymmetrisch verteilt wird, könnte diesem Modell zur Folge jedes Molekül, dessen Expression einer entsprechenden Kinetik folgt, einen Marker für asymmetrische Zellteilungen darstellen (Beckmann et al., 2007). Zur Identifizierung von Kandidaten mit solchen Kinetiken haben wir die Expression verschiedener Antigene in kultivierten $CD34^+$ Zellen analysiert und fanden wie in Abbildung 4 dargestellt, dass die Tetraspanine CD53 und CD63, der Transferrinrezeptor CD71 und L-Selectin (CD62L) entsprechenden Kinetiken folgen (Beckmann et al., 2007).

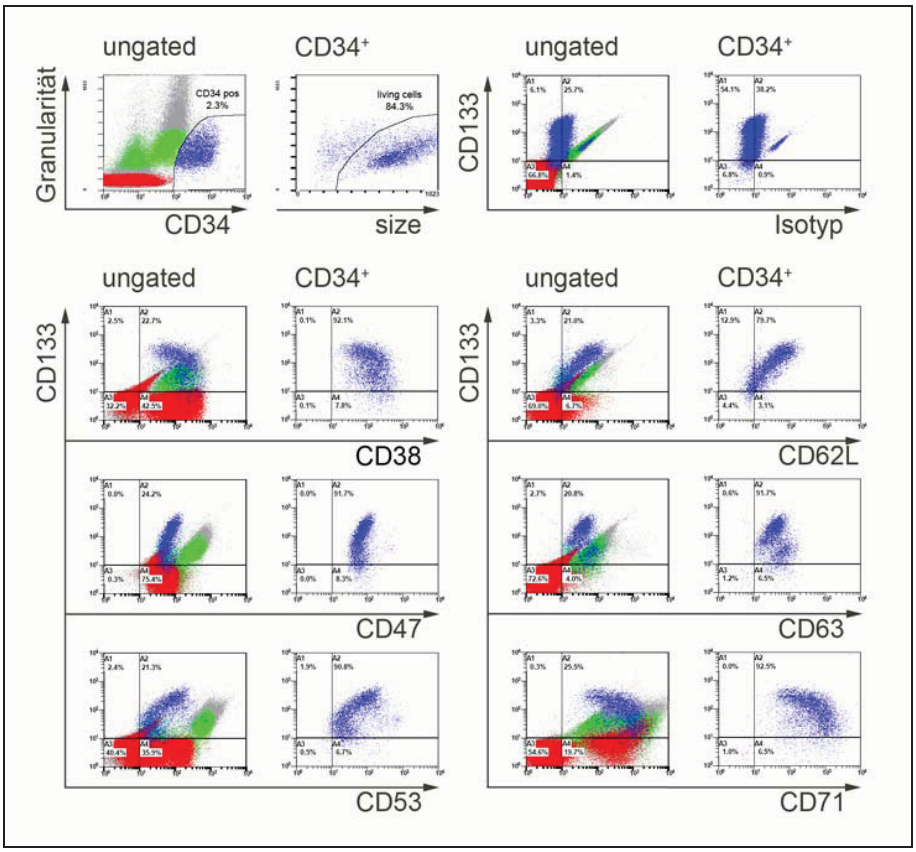

Abbildung 4 *Durchflusszytometrische Darstellung von kulivierten mononukleären Zellen aus dem Nabelschnurrestblut, die für drei Tage kultiviert und anschließend mit verschiedenen fluoreszensmarkierten Antikörpern gefärbt worden sind. Durch Darstellung der CD34 Expressionsstärke gegen die Granularität lässt sich sehr gut die Population der $CD34^+$ Zellen (CD34 pos) von den $CD34^-$ Zellen diskriminieren (1. Plot links oben), erstere sind durchgängig blau markiert (rot: Lymphozyten, grün Monozyten). Im 2. Plot der oberen Reihe ist die Größe der $CD34^+$ Zellen gegen deren Granularität aufgetragen. In allen folgenden Plots, werden variierende Fluoreszenzen mit der von CD133 dargestellt, für alle gemessenen Zellen (ungated) bzw. nur für die $CD34^+$ Zellen. Hierbei wird in der oberen Reihe die Isotyp-Kontrolle gezeigt. Im Weiteren wird CD38 als bekannter Unterscheidungsmarker für reifere und primitivere $CD34^+$ Zellen dargestellt. CD47 dient als Beispiel für Oberflächenantigene, die auf allen $CD34^+$ Zellen in etwa gleich stark exprimiert werden. Die Marker CD53 und CD62L sind deutlich vermehrt auf den $CD34^+$ Zellen zu finden, die mehr CD133 exprimieren, während CD63 und CD71 stärker auf den $CD34^+CD133^{low/-}$ Zellen exprimiert werden (modifiziert aus Beckmann et al., 2007).*

Subzelluläre Lokalisierungsexperimente zeigten, dass CD62L an der Spitze von Uropoden angereichert wird, während CD53 und CD63 in vesikulären Strukturen in einer bis dahin noch nicht beschriebenen Region an der Basis von Uropoden zu finden sind. Hier fanden wir auch eine hohe, vesikuläre Anreicherung von CD71, das ansonsten auf der gesamten Membran verteilt vorliegt. Durch Zugabe von Antikörpern zu lebenden Zellen als auch durch intrazelluläre Färbungen konnten wir nachweisen, dass es sich bei den vesikulären Strukturen um sich bildende und ins Innere der Zellen abknospende Endosomen handelt (Beckmann et al., 2007).

Schließlich analysierten wir die subzelluläre Expression der vier identifizierten Proteine in sich teilenden $CD34^{+}CD133^{+}$ Zellen und fanden, dass in ca. 20% aller analysierten Mitosen diese Marker asymmetrisch segregieren (Abbildung 5). Somit konnten wir zeigen, dass sich primitive humane hämatopoietische Zellen in der Tat asymmetrisch teilen können (Beckmann et al., 2007). Bemerkenswert ist, dass die ermittelte Frequenz in etwa der entspricht, mit der sich Tochterzellen von primitiven hämatopoietischen Zellen unterschiedlich entwickeln. Somit lässt sich vermuten, dass sich die beschriebenen Unterschiede in den Zellschicksalen analysierter Tochterzellen in der Tat durch asymmetrische Zellteilungen manifestieren.

In diesem Zusammenhang fanden wir auch, dass die asymmetrisch segregierenden Marker in Kombination mit CD133 verwendet werden können, um primitivere von reiferen kultivierten $CD34^{+}$ Zellen zu trennen (Beckmann et al., 2007).

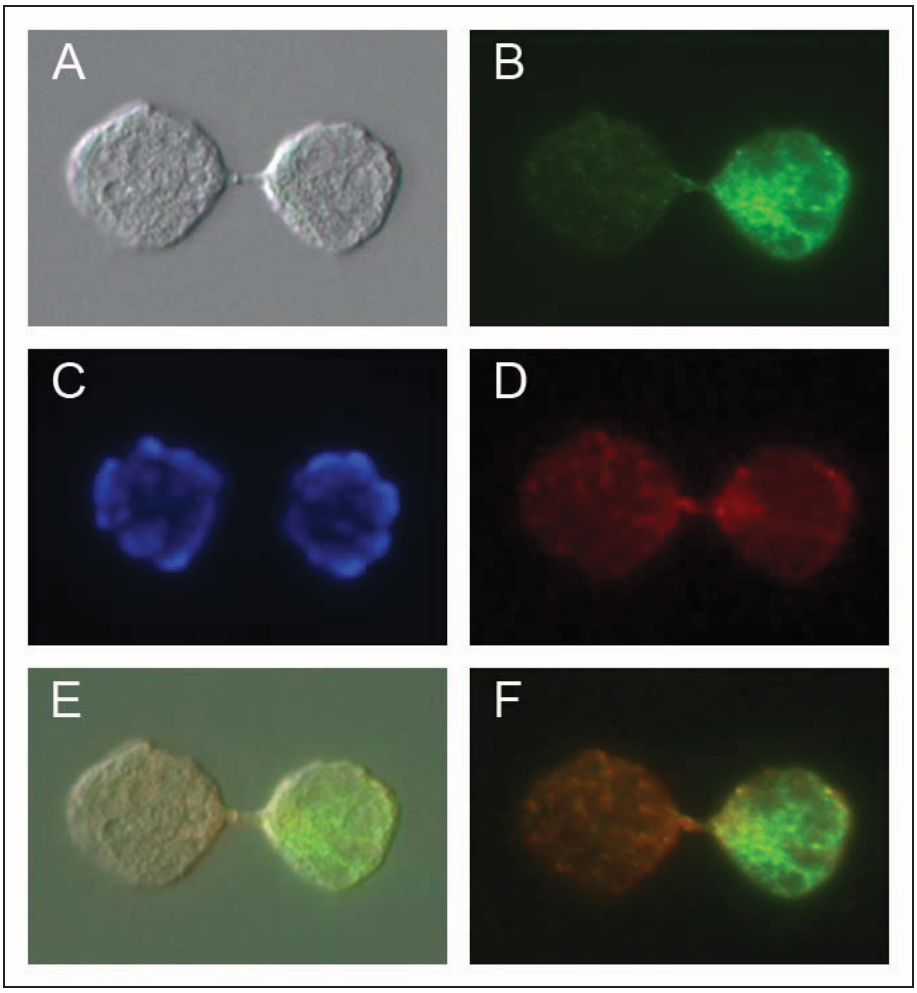

Abbildung 5 *Beispiel für eine sich asymmetrisch teilende $CD34^+CD133^+$ Zelle; A: Durchlicht, B: CD62L; C: DAPI, D: CD133, E: Durchlicht mit CD62L und CD133, F: CD62L und CD133. Während CD62L eindeutig asymmetrisch verteilt ist, ist CD133 stark in der Teilungsebene angereichert.*

2.5 Mechanistische Analysen zur Entscheidung Selbsterneuerung *versus* Differenzierung (von Levetzow et al., 2006; Schneider et al., 2004; Bracker et al., 2006; Feldhahn et al., 2007)

Zur Analyse der molekularen Mechanismen, welche die Entscheidung Selbsterneuerung *versus* Differenzierung steuern, haben wir uns im Rahmen eines weiteren Teilprojekts entschieden, verschiedene Gene zunächst überzuexprimieren. Aufgrund der eigenen Erfahrung aus *Drosophila* und Morbus Hodgkin Studien und der wichtigen Bedeutung

für den Selbsterhalt primitiver hämatopoietischer Zellen haben wir spezielle Komponenten des Notch-Signalwegs und verschiedene Transkriptionsfaktoren ausgewählt (Giebel, 1999; Giebel and Campos-Ortega, 1997; Giebel et al., 1997; Hinz et al., 1994; Schneider et al., 2004). Als Grundlage für solche Experimente benötigten wir effiziente Transfektionstechniken, die es zunächst in unserer Arbeitsgruppe zu etablieren galt. Hierzu wählten wir zum einen die Methode der Nukleofektion, die wir für unsere Zwecke optimierten und mit der wir $CD34^+$ Zellen effizient und transient transfizieren können, ohne ihr Schicksal alleine durch die Methode selbst nennenswert zu modifizieren (Giebel et al., 2004; von Levetzow et al., 2006). Für stabile Transfektionen wählten wir eine auf Lentiviren basierende Technik, die wir mit Unterstützung von Prof. Helmut Hanenberg in unserer Arbeitsgruppe etablieren konnten.

Zur Identifizierung neuer Transkriptionsfaktoren, die in der frühen Hämatopoiese eine entscheidende Rolle spielen könnten, führten wir in Kollaboration mit Prof. Ihor Lemischka und Dr. Natalia Ivanova (Princeton University) sowie mit Prof. Thomas Moritz, PD. Jürgen Thomale und PD. Ludger Klein-Hitpass (Universitätsklinikum Essen) komplexe Genexpressionsanalysen durch, von denen letztere in Zusammenhang mit der Analyse von DNA-Reperaturmechanismen veröffentlicht worden sind (Bracker et al., 2006).

Bislang haben wir die kodierenden Regionen verschiedener identifizierter Transkriptionsfaktoren in den von uns verwendeten lentiviralen Vektor kloniert. Mit einem dieser erhaltenen lentiviralen Plasmide, das die kodierende Region des Transkriptionsfaktors ID2 enthält, haben wir erfolgreich leukämische Zelllinien stabil transfizieren können, die dann von der Gruppe um Prof. Markus Müschen näher charakterisiert wurden (Feldhahn et al., 2007).

Derzeit analysieren wir Effekte nach Überexpression solcher Transkriptionsfaktoren in $CD34^+$ Zellen. Unseren vorläufigen Daten zur Folge konnten wir in der Tat neue Transkriptionsfaktoren identifizieren, deren Aktivität $CD34^+$ Zellen in einem primitiveren Zustand hält.

3 Zusammenfassung

Zur Aufrechterhaltung der Blutbildung müssen sich hämatopoietische Stammzellen sowohl selbst erneuern als auch Zellen hervorbringen, die sich in ihrem weiteren Entwicklungsverlauf in Zellen der unterschiedlichen hämatopoietischen Entwicklungslinien differenzieren. Die Entscheidung, ob entsprechende Tochterzellen als Stammzellen erhalten bleiben oder heranreifen, muss hierbei genau kontrolliert werden. In unseren Studien fanden wir, dass sehr frühe hämatopoietische Zellen häufig Tochterzellen hervorbringen, die sich unterschiedlich entwickeln. Während die eine Tochterzelle das Schicksal der Mutterzelle übernimmt, reduziert sich das Entwicklungspotential der anderen Tochterzelle. Diese Befunde lassen sich gut durch das Modell der asymmetrischen Zellteilung erklären, nachdem durch die Ungleichverteilung von als Zellschicksalsdeterminanten fungierenden Molekülen nur eine Tochterzelle als Stammzelle erhalten bleibt. Da solche Zellschicksalsunterschiede theoretisch auch erst postmitotisch etabliert werden könnten, haben wir nach konkreteren Hinweisen für asymmetrische Zellteilungen im frühen hämatopoietischen Kompartiment gesucht.

Ausgehend von der Erkenntnis, dass sich asymmetrisch teilende Zellen in Modellorganismen polarisiert sind, über die Zellpolarität in frühen hämatopoietischen Zellen zu Beginn unserer Arbeiten aber so gut wie nichts bekannt war, haben wir diese zunächst untersucht. In unseren Studien konnten wir zeigen, dass frühe, anfangs nicht-polar erscheinende hämatopoietische Zellen nach kurzzeitiger Kultivierung einen für ihre Wanderung erforderlichen, polaren Migrationsphänotyp annehmen und verschiedene Oberflächenantigene umverteilen. In diesem Zusammenhang

qualifizierten wir den Stammzellmarker CD133 (Prominin-1) als Uropodmarker früher hämatopoietischer Zellen.

In unseren weiterführenden Untersuchungen fanden wir, dass sich CD133 und andere untersuchte Uropodmarker in mitotischen Zellen stets in der Teilungsfurche anreichern bzw. in der als *Midbody* bezeichneten Zytoplasmabrücke, welche die entstehenden Tochterzellen verbindet. Da wir keine mitotische Zelle fanden, in denen diese Marker asymmetrisch verteilt waren, setzten wir unsere Suche nach asymmetrisch segregierenden Molekülen fort. Unter Verwendung eines auf Durchflusszytometrie basierenden Versuchsansatzes konnten wir Oberflächenantigene identifizieren, deren Expression einer Kinetik folgt, wie wir sie für asymmetrisch segregierende Moleküle postuliert haben. Immunohistochemische Analysen zeigten, dass in der Tat in ca. 20% der sich teilenden frühen hämatopoietischen Zellen die identifizierten Antigene, L-Selektin, der Transferrinrezeptor und die Tetraspanine, CD53 und CD63, asymmetrisch verteilt werden. Somit konnten wir erstmals nachweisen, dass sich primitive hämatopoietische Zellen in der Tat asymmetrisch teilen können.

Unsere neueren Arbeiten werden dazu beitragen, molekularbiologische Mechanismen aufzuklären, welche die Entscheidung Selbsterneuerung *versus* Differenzierung primitiver hämatopoietischer Zellen steuern. Hierbei konzentrieren wir uns im Wesentlichen auf Transkriptionsfaktoren und ausgewählte Mediatoren des Notch-Signaltransduktionsweges. Neben der Selektion spezifischer Kandidaten durch komplexe Expressionsanalysen haben wir uns bereits eine technische Plattform zur Manipulation primärer, humaner hämatpoietischer Stamm- und Vorläuferzellen geschaffen.

4 Literatur:

Adolfsson, J., Mansson, R., Buza-Vidas, N., Hultquist, A., Liuba, K., Jensen, C. T., Bryder, D., Yang, L., Borge, O. J., Thoren, L. A.*, et al.* (2005). Identification of Flt3+ lympho-myeloid stem cells lacking erythro-megakaryocytic potential a revised road map for adult blood lineage commitment. Cell *121*, 295-306.

Al-Hajj, M. (2007). Cancer stem cells and oncology therapeutics. Curr Opin Oncol *19*, 61-64.

Anversa, P., Rota, M., Urbanek, K., Hosoda, T., Sonnenblick, E. H., Leri, A., Kajstura, J., and Bolli, R. (2005). Myocardial aging--a stem cell problem. Basic Res Cardiol *100*, 482-493.

Arai, F., Hirao, A., Ohmura, M., Sato, H., Matsuoka, S., Takubo, K., Ito, K., Koh, G. Y., and Suda, T. (2004). Tie2/Angiopoietin-1 signaling regulates hematopoietic stem cell quiescence in the bone marrow niche. Cell *118*, 149-161.

Artavanis-Tsakonas, S., Rand, M. D., and Lake, R. J. (1999). Notch signaling: cell fate control and signal integration in development. Science *284*, 770-776.

Bate, M. (1990). The embryonic development of larval muscles in Drosophila. Development *110*, 791-804.

Bate, M., Rushton, E., and Frasch, M. (1993). A dual requirement for neurogenic genes in Drosophila myogenesis. Dev Suppl, 149-161.

Beachy, P. A., Karhadkar, S. S., and Berman, D. M. (2004). Tissue repair and stem cell renewal in carcinogenesis. Nature *432*, 324-331.

Beckmann, J., Scheitza, S., Wernet, P., Fischer, J. C., and Giebel, B. (2007). Asymmetric cell division within the human hematopoietic stem and progenitor cell compartment: identification of asymmetrically segregating proteins. Blood *109*, 5494-5501.

Bhatia, M., Bonnet, D., Kapp, U., Wang, J. C., Murdoch, B., and Dick, J. E. (1997a). Quantitative analysis reveals expansion of human hematopoietic repopulating cells after short-term ex vivo culture. J Exp Med *186*, 619-624.

Bhatia, M., Bonnet, D., Murdoch, B., Gan, O. I., and Dick, J. E. (1998). A newly discovered class of human hematopoietic cells with SCID-repopulating activity. Nat Med *4*, 1038-1045.

Bhatia, M., Wang, J. C., Kapp, U., Bonnet, D., and Dick, J. E. (1997b). Purification of primitive human hematopoietic cells capable of repopulating immune-deficient mice. Proc Natl Acad Sci U S A *94*, 5320-5325.

Brummendorf, T. H., Dragowska, W., Zijlmans, J., Thornbury, G., and Lansdorp, P. M. (1998). Asymmetric cell divisions sustain long-term hematopoiesis from single-sorted human fetal liver cells. J Exp Med *188*, 1117-1124.

Buza-Vidas, N., Luc, S., and Jacobsen, S. E. (2007). Delineation of the earliest lineage commitment steps of haematopoietic stem cells: new developments, controversies and major challenges. Curr Opin Hematol *14*, 315-321.

Cabrera, C. V., Martinez-Arias, A., and Bate, M. (1987). The expression of three members of the achaete-scute gene complex correlates with neuroblast segregation in Drosophila. Cell *50*, 425-433.

Calvi, L. M., Adams, G. B., Weibrecht, K. W., Weber, J. M., Olson, D. P., Knight, M. C., Martin, R. P., Schipani, E., Divieti, P., Bringhurst, F. R.*, et al.* (2003). Osteoblastic cells regulate the haematopoietic stem cell niche. Nature *425*, 841-846.

Carmena, A., Bate, M., and Jimenez, F. (1995). Lethal of scute, a proneural gene, participates in the specification of muscle progenitors during Drosophila embryogenesis. Genes Dev *9*, 2373-2383.

Chiba, S. (2006). Notch signaling in stem cell systems. Stem Cells *24*, 2437-2447.

Civin, C. I., Almeida-Porada, G., Lee, M. J., Olweus, J., Terstappen, L. W., and Zanjani, E. D. (1996). Sustained, retransplantable, multilineage engraftment of highly purified adult human bone marrow stem cells in vivo. Blood *88*, 4102-4109.

Conneally, E., Cashman, J., Petzer, A., and Eaves, C. (1997). Expansion in vitro of transplantable human cord blood stem cells demonstrated using a quantitative assay of their lympho-myeloid repopulating activity in nonobese diabetic-scid/scid mice. Proc Natl Acad Sci U S A *94*, 9836-9841.

Corbin, V., Michelson, A. M., Abmayr, S. M., Neel, V., Alcamo, E., Maniatis, T., and Young, M. W. (1991). A role for the Drosophila neurogenic genes in mesoderm differentiation. Cell *67*, 311-323.

Dzierzak, E. (2005). The emergence of definitive hematopoietic stem cells in the mammal. Curr Opin Hematol *12*, 197-202.

Feldhahn, N., Henke, N., Melchior, K., Duy, C., Soh, B. N., Klein, F., von Levetzow, G., Giebel, B., Li, A., Hofmann, W. K.*, et al.* (2007). Activation-induced cytidine deaminase acts as a mutator in BCR-ABL1-transformed acute lymphoblastic leukemia cells. J Exp Med *204*, 1157-1166.

Gallacher, L., Murdoch, B., Wu, D. M., Karanu, F. N., Keeney, M., and Bhatia, M. (2000). Isolation and characterization of human CD34(-)Lin(-) and CD34(+)Lin(-) hematopoietic stem cells using cell surface markers AC133 and CD7. Blood *95*, 2813-2820.

Giebel, B. (1999). The notch signaling pathway is required to specify muscle progenitor cells in Drosophila. Mech Dev *86*, 137-145.

Giebel, B., and Campos-Ortega, J. A. (1997). Functional dissection of the Drosophila enhancer of split protein, a suppressor of neurogenesis. Proc Natl Acad Sci U S A *94*, 6250-6254.

Giebel, B., Corbeil, D., Beckmann, J., Hohn, J., Freund, D., Giesen, K., Fischer, J., Kogler, G., and Wernet, P. (2004). Segregation of lipid raft markers including CD133 in polarized human hematopoietic stem and progenitor cells. Blood *104*, 2332-2338.

Giebel, B., Stuttem, I., Hinz, U., and Campos-Ortega, J. A. (1997). Lethal of scute requires overexpression of daughterless to elicit ectopic neuronal development during embryogenesis in Drosophila. Mech Dev *63*, 75-87.

Giebel, B., Zhang, T., Beckmann, J., Spanholtz, J., Wernet, P., Ho, A. D., and Punzel, M. (2006). Primitive human hematopoietic cells give rise to differentially specified daughter cells upon their initial cell division. Blood *107*, 2146-2152.

Hinz, U., Giebel, B., and Campos-Ortega, J. A. (1994). The basic-helix-loop-helix domain of Drosophila lethal of scute protein is sufficient for proneural function and activates neurogenic genes. Cell *76*, 77-87.

Huang, S., Law, P., Francis, K., Palsson, B. O., and Ho, A. D. (1999). Symmetry of initial cell divisions among primitive hematopoietic progenitors is independent of ontogenic age and regulatory molecules. Blood *94*, 2595-2604.

Iscove, N. N., and Nawa, K. (1997). Hematopoietic stem cells expand during serial transplantation in vivo without apparent exhaustion. Curr Biol *7*, 805-808.

Iwasaki, H., and Akashi, K. (2007). Myeloid lineage commitment from the hematopoietic stem cell. Immunity *26*, 726-740.

Kamel-Reid, S., and Dick, J. E. (1988). Engraftment of immune-deficient mice with human hematopoietic stem cells. Science *242*, 1706-1709.

Kamminga, L. M., and de Haan, G. (2006). Cellular memory and hematopoietic stem cell aging. Stem Cells *24*, 1143-1149.

Karanu, F. N., Murdoch, B., Gallacher, L., Wu, D. M., Koremoto, M., Sakano, S., and Bhatia, M. (2000). The notch ligand jagged-1 represents a novel growth factor of human hematopoietic stem cells. J Exp Med *192*, 1365-1372.

Karanu, F. N., Murdoch, B., Miyabayashi, T., Ohno, M., Koremoto, M., Gallacher, L., Wu, D., Itoh, A., Sakano, S., and Bhatia, M. (2001). Human homologues of Delta-1 and Delta-4 function as mitogenic regulators of primitive human hematopoietic cells. Blood *97*, 1960-1967.

Kemphues, K. J., Priess, J. R., Morton, D. G., and Cheng, N. S. (1988). Identification of genes required for cytoplasmic localization in early C. elegans embryos. Cell *52*, 311-320.

Kiel, M. J., Yilmaz, O. H., Iwashita, T., Terhorst, C., and Morrison, S. J. (2005). SLAM family receptors distinguish hematopoietic stem and progenitor cells and reveal endothelial niches for stem cells. Cell *121*, 1109-1121.

Kojika, S., and Griffin, J. D. (2001). Notch receptors and hematopoiesis. Exp Hematol *29*, 1041-1052.

Korbling, M., and Anderlini, P. (2001). Peripheral blood stem cell versus bone marrow allotransplantation: does the source of hematopoietic stem cells matter? Blood *98*, 2900-2908.

Lapidot, T., Pflumio, F., Doedens, M., Murdoch, B., Williams, D. E., and Dick, J. E. (1992). Cytokine stimulation of multilineage hematopoiesis from immature human cells engrafted in SCID mice. Science *255*, 1137-1141.

Larochelle, A., Vormoor, J., Hanenberg, H., Wang, J. C., Bhatia, M., Lapidot, T., Moritz, T., Murdoch, B., Xiao, X. L., Kato, I.*, et al.* (1996). Identification of primitive human hematopoietic cells capable of repopulating NOD/SCID mouse bone marrow: implications for gene therapy. Nat Med *2*, 1329-1337.

Lauret, E., Catelain, C., Titeux, M., Poirault, S., Dando, J. S., Dorsch, M., Villeval, J. L., Groseil, A., Vainchenker, W., Sainteny, F., and Bennaceur-Griscelli, A. (2004). Membrane-bound delta-4 notch ligand reduces the proliferative activity of primitive human hematopoietic CD34+CD38low cells while maintaining their LTC-IC potential. Leukemia *18*, 788-797.

Leary, A. G., Strauss, L. C., Civin, C. I., and Ogawa, M. (1985). Disparate differentiation in hemopoietic colonies derived from human paired progenitors. Blood *66*, 327-332.

Martinez Arias, A., Zecchini, V., and Brennan, K. (2002). CSL-independent Notch signalling: a checkpoint in cell fate decisions during development? Curr Opin Genet Dev *12*, 524-533.

Mayani, H., Dragowska, W., and Lansdorp, P. M. (1993). Lineage commitment in human hemopoiesis involves asymmetric cell division of multipotent progenitors and does not appear to be influenced by cytokines. J Cell Physiol *157*, 579-586.

Mikkola, H. K., Gekas, C., Orkin, S. H., and Dieterlen-Lievre, F. (2005). Placenta as a site for hematopoietic stem cell development. Exp Hematol *33*, 1048-1054.

Milner, L. A., and Bigas, A. (1999). Notch as a mediator of cell fate determination in hematopoiesis: evidence and speculation. Blood *93*, 2431-2448.

Milner, L. A., Kopan, R., Martin, D. I., and Bernstein, I. D. (1994). A human homologue of the Drosophila developmental gene, Notch, is expressed in CD34+ hematopoietic precursors. Blood *83*, 2057-2062.

Moore, K. A., Ema, H., and Lemischka, I. R. (1997). In vitro maintenance of highly purified, transplantable hematopoietic stem cells. Blood *89*, 4337-4347.

Nervi, B., Link, D. C., and DiPersio, J. F. (2006). Cytokines and hematopoietic stem cell mobilization. J Cell Biochem *99*, 690-705.

Nolta, J. A., Thiemann, F. T., Arakawa-Hoyt, J., Dao, M. A., Barsky, L. W., Moore, K. A., Lemischka, I. R., and Crooks, G. M. (2002). The AFT024 stromal cell line supports long-term ex vivo maintenance of engrafting multipotent human hematopoietic progenitors. Leukemia *16*, 352-361.

Ohishi, K., Varnum-Finney, B., and Bernstein, I. D. (2002). Delta-1 enhances marrow and thymus repopulating ability of human CD34(+)CD38(-) cord blood cells. J Clin Invest *110*, 1165-1174.

Ohishi, K., Varnum-Finney, B., Flowers, D., Anasetti, C., Myerson, D., and Bernstein, I. D. (2000). Monocytes express high amounts of Notch and undergo cytokine specific apoptosis following interaction with the Notch ligand, Delta-1. Blood *95*, 2847-2854.

Petzer, A. L., Hogge, D. E., Landsdorp, P. M., Reid, D. S., and Eaves, C. J. (1996). Self-renewal of primitive human hematopoietic cells (long-term-culture-initiating cells) in vitro and their expansion in defined medium. Proc Natl Acad Sci U S A *93*, 1470-1474.

Portin, P. (2002). General outlines of the molecular genetics of the Notch signalling pathway in Drosophila melanogaster: a review. Hereditas *136*, 89-96.

Punzel, M., Moore, K. A., Lemischka, I. R., and Verfaillie, C. M. (1999a). The type of stromal feeder used in limiting dilution assays influences frequency and maintenance assessment of human long-term culture initiating cells. Leukemia *13*, 92-97.

Punzel, M., Wissink, S. D., Miller, J. S., Moore, K. A., Lemischka, I. R., and Verfaillie, C. M. (1999b). The myeloid-lymphoid initiating cell (ML-IC) assay assesses the fate of multipotent human progenitors in vitro. Blood *93*, 3750-3756.

Punzel, M., Zhang, T., Liu, D., Eckstein, V., and Ho, A. D. (2002). Functional analysis of initial cell divisions defines the subsequent fate of individual human CD34(+)CD38(-) cells. Exp Hematol *30*, 464-472.

Reya, T., Morrison, S. J., Clarke, M. F., and Weissman, I. L. (2001). Stem cells, cancer, and cancer stem cells. Nature *414*, 105-111.

Romani, S., Campuzano, S., and Modolell, J. (1987). The achaete-scute complex is expressed in neurogenic regions of Drosophila embryos. Embo J *6*, 2085-2092.

Schneider, E. M., Torlakovic, E., Stuhler, A., Diehl, V., Tesch, H., and Giebel, B. (2004). The early transcription factor GATA-2 is expressed in classical Hodgkin's lymphoma. J Pathol *204*, 538-545.

Schofield, R. (1978). The relationship between the spleen colony-forming cell and the haemopoietic stem cell. Blood Cells *4*, 7-25.

Shih, C. C., Hu, M. C., Hu, J., Medeiros, J., and Forman, S. J. (1999). Long-term ex vivo maintenance and expansion of transplantable human hematopoietic stem cells. Blood *94*, 1623-1636.

Shimizu, Y., Ogawa, M., Kobayashi, M., Almeida-Porada, G., and Zanjani, E. D. (1998). Engraftment of cultured human hematopoietic cells in sheep. Blood *91*, 3688-3692.

Skeath, J. B., and Carroll, S. B. (1992). Regulation of proneural gene expression and cell fate during neuroblast segregation in the Drosophila embryo. Development *114*, 939-946.

Stier, S., Cheng, T., Dombkowski, D., Carlesso, N., and Scadden, D. T. (2002). Notch1 activation increases hematopoietic stem cell self-renewal in vivo and favors lymphoid over myeloid lineage outcome. Blood *99*, 2369-2378.

Suda, J., Suda, T., and Ogawa, M. (1984a). Analysis of differentiation of mouse hemopoietic stem cells in culture by sequential replating of paired progenitors. Blood *64*, 393-399.

Suda, T., Suda, J., and Ogawa, M. (1984b). Disparate differentiation in mouse hemopoietic colonies derived from paired progenitors. Proc Natl Acad Sci U S A *81*, 2520-2524.

Suzuki, T., and Chiba, S. (2005). Notch signaling in hematopoietic stem cells. Int J Hematol *82*, 285-294.

Suzuki, T., Yokoyama, Y., Kumano, K., Takanashi, M., Kozuma, S., Takato, T., Nakahata, T., Nishikawa, M., Sakano, S., Kurokawa, M.*, et al.* (2006). Highly efficient ex vivo expansion of human hematopoietic stem cells using Delta1-Fc chimeric protein. Stem Cells *24*, 2456-2465.

Taupin, P., and Gage, F. H. (2002). Adult neurogenesis and neural stem cells of the central nervous system in mammals. J Neurosci Res *69*, 745-749.

Varnum-Finney, B., Wu, L., Yu, M., Brashem-Stein, C., Staats, S., Flowers, D., Griffin, J. D., and Bernstein, I. D. (2000). Immobilization of Notch ligand, Delta-1, is required for induction of notch signaling. J Cell Sci *113 Pt 23*, 4313-4318.

von Levetzow, G., Spanholtz, J., Beckmann, J., Fischer, J., Kogler, G., Wernet, P., Punzel, M., and Giebel, B. (2006). Nucleofection, an efficient nonviral method to transfer genes into human hematopoietic stem and progenitor cells. Stem Cells Dev *15*, 278-285.

Wagers, A. J., and Conboy, I. M. (2005). Cellular and molecular signatures of muscle regeneration: current concepts and controversies in adult myogenesis. Cell *122*, 659-667.

Watts, J. L., Etemad-Moghadam, B., Guo, S., Boyd, L., Draper, B. W., Mello, C. C., Priess, J. R., and Kemphues, K. J. (1996). par-6, a gene involved in the establishment of asymmetry in early C. elegans embryos, mediates the asymmetric localization of PAR-3. Development *122*, 3133-3140.

Wodarz, A., and Huttner, W. B. (2003). Asymmetric cell division during neurogenesis in Drosophila and vertebrates. Mech Dev *120*, 1297-1309.

Zanjani, E. D., Almeida-Porada, G., Livingston, A. G., Flake, A. W., and Ogawa, M. (1998). Human bone marrow CD34- cells engraft in vivo and undergo multilineage expression that includes giving rise to CD34+ cells. Exp Hematol *26*, 353-360.

Zanjani, E. D., Pallavicini, M. G., Ascensao, J. L., Flake, A. W., Langlois, R. G., Reitsma, M., MacKintosh, F. R., Stutes, D., Harrison, M. R., and Tavassoli, M. (1992). Engraftment and long-term expression of human fetal hemopoietic stem cells in sheep following transplantation in utero. J Clin Invest *89*, 1178-1188.

Zhang, J., Niu, C., Ye, L., Huang, H., He, X., Tong, W. G., Ross, J., Haug, J., Johnson, T., Feng, J. Q.*, et al.* (2003). Identification of the haematopoietic stem cell niche and control of the niche size. Nature *425*, 836-841.

5 Danksagung

Diese Arbeit wurde im Wesentlichen am Institut für Transplantationsdiagnostik und Zelltherapeutika durchgeführt, das bis zum Ende 2006 unter Leitung von Herrn Prof. Peter Wernet stand. Ihm möchte ich für die gewährten Freiheiten danken, die uns eine weitgehend unabhängige und selbständige Forschung ermöglicht haben. Dankbar erwähnen möchte ich meinen leider viel zu früh verstorbenen Doktor Vater Herrn Prof. José Antonio Campos-Ortega, der mich wissenschaftlich stark geprägt hat und mir nach meiner Promotion die Gelegenheit gab, selbständig in seinem Institut als Postdoc zu arbeiten. Auch Herrn Prof. Hans Tesch, der mir als *Fliegenforscher* einen Quereinstieg in die Biologie des Morbus Hodgkin und somit in die Hämatologie ermöglichte, bin ich zu Dank verpflichtet.

Bei Dr. Johannes Fischer und Prof. Gesine Kögler möchte ich mich nicht nur für die Unterstützung mit Materialien bedanken, sondern ebenso wie bei Herrn P.D. Markus Uhrberg für die vielen Diskussionen, die zum Gelingen unserer Arbeiten beigetragen haben. Besonders Dankbar bin ich Herrn Fischer als auch Herrn P.D. Rüdiger Sorg, dass sie mich in die Welt der Durchflusszytometrie eingeweiht haben, die Grundvoraussetzung für die meisten unserer Arbeiten darstellt. Herrn Dr. Jürgen Enczmann und Herrn Dr. Andreas Knipper bin ich für die anfängliche Unterstützung in molekularbiologischen Techniken ebenso dankbar wie Frau Gabi Tillmann. Danke auch an die vielen netten und hilfsbereiten Kollegen, die hier nicht gesondert erwähnt werden.

Einen wichtigen Anschub in Sachen Zellkulturtechniken gab uns Herr P.D. Michael Punzel, ohne den wir sicherlich nicht soweit gekommen wären, und der uns dankenswerterweise als Diskussionspartner stets zur Seite steht.

Dankbar bin ich Herrn Ingmar Bruns und Herrn Prof. Rainer Haas, dass sie uns die maligne Hämatopoiese näher gebracht haben, und uns so neue wissenschaftliche Horizonte eröffneten. Weiterhin bedanke ich mich bei Herrn Prof. Haas, für die Mentorenschaft dieser Arbeit.

Als Eckpfeiler meines bzw. unseres wissenschaftlichen Erfolges stehen natürlich meine jetzigen und ehemaligen Mitarbeiter, vorneweg Frau Julia Beckmann, die auch in schweren Stunden immer Alles gegeben hat, was noch so grade ging. Danke!!!

Danke auch an Johannes Höhn, Jan Spanholtz, Svenja Jünger, Sebastian Scheitza, Ron(ny)-Patrick Cadeddu, Simon Magin, Andre Görgens, Gregor von Levetzow und Liska Horsch.

Dankbar bin ich natürlich auch unseren diversen Kollaborationspartnern, von denen ich stellvertretend Prof. Andreas Wodarz nennen möchte, mit dem ich schon als Fliegenzüchter freundschaftlich zusammengearbeitet habe. Aus dem Freundeskreis hatte Herr Dr. Thomas Menne, ebenfalls ein Ex-Fliegenzüchter, stets ein offenes Ohr und einen Rat, um bei einem Glas Limo auch die unerfreulichen Dinge im Wissenschaftlerleben wieder ins Gerade zu rücken.

Natürlich gilt mein ganz besonderer Danke meiner Familie, sprich meinen Eltern und meiner Partnerin Svetlana Schuster, die mich stets bestens unterstützt haben.

Auch wenn Du erst kurz vor Erstellung dieser Habilitationsschrift in mein Leben getreten bist und Du noch keinen wesentlichen Beitrag zu den zugrunde liegenden Arbeit leisten konntest, möchte ich auch Dir Ian, mein Sohn, danken.

6 Anlagen

Sonderdrucke der folgenden Arbeiten:

Giebel, B., Zhang, T., Beckmann, J., Spanholtz, J., Wernet, P., Ho, A. D., and Punzel, M. (2006). Primitive human hematopoietic cells give rise to differentially specified daughter cells upon their initial cell division. Blood 107, 2146-2152.

Giebel, B. (1999). The Notch signaling pathway is required to specify muscle progenitor cells in Drosophila. Mech. Dev. 86, 137-145.

Giebel, B., Corbeil, D., Beckmann, J., Hohn, J., Freund, D., Giesen, K., Fischer, J., Kogler, G., and Wernet, P. (2004). Segregation of lipid raft markers including CD133 in polarized human hematopoietic stem and progenitor cells. Blood 104, 2332-2338.

Beckmann, J., Scheitza, S., Wernet, P., Fischer, J. C., and **Giebel, B.** (2007). Asymmetric cell division within the human hematopoietic stem and progenitor cell compartment: identification of asymmetrically segregating proteins. Blood 109, 5494-5501.

Levetzow, G. V., Spanholtz, J., Beckmann, J., Fischer, J., Kogler, G., Wernet, P., Punzel, M., and **Giebel, B.** (2006). Nucleofection, an efficient nonviral method to transfer genes into human hematopoietic stem and progenitor cells. Stem Cells Dev 15, 278-285.

Schneider, E. M., Torlakovic, E., Stuhler, A., Diehl, V., Tesch, H., and **Giebel, B.** (2004). The early transcription factor GATA-2 is expressed in classical Hodgkin's lymphoma. J Pathol 204, 538-545.

Bracker, T. U., **Giebel, B.**, Spanholtz, J., Sorg, U. R., Klein-Hitpass, L., Moritz, T., and Thomale, J. (2006). Stringent regulation of DNA repair during human hematopoietic differentiation: a gene expression and functional analysis. Stem Cells 24, 722-730.

Feldhahn, N., Henke, N., Melchior, K., Duy, C., Soh, B.N., Klein, F., von Levetzow, G., **Giebel, B.**, Li, A., Hofmann, W.K., Jumaa, H., and Müschen, M. (2007). Activation-induced cytidine deaminase acts as a mutator in BCR-ABL1-transformed acute lymphoblastic leukemia cells. J Exp Med 204, 1157-1166.

Primitive human hematopoietic cells give rise to differentially specified daughter cells upon their initial cell division

Bernd Giebel, Tao Zhang, Julia Beckmann, Jan Spanholtz, Peter Wernet, Anthony D. Ho, and Michael Punzel

It is often predicted that stem cells divide asymmetrically, creating a daughter cell that maintains the stem-cell capacity, and 1 daughter cell committed to differentiation. While asymmetric stem-cell divisions have been proven to occur in model organisms (eg, in *Drosophila*), it remains illusive whether primitive hematopoietic cells in mammals actually can divide asymmetrically. In our experiments we have challenged this question and analyzed the developmental capacity of separated offspring of primitive human hematopoietic cells at a single-cell level. We show for the first time that the vast majority of the most primitive, in vitro–detectable human hematopoietic cells give rise to daughter cells adopting different cell fates; 1 inheriting the developmental capacity of the mother cell, and 1 becoming more specified. In contrast, approximately half of the committed progenitor cells studied gave rise to daughter cells, both of which adopted the cell fate of their mother. Although our data are compatible with the model of asymmetric cell division, other mechanisms of cell fate specification are discussed. In addition, we describe a novel human hematopoietic progenitor cell that has the capacity to form natural killer (NK) cells as well as macrophages, but not cells of other myeloid lineages. (Blood. 2006;107: 2146-2152)

Introduction

Somatic stem cells are defined as undifferentiated cells, which can self-renew over a long period of time and give rise to progenitor cells that are committed to differentiation upon their further development. Since both an uncontrolled expansion as well as loss of stem cells would be fatal for multicellular organisms, the decision of self-renewal versus differentiation needs to be tightly controlled. Therefore, a key question in stem-cell biology is how and which mechanisms govern this decision.

Hematopoietic stem cells (HSCs) are the most investigated mammalian stem cells. More than 30 years of clinical experience as well as experiments with animals demonstrated that neonatal and adult HSCs retain the ability to reconstitute the hematopoietic systems of patients after myeloablative treatment.[1] Therefore, an important feature of HSCs is the capacity to replenish all lineages of mature blood cells. Beside this, they also have the potential to expand in vivo as revealed by sequential transplantation experiments using limiting numbers of mouse HSCs to reconstitute the hematopoietic systems of primary and secondary lethally irradiated hosts.[2,3] However, although HSCs can be maintained in vitro in close contact to adequate stroma cells,[4-8] no evaluated in vitro condition has been reported so far, which supports the expansion of these cells over a period of several weeks. These findings demonstrate that the surrounding environment has a major influence on the cell fate of HSCs and their daughter cells. In this context, it was recently shown that by participating in the formation of special HSC-supporting niches, osteoblasts regulate the size of the HSC pool in vivo.[9-11]

In addition to data supporting a hematopoietic stem-cell niche model, results of further studies suggest that cells of the hematopoietic stem- and progenitor-cell compartments are able to divide asymmetrically. In an initial set of experiments Ogawa's group analyzed the differentiation of murine and human hematopoietic progenitor cells (HPCs). After separation of paired-progenitor cells they cultured these cells individually and observed that in some cases siblings gave rise to colonies that significantly differed from each other (ie, they gave rise to different cell lineages and/or to colonies of different sizes).[12-14] Recently, some evidence for the occurrence of asymmetric cell division of mouse HSCs was provided in a transplantation model.[15,16]

In studies using human HSC-enriched cells of the $CD34^+CD38^-$ fraction we and others have shown that $CD34^+CD38^-$ cells are heterogeneous in respect to their function and their proliferation kinetics (ie, the proliferation rate of more primitive cells is lower than that of committed ones).[17-19] Furthermore, it was observed that approximately 30% of the $CD34^+CD38^-$ cells gave rise to daughter cells with heterogeneous proliferation kinetics, perhaps the result of an asymmetric cell division.[17,19,20]

To increase the evidence for the occurrence of asymmetric cell divisions within the most primitive in vitro–detectable hematopoietic cell compartment we have separated the progenies of HSC candidates by micromanipulation and analyzed their developmental potential in primitive human progenitor assays.

From the Institute for Transplantation Diagnostics and Cellular Therapeutics, Heinrich-Heine-University Düsseldorf, Germany; Department of Medicine V, Ruprecht-Karls University of Heidelberg, Germany; and Cancer Center Union Hospital, Huazhong University of Science and Technology Wuhan, People's Republic of China.

Submitted August 5, 2005; accepted October 15, 2005. Prepublished online as *Blood* First Edition Paper, October 25, 2005; DOI 10.1182/blood-2005-08-3139.

Supported by grants from the Deutsche Forschungsgemeinschaft (SPP1109 GI 336/1-2 to B.G. and P.W.; HO 914/2-1 to A.D.H.), from the Forschungskommission of the HHU-Düsseldorf (B.G., M.P.), and from the Faculty Research Program of the University of Heidelberg (F203532 to M.P.).

B.G. and T.Z. contributed equally to this work.

Reprints: Michael Punzel or Bernd Giebel, Institute for Transplantation Diagnostics and Cell Therapeutics, Heinrich-Heine-University Düsseldorf, D-40225 Düsseldorf, Germany; e-mail: punzel@itz.uni-duesseldorf.de or giebel@itz.uni-duesseldorf.de.

The publication costs of this article were defrayed in part by page charge payment. Therefore, and solely to indicate this fact, this article is hereby marked "advertisement" in accordance with 18 U.S.C. section 1734.

Materials and methods

Cell source and preparation

Human umbilical cord blood (CB) was obtained from the umbilical vein after delivery of the placenta from mothers after informed consent according to the Declaration of Helsinki. Approval for CB was obtained from the Paul-Ehrlich Institute. Mononuclear cells were isolated from individual sources by Ficoll (Biocoll Separating Solution; Biochrom AG, Berlin, Germany) density gradient centrifugation. $CD34^+$ cells were isolated by magnetic cell separation using the MidiMacs technique according to the manufacturer's instructions (Miltenyi Biotec, Bergisch Gladbach, Germany).

Immunofluorescence

For the proliferation kinetics, freshly isolated $CD34^+$ cells were stained with PKH2 (Sigma-Aldrich Chemie, Taufkirchen, Germany) as described previously.[19] Before the cells were analyzed by flow cytometry they were stained with AC133-phycoerythrin (PE; Miltenyi Biotec) and anti-CD34–PE/Cytochrome 5 (PCy5) antibodies (BD PharMingen, Heidelberg, Germany). Flow cytometric analyses were performed on a Cytomics FC 500 flow cytometer equipped with the RXP software (Beckman Coulter, Krefeld, Germany).

For functional analysis $CD34^+$-enriched cells were stained with anti-CD34–PE (BD PharMingen) and anti-CD38–allophycocyanin (APC; BD PharMingen) antibodies. Individual $CD34^+CD38^-$ cells were sorted into 96-well plates (NUNC, Roskilde, Denmark) using the Automated Cell Deposition Unit (ACDU) on a FACSvantage-SE flow cytometry system (BD Immunosystems, Heidelberg, Germany) equipped with an Apple G3 Power computer (Palo Alto, CA). To ensure that only a single cell was deposited, the ACDU was set up in a low-event "through-put" (200-500 events/second).

Cell culture (bulk proliferation assays)

Freshly enriched and PKH2-stained $CD34^+$ cells were cultured in a humidified atmosphere at 37°C and 5% CO_2 at a density of approximately 1×10^5 cells/mL in serum containing tissue-culture medium (Myelocult H5100; Stemcell Technologies, Vancouver, BC, Canada) supplemented with 1000 U/mL penicillin and 100 U/mL streptomycin (Invitrogen, Karlsruhe, Germany) in the presence of early-acting (recombinant human fetal liver tyrosine kinase 3 ligand [rhFLT3L], recombinant human stem-cell factor [rhSCF], and recombinant human thrombopoietin [rhTPO], each at 10 ng/mL final concentration; PeproTech, Rocky Hill, NJ) or late-acting cytokines (10 ng/mL recombinant human interleukin-3 [rhIL-3], 500 U/mL rhIL-6, 10 ng/mL recombinant human granulocyte-macrophage colony-stimulating factor [rhGM-CSF], 2.5 ng/mL recombinant human basic fibroblast growth factor [rh-bFGF],10 ng/mL recombinant human insulin-like growth factor-1 [rhILGF; all Cell Systems, St Katharinen, Germany], 2.5 U/mL recombinant human erythropoietin [rhEpo; Roche Diagnostics, Mannheim, Germany], and 50 ng/mL rhSCF [R&D Systems, Minneapolis, MN]), respectively.

Functional assays (single-cell experiments)

Individual sorted $CD34^+CD38^-$ cells were cultured for 10 days in Myelocult (Cell Systems) supplemented with 10 ng/mL rhIL-3, 500 U/mL rhIL-6, 10 ng/mL rhGM-CSF, 2.5 ng/mL rhbFGF, 10 ng/mL rhILGF (all Cell Systems), 2.5 U/mL rhEpo (Roche), 50 ng/mL rhSCF (R&D Systems), 1000 U/mL penicillin, and 100 U/mL streptomycin (Invitrogen) as described before.[19]

Before cell deposition the 96-well plates (Nunc) were precoated with bovine serum albumin (BSA) as described previously,[19,21] and each well was subsequently filled with 150 μL culture medium as described. After single-cell deposition, cells were maintained in a humidified atmosphere at 37°C and 5% CO_2 and fed every 48 hours with fresh medium. The proliferation of each cell was determined by light microscopy every 12 to 24 hours.

Immediately after single cells divided, the corresponding daughter cells were separated using a customized micromanipulation-system (Nikon-Germany, Düsseldorf, Germany) and individually transferred into the myeloid-lymphoid–initiating cell (ML-IC) assay.

ML-IC assay

This readout assay was described extensively in our previous reports.[19,21] Briefly, separated daughter cells were individually deposited into 96-well plates (Nunc) containing a confluent, irradiated AFT024 feeder-cell layer. After 2 weeks of culture in a humidified atmosphere at 37°C and 5% CO_2 in RPMI-medium containing 20% fetal bovine serum supplemented with 10 ng/mL rhFLT3L, 10 ng/mL rhSCF, 10 ng rhIL-7, and 10 ng/mL rhTPO (all Cell Systems), the content of each well was harvested by trypsination and split into 4 equal fractions. As described before, 2 fractions were transferred into duplicates of the lymphoid natural killer initiating cell (NK-IC) readout assay;[21,22] the other 2 fractions were transferred into duplicates of the myeloid LTC-IC assay.[19,21]

Culture conditions in readout assays

Lymphoid differentiation readout (NK-IC assay). Transferred cells were cocultured with the murine cell line AFT024 in Dulbecco modified Eagle medium (DMEM) and Ham F12-medium (Invitrogen) mixed in a 2:1 (vol/vol) relation containing 20% heat-inactivated human AB serum (Cambrex, Taufkirchen, Germany), ascorbic acid (20 mg/mL; Invitrogen), selenium selenite (50 μM; Invitrogen), 2-mercaptoethanol (25 μM), and ethanolamine (50 μM; Invitrogen). The following cytokines were added to these cultures: rhIL-2 (1000 U/mL), rhIL-3 (5 ng/mL), rhIL-7 (20 ng/mL), rhSCF (10 ng/mL), and rhFlt3L (10 ng/mL). At weekly intervals half-media exchanges were performed using 10% instead of 20% human AB serum. Starting at week 2, the only cytokine added to the cultures was rhIL-2. After 5 to 7 weeks of culture, wells containing viable cells were harvested and cells were analyzed flow cytometrically using antibodies recognizing the NK cell–specific antigens CD16 and CD56 as well as CD3.

Confirming previous studies from our group and others the cells arising in the NK-IC assay express the NK cell–specific antigens CD16 and CD56 and are negative for the T-cell marker CD3. As such cells are able to kill cells of the commonly used NK cell target cell line K562, they are considered as functional NK cells.[19,21-24] In agreement with this assumption, we found in our ongoing experiments that the arising cells express additional NK cell–specific antigens like NKp30/NKp44/NKp46 and NKG2A/CD94 as well as different killer immunoglobulin-like receptor (KIR) transcripts (M.P. and M. Uhrberg, manuscript in preparation).

Myeloid differentiation readout (LTC-IC assay). Transferred cells were cocultured with the murine cell line AFT024 in Iscove modified Dulbecco medium (IMDM; Invitrogen) supplemented with 12.5% fetal calf serum (FCS), 12.5% horse serum (Cell Systems), 2 mM L-glutamine (Invitrogen), 1000 U/mL penicillin, 100 U/mL streptomycin (Invitrogen), and 10^{-6} M hydrocortisone. Cultures were maintained for 5 weeks in a humidified atmosphere at 37°C and 5% CO_2 and fed once a week. At week 5 all wells were overlaid with clonogenic methylcellulose medium (Methylcellulose [Fluka, Buchs, Switzerland] in a final concentration of 1.12% containing IMDM and supplemented with 30% FCS, 3 U/mL erythropoietin [Cell Systems], and supernatant of the bladder carcinoma cell line 5637 [10%]). Wells were scored for the occurrence of secondary colony-forming cells (CFCs) after an additional 2 weeks. As the initially deposited cells and their offspring were cultured for more than 8 weeks before reading out the secondary colony-forming cells as LTC-ICs, our myeloid readout reflects more primitive myeloid progenitors than those detected in conventional LTC-IC assays.

Statistics

Experimental results from different experiments were reported as mean ± standard deviation of the mean (SD). Significance analyses were performed with the paired Student *t* test.

Results

Experimental design

We and others have demonstrated that primitive human hematopoietic cells give rise to daughter cells following different proliferation kinetics.[17,19,20] However, the cell fate of primitive hematopoietic cell siblings has not been analyzed at the single-cell level until now. Therefore, we decided to determine the developmental capacity of arising daughter cells individually. Because it is challenging to identify a single human primitive hematopoietic cell and subsequently separate its offspring, we compared the effect of 2 different culture conditions on the proliferation kinetics of primitive hematopoietic cells in bulk experiments first. For these analyses we assessed effects of 2 distinct cytokine cocktails, which we have successfully applied in our previous analysis,[19,24] 1 cocktail containing late-acting cytokines (LACs), and the other consisting of early-acting cytokines (EAC; ie, SCF, FLT3L, and TPO). The latter cocktail has been shown to be particularly effective in maintaining and slightly expanding human HSCs in suspension cultures up to 7 days.[25-27] In order to compare the data presented here with our former results we performed our experiments in Dexter-type cultures.

Proliferation kinetics of primitive hematopoietic cells under different cytokine conditions

Isolated $CD34^+$ cells (89.9% ± 5.9% purity; n = 3) were labeled with the fluorescent dye PKH2 and cultured up to a week in serum containing media supplemented either with EACs or LACs. Starting at day 3 cultured cells from individual aliquots were harvested every other day and simultaneously counterstained with antibodies recognizing the human stem-cell surrogate markers CD34 and CD133.[28,29]

By analyzing the influence of the culture conditions on $CD34^+$ cells we observed that under both conditions cells increase in size and granularity (Figure 1A). Cells cultured in the presence of LACs expand more (45.2-fold ± 17.7-fold at day 5 compared with day 0; n = 3) than in the presence of EACs (14.7-fold ± 5.6-fold at day 5 compared with day 0; n = 3). Under both conditions most cells remain $CD34^+$ until day 5 (Figure 1B) (LACs, 61.4% ± 20.2%; n = 3; EACs, 85.5% ± 10.4%; n = 3), while the percentage of $CD133^+$ cells decreases over time (Figure 1B) (LACs, 14.6% ± 6.7%; n = 3; EACs, 33.0% ± 5.2%; n = 3 at day 5). However, the absolute numbers of $CD133^+$ cells increase under both conditions (LACs, 8.6-fold ± 1.0-fold; n = 3; EACs, 5.4-fold ± 1.0-fold at day 5 compared with day 0; n = 3).

In addition, we show that under both conditions the average of the newly detected $CD34^+CD133^-$ cells is less positive for PKH2 than $CD34^+CD133^+$ cells, suggesting that most arising $CD34^+CD133^-$ cells have had a higher proliferation rate than the $CD34^+CD133^+$ cells (Figure 1C). Regarding their PKH2 staining, the LAC-stimulated $CD34^+CD133^+$ cell fraction is more heterogeneous than the corresponding EAC-stimulated fraction (Figure 1C), suggesting that EACs stimulate proliferation of $CD34^+CD133^+$ cells more homogeneously than LAC conditions. Within the LAC-stimulated fraction we observed more remaining PKH^{bright} $CD34^+CD133^+$ cells than in the EAC-stimulated fraction (at day 5: LACs, 47.7% ± 24.1%; EACs, 39.4% ± 28.3% of the initially cultured PKH^{bright} $CD34^+CD133^+$ cells, n = 3, $P = .05$; Figure 1C). Remarkably, the PKH^{bright} fraction of LAC-stimulated cells contain less $CD133^-$ cells than the EAC-stimulated fraction, resulting in a sharp contrast of PKH^{bright} $CD34^+CD133^+$ versus PKH^+ $CD34^+CD133^-$ cells within the LAC-stimulated fraction (Figure 1C).

According to our previous results primitive hematopoietic cells cultured under LAC conditions get highly enriched in the PKH^{bright} or the so-called slow dividing fraction.[19,24] This is most likely due

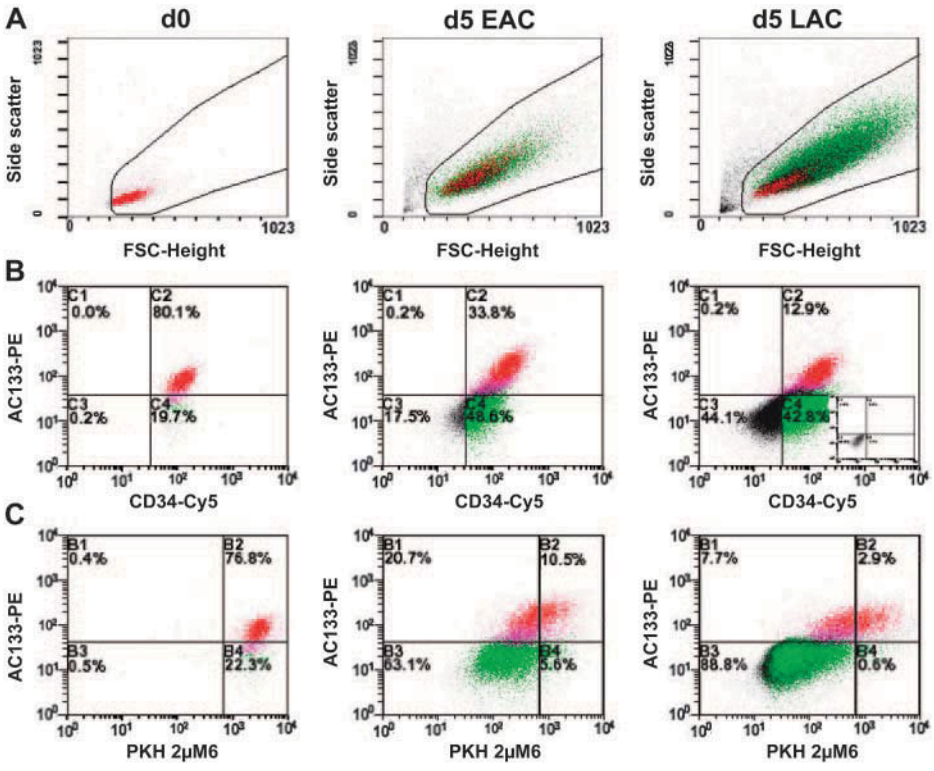

Figure 1. Flow cytometric analysis of bulk experiments. Since the amount of cells depicted in the plots is normalized to the cell number initially used, plots can be compared semiquantitatively. Cells analyzed in panels B and C were gated according to the morphology depicted on the forward scatter/side scatter plots shown in panel A. Plots in panel B represent the distribution of CD34 and CD133 antigens in freshly isolated or in expanded $CD34^+$ cells, respectively. A characteristic isotype control of expanded cells is shown as inlet in the right panels. To identify the individual subpopulations in panels A or C, $CD34^+CD133^+$ cells are labeled in red, $CD34^+CD133^-$ cells in green, and $CD34^-CD133^-$ cells in black. The PKH2 staining, representing the number of cell divisions single cells have performed, is plotted against the CD133 antigen distribution in panel C. $PKH2^{bright}$ cells are plotted within the right quadrants of the diagrams shown in panel C. See "Results" for more details.

to the fact that the most primitive hematopoietic cells do not immediately respond to LACs and therefore remain quiescent for the first few days under LAC conditions. Since the vast majority of the $CD34^+$ cells get activated under EAC conditions and show similar cell division kinetics, the LAC conditions provide an opportunity to discriminate between primitive and more mature $CD34^+$ cells according to just the way they initiate their cell division. Therefore, we concluded that LAC conditions were more suitable for our intended single-cell studies on primitive hematopoietic cells than EAC conditions.

Our conclusion was additionally supported by the finding that the percentage of the stem-cell surrogate marker CD133 within the slow dividing fraction (PKH^{bright} cells) was significantly higher under LAC than under EAC conditions (at day 5: LAC, 61.1% ± 3.1%; EAC, 50.3% ± 3.9%; n = 3, $P = .005$).

Proliferation of individual primitive human hematopoietic cells

Due to the fact that freshly isolated $CD34^+$ cells express similar amounts of CD133 (Figure 1B) and with the necessity to enrich the most primitive hematopoietic cells as much as possible, we decided to perform our single-cell analyses with $CD34^+CD38^-$ cells.

In 4 independent experiments we sorted a total of 176 single $CD34^+CD38^-$ cells per experiment into individual wells of 96-well plates. To determine the deposition frequency we analyzed each well 12 hours after finishing the sorting procedure by bright-field microscopy. We recovered a total of 556 single deposited cells, which corresponds to a deposition frequency of 79.0% ± 4.0%.

In previous experiments under LAC conditions, the most primitive hematopoietic cells remained quiescent for up to 5 days and underwent their first in vitro cell division between day 5 and day 10 after deposition.[19] Therefore, we tracked the division process of each single cell within the first 10 days and grouped them into 3 different categories as shown in Table 1: (1) category I indicates cells that divided before day 5 (59% ± 12%); (2) category II, cells that performed their first cell division between day 5 and day 10 (31% ± 11%); and (3) category III, cells which did not perform any cell division within the first 10 days of culture (10% ± 4%).

Analyses of the developmental potential of individually separated daughter cells

According to our focus on the most primitive human hematopoietic cells we only included cells from category II for the micromanipulation-based daughter cell analyses. Within 24 hours after performing their initial cell division, emerging daughter cells of category II cells were separated by micromanipulation and individually transferred into expansion cultures containing the murine fetal liver–derived stromal cell line AFT024.[21] As shown in Figure 2, the expansion cultures were harvested after 2 weeks and split into 4 separate aliquots, which were transferred into secondary readout systems: 2 into primitive myeloid assays (LTC-IC) and 2 into primitive lymphoid assays (NK-IC). This enabled us to determine whether initially deposited cells gave rise to primitive progeny in any of the functional assays.

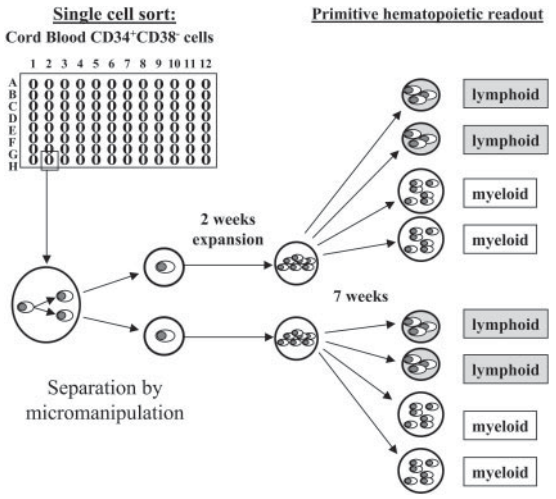

Figure 2. Experimental setup. Individual $CD34^+CD38^-$ cells were deposited by fluorescent cell sorting into 96-well plates (1 cell/well), and observed at half-daily intervals. Initially deposited cells that performed their initial cell division between culture days 5 and 10 (category II) were considered for further analyses. Shortly after the first cell division, the arising daughter cells were separated by micromanipulation and individually transferred into secondary plates containing irradiated AFT024 cells as a stromal feeder. After 2 weeks of expansion the entire progeny of each individual daughter cell was split into 4 aliquots and transferred in equal amounts (in duplicates) into primitive myeloid (LTC-IC) or primitive lymphoid (NK-IC) readout assays, respectively. After an additional 7 weeks the assays were analyzed as described in "Materials and methods." Originally deposited cells as well as singularized daughter cells that had both LTC-IC as well as NK-IC capacity were retrospectively considered ML-ICs.[21]

As shown in Table 2 we formed 3 groups, discriminating initially deposited cells which gave rise to (1) 2 colony forming daughter cells (category IIa; 55 pairs of daughter cells); (2) those in which only 1 daughter cell formed colonies (category IIb; 21 pairs); and (3) the ones in which none of the daughter cells formed any colonies (category IIc; 101 pairs).

Category IIa and IIb cells, 76 cells in total, were further subgrouped regarding to the cell fate adopted by the individual daughter cells (Table 3). We used the following definitions: (1) initially plated cells that only gave rise to primitive myeloid hematopoiesis were defined as LTC-ICs; (2) those that gave rise only to NK cells were defined as NK-ICs; and (3) cells that were able to generate both LTC-ICs as well as NK-ICs were defined as ML-ICs, closely related to the most primitive human hematopoietic compartment.[21]

In several cases colonies were found in the LTC-IC assays that did not fulfill the well-defined morphologic criteria of secondary colony formation. Since they resembled a macrophage-like morphology without clonogenic proliferation we did not categorize them as

Table 1. Categorization of individual $CD34^+CD38^-$ cells according to the occurrence of their initial in vitro cell division under LAC-stimulated culture conditions

	Deposited cells	Category I: first division before day 5	Category II: first division days 5-10	Category III: first division after day 10
Experiment 1	130	93	26	11
Experiment 2	147	65	63	19
Experiment 3	139	78	54	7
Experiment 4	140	90	34	16
Total cell no. (mean % ± SEM)	556	326 (59.0 ± 11.7)	177 (31.5 ± 11.1)	53 (9.5 ± 3.5)

Values in table are total numbers of cells except where indicated.

Table 2. Categorization of individual CD34$^+$CD38$^-$ cells performing their initial in vitro cell division under LAC-stimulated culture conditions between days 5 and 10

	Investigated daughter cell pairs	Category IIa: 2 colony-initiating daughter cells	Category IIb: 1 colony-initiating daughter cell	Category IIc: No colony-initiating daughter cells
Experiment 1	26	3	1	22
Experiment 2	63	16	5	42
Experiment 3	54	13	7	34
Experiment 4	34	23	8	3
Total cell no. (mean % ± SEM)	177	55 (32.2 ± 24.5)	21 (12.1 ± 8.5)	101 (55.8 ± 32.7)

Values in table are total numbers of cells except where indicated.

LTC-ICs but as macrophage colony-forming units (CFUs-M). Remarkably, we found many cases in which individual cells had the NK-IC capacity and gave rise to CFU-M–forming progeny. To discriminate these cells from ML-ICs we called them macrophage/NK cell–initiating cells (M-NK-ICs).

In total, 15 of the original deposited cells had the ML-IC capacity; 2 of them transmitted the ML-IC fate to both daughter cells, and in the remaining cases only 1 of the daughter cells adopted both, the LTC-IC as well as the NK-IC capacity (Table 4). Remarkably, in 6 (40%) cases the non–ML-IC daughter cell gave rise to NK-ICs and formed macrophage-like colonies in the LTC-IC assay, demonstrating that viable offspring of the corresponding daughter cells were transferred into the latter assay. These results suggest that in these cases the first-generation ML-IC daughter cells contained different developmental capacities. Surprisingly, we never found the constellation in which 1 ML-IC daughter cell adopted the myeloid and the other 1 the lymphoid potential.

Only 3 of the 76 originally deposited cells were determined exclusively as LTC-ICs; 2 of them gave rise to daughter cells, both containing the LTC-IC potential (Table 4). Originally deposited cells of the newly defined M-NK-IC group transmitted this cell fate to both daughter cells in 46% of the cases studied, and to only 1 daughter cell in 54% (Table 4). In the latter cases the non–M-NK-IC daughter cell died or gave rise to macrophage-like cells in LTC-IC assays. We never found any daughter cell that had the NK-IC potential only. Seventeen of the originally deposited cells had NK-IC potential only, which was transmitted in 7 cases to both daughter cells; in the remaining 10 cases only 1 of the siblings gave rise to NK cells in our assays (Table 4). Most of the cells (13 of 17) that were retrospectively named CFUs-M transmitted this fate to both daughter cells; in the remaining cases, only 1 daughter cell gave rise to the macrophage-like cells.

In summary, most of the originally deposited cells, retrospectively determined as ML-ICs, gave rise to daughter cells with different cell fates. In contrast, siblings of more-committed mother cells seem to inherit a higher ratio of identical cell fates in our assays (Table 4).

Discussion

Here, we analyzed primitive human hematopoietic cells in bulk cultures and at a single-cell level, and report 3 major findings: (1) we realized that upon cultivation CD34$^+$ cells split up into a CD34$^+$CD133$^+$ and a CD34$^+$CD133$^-$ fraction; (2) using our newly established single-cell separation approach we determined the cell fate of primitive human hematopoietic cells and their first-generation daughter cells individually and present evidence for the existence of progenitor cells containing the capacity to form NK cells and macrophages, but which lack more primitive myeloid capacities (LTC-ICs); and (3) we demonstrate that the most primitive ML-ICs have a high tendency (87%) to transmit their cell fate to only 1 of the arising daughter cells. In contrast, the ratio of more-committed progenitor cells giving rise to progeny adopting identical cell fates to those adopting different cell fates is more balanced.

Although there is increasing evidence that special hematopoietic niches are required to maintain HSCs,[9-11] it is often suggested that hematopoietic stem cells can divide asymmetrically to form another HSC and a more-specified daughter cell.[30] The latter hypothesis is highly supported by the finding that immediate progeny of primitive hematopoietic progenitor cells often adopt different cell fates in myeloid readout systems.[12-14,16,18] However, as mentioned by Takano and colleagues, due to the lack of an appropriate assay, the lymphoid potential of separated cells was not analyzed in these studies.[16] In this study we used the ML-IC assay, a sensitive and efficient assay for the detection of both the myeloid and lymphoid potentials of individual cells,[19,21] and analyzed the myeloid and lymphoid potentials of progenies of primitive human hematopoietic cells at the single-cell level.

Supporting our previous data, we found that under LAC conditions approximately 30% of the deposited CD34$^+$CD38$^-$ cells performed their initial cell division between culture day 5 and 10.[19] We were able to determine retrospectively the cell fate of approximately 45% of the initially deposited cells that performed their first cell division between culture days 5 and 10. In 55% of the cases studied none of the separated daughter cells gave rise to any recognizable colony in our readout systems. Since similar frequencies were obtained in our previous and other studies, in which nonseparated CD34$^+$CD38$^-$ cells were analyzed in ML-IC assays,[19,31] we suggest that loss of cells during the micromanipulation procedure is more or less negligible. The efficiency of our micromanipulation procedure is additionally supported by the fact that we obtain similar ML-IC frequencies of nonseparated and separated CD34$^+$CD38$^-$ cells performing their first cell division under LAC conditions between culture days 5 and 10 (15 [8.5%] cells of 177) or after day 5 (10.3% ± 3.5%),[19] respectively.

In this context it should be mentioned that all but 1 initially deposited cell, which gave rise to only 1 colony-forming daughter cell, were retrospectively determined to be more mature cells (M-NK-ICs, NK-ICs, or CFUs-M), suggesting that the non–colony-forming daughter cell was more committed and terminally differentiated during the long-term culture period.

It is interesting to note that using the ML-IC assay we could identify a novel human progenitor cell that has not been described before. This progenitor, which we called M-NK-IC, has the capability to initiate NK cell development and also gives rise to macrophages but not to secondary clonogenic myeloid colonies in LTC-IC assays. Similar to our findings, murine fetal liver but not adult hematopoietic progenitors have been described as containing

Table 3. Cell fate classification of initially deposited colony-initiating CD34$^+$CD38$^-$ cells

	Category IIa and IIb cells	ML-ICs	LTC-ICs	M-NK-ICs	NK-ICs	CFUs-M
Experiment 1	4	1	0	1	2	0
Experiment 2	21	5	2	5	2	7
Experiment 3	20	4	0	5	8	3
Experiment 4	31	5	1	13	5	7
Total cell no. (mean % ± SEM)	76	15 (21.2 ± 4.0)	3 (3.2 ± 4.5)	24 (28.9 ± 8.7)	17 (28.9 ± 19.2)	17 (17.7 ± 14.0)

Values in table are total numbers of cells except where indicated.

lymphoid and macrophage potential in short-term murine readout systems.[32,33]

According to the prevailing model of hematopoiesis, primitive hematopoietic cells give rise to common myeloid and common lymphoid progenitor cells, which have the developmental capacity to form all myeloid or lymphoid lineages, respectively.[34] Because macrophages belong to the myeloid compartment, the discovery of progenitors containing the M-NK-IC capacity is not compatible with this model. In addition, the recent discovery of primitive hematopoietic cells in mice and humans which contain the lymphoid potential as well as the capacity to form granulocytes and macrophages but not cells of the erythromegakaryocytic lineage, is contrary to this model as well.[35-37] In this context, Adolfsson and colleagues offered a so-called composite model in which primitive hematopoietic cells sequentially lose the capacity to form cells of the megakaryocyte/erythroid and then of the granulocyte/macrophage potential during lymphoid commitment.[35] Our findings together with those of others[32,33,38] support this hypothesis and further suggest that next to the megakaryocyte/erythroid potential the granulocytic developmental capacity is lost during early lymphoid commitment, leaving cells containing the capacity to initiate lymphoid and macrophage development.

In previous studies it was found that siblings of primitive hematopoietic cells often adopt different proliferation kinetics, whereas more-committed progenitor cells give rise to daughter cells dividing in a more uniform fashion. Differences in the proliferation kinetics are often interpreted as a result of an asymmetric cell division.[17,19,20] The theory of asymmetric cell division is further supported by the finding that individual daughter cells of primitive hematopoietic cells frequently adopt different cell fates in myeloid progenitor assays.[12-14,16] However, until now there was no evidence that the most primitive hematopoietic cells containing the lymphoid as well as the myeloid developmental potential give rise to daughter cells adopting different cell fates. Therefore, we demonstrate here for the first time evidence that the most primitive, in vitro–detectable hematopoietic cells, the ML-ICs, give rise to daughter cells adopting different cell fates, which could be the result of an asymmetric cell division. In addition, we provide evidence that offspring of more-committed progenitors that seem to contain similar proliferation kinetics also give rise to cells adopting different cell fates in approximately 50% of the cases studied. These findings demonstrate that proliferation kinetics of arising daughter cells cannot be interpreted as indication for the occurrence of asymmetric cell divisions.

Table 4. Cell fate classification of separated offspring of initially deposited colony-initiating CD34$^+$CD38$^-$ cells

	DC no. 1				
DC no. 2	ML-ICs	LTC-ICs	M-NK-ICs	NK-ICs	CFUs-M
ML-ICs	2	—	—	—	—
LTC-ICs	3	2	—	—	—
M-NK-ICs	6	0	11	0	—
NK-ICs	1	1	0	7	—
CFUs-M	2	0	8	0	13
Dead	1	0	5	10	4
Identical cell fate, no. (%)	2 (13.3)	2 (66.7)	11 (45.8)	7 (41.2)	13 (76.5)
Different cell fate, no. (%)	13 (86.7)	1 (33.3)	13 (54.2)	10 (58.8)	4 (23.5)

The more primitive separated daughter cell is defined as DC no. 1, the other as DC no. 2. Values in table are total numbers of cells except where indicated.

— indicates not applicable.

Surprisingly, none of the deposited cells gave rise to siblings that both adopted only partial capacities of their mother cells. In all cases studied at least 1 of the arising daughter cells took over the developmental capacity of the mother cell, most likely resembling the predicted process of self-renewal. Committed progenitors have a high tendency to expand their cell fate, especially by forming 2 daughter cells containing the same developmental capacity. Cells of the most primitive compartment, the ML-ICs, have a very low tendency to transmit their cell fate to both of the arising daughter cells, which is consistent with the hypothesis that primitive hematopoietic cells have a high tendency to divide asymmetrically.[30]

However, can we really conclude from these data that there are asymmetric cell divisions within the primitive hematopoietic cell compartment? It depends how we define "asymmetric cell division." If we define it from the point of the adopted cell fate, our data would fulfill these criteria. If we define asymmetric cell division as it is used in model organisms such as *Drosophila* or *Caenorhabditis elegans,* in which an asymmetric cell division describes the process in which 2 qualitatively different cells are formed by the different distribution of certain factors which might act as cell fate determinants,[39] our data will not fulfill these criteria. In principle, it could be that even cells that form daughter cells adopting different cell fates divide in a symmetric way, giving rise to 2 equally specified daughter cells. Since the daughter cells in our as well as in other experiments had the ability to stay in close contact with each other before they were separated, they could theoretically have influenced each other's developmental capacity after mitosis. Developmental processes like that are well described. For example, the Notch-mediated process of lateral inhibition selects a single cell within a group of equivalent cells to adopt another cell fate than the remaining cells of that group.[40,41] As Notch is required to maintain primitive hematopoietic cells in an undifferentiated state,[42] it might be possible that 1 of the daughter cells activates the Notch signaling pathway in a process of lateral inhibition in its sister cell, resulting in the maintenance of the primitive cell fate in only 1 of the 2 cells.

Thus, we summarize that our data and data presented before are not sufficient to conclude that primitive hematopoietic cells can indeed divide asymmetrically. To unequivocally demonstrate that hematopoietic cells can divide asymmetrically, markers need to be defined which clearly segregate unequally within mitotic cells. We have learned from model organisms that all cells which divide asymmetrically are polarized during cell division and localize certain molecules to distinct regions of the cells, which then get

transmitted in an unequal way.[39] As we recently could show that several surface molecules, especially CD133, become distributed in a localized fashion in cultivated primitive hematopoietic cells,[43] it will be interesting to analyze the distribution of these markers in dividing primitive hematopoietic cells. As we realized that the more primitive $CD34^+$ cells of the slow-dividing fraction specifically express CD133, it might be possible that upon cell division CD133 segregates into one of the arising daughter cells, perhaps confirming the concept of asymmetric cell division within the primitive hematopoietic cell compartment.

Acknowledgments

The authors like to thank Rainer Saffrich and Martin Peschel (Nikon-Germany) for their excellent support in establishing the micromanipulation system, as well as Volker Eckstein, Johannes Fischer, and Katrin Miesala for their technical support. Umbilical cord blood samples were kindly provided by the Department of Gynecology and Obstetrics of the University of Heidelberg and by Gesine Kögler of the Heinrich-Heine University, Düsseldorf.

References

1. Korbling M, Anderlini P. Peripheral blood stem cell versus bone marrow allotransplantation: does the source of hematopoietic stem cells matter? Blood. 2001;98:2900-2908.
2. Iscove NN, Nawa K. Hematopoietic stem cells expand during serial transplantation in vivo without apparent exhaustion. Curr Biol. 1997;7:805-808.
3. Krause DS, Theise ND, Collector MI, et al. Multi-organ, multi-lineage engraftment by a single bone marrow-derived stem cell. Cell. 2001;105:369-377.
4. Moore KA, Ema H, Lemischka IR. In vitro maintenance of highly purified, transplantable hematopoietic stem cells. Blood. 1997;89:4337-4347.
5. Nolta JA, Thiemann FT, Arakawa-Hoyt J, et al. The AFT024 stromal cell line supports long-term ex vivo maintenance of engrafting multipotent human hematopoietic progenitors. Leukemia. 2002;16:352-361.
6. Punzel M, Moore KA, Lemischka IR, Verfaillie CM. The type of stromal feeder used in limiting dilution assays influences frequency and maintenance assessment of human long-term culture initiating cells. Leukemia. 1999;13:92-97.
7. Thiemann FT, Moore KA, Smogorzewska EM, Lemischka IR, Crooks GM. The murine stromal cell line AFT024 acts specifically on human CD34+CD38- progenitors to maintain primitive function and immunophenotype in vitro. Exp Hematol. 1998;26:612-619.
8. Shih CC, Hu MC, Hu J, Medeiros J, Forman SJ. Long-term ex vivo maintenance and expansion of transplantable human hematopoietic stem cells. Blood. 1999;94:1623-1636.
9. Arai F, Hirao A, Ohmura M, et al. Tie2/Angiopoietin-1 signaling regulates hematopoietic stem cell quiescence in the bone marrow niche. Cell. 2004; 118:149-161.
10. Calvi LM, Adams GB, Weibrecht KW, et al. Osteoblastic cells regulate the haematopoietic stem cell niche. Nature. 2003;425:841-846.
11. Zhang J, Niu C, Ye L, et al. Identification of the haematopoietic stem cell niche and control of the niche size. Nature. 2003;425:836-841.
12. Suda T, Suda J, Ogawa M. Disparate differentiation in mouse hemopoietic colonies derived from paired progenitors. Proc Natl Acad Sci U S A. 1984;81:2520-2524.
13. Suda J, Suda T, Ogawa M. Analysis of differentiation of mouse hemopoietic stem cells in culture by sequential replating of paired progenitors. Blood. 1984;64:393-399.
14. Leary AG, Strauss LC, Civin CI, Ogawa M. Disparate differentiation in hemopoietic colonies derived from human paired progenitors. Blood. 1985;66:327-332.
15. Ema H, Takano H, Sudo K, Nakauchi H. In vitro self-renewal division of hematopoietic stem cells. J Exp Med. 2000;192:1281-1288.
16. Takano H, Ema H, Sudo K, Nakauchi H. Asymmetric division and lineage commitment at the level of hematopoietic stem cells: inference from differentiation in daughter cell and granddaughter cell pairs. J Exp Med. 2004;199:295-302.
17. Brummendorf TH, Dragowska W, Zijlmans J, Thornbury G, Lansdorp PM. Asymmetric cell divisions sustain long-term hematopoiesis from single-sorted human fetal liver cells. J Exp Med. 1998;188:1117-1124.
18. Mayani H, Dragowska W, Lansdorp PM. Lineage commitment in human hemopoiesis involves asymmetric cell division of multipotent progenitors and does not appear to be influenced by cytokines. J Cell Physiol. 1993;157:579-586.
19. Punzel M, Zhang T, Liu D, Eckstein V, Ho AD. Functional analysis of initial cell divisions defines the subsequent fate of individual human CD34(+)CD38(-) cells. Exp Hematol. 2002;30: 464-472.
20. Huang S, Law P, Francis K, Palsson BO, Ho AD. Symmetry of initial cell divisions among primitive hematopoietic progenitors is independent of ontogenic age and regulatory molecules. Blood. 1999; 94:2595-2604.
21. Punzel M, Wissink SD, Miller JS, Moore KA, Lemischka IR, Verfaillie CM. The myeloid-lymphoid initiating cell (ML-IC) assay assesses the fate of multipotent human progenitors in vitro. Blood. 1999;93:3750-3756.
22. Miller JS, McCullar V, Punzel M, Lemischka IR, Moore KA. Single adult human CD34(+)/Lin-/CD38(-) progenitors give rise to natural killer cells, B-lineage cells, dendritic cells, and myeloid cells. Blood. 1999;93:96-106.
23. Miller JS, McCullar V. Human natural killer cells with polyclonal lectin and immunoglobulinlike receptors develop from single hematopoietic stem cells with preferential expression of NKG2A and KIR2DL2/L3/S2. Blood. 2001;98:705-713.
24. Punzel M, Liu D, Zhang T, Eckstein V, Miesala K, Ho AD. The symmetry of initial divisions of human hematopoietic progenitors is altered only by the cellular microenvironment. Exp Hematol. 2003; 31:339-347.
25. Kobayashi M, Laver JH, Lyman SD, Kato T, Miyazaki H, Ogawa M. Thrombopoietin, steel factor and the ligand for flt3/flk2 interact to stimulate the proliferation of human hematopoietic progenitors in culture. Int J Hematol. 1997;66:423-434.
26. Luens KM, Travis MA, Chen BP, Hill BL, Scollay R, Murray LJ. Thrombopoietin, kit ligand, and flk2/flt3 ligand together induce increased numbers of primitive hematopoietic progenitors from human CD34+Thy-1+Lin- cells with preserved ability to engraft SCID-hu bone. Blood. 1998;91: 1206-1215.
27. Ohmizono Y, Sakabe H, Kimura T, et al. Thrombopoietin augments ex vivo expansion of human cord blood-derived hematopoietic progenitors in combination with stem cell factor and flt3 ligand. Leukemia. 1997;11:524-530.
28. Krause DS, Fackler MJ, Civin CI, May WS. CD34: structure, biology, and clinical utility. Blood. 1996; 87:1-13.
29. Yin AH, Miraglia S, Zanjani ED, et al. AC133, a novel marker for human hematopoietic stem and progenitor cells. Blood. 1997;90:5002-5012.
30. Ho AD. Kinetics and symmetry of divisions of hematopoietic stem cells. Exp Hematol. 2005;33: 1-8.
31. Theunissen K, Verfaillie CM. A multifactorial analysis of umbilical cord blood, adult bone marrow and mobilized peripheral blood progenitors using the improved ML-IC assay. Exp Hematol. 2005; 33:165-172.
32. Lacaud G, Carlsson L, Keller G. Identification of a fetal hematopoietic precursor with B cell, T cell, and macrophage potential. Immunity. 1998;9: 827-838.
33. Mebius RE, Miyamoto T, Christensen J, et al. The fetal liver counterpart of adult common lymphoid progenitors gives rise to all lymphoid lineages, CD45+CD4+CD3- cells, as well as macrophages. J Immunol. 2001;166:6593-6601.
34. Reya T, Morrison SJ, Clarke MF, Weissman IL. Stem cells, cancer, and cancer stem cells. Nature. 2001;414:105-111.
35. Adolfsson J, Mansson R, Buza-Vidas N, et al. Identification of Flt3+ lympho-myeloid stem cells lacking erythro-megakaryocytic potential a revised road map for adult blood lineage commitment. Cell. 2005;121:295-306.
36. Haddad R, Guardiola P, Izac B, et al. Molecular characterization of early human T/NK and B-lymphoid progenitor cells in umbilical cord blood. Blood. 2004;104:3918-3926.
37. Lu M, Kawamoto H, Katsube Y, Ikawa T, Katsura Y. The common myelolymphoid progenitor: a key intermediate stage in hemopoiesis generating T and B cells. J Immunol. 2002;169:3519-3525.
38. Cumano A, Paige CJ, Iscove NN, Brady G. Bipotential precursors of B cells and macrophages in murine fetal liver. Nature. 1992;356:612-615.
39. Betschinger J, Knoblich JA. Dare to be different: asymmetric cell division in Drosophila, C. elegans and vertebrates. Curr Biol. 2004;14: R674–685.
40. Giebel B. The notch signaling pathway is required to specify muscle progenitor cells in Drosophila. Mech Dev. 1999;86:137-145.
41. Martinez Arias A, Zecchini V, Brennan K. CSL-independent Notch signalling: a checkpoint in cell fate decisions during development? Curr Opin Genet Dev. 2002;12:524-533.
42. Ohishi K, Varnum-Finney B, Bernstein ID. The notch pathway: modulation of cell fate decisions in hematopoiesis. Int J Hematol. 2002;75:449-459.
43. Giebel B, Corbeil D, Beckmann J, et al. Segregation of lipid raft markers including CD133 in polarized human hematopoietic stem and progenitor cells. Blood. 2004;104:2332-2338.

ELSEVIER

Mechanisms of Development 86 (1999) 137–145

The Notch signaling pathway is required to specify muscle progenitor cells in *Drosophila*

Bernd Giebel*

Institut für Entwicklungsbiologie, Universität zu Köln, 50923 Köln, Germany

Received 3 March 1999; received in revised form 19 May 1999; accepted 26 May 1999

Abstract

Organization and function of the Notch signaling pathway in *Drosophila* are best understood with respect to its role in the process of selection of neural progenitor cells. However, there is evidence that, besides neurogenesis, the Notch signaling pathway is involved in several other developmental processes, one of which is the selection of muscle progenitor cells. Thus, the number of these cells is increased in neurogenic mutants, and it has been proposed that muscle progenitor cells are selected from clusters of equivalent cells expressing genes of the *achaete-scute* gene complex (AS-C). Here, I present evidence for the participation of additional elements of the Notch signaling pathway in myogenesis. Gal4 mediated expression of a *Notch* variant, *E(spl)* and *Hairless* shows that the selection of muscle progenitor cells obeys principles apparently identical to those acting at the selection of neural progenitor cells.

Keywords: Neurogenic genes; Proneural genes; Gal4 system; Myogenesis; Drosophila

1. Introduction

Specification of neural progenitor cells in *Drosophila*, i.e. neuroblasts and sensory organ mother cells (SMCs), requires a complex network of interlinked functions mediated by the products of proneural and neurogenic genes (see Campos-Ortega, 1993; Ghysen et al., 1993; Jan and Jan, 1993, for reviews). The neurogenic network acts during embryogenesis within relatively small groups of equivalent cells, called proneural clusters, from which individual cells are selected. All the cells in these clusters express initially proneural genes (Cabrera et al. 1987; Romani et al., 1987; Cabrera, 1990; Martín-Bermudo et al., 1991), which encode transcriptional activators of the bHLH family (Villares and Cabrera, 1987; Alonso and Cabrera, 1988; González et al., 1989). Expression becomes restricted to an individual cell of the cluster, which delaminates as neural progenitor cells. This decision process is controlled by lateral inhibition mediated by the neurogenic genes. In neurogenic mutants (Lehmann et al., 1983), in which lateral inhibition is perturbed, expression of *achaete*, *scute* and *lethal of scute* does not become restricted to individual cells, but persists in all cells of the proneural cluster (Brand and Campos-Ortega, 1988; Cabrera, 1990; Skeath and Carroll, 1992; Ruiz-Gómez and Ghysen, 1993; Martín-Bermudo et al., 1995). The neurogenic genes can be ordered in an epistatic chain whose last link is the *Enhancer of split* complex (E(SPL)-C) (de la Concha et al., 1988; Lieber et al., 1993). *Notch*, *Suppressor of Hairless* (*Su(H)*) and the E(SPL)-C participate in the reception and processing of the regulatory signals, whereas *Delta* acts as the source of these signals (Technau and Campos-Ortega, 1987; Heitzler and Simpson, 1991; Lieber et al., 1993; Rebay et al., 1993; Struhl et al., 1993; Bailey and Posakony, 1995; Lecourtois and Schweissguth, 1995). The genes of the E(SPL)-C (Knust et al., 1987a) encode transcription factors of the bHLH family (Klämbt et al., 1989; Delidakis and Artavanis-Tsakonas, 1992; Knust et al., 1992), which upon Notch-mediated activation (Jennings et al., 1994; Bailey and Posakony, 1995; Lecourtois and Schweissguth, 1995) suppress the function of the proneural genes (Oellers et al., 1994; Singson et al., 1994; Van Doren et al., 1994; Tata and Hartley, 1995; Heitzler et al., 1996; Nakao and Campos-Ortega, 1996; Giebel and Campos-Ortega, 1997). Genetic data suggest that the level of expression and activity of proneural gene products decide the neural or epidermal fate of each cell in the proneural clusters. In vitro experiments suggest that the proteins encoded by the AS-C genes function as

* Present address. Institut für Transplantationsdiagnostik und Zelltherapeutika, Heinrich Heine Universität, Düsseldorf, Germany. Tel.: +49-211-81-16793; fax: +49-21-81-16792.

E-mail address: giebel@kmsz.uni-duesseldorf.de (B. Giebel)

0925-4773/99/$ - see front matter
PII: S0925-4773(99)00128-8

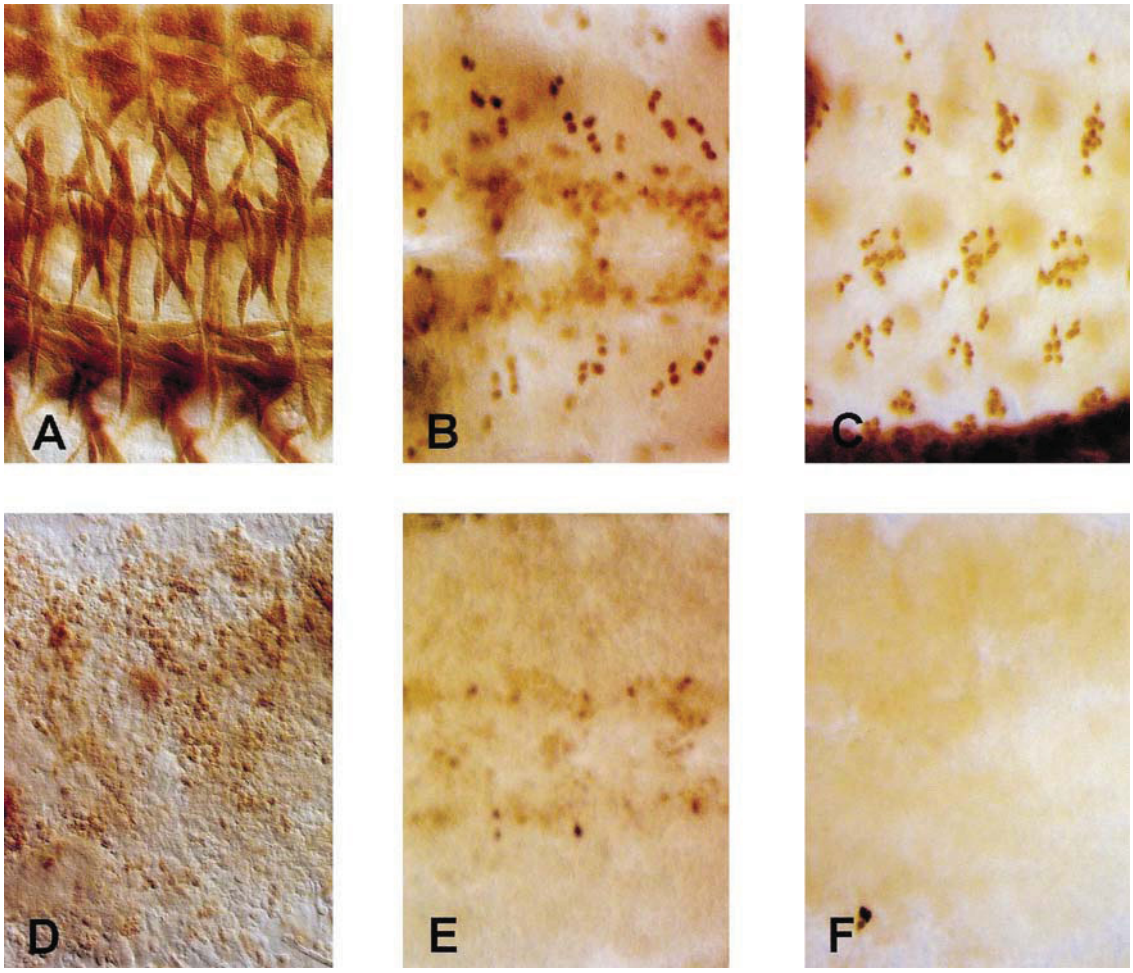

Fig. 1. Muscle and PNS formation is suppressed in embryos expressing *Notch*^{intra} (D–F). In all views anterior is to the left. (A,D) Lateral view of stage 16 embryos, carrying one copy of the MHC-*lacZ* reportergene, stained with an anti-β-Gal antibody. The embryo shown in (A) represents the wildtype pattern of the larval muscles. (D) Although embryos expressing UAS-*Notch*^{intra} under control of the 24B-Gal4 activator do not form any muscles, certain fusion competent myoblasts express the MHC-*lacZ* reportergene. (B,E) Ventral view of late stage 11 embryos stained with an anti-Krüppel antibody. In the wildtype embryo shown in (B) most of the Krüppel positive progenitor cells have already separated to give rise to a pair of founder cells. The dorsal and the most ventral progenitor cells or their offspring, respectively, are out of focus. Embryos expressing UAS-*Notch*^{intra} under control of the 24B-Gal4 activator do not develop any Krüppel positive founder cells (E). (C,F) Lateral view of stage 16 embryos stained with the MAb 44C11. (C) Wildtype pattern of PNS cells expressing Elav, the antigen recognized by MAb44C11. In embryos expressing UAS-*Notch*^{intra} under control of daG32 no PNS structures are formed as visualized by the absence of 44C11 positive cells.

heterodimers with another, ubiquitously distributed bHLH protein, encoded by *daughterless* (Caudy et al., 1988a,b; Cronmiller et al., 1988; Murre et al., 1989; Cabrera and Alonso, 1991; Cronmiller and Cummings, 1993; Oellers et al., 1994; van Doren et al., 1994); in vivo evidence has been obtained that Lethal of scute requires Daughterless to elicit neural development ectopically (Giebel et al., 1997).

For many years, the neurogenic genes have been studied solely from the point of view of neurogenesis. However, the neurogenic mutations cause phenotypic abnormalities in many other organs and processes, besides the neural tissue. For example, as early as 1937 Poulson described muscle defects associated with *Notch* mutations (Poulson, 1937). Since then defects in myogenesis, oogenesis, gut and heart development have been described as associated with *Notch* and other neurogenic mutations (Corbin et al., 1991; Ruohola et al., 1991; Xu et al., 1992; Bate et al., 1993; Tepass and Hartenstein, 1994; Carmena et al., 1995). Carmena et al. (1995) have reported that *lethal of scute* is expressed in mesodermal cell clusters. During early myogenesis its expression becomes restricted to one cell of each cluster which segregates thereafter as muscle progenitor cell. Division of the progenitor cells creates two muscle founder cells, each of which recruits neighboring non-founder myoblasts to form the syncytial precursors of a distinct mature muscle (Bate 1990; Dohrmann et al., 1990). As previously shown in the neuroectoderm, restriction of expression to one cell is impaired in neurogenic mutants leading to severe abnormalities in muscle patterning and muscle differentiation (Corbin et al., 1991; Bate et al., 1993; Carmena et al., 1995). In addition, loss of *lethal of scute* function leads to loss, and overexpression to duplica-

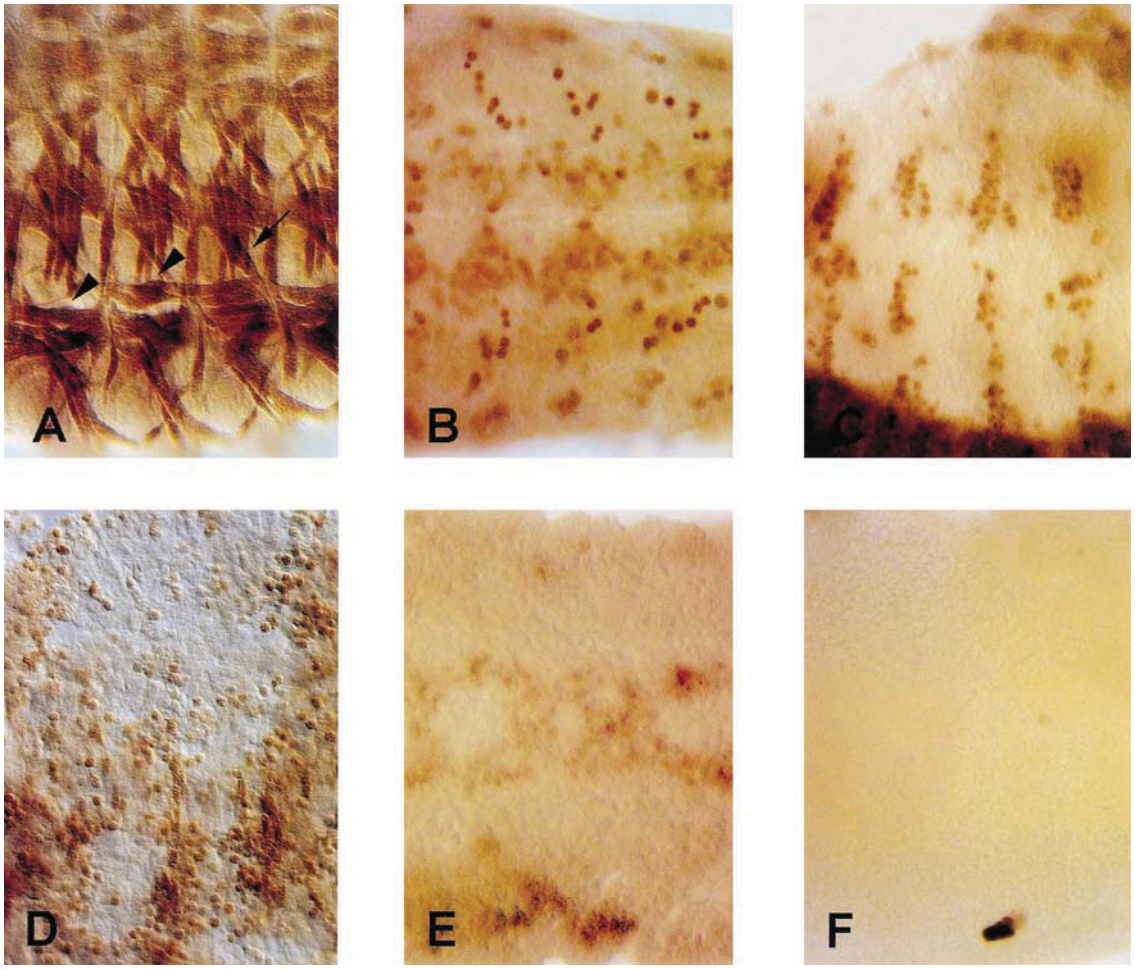

Fig. 2. Mesoderm and PNS formation in embryos expressing UAS-*daughterless* and UAS-*lethal of scute* without (A–C) or with coexpression of *Notch*^{intra} (D–F). The stages and the antibody stainings of the illustrated embryos correspond to those in Fig. 1. The expression of the Gal4 effector genes is under control of the 24B-Gal4 activator (A,B,D,E) or of daG32 (C,F), respectively. Coexpression of UAS-*da*52.2 and UAS-*l'sc*W3h results in muscle (A) and PNS (C) pattern formation defects and in very rare cases in muscle duplications (A). The embryo shown in A has a duplication of a LO1 muscle (arrow); pattern formation defects are easily recognizable in the arrangement of the VL muscles (arrowheads). No striking defects were detected in the pattern of Krüppel positive founder cells (B). *Notch*^{intra} dominates over the function of *daughterless* and *lethal of scute*, since embryos expressing all of these three effector genes do not develop any of the larval muscles (D), any of the Krüppel positive founder cells (E) or any structures of the PNS (F). These phenotypes are comparable to those of *Notch*^{intra} expressing embryos (see Fig. 1D–F).

tion of specific founder cells and muscles (Carmena et al., 1995). These results suggest that the function of the proneural gene *lethal of scute* in myogenesis is analogous to its function in neurogenesis.

I have sought to obtain more evidence for the participation of the Notch signaling pathway during *Drosophila* myogenesis by overexpressing genes encoding various members of this pathway by means of the Gal4 system (Fischer et al., 1988; Brand and Perrimon, 1993). I found that Gal4-mediated expression of a constitutively active Notch receptor inhibits the development of muscle founder cells, as visualized with the markers S59 (Dohrmann et al., 1990) and Krüppel (Ruiz-Gómez et al., 1997); however, mesodermal cells express the muscle specific myosin heavy chain. This effect on the muscle founder cells persists after simultaneous overexpression of *lethal of scute* and *daughterless*, but is partially compensated by *Hairless*. Finally, Gal4-mediated overexpression of *E(spl)* leads to a dramatic reduction of S59 and Krüppel positive cells. These findings strongly suggest that the Notch signaling pathway in myogenesis is similar organized as in neurogenesis.

2. Results

In the experiments described, I mainly used two activator insertions. One, daG32 (Wodarz et al., 1995; Nakao and Campos-Ortega, 1996; Giebel et al., 1997) efficiently activates reporter gene transcription ubiquitously from blastoderm stages onwards. The other activator insertion, 24B-Gal4 (Brand and Perrimon, 1993), directs transcription exclusively in the mesoderm from stage 8 on (Carmena et al., 1995). The results were identical with both activators, at

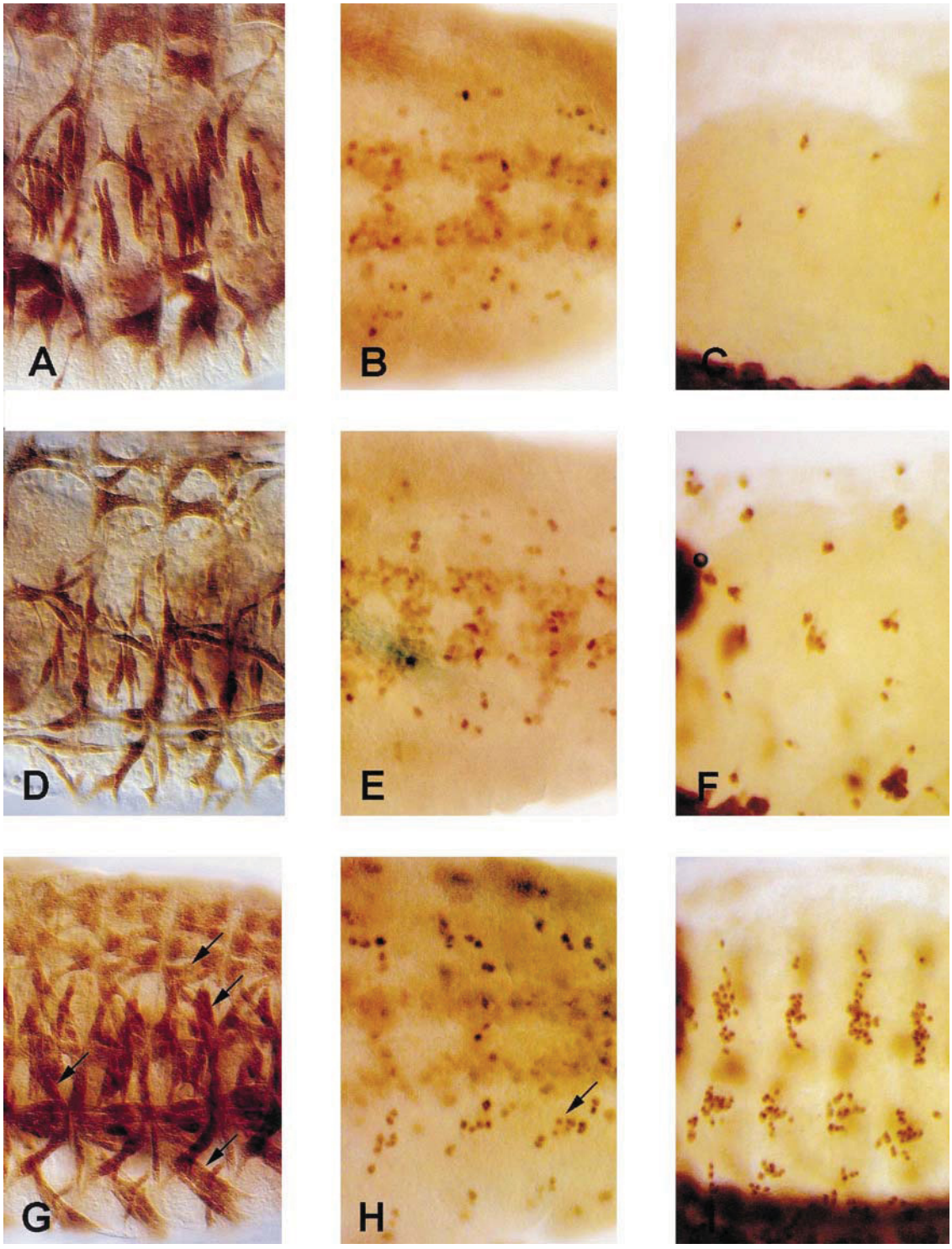

Fig. 3. The stages and the antibody stainings of the illustrated embryos correspond to those of Fig. 1. The expression of the Gal4 effector genes is controlled by the 24B-Gal4 activator (A,B,E,G,H) or by daG32 (C,F,I), respectively. Embryos expressing UAS-*E(spl)* (UAS-*E(spl)*.J5,19) have a reduced number of Krüppel positive founder cells (B), consistent with this observation the number of larval muscles is strongly reduced in older embryos (A); notice the single MHC-*lacZ* positive fusion competent myoblasts (A). Neuroectodermal expression of UAS-*E(spl)* leads to suppression of PNS structures, too (C). Similar phenotypes are observed when UAS-*Hairless* (UAS-*H*.37or) and UAS-*Notch*^{intra} are coexpressed (D–F). Indicating that Hairless antagonizes the function of Notch^{intra} (compare with Fig. 1: D–F). Gal4 mediated expression of UAS-*Hairless* (UAS-*H*.27sh,37or) by itself leads to the development of additional muscles. The illustrated embryo has duplications in one of the DA3 muscles, in one of the DT1 muscles, in one of the LO1 muscles and in one muscle of a VO4-VO6 group (arrows, dorsal to ventral, G). Consistent with this, the number of Krüppel positive foundercells (arrow in H) and the number of PNS cells (I, compare with wildtype Fig. 1C) are increased as well.

least with respect to the aspects of myogenesis covered in our study.

2.1. The active form of Notch suppresses development of muscle founder cells and is dominant over Daughterless and Lethal of scute function

To test whether the Notch signaling pathway is involved in myogenesis, I studied the effects of expression of a constitutively active Notch protein (Notch^{intra}; Lieber et al., 1993; Struhl et al., 1993). A second chromosomal effector line with an UAS-*Notch^{intra}* construct was used. As described in Giebel et al. (1997) this construct led to complete blocking of neural development upon activation with daG32 (Fig. 1F). Embryos carrying that construct driven by daG32 or by 24B-Gal4, respectively, do not express any of the muscle founder cell markers S59 and Krüppel (Fig. 1E) in the mesoderm. Therefore, I assume that no muscle progenitor cells are specified in these animals. Confirmation of this assumption is provided by the observation that no muscle fibers differentiate in these embryos, as shown by means of the expression of a myosin heavy chain (MHC) reporter gene (Fig. 1D). In mutants where fusion of myoblasts is blocked, founder cells express corresponding founder cell markers, while the non-founder myoblasts remain as undifferentiated rounded cells, which expresses certain muscle specific genes like *myosin* (Rushton et al., 1995). Since *Notch^{intra}* expressing mesodermal cells are rounded and many of them express the MHC reporter (Fig. 1D), I assume that the MHC expressing cells are non-founder myoblasts which have failed to undergo fusion due to the lack of muscle founder cells.

In view of the myogenic abilities of the proneural gene *lethal of scute* (Carmena et al., 1995), whose gene products function as heterodimers with Daughterless (Caudy et al., 1988a,b; Cronmiller et al., 1988; Murre et al., 1989; Cabrera and Alonso, 1991; Cronmiller and Cummings, 1993; van Doren et al., 1994; Oellers et al., 1994), I have tested whether the effects of constitutively activation of Notch can be compensated by the simultaneous Gal4 mediated expression of *daughterless*, *lethal of scute* and *Notch^{intra}*. I found no difference as compared to embryos which do not express UAS-*daughterless* and UAS-*lethal of scute* (Fig. 2D–F). These results indicate that the Notch^{intra}-mediated inhibitory signals are dominant over the action of both endogenous and exogenous provided proneural proteins.

The Gal4 mediated expression of *daughterless* and *lethal of scute* by itself causes just minor defects in the pattern of mature muscles (Fig. 2A,B). I rarely detected any duplication of founder cells or muscles after overexpression of both *lethal of scute* alone or in combination with *daughterless*. During neurogenesis daG32 mediated expression of UAS-*lethal of scute* or *UAS-daughterless* effectors compensates for loss of AS-C or *daughterless* function, respectively (Giebel et al., 1997), this suggests that both constructs are functionally expressed in the mesoderm, at least after activation with daG32. Therefore, I conclude that the inhibitory signals mediated by exogenously provided Notch^{intra} and those mediated by the endogenous Notch dominate over the function of Lethal of scute and Daughterless. These results are consistent with results obtained on the development of the embryonic nervous-system (Fig. 2C,F; Giebel et al., 1997).

2.2. Gal4-mediated overexpression of Enhancer of split reduces the number of muscle founder cells

Further evidence for a role of the Notch pathway in myogenesis was obtained by overexpressing UAS-*E(spl)* in the mesoderm. In neurogenesis, Suppressor of Hairless (Su(H)) activates the transcription of genes of the (E(SPL)-C (Jennings et al., 1994; Bailey and Posakony, 1995; Lecourtois and Schweissguth, 1995), which on their turn will suppress the activity of the proneural genes (Oellers et al., 1994; Singson et al., 1994; van Doren et al., 1994; Tata and Hartley, 1995; Heitzler et al., 1996; Nakao and Campos-Ortega, 1996; Giebel and Campos-Ortega, 1997). Following Gal4 mediated activation of UAS-*E(spl)*, the number of S59 and Krüppel positive cells is strongly reduced (Fig. 3B). This correlates with a defect in the number of differentiated muscle cells, as shown by MHC reporter gene expression (Fig. 3A). Again these data fit well with the results obtained on the development of the neuroectoderm, in which Gal4 driven UAS-*E(spl)* expression leads to strong reduction of CNS and PNS structures (Fig. 3C; Nakao and Campos-Ortega, 1996).

2.3. Gal4 mediated overexpression of Hairless increases the number of muscle founder cells

During neurogenesis Su(H) becomes active if Notch^{intra} is expressed (Bailey and Posakony, 1995; Lecourtois and Schweissguth, 1995). During imaginal neurogenesis the function of Su(H) is antagonized by proteins encoded by *Hairless*; this effect is mediated by direct protein-protein interactions (Brou et al., 1994; Schweisguth and Posakony, 1994; Bang et al., 1995). During specification of imaginal sensory organ precursors, overexpression of *Hairless* counteracts the phenotypic effects of activated Notch (Bang et al., 1995). If Su(H) is involved in transducing the inhibitory signals mediated by activated Notch during myogenesis, Gal4 mediated expression of *Hairless* could theoretically weaken the effect of Notch^{intra} on the course of myogenesis. To test the relationships between active Notch and Hairless during myogenesis, I have expressed UAS-*Hairless* and UAS-*Notch^{intra}* in the mesoderm of the same embryos. S59 and Krüppel positive cells are present in these embryos (Fig. 3E), although in a much lower number than in wildtype embryos (Fig. 1B). Well differentiated muscles are also present in these embryos (Fig. 3D). I obtained similar results in the course of embryonic neurogenesis. Embryos with daG32 driven UAS-*Notch^{intra}* are completely aneural (Fig. 1F; Giebel et al., 1997). After coexpression of UAS-*Hair-*

less structures of the CNS as well as of the PNS differentiate as visualized with 22C10 and 44C11 antibody stainings (Fig. 3F).

Gal4 mediated expression of UAS-*Hairless* alone leads to a slight increase in the number of S59 and Krüppel positive cells in the mesoderm (Fig. 3H). This correlates with an increase in the number of differentiated muscle fibers, shown by the expression of the MHC reporter gene (Fig. 3G). In correspondence to those data the neuroectodermal Gal4 mediated expression of UAS-*Hairless* leads to the development of a weakly hyperplasic nervous system, as shown by stainings using the neural antibodies 22C10 and 44C11 (Fig. 3I compared to Fig. 1C).

3. Discussion

Derivatives of the mesoderm, like the skeletal muscles, and descendants of the neuroectoderm (cells of the central nervous system and epidermis) are morphologically completely different. One of the most striking differences is the formation of multinuclear syncytia of skeletal muscle compared to the mononuclear cells of the neuroectoderm. Therefore, it seems reasonable that the development of both germ layers is mechanistically completely different. However, there is growing evidence, which is strongly enhanced by the presented data, that the first steps in mesodermal development follow the same rules than those in the neuroectoderm.

Specification of at least some muscle progenitor cells requires the expression of the proneural gene *lethal of scute* (Carmena et al., 1995). *l'sc* is expressed in the mesoderm from stage 10 onward in several groups of cells (Carmena et al., 1995), in a similar manner as its expression in proneural clusters during early neurogenesis (Cabrera et al., 1987; Romani et al., 1987; Martín-Bermudo et al., 1991). As during neurogenesis one cell of a given mesodermal *l'sc* expression domain accumulates higher levels of the protein than the other cells (Carmena et al., 1995). Since some of those cells also express the founder cell marker S59 it is thought that the cells with high Lethal of scute concentration are committed to become muscle progenitor cells (Carmena et al., 1995). This is again analogous to neurogenesis, where the cells with higher proneural gene product are singled out to form neural precursors and express certain neuroblast or sensory organ mother cell markers; while the other cells develop as epidermoblasts (reviewed in Campos-Ortega, 1993; Goodman and Doe, 1993). Furthermore, neurogenic mutants have an excess development of neural precursor cells (reviewed in Campos-Ortega, 1993) and of muscle progenitor cells (Corbin et al., 1991; Bate et al., 1993; Carmena et al., 1995). Therefore, muscle progenitor cells are specified by similar mechanisms as the precursors of the nervous system.

3.1. Lateral inhibition dominates over proneural gene function during muscle progenitor cell specification

As we have reported recently there are no supernumerary neuroblasts or supernumerary SMCs in the anlage of the nervous system of embryos overexpressing the proneural genes *lethal of scute* and *daughterless*, although there are pattern formation defects in the differentiated nervous system (Giebel et al., 1997). Consistent with those data embryos overexpressing *lethal of scute* alone or in combination with *daughterless* have some defects in muscle patterning. Only occasionally I have detected additional muscles in such embryos, confirming the data of Carmena et al. (1995). Since daG32 mediated *l'sc* expression is sufficient to rescue the neural defects of AS-C deficiency embryos (Giebel et al., 1997), and Gal4 mediated expression of $Notch^{intra}$ causes drastic developmental defects in the mesoderm, I conclude that the proneural transgenes are expressed in the mesoderm and that a certain mechanism represses their proneural protein function. Because the coexpression of *lethal of scute* and *daughterless* does neither modify the amuscular nor the aneural phenotype of $Notch^{intra}$ expressing embryos (Giebel et al., 1997), this inhibitory mechanism is most probably a process of lateral inhibition, in which the active form of Notch dominates over the function of Lethal of scute and Daughterless.

I have tested whether genes that mediate the Notch signal during neurogenesis, are involved in myogenesis as well. Since Su(H) is maternally and zygoticly expressed (Schweisguth and Posakony, 1992) and mutants die at late larval and early pupal stages, the maternal expression component is sufficient for the whole embryogenesis (Furukawa et al., 1992; Schweisguth and Posakony, 1992), while loss of maternal and zygotic *Su(H)* gene function results in embryos showing a neurogenic phenotype (Lecourtois and Schweissguth, 1995). It has been shown that *Hairless* antagonizes the function of *Su(H)* at least during imaginal neurogenesis (Brou et al., 1994; Schweisguth and Posakony, 1994; Bang et al., 1995). Although *Hairless* has no essential function during embryonic neurogenesis (Schweisguth and Lecourtois, 1998), I could show that Gal4 mediated expression of *Hairless* leads to suppression of the aneural and amuscular phenotype of embryos expressing a constitutive active form of Notch, while Gal4 mediated *Hairless* expression by itself causes the development of a weak hyperplasic embryonic nervous system and results in the development of few additional muscle founder cells and muscles, respectively. In summary this results suggest that at least ectopically expressed Hairless titrates maternal and zygotic expressed Su(H) during embryonic neurogenesis and myogenesis, resulting in a weakening of the process of lateral inhibition. Therefore it is reasonable that Su(H) mediates the Notch signal during muscle progenitor development as well as during neurogenesis.

E(SPL)-C is at least during neurogenesis the last link in the epistatic chain of the Notch signaling pathway (de la

Concha et al., 1988; Lieber et al., 1993) and as fare as analyzed its genes are also expressed in the mesoderm at stage 11–12 (Knust et al., 1987b) at the time where muscle progenitor cells are specified (Dohrmann et al., 1990; Carmena et al., 1995). Overexpression of certain genes of the E(SPL)-C, especially *E(spl)*, leads to a suppression of neural fate (Tata and Hartley, 1995; Nakao and Campos-Ortega, 1996; Giebel and Campos-Ortega, 1997). Consistent with this, Gal4 mediated expression of *E(spl)* leads to suppression of muscle founder cells and therefore most likely to suppression of muscle progenitor specification. Again the obtained results are similar for myogenesis and neurogenesis, suggesting that the E(SPL)-C has the same function in both processes, namely to suppress one of two different possible cell fates, in the anlagen of the nervous system the development of the neural precursor cell and in the mesoderm the development of muscle progenitor cells.

The analogy between neurogenesis and myogenesis is further reinforced by the finding that the specified neural precursor cells and the muscle progenitor cells divide asymmetrically. This asymmetry depends in both cases on the cytoplasmatic membrane-associated protein Numb (Uemura et al., 1989; Rhyu et al., 1994; Spana et al., 1995; Guo et al., 1996; Spana and Doe, 1996; Ruiz-Gómez and Bate, 1997; Carmena et al., 1998), on the gene-product of *inscutable* (Kraut et al., 1996; Ruiz-Gómez and Bate, 1997; Carmena et al., 1998) and on *Notch* (Guo et al., 1996; Spana and Doe, 1996; Ruiz-Gómez and Bate, 1997). Taken together the results of this study and of previously published data (see Section 1 and Giebel et al., 1997) suggest that the mechanism of lateral inhibition and its functional components is evolutionary conserved along the different germlayers.

4. Materials and methods

4.1. Plasmid constructions and germ line transformation

To construct pUAST-*Hairless* a 4386 bp *Asp*718I/*Ssp*I fragment from pNBH2-10 (Brown and Kafatos, 1988; Bang and Posakony, 1992), comprising the *Hairless* coding region, was initially ligated into the *Asp*718I/*Eco*RV-site of pBluescript KS + (Stratagene) yielding pBH. An *Asp*718I/*Xba*I fragment was excised from the pBH plasmid and ligated into the corresponding site of pUAST (Brand and Perrimon, 1993). DNA injection of w^{1118} embryos (Lindsley and Zimm, 1992) were performed as described previously (Rubin and Spradling, 1982). As a source of transposase the plasmid pPΔ2–3 (Laski et al., 1986) was used. I have established 15 independent UAS-*Hairless* lines. The strength of the individual effector insertions was determined in crosses with flies of the ubiquitous activator line daG32. The effects of particular insertions was considered to be strong if they led to a clearly visible hyperplasia in the PNS and CNS of embryos activated with daG32. The strongest homozygous effectors were used in this study.

4.2. Drosophila stocks

I used a homozygous third chromosomal daughterless-Gal4 line (daG32, Wodarz et al., 1995) and the homozygous 24B-Gal4 enhancer trap line (Brand and Perrimon, 1993) as activators. Both lines were combined with a second chromosomal insertion of a MHC-*lacZ* reportergene (Hess et al., 1989).

Homozygous effector lines carried insertions in either the second or the third chromosome. I used UAS-*lethal of scute* lines (UAS-$l^{l}sc$W3h, UAS-$l^{l}sc$M3h) described in Hinz et al. (1994); a UAS-*daughterless* line (UAS-*da*52.2) described in Giebel et al. (1997), and UAS-*Enhancer of split* lines described in Giebel and Campos-Ortega (1997). In addition, I used a UAS-$Notch^{intra}$ line, kindly provided by Laurent Seugnet, Marc Haenlin and Pat Simpson (Strasbourg).

4.3. Immunohistochemical staining of embryos

Antibody stainings, i.e. MAb22C10 (Fujita et al., 1982), MAb44C11 (Bier et al., 1988) and anti-β-Galactosidase (Cappel) of embryos were performed according to standard protocols. For anti-Krüppel (Gaul et al., 1987) and anti-S59 (Dohrmann et al., 1990) stainings, the horseradish peroxidase vectastain elite ABC reagents (Vector Laboratories) were used. Staging of embryos was following Campos-Ortega and Hartenstein (1985). Since all activator and effector strains were homozygous for the corresponding inserts, all embryos of a given cross had the same genotype resulting in fully penetrant phenotypes.

Acknowledgements

I thank A. Brand, M. Haenlin, N. Perrimon, L. Seugnet and P. Simpson for fly stocks; M. Bate and R. Reuter for antibodies; J. Posakony for the *Hairless* cDNA; M. Bate, J. A. Campos-Ortega, U. Hinz and I. Stüttem for general discussion; J. A. Campos-Ortega, P. Hardy, U. Hinz and A. Stühler for critical reading of the manuscript. This work was supported by grants from the Deutsche Forschungsgemeinschaft (DFG, SFB 243) and the Fonds der Chemischen Industrie to J.A. Campos-Ortega.

References

Alonso, M.C., Cabrera, C.V., 1988. The *achaete-scute* gene complex of *Drosophila melanogaster* comprises four homologous genes. EMBO J. 7, 2585–2591.

Bailey, A.M., Posakony, J.W., 1995. Suppressor of Hairless directly activates transcription of *Enhancer of split* complex genes in response to Notch receptor activity. Genes Dev. 9, 2609–2622.

Bang, A.G., Posakony, J.W., 1992. The *Drosophila* gene *Hairless* encodes

a novel basic protein that controls alternative cell fates in adult sensory organ development. Genes Dev. 6, 1752–1769.

Bang, A.G., Bailey, A.M., Posakony, J.W., 1995. *Hairless* promotes stable commitment to the sensory organ precursor cell fate by negatively regulating the activity of the *Notch* signaling pathway. Dev. Biol. 172, 479–494.

Bate, M., Rushton, E., Frasch, M., 1993. A dual requirement for neurogenic genes in *Drosophila* myogenesis. Development 1993, 149–161.

Bate, M., 1990. The embryonic development of larval muscles in *Drosophila*. Development 110, 791–804.

Bier, E., Ackerman, L., Barbel, S., Jan, L.Y., Jan, Y.N., 1988. Identification and characterization of a neuron-specific nuclear antigen in *Drosophila*. Science 240, 913–916.

Brand, M., Campos-Ortega, J.A., 1988. Two groups of interrelated genes regulate early neurogenesis in *Drosophila melanogaster*. Wilhelm Roux's Arch. Dev. Biol. 197, 457–470.

Brand, A.H., Perrimon, N., 1993. Targeted gene expression as a means of altering cell fates and generating dominant phenotypes. Development 118, 401–415.

Brou, C., Logeat, F., Lecourtois, M., Vandekerckhove, J., Kourilsky, P., Schweisguth, F., Israèl, A., 1994. Inhibition of the DNA-binding activity of *Drosophila* Suppressor of Hairless and of its human homolog. KBF2/RBP-Jκ, by direct protein–protein interaction with *Drosophila* Hairless. Genes Dev. 8, 2491–2503.

Brown, N.M., Kafatos, F.C., 1988. Functional cDNA libraries from *Drosophila* embryos. J. molec. Biol. 203, 425–437.

Cabrera, C.V., Alonso, M.C., 1991. Trancriptional activation by heterodimers of the *achaete-scute* and *daughterless* gene products of *Drosophila*. EMBO J. 10, 2965–2973.

Cabrera, C.V., Martinez-Arias, A., Bate, M., 1987. The expression of three members of the *achaete-scute* gene complex correlates with neuroblast segregation in *Drosophila*. Cell 50, 425–433.

Cabrera, C.V., 1990. Lateral inhibition and cell fate during neurogenesis in *Drosophila*: the interaction between *scute*. *Notch*, and *Delta*. Development 109, 733–742.

Campos-Ortega, J.A., Hartenstein, V., 1985. The embryonic development of *Drosophila melanogaster*, Springer Verlag, Berlin.

Campos-Ortega, J.A., 1993. Early neurogenesis in *Drosophila melanogaster*. In: Bate, M., Martinez-Arias, A. (Eds.). Development of *Drosophila melanogaster*, 2Cold Spring Harbor Laboratory Press, New York, pp. 1091–1129.

Carmena, A., Bate, M., Jiménez, F., 1995. *lethal of scute*, a proneural gene, participates in the specification of muscle progenitors during *Drosophila* embryogenesis. Genes Dev. 9, 2373–2383.

Carmena, A., Murugasu-Oei, B., Menon, D., Jiménez, F., Chia, W., 1998. *inscutable* and *numb* mediate asymmetric muscle progenitor cell division during *Drosophila* myogenesis. Genes Dev. 12, 304–315.

Caudy, M., Grell, E.H., Dambly-Chaudière, C., Ghysen, A., Jan, L.Y., Jan, L.N., 1988a. The maternal sex determination gene *daughterless* has zygotic activity necessary for the formation of peripheral neurons in *Drosophila*. Genes Dev. 2, 843–852.

Caudy, M., Vässin, H., Brand, M., Tuma, R., Jan, L.Y., Jan, L.N., 1988b. *daughterless*, a gene essential for both neurogenesis and sex determination in *Drosophila*, has sequence similarities to myc and the achaete-scute complex. Cell 55, 1061–1067.

Corbin, V., Michelson, A.M., Abmayr, S.M., Neel, V., Alcamo, E., Maniatis, T., Young, M., 1991. A role for the *Drosophila* neurogenic genes in mesoderm differentiation. Cell 67, 311–323.

Cronmiller, C., Cummings, C.A., 1993. The *daughterless* gene product in *Drosophila* is a nuclear protein that is broadly expressed throughout the organism during development. Mech. Dev. 42, 159–169.

Cronmiller, C., Schedl, P., Cline, T.W., 1988. Molecular characterization of *daughterless*, a *Drosophila* sex determination gene with multiple roles in development. Dev. Genet. 2, 1666–1676.

de la Concha, A., Dietrich, U., Weigel, D., Campos-Ortega, J.A., 1988. Functional interactions of neurogenic genes of *Drosophila melanogaster*. Genetics 118, 499–508.

Delidakis, C., Artavanis-Tsakonas, S., 1992. The *Enhancer of split* [*E(spl)*] locus of *Drosophila* encodes seven independent helix-loop-helix proteins. Proc. Natl. Acad. Sci. USA 89, 8731–8735.

Dohrmann, C., Azpiazu, N., Frasch, M., 1990. A new *Drosophila* homeobox gene is expressed in mesodermal precursor cells of distinct muscles during embryogenesis. Genes Dev. 4, 2098–2111.

Fischer, J.A., Giniger, E., Maniatis, T., Ptashne, M., 1988. Gal4 activates transcription in *Drosophila*. Nature 332, 853–856.

Fujita, S.C., Zipursky, S.L., Benzer, S., Ferrus, A., Shotwell, S.L., 1982. Monoclonal antibodies against the *Drosophila* nervous system. Proc. Natl. Acad. Sci. USA 79, 7929–7933.

Furukawa, T., Maruyama, S., Kawaichi, M., Honjo, T., 1992. The *Drosophila* homolog of the immunglobulin recombination signal-binding protein regulates peripheral nervous system development. Cell 69, 1191–1197.

Gaul, U., Seifert, E., Schuh, R., Jäckle, H., 1987. Analysis of Krüppel protein distribution during early *Drosophila* development reveals post-transcriptional regulation. Cell 50, 639–647.

Ghysen, A., Dambly-Chaudière, C., Jan, L.Y., Jan, Y.N., 1993. Cell interactions and gene interactions in peripheral neurogenesis. Genes Dev. 7, 723–733.

Giebel, B., Campos-Ortega, J.A., 1997. Functional dissection of the *Drosophila* Enhancer of Split protein, a suppressor of neurogenesis. Proc. Natl. Acad. Sci. USA 94, 6250–6254.

Giebel, B., Stüttem, I., Hinz, U., Campos-Ortega, J.A., 1997. Lethal of scute requires overexpression of Daughterless to elict ectopic neuronal development during embryogenesis in *Drosophila*. Mech. Dev. 63, 75–87.

González, F., Romani, S., Cubas, P., Modolell, J., Campuzano, S., 1989. Molecular analysis of *asense*, a member of the *achaete-scute* complex of *Drosophila melanogaster*, and its novel role in optic lobe development. EMBO J. 8, 3553–3562.

Goodman, C.S., Doe, C.Q., 1993. In: Bate, M., Martinez-Arias, M. (Eds.). Embryonic Development of the *Drosophila* Central Nervous System, vol. 2. Cold Spring Harbor Laboratory Press, New York, pp. 1131–1206.

Guo, M., Jan, L.Y., Jan, N.Y., 1996. Control of daughter cell fates during asymmetric division: interaction of Numb and Notch. Neuron 17, 27–41.

Heitzler, P., Simpson, P., 1991. The choice of cell fate in the epidermis of *Drosophila*. Cell 64, 1083–1092.

Heitzler, P., Bourouis, M., Ruel, L., Carteret, C., Simpson, P., 1996. Genes of the *Enhancer of split* and *achaete-scute* complexes are required for a regulatory loop between Notch and Delta during lateral signaling in *Drosophila*. Development 122, 161–171.

Hess, N., Kronert, W.A., Bernstein, S.I., 1989. Transcriptional and post-transcriptional regulation of *Drosophila* myosin heavy chain gene expression. In: Cellular and Molecular Biology of Muscle Development, Alan R Liss Inc., New York.

Hinz, U., Giebel, B., Campos-Ortega, J.A., 1994. The basic-helix-loop-helix domain of *Drosophila* lethal of scute protein is sufficient for proneural function and activates neurogenic genes. Cell 76, 1–11.

Jan, Y.N., Jan, Y.L., 1993. In: Bate, M., Martinez-Arias, A. (Eds.). The Peripheral Nervous System, vol. 2. Cold Spring Harbor Laboratory Press, New York, pp. 1207–1244.

Jennings, B., Preiss, A., Delidakis, C., Bray, S., 1994. The Notch signaling pathway is required for Enhancer of split bHLH protein expression during neurogenesis in the *Drosophila* embryo. Development 120, 3537–3548.

Klämbt, C., Knust, E., Tietze, K., Campos-Ortega, J.A., 1989. Closely related transcripts encoded by the neurogenic gene complex *Enhancer of split* of *Drosophila melanogaster*. EMBO J. 8, 203–210.

Knust, E., Bremer, K.A., Vässin, H., Ziemer, A., Tepass, U., Campos-Ortega, J.A., 1987a. The *Enhancer of split* locus and neurogenesis in *Drosophila melanogaster*. Dev. Biol. 122, 262–273.

Knust, E., Tietze, K., Campos-Ortega, J.A., 1987b. Molecular analysis of the neurogenic locus *Enhancer of split* of *Drosophila melanogaster*. EMBO J. 6, 1123–4113.

Knust, E., Schrons, H., Grawe, F., Campos-Ortega, J.A., 1992. Seven genes of the *Enhancer of split* Complex of *Drosophila melanogaster* encode Helix-Loop-Helix proteins. Genetics 132, 505–518.

Kraut, R., Chia, W., Jan, L.Y., Jan, N.Y., Knoblich, J.A., 1996. Role of *inscutable* in orienting asymmetric cell divisions in *Drosophila*. Nature 383, 50–55.

Laski, F.A., Rio, D.C., Rubin, G.M., 1986. Tissue specificity of *Drosophila* P-Element transposition is regulated at the level of mRNA splicing. Cell 44, 7–19.

Lecourtois, M., Schweissguth, F., 1995. The neurogenic Suppressor of Hairless DNA-binding protein mediates the transcriptional activation of the *Enhancer of split* Complex genes triggered by Notch signaling. Genes Dev. 9, 2598–2608.

Lehmann, R., Jiménez, F., Dietrich, U., Campos-Ortega, J.A., 1983. On the phenotype and development of mutants of early neurogenesis in *Drosophila melanogaster*. Wilhelm Roux's Arch. Dev. Biol. 192, 62–74.

Lieber, T., Kidd, S., Alcamo, E., Corbin, V., Young, M.W., 1993. Antineurogenic phenotypes induced by truncated Notch proteins indicate a role in signal transduction and may point to a novel function for Notch in the nuclei. Genes Dev. 7, 1949–1965.

Lindsley, D.L., Zimm, G., 1992. The genome of *Drosophila melanogaster*, Academic Press Inc, San Diego.

Martín-Bermudo, M.D., Martínez, C., Rodríguez, A., Jiménez, F., 1991. Distribution and function of the *lethal of scute* gene product during early neurogenesis in *Drosophila*. Development 113, 445–454.

Martín-Bermudo, M.D., Carmena, A., Jiménez, F., 1995. Neurogenic genes control gene expression at the transcriptional level in early neurogenesis and in mesectoderm specification. Development 121, 219–224.

Murre, C., Schonleber McCaw, P., Vässin, H., Caudy, M., Jan, L.Y., Jan, L.N., Cabrera, C.V., Buskin, J.N., Hauschka, S.D., Lassar, A.B., Weintraub, H. and Baltimore, D., 1989. Interactions between heterologous helix-loop-helix proteins generate complexes that bind specifically to a common DNA sequence. Cell 58, 537–544.

Nakao, K., Campos-Ortega, J.A., 1996. Persistent expression of genes of the Enhancer of split-Complex suppresses neural development in *Drosophila*. Neuron 16, 275–286.

Oellers, N., Dehio, M., Knust, E., 1994. bHLH proteins encoded by the *Enhancer of split* complex of *Drosophila* negatively interfere with transcriptional activation mediated by proneural genes. Mol. Gen. Genet. 244, 465–473.

Poulson, D.F., 1937. Chromosomal deficiencies and development of *Drosophila melanogaster*. Proc. Natl. Acad. Sci. USA 23, 133–137.

Rebay, I., Fehon, R.G., Artavanis-Tsakonas, S., 1993. Specific truncations of *Drosophila* Notch define dominant activated and dominant negative forms of the receptor. Cell 74, 319–329.

Rhyu, M.S., Jan, L.Y., Jan, N.Y., 1994. Asymmetric distribution of Numb protein during division of the sensory organ precursor cell confers distinct fates on daughter cells. Cell 76, 477–491.

Romani, S., Campuzano, S., Modolell, J., 1987. The *achaete-scute* complex is expressed in neurogenic regions of *Drosophila* embryos. EMBO J. 6, 2085–2092.

Rubin, G.M., Spradling, A.C., 1982. Genetic transformation of *Drosophila* with transposable element vectors. Science 218, 348–353.

Ruiz-Gómez, M., Bate, M., 1997. Segregation of myogenic lineages in *Drosophila* requires Numb. Development 124, 4857–4866.

Ruiz-Gómez, M., Ghysen, A., 1993. The expression and role of a proneural gene. *achaete*, in the development of the larval *Drosophila* nervous system. EMBO J. 12, 1121–1130.

Ruiz-Gómez, M., Hartmann, C., Jäckle, H., Bate, M., 1997. Specific muscle identities are regulated by *Krüppel* during *Drosophila* embryogenesis. Development 124, 3407–3414.

Ruohola, H., Bremer, K.A., Baker, D., Swedlow, J.R., Jan, L.Y., Jan, Y.N., 1991. Role of neurogenic genes in establishment of follicle cell fate and oocyte polarity during oogenesis in *Drosophila*. Cell 66, 433–449.

Rushton, E., Drysdale, R., Abmayr, S.M., Michelson, A.M., Bate, M., 1995. Mutations in a novel gene. *myoblast city*, provide evidence in support of the founder cell hypothesis for Drosophila muscle development. Development 121, 1979–1988.

Schweisguth, F., Lecourtois, M., 1998. The activity of *Drosophila Hairless* is required in pupae but not in embryos to inhibit Notch signal transduction. Dev. Genes Evol. 208, 19–27.

Schweisguth, F., Posakony, J., 1992. *Suppressor of Hairless*, the *Drosophila* homolog of the mouse recombination signal-binding protein gene, controls sensory organ cell fates. Cell 69, 1199–1212.

Schweisguth, F., Posakony, J., 1994. Antagonistic activities of *Suppressor of Hairless* and *Hairless* control alternative cell fates in the *Drosophila* adult epidermis. Development 120, 1433–1441.

Singson, A., Leviten, M.W., Bang, A.G., Hua, X.H., Posakony, J.W., 1994. Direct downstream targets of proneural activators in the imaginal disc include genes involved in lateral inhibitory signaling. Genes Dev. 8, 2058–2071.

Skeath, J.B., Carroll, S.B., 1992. Regulation of proneural gene expression and cell fate during neuroblast segregation in *Drosophila* embryo. Development 114, 939–946.

Spana, E.P., Doe, C.Q., 1996. Numb antagonises Notch signaling to specify sibling neuron cell fates. Neuron 17, 21–26.

Spana, E.P., Kopczynski, C., Goodman, C.S., Doe, C.Q., 1995. Asymmetric localization of Numb autonomously determines sibling neuron identity in the *Drosophila* CNS. Development 121, 3489–3494.

Struhl, G., Fitzgerald, K., Greenwald, I., 1993. Intrinsic activity of the Lin-12 and Notch intracellular domains *in vivo*. Cell 74, 331–345.

Tata, F., Hartley, D.A., 1995. Inhibition of cell fate in *Drosophila* by *Enhancer of split* genes. Mech. Dev. 51, 305–315.

Technau, G.M., Campos-Ortega, J.A., 1987. Cell autonomy of expression of neurogenic genes of *Drosophila melanogaster*. Proc. Natl. Acad. Sci. USA 84, 4500–4504.

Tepass, U., Hartenstein, V., 1994. The formation of the midgut epithelium in *Drosophila* depends on the interaction of endoderm and mesoderm. Development 120, 579–590.

Uemura, T., Shepherd, S., Ackermanns, L., Jan, L.Y., Jan, N.Y., 1989. *numb*, a gene required in determination of cell fate during sensory organ formation in *Drosophila* embryos. Cell 58, 349–360.

van Doren, M., Bailey, A.M., Esnayra, J., Ede, K., Posakony, J.W., 1994. Negative regulation of proneural gene activity: hairy is a direct transcriptional repressor of *achaete*. Genes Dev. 8, 2729–2742.

Villares, R., Cabrera, C.V., 1987. The *achaete-scute* gene complex of *Drosophila melanogaster*: conserved domains in a subset of genes required for neurogenesis and their homology to *myc*. Cell 50, 415–424.

Wodarz, A., Hinz, U., Engelbert, M., Knust, E., 1995. Expression of *crumbs* confers apical character on plasma membrane domains of ectodermal epithelia of *Drosophila*. Cell 82, 67–76.

Xu, T., Caron, L.A., Fehon, R.G., Artavanis-Tsakonas, S., 1992. The involvement of the *Notch* locus in *Drosophila* oogenesis. Development 115, 913–922.

Segregation of lipid raft markers including CD133 in polarized human hematopoietic stem and progenitor cells

Bernd Giebel, Denis Corbeil, Julia Beckmann, Johannes Höhn, Daniel Freund, Kay Giesen, Johannes Fischer, Gesine Kögler, and Peter Wernet

During ontogenesis and the entire adult life hematopoietic stem and progenitor cells have the capability to migrate. In comparison to the process of peripheral leukocyte migration in inflammatory responses, the molecular and cellular mechanisms governing the migration of these cells remain poorly understood. A common feature of migrating cells is that they need to become polarized before they migrate. Here we have investigated the issue of cell polarity of hematopoietic stem/progenitor cells in detail. We found that human CD34$^+$ hematopoietic cells (1) acquire a polarized cell shape upon cultivation, with the formation of a leading edge at the front pole and a uropod at the rear pole; (2) exhibit an amoeboid movement, which is similar to the one described for migrating peripheral leukocytes; and (3) redistribute several lipid raft markers including cholesterol-binding protein prominin-1 (CD133) in specialized plasma membrane domains. Furthermore, polarization of CD34$^+$ cells is stimulated by early acting cytokines and requires the activity of phosphoinositol-3-kinase as previously reported for peripheral leukocyte polarization. Together, our data reveal a strong correlation between polarization and migration of peripheral leukocytes and hematopoietic stem/progenitor cells and suggest that they are governed by similar mechanisms. (Blood. 2004;104:2332-2338)

Introduction

During ontogenesis the earliest progenitors of the mammalian adult hematopoietic system are initially formed in the intraembryonic aorta-gonad-mesonephros (AGM) and it seems very likely that such AGM-derived hematopoietic stem cells (HSCs) emigrate and colonize the fetal liver, the main site of embryonic hematopoiesis. During neonatal stages, HSCs migrate again; they leave the fetal liver to enter the blood stream and home to the bone marrow (BM), the main side of adult hematopoiesis.[1] More than 30 years of clinical experience as well as several animal models have demonstrated that neonatal and adult HSCs retain their ability to migrate into the BM and the capacity to reconstitute the entire hematopoietic system.[2] It appears that the homing process of transplanted HSCs is based on a naturally occurring process in which adult HSCs and progenitors travel from BM to blood and back to functional niches in BM and maybe into other organs.[3] Remarkably, despite the central role of these phenomena in hematopoietic stem cell biology and their therapeutic relevance, the molecular and cellular mechanisms, which involve chemokines for navigation, and adhesive proteins for interactions, to guide them to their appropriate niche, remain poorly understood.[4-8]

In contrast, more is known about the migration process of peripheral leukocytes in inflammatory responses in which they are attracted to leave the blood stream and enter tissues by crossing the vascular endothelium. As reviewed by Sanchez-Madrid and del Pozo,[9] the first requirement for cells that initiate migration is the acquisition of a polarized morphology that enables them to turn intracellularly generated forces into net cell locomotion. In this context it has been shown that chemokines trigger processes that induce changes in the organization of the cytoskeleton, resulting in an observable switch from a spherical into a polarized cell shape. It is established that this polarization requires the activity of phosphoinositol-3-kinase (PI3K), an enzyme involved in signal transduction events.[10,11] Polarized leukocytes form lamellipodia-like structures at the front side (ie, the leading edge) and contain a pseudopod-like projection at the rear pole called a uropod, a leukocyte-specific structure that plays an important role in cell motility and adhesion.[9] These morphologic changes are accompanied not only by the redistribution of several intracellular but also transmembrane proteins (eg, chemokine receptors become localized at the leading edge while other intercellular cell adhesion molecules, including intercellular adhesion molecules [ICAMs], CD43, and CD44, concentrate at the uropod).[9]

In our current studies we have observed that human CD34$^+$ cells acquire a polarized cell shape resembling the morphologic phenotype of migrating peripheral leukocytes when they are cultured ex vivo. Since the human CD34$^+$ cell fraction is highly enriched for HSCs and hematopoietic progenitor cells (HPCs),[12] we wondered whether there are parallels between the polarization

From the Institut für Transplantationsdiagnostik and Zelltherapeutika, Heinrich-Heine-Universität Düsseldorf, Düsseldorf, Germany; Medical Clinic and Polyclinic I, University Carl Gustav Carus, Dresden, Germany; and Max-Planck-Institute of Molecular Cell Biology and Genetics, Dresden, Germany.

Submitted February 10, 2004; accepted April 10, 2004. Prepublished online as Blood First Edition Paper, July 1, 2004; DOI 10.1182/blood-2004-02-0511.

Supported by grants from the Deutsche Forschungsgemeinschaft (SPP1109 GI 336/1-1, B.G. and P.W.; CO298/2-1, D.C.) as well as from the Forschungskommission of the Heinrich-Heine-Universität-Düsseldorf and the Stem Cell Network Nordrhein-Westfalen.

The online version of the article contains a data supplement.

Reprints: Bernd Giebel, Institut für Transplantationsdiagnostik and Zelltherapeutika, Heinrich Heine Universität Düsseldorf, Moorenstr 5, Geb 14.80, D-40225 Düsseldorf, Germany; e-mail: giebel@itz.uni-duesseldorf.de.

The publication costs of this article were defrayed in part by page charge payment. Therefore, and solely to indicate this fact, this article is hereby marked "advertisement" in accordance with 18 U.S.C. section 1734.

and migration processes of HSCs/HPCs and peripheral leukocytes. Here we have investigated this issue by immunochemistry and green fluorescent protein (GFP)–based approaches using a panel of uropod and leading-edge protein and lipid markers as well as the new hematopoietic stem and progenitor cell marker prominin-1/CD133 (human AC133 antigen)[13-15] (for review see Bhatia[16] and Corbeil et al[17]).

Materials and methods

Cell preparation and culture conditions

Umbilical cord blood (CB), BM, and peripheral blood (PB) of granulocyte colony-stimulating factor (G-CSF)–treated stem cell donors were obtained from unrelated donors after informed consent. Approval for BM and PB was obtained from the ethics commission of the Heinrich-Heine University, and approval for CB was obtained from the Paul-Ehrlich Institute. Informed consent was provided according to the Declaration of Helsinki. Mononuclear cells were isolated from individual sources by Ficoll (Biocoll Separating Solution; Biochrom, Berlin, Germany) density gradient centrifugation. Remaining red blood cells were lysed at 4°C in 0.83% ammonium chloride with 0.1% potassium hydrogen carbonate, followed by a phosphate-buffered saline (PBS) washing step. $CD34^+$ cells were isolated by magnetic cell separation using the MidiMacs technique according to the manufacturer's instructions (Miltenyi Biotec, Bergisch Gladbach, Germany), yielding $CD34^+$ cells of 65.5% ± 14.3% purity.

Freshly enriched $CD34^+$ cells were cultured in a humidified atmosphere at 37°C and 5% CO_2 at a density of approximately 1×10^5 cells/mL in serum-free (Stemspan H3000; Stemcell Technologies Inc, Vancouver, BC, Canada) or serum-containing tissue culture medium (Myelocult H5100; Stemcell Technologies Inc) in the absence or presence of early acting cytokines (fetal liver tyrosine kinase 3 ligand [FLT3L], stem cell factor [SCF], thrombopoietin [TPO]; each at 10 ng/mL final concentration; PeproTech Inc, Rocky Hill, NJ). To inhibit the PI3K activity of isolated cells we have added Ly294002 (Calbiochem, Bad Soden, Germany) at a final concentration of 50 μM to serum-free or serum-containing media supplemented with early acting cytokines.

Migration assays

Migratory potential of cultivated cells was analyzed by transmigration assays using 3-μm pore filters (Costar Transwell, 6.5-mm diameter; Corning Incorporated, Corning, NY). CB-derived $CD34^+$ cells were cultured for 2 days in Myelocult H5100 supplemented with early acting cytokines as described under "cell preparation and culture conditions." The Transwell filters were washed with Myelocult H5100 before they were loaded with 100-μL cell suspension of cultivated cells. Afterward they were carefully transferred to another well containing 600 μL Myelocult H5100 supplemented with early acting cytokines and 100 ng/mL stromal cell–derived factor-1α (SDF-1α; R&D Systems Inc, Minneapolis, MN) and cultured overnight in a humidified atmosphere at 37°C and 5% CO_2. To study the influence of PI3K activity on cell migration, the same assays were performed and Ly294002 was added at a final concentration of 100 μM to both to the top cell suspension and to the medium in the bottom chambers. The cultivation of the same amount of cells in 600 μL Myelocult H5100 supplemented with early acting cytokines and 100 ng/mL SDF-1α in the absence or presence of Ly294002 (100 μM) served as controls. Following overnight incubation, filters were carefully removed and the percentage of cells recovered in the bottom compartment was evaluated.

Immunofluorescence and microscopy

$CD34^+$ cells were generally cultured for 2 days in the presence of early acting cytokines in Myelocult H5100 medium before immunostaining. To conserve their polarized morphology, the $CD34^+$ cells were prefixed for 5 minutes at room temperature with paraformaldehyde (Sigma-Aldrich Chemie, Taufkirchen, Germany) at a final concentration of 0.2% in the medium. Cells were then incubated with the AC133-phycoerythrin (PE) antibody (1:10; AC133/1; Miltenyi Biotec) diluted in PBS containing 10% donkey serum (Jackson Immuno Research Laboratories, West Grove, PA) for at least 10 minutes at 4°C and postfixed with 4% paraformaldehyde in PBS for 20 minutes at 4°C. Because PE is not a suitable fluorochrome for immunofluorescence microscopy, we counterstained the AC133-labeled cells with cyanin 3 (Cy3)–conjugated AffiniPure Fab fragment donkey antimouse immunoglobulin G (IgG; 1:50; Jackson Immuno Research Laboratories) diluted in PBS containing 10% donkey serum for at least 10 minutes at 4°C. Remaining mouse epitopes were saturated with unconjugated AffiniPure Fab fragment rabbit antimouse IgG (1:10; Jackson Immuno Research Laboratories). Cells were divided in different aliquots and stained with one of the following primary mouse antibodies: anti-CD34–fluorescein isothiocyanate (FITC; HPCA-2; BD PharMingen, Heidelberg, Germany), anti-CD43 (1G10; BD PharMingen), anti-CD44–FITC (J173; Immunotech, Marseille, France), anti-CD45–FITC (2D1; BD PharMingen), anti-CD50 (TU41; BD PharMingen), anti-CD54–FITC (84H10; Immunotech), anti-GM3 IgM (GMR6; Seikagaku America, East Falmouth, MA), or rat anti-CXCR4 (1D9; BD PharMingen). These antibodies were counterstained using Cy2-conjugated secondary antibodies (goat antimouse IgG, donkey antimouse IgM, and goat antirat IgG + IgM; Jackson Immuno Research Laboratories). Labeled cells were mounted in 75% glycerin containing propylgallat (50 mg/mL) and DAPI (4,6 diamidino-2-phenylindole; 200 ng/mL; Roche, Mannheim, Germany).

Cells were observed with an Axioplan 2 fluorescence microscope (Carl Zeiss, Goettingen, Germany) using a ×20 dry (Figure 2A-B) or a ×100 oil immersion objective (Figures 2Ci-2Dii, 3), respectively. In general, analyses of living cells were performed at 37°C in a humidified 5% CO_2 atmosphere using a DMIRB inverse fluorescence microscope equipped with a CO_2 incubator chamber and a ×20 dry objective (Figures 1,4) (Leica, Bensheim, Germany). All pictures and videos were taken with an Axiocam digital camera and processed using Axiovision 3.1 Software (Carl Zeiss).

To analyze the degree of cell polarization, the living cells were photographed and their structure was evaluated. Cells with a comma-shaped morphology or with a recognizable tip (uropod) were determined as being polarized, whereas round and oval cells were determined as being nonpolarized. The percentage of viable cells was evaluated by trypan blue staining (0.4% solution; Sigma-Aldrich).

Plasmid construction and transfection of $CD34^+$ cells

The eukaryotic expression vector plasmid enhanced GFP (pEGFP)–N1-CD133, containing the entire coding sequence of human CD133 fused in-frame to the N-terminus of GFP, was constructed by selective polymerase chain reaction (PCR) amplification of the corresponding cDNA (GenBank accession no. AF027208) using the oligonucleotides 5′-TTGGAGTTTCTCGAGCTATGGCCCTCGTACT-3′ and 5′-TTCAACATCAGCTCGAGATGTTGTGATGG-3′ as 5′ and 3′ primers, respectively. The resulting PCR fragment was digested with *Xho*I and cloned into the corresponding site of pEGFP-N1 vector (BD Clontech, Heidelberg, Germany). The pEGFP-N1-CD44 plasmid encoding for human CD44 fused in-frame to the N-terminus of GFP was obtained by selective PCR amplification of the corresponding cDNA (GenBank accession no. AY101192) with the oligonucleotides 5′-CGCCTCGAGATCCTCCAGCTCCTTT-3′ and 5′-ATGGTGTAGAATTCGCACCCCAATC-3′ as 5′ and 3′ primers, respectively. The resulting PCR fragment was digested with *Xho*I and *Eco*RI and cloned into the corresponding sites of pEGFP-N1 vector. In both constructs, GFP is fused in-frame to the cytosolic C-terminal domain of the CD marker and their expression is under control of the cytomegalovirus (CMV) promoter.

CB-derived $CD34^+$ cells (1.5×10^5 to 3×10^5 cells) were transfected with 10 μg of plasmid DNA using the new Amaxa Nucleofection technology according to the manufacturer's instructions (Amaxa Biosystems, Cologne, Germany). As effectors we have used the pEGFP-N1-CD133 or pEGFP-N1-CD44 plasmids and, as a control, the plasmid yellow fluorescent protein–N1 (pEYFP-N1) or pEGFP-N1 vector, respectively. Following transfection, cells were immediately transferred into Myelocult H5100 supplemented with early acting cytokines. The

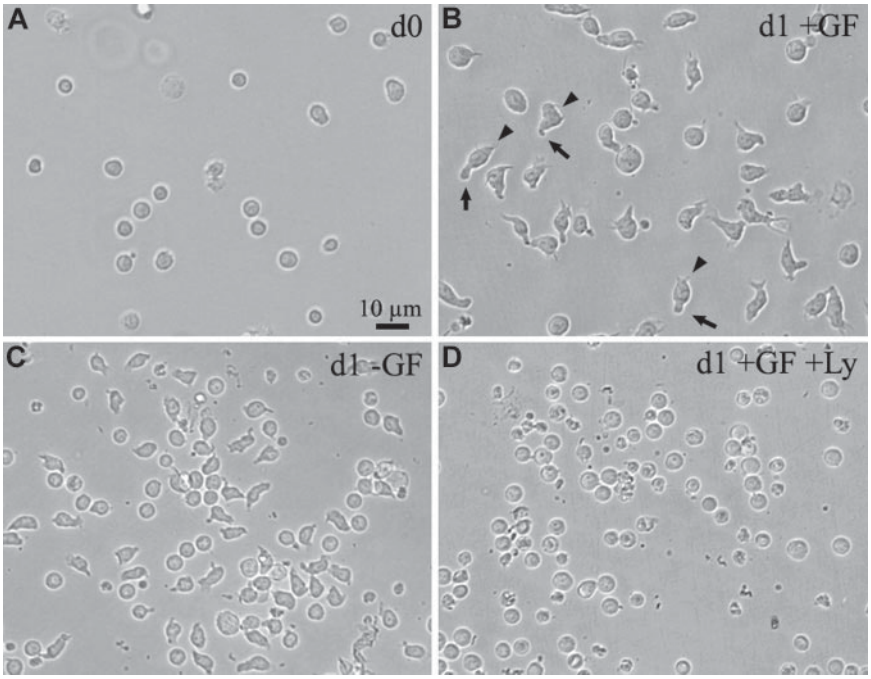

Figure 1. The human CD34$^+$ cells acquire a morphologic polarity upon in vitro cultivation. (A-C) Light micrographs of human CD34$^+$ cells freshly isolated from the umbilical cord blood (A) or cultured for 1 day (d1) in serum-free medium in the presence (B) or absence (C) of early acting cytokines as growth factors (GF). (D) The human CD34$^+$ cells were cultured in serum-free medium in the presence of early acting cytokines and PI3K inhibitor Ly294002 (Ly). All panels are shown at the same magnification. Note, CD34$^+$ cells that were cultured for 1 day in the presence of early acting cytokines (B) increase in size and acquire a polarized cell shape forming a leading edge at the front (arrowheads) and a uropod at the rear pole (arrows). Even in the absence of early acting cytokines, CD34$^+$ cells can acquire a polarized cell shape, although they do not increase in size (C). The cell polarization and the growth process are inhibited by the PI3K inhibitor (D).

efficiency of individual transfections was evaluated by staining the transfected cells 24 hours after the DNA incorporation with an anti-CD34–PE antibody (8G12; BD PharMingen) and analyzed by flow cytometry or fluorescence microscopy (see "Immunofluorescence and microscopy").

Flow cytometry

Flow cytometric analyses were performed on a Cytomics FC 500 flow cytometer equipped with the RXP software (Beckman Coulter, Krefeld, Germany).

Results

Morphologic polarization of human CD34$^+$ cells

Human CD34$^+$ cells freshly isolated from different sources (CB, BM, and PB) are small (ie, 5-6 μm), round, and without any morphologic sign of cell polarity (Figure 1A). Remarkably, a high proportion of these cells increase in size and acquire a polarized cell shape when grown on uncoated plastic dishes in the presence of early acting cytokines (SCF, TPO, FLT3L; 10 ng/mL each) in either serum-supplemented or serum-free tissue culture medium (Table 1; Figure 1B). It should be mentioned that these early acting cytokines have been reported to preserve the multipotency and engraftment potential of human HSCs/HPCs in short-term cultures.[18] Although the number of cells possessing a polarized shape is high and comparable between individual donor samples under serum-containing conditions, it is more variable under serum-free conditions (Table 1). Cells acquiring a polarized morphology form a leading-edge–like structure at one end and a uropod-like structure at the opposite side (Figure 1B, arrowheads and arrows, respectively). Even in the absence of any growth factor, some cells acquire a polarized cell shape in serum-containing or serum-free medium (Table 1), but they neither increase in size (Figure 1C) nor proliferate (data not shown). Although we did not add SDF-1 or any other chemokine, the cultivated cells were highly dynamic and exhibited an amoeboid movement that is very similar to the one described for migrating peripheral leukocytes[9] (see the time-lapse videomicroscopy imaging in supplemented material). Additionally, we have observed that flow cytometrically sorted lin$^-$CD34$^+$CD38$^{low/-}$ cells as well as lin$^-$CD34$^+$CD38$^+$ cells acquire a polarized cell shape upon cultivation in cytokine-containing media (data not shown).

Table 1. Polarization and migration of CD34$^+$ cells depend on PI3K activity

	% polarized cells	n	% living cells	n	% migrated cells	n
Culture condition d0-d1; values d1						
Serum-free + GF	64.90 ± 18.70	7	97.37 ± 1.84	3	NE	0
Serum-free	37.75 ± 19.91	7	90.91 ± 1.91	3	NE	0
Serum-free + GF + Ly294002	3.91 ± 1.47	3	92.55 ± 1.11	3	NE	0
Serum + GF	82.86 ± 5.84	7	96.74 ± 2.02	3	NE	0
Serum	42.84 ± 25.61	3	83.53 ± 16.22	3	NE	0
Serum + GF + Ly294002	9.73 ± 3.20	3	91.05 ± 1.41	3	NE	0
Culture condition d2-d3; values d3						
Serum + GF + SDF-1α	73.10 ± 3.85	3	94.48 ± 1.51	3	15.6 ± 4.20	3
Serum + GF + SDF-1α + Ly294002	14.60 ± 7.12	3	87.39 ± 4.74	3	3.3 ± 0.25	3

Data are for CB-derived CD34$^+$ cells; mean ± SD.
n indicates number of independent experiments; d0, freshly isolated cells; GF, growth factors (SCF, TPO, FLT3L); and NE, not estimated.

Polarization and migration of CD34$^+$ cells depends on PI3K activity

When PI3K activity is inhibited by addition of Ly294002, peripheral leukocytes lose their polarized shape and round up.[10] To investigate if PI3K activity is also required for the polarization of CD34$^+$ cells we have cultured CB-derived CD34$^+$ cells in early acting cytokine-supplemented media, in the presence or absence of Ly294002. While most of the CD34$^+$ cells present in the control group acquired a polarized cell shape after 1 day (Table 1; Figure 1B), treated cells remained round (Table 1; Figure 1D) and viable (Table 1). Furthermore, when adding Ly294002 to polarized CD34$^+$ cells cultured for 2 days in serum and early acting cytokine-containing medium, many of them lose their polarized morphology and round up but remain viable (Table 1). Taken together these data suggest that the PI3K pathway is involved in the polarization process of CD34$^+$ cells.

Because cell polarity is an essential prerequisite for the migration process of several cell types,[9] we have tested whether CD34$^+$ cells that lose their polarized cell shape have a reduced migration capacity. Therefore, we have examined the migration rate of CB-derived CD34$^+$ cells, which were originally cultured for 2 days in serum and early acting cytokine-containing medium, in the presence or absence of the PI3K inhibitor Ly294002 using a transmigration assay. In the absence of Ly294002, 15.6% ± 4.20% of the CD34$^+$ cells migrated through 3-μm pores of Transwell filters, whereas only 3.3% ± 0.25% of the cells treated with this PI3K inhibitor passed through the pores (Table 1).

The hematopoietic stem cell marker CD133 is redistributed to the uropod-like structure of migrating human CD34$^+$ cells

A hallmark of the polarization of migrating peripheral leukocytes is an asymmetric redistribution of certain cell surface proteins into the well-defined architectural structures, the uropod and the leading edge.[9] This prompted us to examine, by immunochemistry, the distribution of hematopoietic stem and progenitor marker CD133 in nonpolarized and polarized (ie, migrating) CD34$^+$ cells. In our hands more than 90% of CD34$^+$ cells isolated from CB, PB, or BM express CD133 (data not shown). Interestingly, we found that CD133, which is distributed over the entire cell surface of freshly isolated CB-derived CD34$^+$ cells (Figure 2A,Ci-ii), is redistributed into the tip of the uropod-like structure in polarized CD34$^+$ cells (Figure 2B,Di-ii). Under the same conditions, the cell surface redistribution of CD133 is not observed in nonpolarized cells (Figure 2B arrowhead). The same phenomenon is observed with CD34$^+$ cells isolated from BM and PB (data not shown).

Segregation of several plasma membrane markers in polarized human CD34$^+$ cells

Given the high similarity observed between the migrating CD34$^+$ cells and peripheral leukocytes we decided to investigate the subcellular distribution of several membrane protein markers, including adhesion molecules and one membrane receptor, known to be enriched either in the uropod or at the leading edge of migrating peripheral leukocytes.[9] Immunochemistry revealed that CD markers previously reported to be concentrated into the uropod of migrating peripheral leukocytes,[9] including CD43, CD44, CD50 (ICAM3), and CD54 (ICAM1), are also enriched in the uropod-like structure of CB-derived CD34$^+$ cells and colocalized with CD133 (Figure 3A-D). Similar data were obtained with PB-derived CD34$^+$ cells (data not shown).

In contrast, we found that the CXCR4 chemokine receptor, which has been reported to be redistributed at the leading edge of B and T lymphocytes upon exposure to chemokines,[19-21] appeared as a gradient with its highest expression in the leading edge of CD34$^+$ cells (Figure 3G). Finally, the segregation of CD

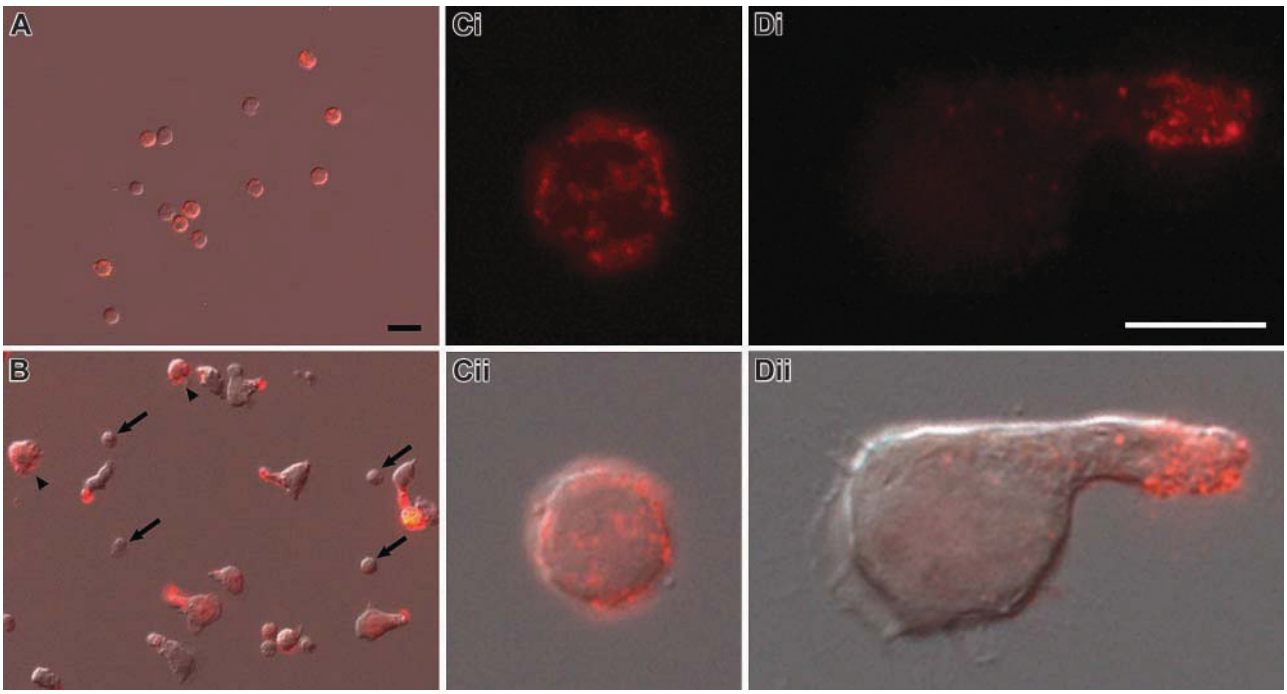

Figure 2. Cell surface redistribution of CD133 into the uropod of polarized CD34$^+$ cells. (A-D) Human CD34$^+$ cells, freshly isolated from umbilical cord blood (A,Ci-ii) or cultured for 2 days in the presence of early acting cytokines (B,Di-ii), were labeled with AC133 antibody (anti-CD133; red) and observed by immunofluorescence (Ci,Di). The overlays with the corresponding differential interference contrast images are shown (A-B,Cii,Dii). Note that the cultured CD133$^-$ cells remain small and round (arrows in B), whereas cultured CD133$^+$ cells increase in size and CD133 becomes localized into the uropod of polarized cells (B,Di-ii) but remains distributed all over the surface of nonpolarized CD133$^+$ cells (arrowheads in B). Same magnification was used in panels A and B (scale bar = 10 μm; A) or in panels Ci and Di (scale bar = 5 μm; Di), respectively.

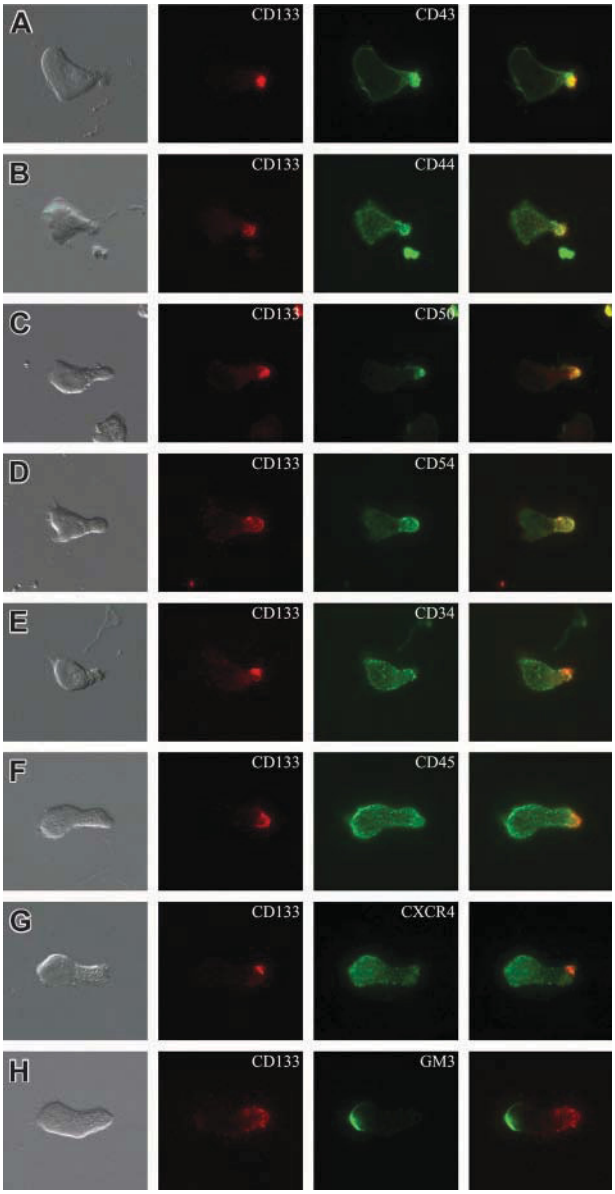

Figure 3. Cell surface distribution of plasma membrane markers in polarized CD34⁺ cells. (A-H) CD34⁺ cells isolated from umbilical cord blood and cultured for 2 days in serum-containing medium supplemented with early acting cytokines were subjected to double labeling using AC133 antibody (anti-CD133) and an antibody directed against another cell surface antigen, as indicated, and analyzed by double immunofluorescence. The CD133 immunofluorescence (red) is shown in the second column, the immunofluorescence of various cell surface antigens (green) in the third column, and the corresponding differential interference contrast image as well as the merge are shown in the first and the fourth column, respectively. Note that the chemokine receptor CXCR4 (G) and the ganglioside GM3 (H) are concentrated in the leading edge of the front pole, whereas CD43 (A), CD44 (B), ICAM3/CD50 (C), and ICAM1/CD54 (D) are enriched in the uropod of the polarized cells and colocalized with CD133. All panels are shown at the same magnification.

markers observed here is not a common characteristic shared by all of them since CD34 and CD45 are found equally distributed all over the surface of polarized CD34⁺ cells (Figure 3E and F, respectively).

Recently, it has been demonstrated that during polarization of T cells the monosi θ alogangliosi de GM3, a raft-associated lipid, redistributes to the leading edge of activated leukocytes.[22] To corroborate further the similarity underlying the polarization process between CD34⁺ cells and activated leukocytes, we analyzed the distribution of GM3 in CD34⁺ cells by immunochemistry. Remarkably, we found that GM3 is localized at the leading edge of polarized CD34⁺ cells (Figure 3H).

CD44-GFP and CD133-GFP fusion proteins are localized in the uropod of transfected human CD34⁺ cells

The morphologic data strongly suggest that certain plasma membrane markers are partitioned into specialized regions or domains of migrating human CD34⁺ cells. To rule out that the compartmentalization observed is generated by the use of antibodies creating an artificial cluster of a given membrane marker, we monitored the distribution of the protein markers CD44 and CD133 fused to green fluorescent protein (GFP) in living CB-derived CD34⁺ cells. Under the specific and new nonviral transfection conditions described here (see "Plasmid construction and transfection of CD34 cells" in "Materials and methods"), up to 80% of CB transfected cells expressed the fluorescence protein reporter gene (Figure 4Cii quadrants A2 and A4), which is distributed into the entire cytoplasm (Figure 4Ci). No fluorescence is observed with untransfected cells (Figure 4B quadrants A2 and A4). Interestingly, fluorescence microscopy revealed that CD44-GFP fusion protein, which is expressed in more than 75% of transfected cells (Figure 4Dii quadrants A2 and A4), is associated with the entire plasma membrane being enriched in the uropod of the CB-derived cells (Figure 4Di). Likewise, CD133-GFP is selectively concentrated at the tip of the uropod of polarized CD34⁺ cells (Figure 4Ei), as previously observed by immunochemistry for the endogenous CD133 (Figures 2-3). It should be mentioned that in comparison to fluorescence protein alone and CD44-GFP, CD133-GFP is detected only in a specific subpopulation of CB-derived cells (ie, CD34⁺ cells; Figure 4Ei quadrant A2).

Discussion

Here we report 4 major observations. First, HSCs/HPCs acquire a polarized cell shape by a molecular mechanism dependent on the PI3K pathway. Second, polarized HSCs/HPCs exhibit an amoeboid movement, which is similar to the one described for migrating peripheral leukocytes. Third, the polarization of HSC/HPC plasma membrane leads to a redistribution of a particular set of markers from which several of them have been previously reported to be associated with lipid microdomains (lipid rafts). Fourth, the stem cell marker CD133 is selectively concentrated in the uropod of polarized HSCs/HPCs.

It is well established that HSCs/HPCs have the ability to migrate.[1-3] Despite the evidence that SDF-1 triggers migration of HSCs/HPCs,[4-8] the current knowledge of the mechanisms governing stem cell migration remains limited. For other cell types it has been shown that the acquisition of cell polarity is an essential prerequisite for the migration process.[9] Although it has been noticed that some CD34⁺ cells acquire a polarized cell shape upon adhesion to fibronectin[23] or when migrating under the influence of SDF-1 through a fibronectin-coated Transwell filter or a 3-dimensional meshwork of extracellular matrix components,[5,24] the issue of cell polarity in HSCs/HPCs has not been analyzed in detail.

We were able to document that the CD34⁺ cells grown in suspension cultures in the presence of early acting cytokines acquire a polarized cell shape with a defined leading edge at the front pole and a uropod at the rear pole. This morphologic phenotype is highly related to the one described for polarized, migrating peripheral leukocytes. Since the polarization of peripheral leukocytes depends on the activity of chemokines,[20,25,26] it is

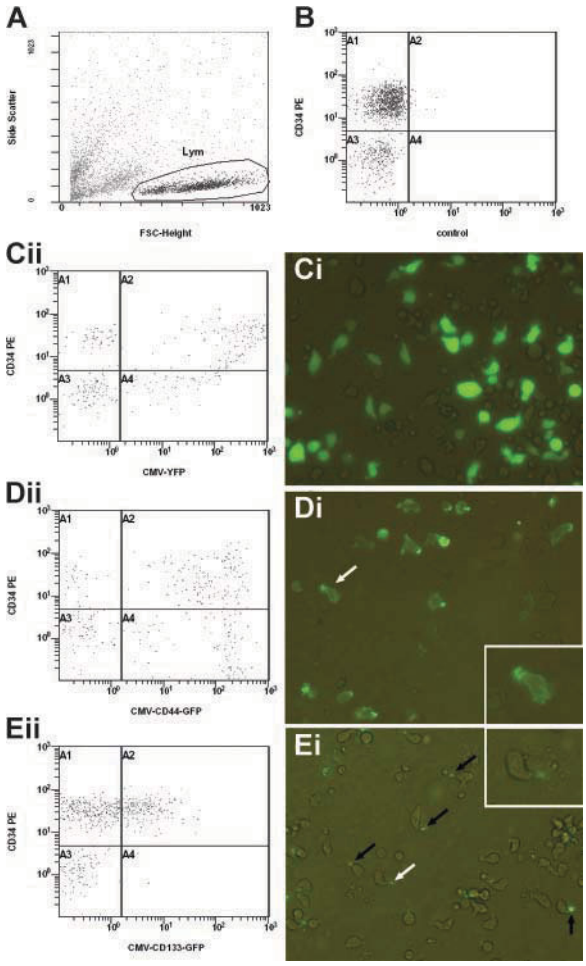

Figure 4. Subcellular localization of CD44-GFP and CD133-GFP fusion proteins in transfected CD34$^+$ cells. Using the new Amaxa nucleofection technology, human CD34$^+$ cells enriched from umbilical cord blood were transfected with the expression plasmid encoding either for YFP (Ci), CD44-GFP (Di-ii) or CD133-GFP (Ei-ii) under the control of the cytomegalovirus promoter. Transfected cells and, as negative control, untransfected cells (B) were cultivated for 1 day in serum-containing medium supplemented with early acting cytokines and were analyzed by flow cytometry (A-B,Cii,Dii,Eii) and fluorescence microscopy (Ci,Di,Ei). (A-B,Cii,Dii,Eii) A representative experiment (n = 5) of the CB-derived cells untransfected (B) or transfected with different expression plasmids (Cii,Dii,Eii) was stained with a PE-conjugated anti-CD34 antibody and analyzed by flow cytometry. The cells analyzed in panels B, Cii, Dii, and Eii were gated according to the morphology depicted on a forward scatter/side scatter plot (A). Note, cells shown in panel Cii are extremely positive for YFP; most of them stick to the right border of the plot. (Ci,Di,Ei). Differential interference contrast image shows fluorescence overlay of YFP (Ci), CD44-GFP (Di), or CD133-GFP (Ei) in living transfected CD34$^+$-enriched cells. The YFP is strongly expressed throughout the cytoplasm of the cells, whereas CD44-GFP and CD133-GFP are concentrated in the uropod of the migrating cells (arrows in Di and Ei). The white arrows indicate the cells shown in the insets (high magnification).

very suggestive that similar factors are not only involved in the migration process of HSCs but also required for the polarization of these cells. However, our data show that chemokines, including SDF-1, do not appear essential for the polarization of CD34$^+$ cells. Moreover, although it is not known yet which factor triggers such polarization, we provide evidence that the activation of the PI3K pathway is crucial for this process, being consistent with results obtained for peripheral leukocytes.[10,11] It is interesting to note that SCF, which was added to most of our cultures, has been reported to activate the PI3K signaling pathway similarly to SDF-1.[10,11,27-29] SCF also has the capability to act as a chemoattractant for human HPCs,[8] arguing that other factors than chemokines can induce polarization and migration of CD34$^+$ cells. Finally, it is important to point out that the serum-free culture medium used in our assays contains insulin, which is another potential activator of the PI3K.[30] Therefore, insulin might be responsible for the polarization of CD34$^+$ cells under serum-free conditions in the absence of cytokines.

As mentioned in "Introduction," the polarization process seems to be a prerequisite for cell migration. Indeed we show that CD34$^+$ cells treated with a PI3K inhibitor lose not only their polarized morphology but also their ability to migrate, suggesting that polarization and migration are closely connected to each other in CD34$^+$ cells, as they are in other cell types. The inhibition of these cellular processes may explain why the homing of CD34$^+$ cells is disturbed when PI3K signaling is perturbed.[31]

In addition to the importance of the PI3K signaling, we have demonstrated that polarization of CD34$^+$ cells is accompanied by the redistribution of certain transmembrane proteins. As in other leukocytes, CD43, CD44, CD50 (ICAM3), and CD54 (ICAM1) become concentrated into the uropod of CD34$^+$ cells, whereas other molecules such as CD34 or CD45 remain distributed all over the plasma membrane.

The phenotypic similarity between polarized progenitor cells and other leukocytes is not restricted to their morphology and the distribution of uropod markers. We show that the chemokine receptor CXCR4, which is known to be enriched in the leading edge of migrating lymphocytes, is distributed in a gradient-like fashion with its maximal concentration in the leading edge of polarized CD34$^+$ cells. In agreement with this finding, van Buul and colleagues[32] have reported recently that a CXCR4-GFP fusion protein redistributes to the leading edge of the KG1a cells, an acute myeloid leukemia (AML)–derived cell line.

There is growing evidence that many membrane proteins are associated with certain lipids (eg, sphingolipid or cholesterol-based lipids). Such lipids are often clustered in special microdomains, in so-called lipid rafts.[33] Depending on the lipids that form a special raft, lipid rafts traffic to certain plasma membrane domains (eg, the apical or basal plasma membrane). In this context they seem to function as platforms that are important to govern the subcellular distribution of associated membrane proteins.[33] Indeed, it has been shown that polarization of peripheral leukocytes depends on the controlled redistribution of such specialized lipid rafts.[22,34] In activated T cells for example, the monosialoganglioside GM3-enriched lipid rafts traffic to the leading edge, while others redistribute to the uropod pole, concentrating a specific set of membrane proteins, such as ICAM3, CD43, and CD44, there.[22,34] The observation that these raft-associated markers are also concentrated at the uropod pole and GM3 at the leading edge of CD34$^+$ cells further reinforces existing parallels in the polarization process of HSCs/HPCs with peripheral leukocytes and suggests that lipid rafts are also important for the polarization of HSCs/HPCs. Therefore, it is tempting to speculate that cues and mechanisms underlying the polarization and migration of precursors and more mature hematopoietic cells appear common to all of them.

Interestingly, we found that the stem cell marker CD133, a cholesterol-binding protein,[35] is also redistributed into the uropod of migrating CD34$^+$ cells. Since CD133 is preferentially associated with plasma membrane protrusions in all cell types where it is expressed,[35-38] and is incorporated into lipid rafts,[35] it seems very likely that special lipid rafts organize the delivery and/or retention of CD133 in the uropod. As CD133 is selectively associated with microvilli and other plasma membrane protrusions within the apical plasma membrane in different epithelia of embryonic and adult tissues,[37,38] it might be possible that epithelial cells and

HSCs/HPCs use a similar mechanism to distribute CD133. In agreement with the postulation that the targeting and retention of proteins into a specialized plasma membrane domain of distinct cell types are mediated by a common intracellular machinery,[39] the uropod of polarized HSCs/HPCs and therefore of other leukocytes would correspond to the apical domain of polarized epithelial cells.

In conclusion, our data show for the first time that the polarization and migration processes of $CD34^+$ cells are highly related to those reported for migrating peripheral leukocytes. The comprehensive knowledge about these mechanisms in peripheral leukocyte biology should increase our understanding about HSC/HPC traffic during normal and malignant hematopoiesis and should help to improve the process of homing and engraftment of stem cells in clinical trials.

Acknowledgment

We thank Michael Punzel for general discussion, comments on the manuscript, and providing us with PB and BM samples.

References

1. Dzierzak E. Hematopoietic stem cells and their precursors: developmental diversity and lineage relationships. Immunol Rev. 2002;187:126-138.
2. Weissman IL. Translating stem and progenitor cell biology to the clinic: barriers and opportunities. Science. 2000;287:1442-1446.
3. Wright DE, Wagers AJ, Gulati AP, Johnson FL, Weissman IL. Physiological migration of hematopoietic stem and progenitor cells. Science. 2001; 294:1933-1936.
4. Peled A, Petit I, Kollet O, et al. Dependence of human stem cell engraftment and repopulation of NOD/SCID mice on CXCR4. Science. 1999;283: 845-848.
5. Peled A, Kollet O, Ponomaryov T, et al. The chemokine SDF-1 activates the integrins LFA-1, VLA-4, and VLA-5 on immature human CD34(+) cells: role in transendothelial/stromal migration and engraftment of NOD/SCID mice. Blood. 2000;95:3289-3296.
6. Aiuti A, Webb IJ, Bleul C, Springer T, Gutierrez-Ramos JC. The chemokine SDF-1 is a chemoattractant for human CD34+ hematopoietic progenitor cells and provides a new mechanism to explain the mobilization of CD34+ progenitors to peripheral blood. J Exp Med. 1997;185:111-120.
7. Mohle R, Bautz F, Rafii S, Moore MA, Brugger W, Kanz L. The chemokine receptor CXCR-4 is expressed on CD34+ hematopoietic progenitors and leukemic cells and mediates transendothelial migration induced by stromal cell-derived factor-1. Blood. 1998;91:4523-4530.
8. Kim CH, Broxmeyer HE. In vitro behavior of hematopoietic progenitor cells under the influence of chemoattractants: stromal cell-derived factor-1, steel factor, and the bone marrow environment. Blood. 1998;91:100-110.
9. Sanchez-Madrid F, del Pozo MA. Leukocyte polarization in cell migration and immune interactions. EMBO J. 1999;18:501-511.
10. Sotsios Y, Whittaker GC, Westwick J, Ward SG. The CXC chemokine stromal cell-derived factor activates a Gi-coupled phosphoinositide 3-kinase in T lymphocytes. J Immunol. 1999;163:5954-5963.
11. Vicente-Manzanares M, Rey M, Jones DR, et al. Involvement of phosphatidylinositol 3-kinase in stromal cell-derived factor-1 alpha-induced lymphocyte polarization and chemotaxis. J Immunol. 1999;163:4001-4012.
12. Krause DS, Fackler MJ, Civin CI, May WS. CD34: structure, biology, and clinical utility. Blood. 1996; 87:1-13.
13. Fargeas CA, Corbeil D, Huttner WB. AC133 antigen, CD133, prominin-1, prominin-2, etc: prominin family gene products in need of a rational nomenclature. Stem Cells. 2003;21:506-508.
14. Miraglia S, Godfrey W, Yin AH, et al. A novel five-transmembrane hematopoietic stem cell antigen: isolation, characterization, and molecular cloning. Blood. 1997;90:5013-5021.
15. Yin AH, Miraglia S, Zanjani ED, et al. AC133, a novel marker for human hematopoietic stem and progenitor cells. Blood. 1997;90:5002-5012.
16. Bhatia M. AC133 expression in human stem cells. Leukemia. 2001;15:1685-1688.
17. Corbeil D, Roper K, Fargeas CA, Joester A, Huttner WB. Prominin: a story of cholesterol, plasma membrane protrusions and human pathology. Traffic. 2001;2:82-91.
18. Luens KM, Travis MA, Chen BP, Hill BL, Scollay R, Murray LJ. Thrombopoietin, kit ligand, and flk2/flt3 ligand together induce increased numbers of primitive hematopoietic progenitors from human CD34+Thy-1+Lin- cells with preserved ability to engraft SCID-hu bone. Blood. 1998;91: 1206-1215.
19. Nieto M, Frade JM, Sancho D, Mellado M, Martinez AC, Sanchez-Madrid F. Polarization of chemokine receptors to the leading edge during lymphocyte chemotaxis. J Exp Med. 1997;186:153-158.
20. Vicente-Manzanares M, Montoya MC, Mellado M, et al. The chemokine SDF-1alpha triggers a chemotactic response and induces cell polarization in human B lymphocytes. Eur J Immunol. 1998;28: 2197-2207.
21. Pelletier AJ, van der Laan LJ, Hildbrand P, et al. Presentation of chemokine SDF-1 alpha by fibronectin mediates directed migration of T cells. Blood. 2000;96:2682-2690.
22. Gomez-Mouton C, Abad JL, Mira E, et al. Segregation of leading-edge and uropod components into specific lipid rafts during T cell polarization. Proc Natl Acad Sci U S A. 2001;98:9642-9647.
23. Fruehauf S, Srbic K, Seggewiss R, Topaly J, Ho AD. Functional characterization of podia formation in normal and malignant hematopoietic cells. J Leukoc Biol. 2002;71:425-432.
24. Voermans C, Anthony EC, Mul E, van der Schoot E, Hordijk P. SDF-1-induced actin polymerization and migration in human hematopoietic progenitor cells. Exp Hematol. 2001;29:1456-1464.
25. del Pozo MA, Sanchez-Mateos P, Nieto M, Sanchez-Madrid F. Chemokines regulate cellular polarization and adhesion receptor redistribution during lymphocyte interaction with endothelium and extracellular matrix: involvement of cAMP signaling pathway. J Cell Biol. 1995;131:495-508.
26. Nieto M, Navarro F, Perez-Villar JJ, et al. Roles of chemokines and receptor polarization in NK-target cell interactions. J Immunol. 1998;161:3330-3339.
27. Lev S, Givol D, Yarden Y. Interkinase domain of kit contains the binding site for phosphatidylinositol 3' kinase. Proc Natl Acad Sci U S A. 1992;89: 678-682.
28. Timokhina I, Kissel H, Stella G, Besmer P. Kit signaling through PI 3-kinase and Src kinase pathways: an essential role for Rac1 and JNK activation in mast cell proliferation. EMBO J. 1998;17: 6250-6262.
29. Feng LX, Ravindranath N, Dym M. Stem cell factor/c-kit up-regulates cyclin D3 and promotes cell cycle progression via the phosphoinositide 3-kinase/p70 S6 kinase pathway in spermatogonia. J Biol Chem. 2000;275:25572-25576.
30. Cheatham B, Vlahos CJ, Cheatham L, Wang L, Blenis J, Kahn CR. Phosphatidylinositol 3-kinase activation is required for insulin stimulation of pp70 S6 kinase, DNA synthesis, and glucose transporter translocation. Mol Cell Biol. 1994;14: 4902-4911.
31. Wang JF, Park IW, Groopman JE. Stromal cell-derived factor-1alpha stimulates tyrosine phosphorylation of multiple focal adhesion proteins and induces migration of hematopoietic progenitor cells: roles of phosphoinositide-3 kinase and protein kinase C. Blood. 2000;95:2505-2513.
32. van Buul JD, Voermans C, van Gelderen J, Anthony EC, van der Schoot CE, Hordijk PL. Leukocyte-endothelium interaction promotes SDF-1-dependent polarization of CXCR4. J Biol Chem. 2003;278:30302-30310.
33. Simons K, Ikonen E. Functional rafts in cell membranes. Nature. 1997;387:569-572.
34. Millan J, Montoya MC, Sancho D, Sanchez-Madrid F, Alonso MA. Lipid rafts mediate biosynthetic transport to the T lymphocyte uropod subdomain and are necessary for uropod integrity and function. Blood. 2002;99:978-984.
35. Roper K, Corbeil D, Huttner WB. Retention of prominin in microvilli reveals distinct cholesterol-based lipid micro-domains in the apical plasma membrane. Nat Cell Biol. 2000;2:582-592.
36. Corbeil D, Roper K, Hannah MJ, Hellwig A, Huttner WB. Selective localization of the polytopic membrane protein prominin in microvilli of epithelial cells: a combination of apical sorting and retention in plasma membrane protrusions. J Cell Sci. 1999;112(pt 7):1023-1033.
37. Weigmann A, Corbeil D, Hellwig A, Huttner WB. Prominin, a novel microvilli-specific polytopic membrane protein of the apical surface of epithelial cells, is targeted to plasmalemmal protrusions of non-epithelial cells. Proc Natl Acad Sci U S A. 1997;94:12425-12430.
38. Corbeil D, Roper K, Hellwig A, et al. The human AC133 hematopoietic stem cell antigen is also expressed in epithelial cells and targeted to plasma membrane protrusions. J Biol Chem. 2000;275:5512-5520.
39. Keller P, Simons K. Post-Golgi biosynthetic trafficking. J Cell Sci. 1997;110(pt 24):3001-3009.

Asymmetric cell division within the human hematopoietic stem and progenitor cell compartment: identification of asymmetrically segregating proteins

Julia Beckmann,[1] Sebastian Scheitza,[1] Peter Wernet,[1] Johannes C. Fischer,[1] and Bernd Giebel[1]

[1]Institute for Transplantation Diagnostics and Cellular Therapeutics, Heinrich-Heine-University Düsseldorf, Germany

The findings that many primitive human hematopoietic cells give rise to daughter cells that adopt different cell fates and/or show different proliferation kinetics suggest that hematopoietic stem cells (HSCs) and hematopoietic progenitor cells (HPCs) can divide asymmetrically. However, definitive experimental demonstration is lacking due to the current absence of asymmetrically segregating marker molecules within the primitive hematopoietic cell compartment. Thus, it remains an open question as to whether HSCs/HPCs have the capability to divide asymmetrically, or whether the differences that have been observed are established by extrinsic mechanisms that act on postmitotic progenitors. Here, we have identified 4 proteins (CD53, CD62L/L-selectin, CD63/lamp-3, and CD71/transferrin receptor) that segregate differentially in about 20% of primitive human hematopoietic cells that divide in stroma-free cultures. Therefore, this indicates for the first time that HSCs/HPCs have the capability to divide asymmetrically. Remarkably, these proteins, in combination with the surrogate stem-cell marker CD133, help to discriminate the more primitive human cultivated HSCs/HPCs. Since 3 of these proteins, the transferrin receptor and the tetraspanins CD53 and CD63, are endosomal-associated proteins, they may provide a link between the endosomal compartment and the process of asymmetric cell division within the HSC/HPC compartment. (Blood. 2007;109:5494-5501)

Introduction

Somatic stem cells are undifferentiated cells that can self-renew over a long period of time in vivo and give rise to progenitor cells that are committed to differentiate. Since both uncontrolled expansion as well as loss of stem cells would be fatal for multicellular organisms, the decision of self-renewal versus differentiation needs to be tightly controlled. Therefore, key questions in stem cell biology are how and which mechanisms govern these decisions. Although mammalian hematopoietic stem cells (HSCs) are the most intensively investigated somatic stem cells, the nature of the factors controlling self-renewal and differentiation remain largely unknown.

There is good evidence that HSCs can expand in vivo[1] and be maintained in vitro in close contact to adequate stroma cells.[2-5] These observations point toward the existence of specialized HSC niches, which was already hypothesized as early as 1978.[6] Indeed, it was recently shown that osteoblasts are key elements of HSC niches in the endosteum of bone marrow (BM) and sinusoidal endothelial cells of vascular HSC niches found in the spleen and BM.[7-9] In addition to the data supporting the HSC niche model that likely provides cell extrinsic cue, evidence suggest that cells of the HSC and hematopoietic progenitor cell (HPC) compartment contain capabilities to divide asymmetrically. Ogawa and colleagues showed that after separation of paired murine and human HPCs that were cultured in stroma-free suspension conditions, siblings gave rise to colonies with significantly different characteristics.[10-12] More recently, HSC-enriched cell populations were found to be highly heterogeneous in respect to their function and their proliferation kinetics (ie, the proliferation rate of more primitive cells is slower than that of committed ones).[13-15] Furthermore, it was observed that approximately 30% of primitive hematopoietic cells ($CD34^+CD38^-$ cells) give rise to daughter cells with heterogeneous proliferation kinetics and functions.[14-16]

Recently, we showed that human myeloid-lymphoid initiating cells (ML-ICs), a subfraction of the $CD34^+CD38^-$ cells, when cultured under stroma-free conditions give rise to daughters that adopt different cell fates, with 1 cell inheriting the developmental capacity of the mother cell, and 1 cell becoming more specified.[17] Similarly, in mice, up to 62% of primitive hematopoietic cells ($lin^-CD34^{low/-}c\text{-}kit^+Sca\text{-}1^+$) give rise to daughter cells with different myeloid developmental potentials.[18,19] Although all these observations are in accordance with the model of asymmetric cell division in which primitive hematopoietic cells contain the potential to give birth to 2 intrinsically different daughter cells, it cannot be concluded that the observed differences are indeed the result of an asymmetric cell division. In principle, these differences could have been established by postmitotic, extrinsic decision processes.[17,20,21]

In organisms like *Drosophila melanogaster* and *Caenorhabditis elegans*, in which asymmetric cell divisions have been proven to occur, cells that divide asymmetrically are polarized during cell division and localize specific molecules to distinct regions of the cell, which are then transmitted unequally into the daughters.[22] Therefore, to demonstrate that primitive hematopoietic cells can indeed divide asymmetrically, molecules that clearly segregate asymmetrically during mitoses of these cells need to be identified. Here, we describe the identification of proteins containing extracellular epitopes, which segregate differentially to daughters during mitosis of approximately 20% of the human $CD34^+CD133^+$

Submitted November 2, 2006; accepted February 25, 2007. Prepublished online as *Blood* First Edition Paper, March 1, 2007; DOI 10.1182/blood-2006-11-055921.

The online version of this article contains a data supplement.

The publication costs of this article were defrayed in part by page charge payment. Therefore, and solely to indicate this fact, this article is hereby marked "advertisement" in accordance with 18 USC section 1734.

hematopoietic cells and confirm the occurrence of asymmetric cell division within the human HSC and HPC compartment.

Materials and methods

Cell source and preparation

Human umbilical cord blood (CB), BM, and peripheral blood (PB) of granulocyte colony-stimulating factor (G-CSF)–treated stem cell donors were obtained from unrelated donors after informed consent was obtained in accordance with the Declaration of Helsinki. The use of human cord blood was approved by the ethics committee of Heinrich-Heine University. Mononuclear cells (MNCs) were isolated from individual sources by Ficoll (Biocoll Separating Solution; Biochrom AG, Berlin, Germany) density gradient centrifugation as described previously.[23] $CD34^+$ cells were isolated by magnetic cell separation using the MidiMacs technique according to the manufacturer's instructions (Miltenyi Biotec, Bergisch Gladbach, Germany).

If not stained immediately, freshly purified MNCs were cultured in a humidified atmosphere at 37°C and 5% CO_2 at a density of approximately 1×10^6 cells/mL and freshly enriched $CD34^+$ cells at a density of approximately 1×10^5 cells/mL in I20 (Iscove modified Dulbecco medium [IMDM; Invitrogen, Karlsruhe, Germany] supplemented with 20% fetal calf serum [FCS; Biochrom AG], 1000 U/mL penicillin, and 100 U/mL streptomycin [Invitrogen]) in the presence of early-acting cytokines (fetal liver tyrosine kinase 3 ligand [FLT3L], stem cell factor [SCF], and thrombopoietin [TPO], each at 10 ng/mL final concentration [all from PeproTech, Rocky Hill, NJ]).

Flow cytometry

For the proliferation kinetics, freshly isolated $CD34^+$ cells were stained for 4 minutes with 2 μM PKH2 (Sigma-Aldrich Chemie, Taufkirchen, Germany). After 1 washing step, stained cells were cultured in I20 in the presence of early-acting cytokines. For flow cytometric analyses, cells were stained with AC133-phycoerythrin (PE; Miltenyi Biotec) and anti-CD34–PE/cytochrome 5 (PCy5) antibodies (BD PharMingen, Heidelberg, Germany).

For the screening procedure, MNCs were stained with different combinations of 3 different antibodies as described in paragraph 3 of Results. A list of the antibodies used is given in Table S1, available on the *Blood* website; see the Supplemental Table link at the top of the online article).

Flow cytometric analyses were performed on a Cytomics FC 500 flow cytometer equipped with the RXP software (Beckman Coulter, Krefeld, Germany).

For the functional assays, the cells were highly purified using a Coulter EPICS Elite ESP fluorescence cell sorting system equipped with the Expo32 software (Beckman Coulter).

Immunofluorescence and microscopy

For subcellular localization studies of polarized and dividing primitive hematopoietic cells, $CD34^+$ cells were cultured for 3 or 4 days in the presence of early-acting cytokines in I20 medium before immunostaining. To conserve their morphology, the $CD34^+$ cells were prefixed for 5 minutes at room temperature with paraformaldehyde (Sigma-Aldrich Chemie) at a final concentration of 0.2% in the medium. As the AC133 epitope of CD133 is sensitive to formaldehyde and paraformaldehyde fixation, the cells for the extracellular staining procedure were then incubated with the AC133-PE antibody (1:10; AC133/1; Miltenyi Biotec) diluted in PBS containing 10% donkey serum (Jackson ImmunoResearch Laboratories, West Grove, PA). They were stained for at least 10 minutes at 4°C, and then postfixed with 4% paraformaldehyde in PBS for 20 minutes at 4°C. Because PE is not a suitable fluorochrome for immunofluorescence microscopy, we counterstained the AC133-labeled cells with Cy3-conjugated AffiniPure Fab fragment donkey anti-mouse IgG (1:20; Jackson ImmunoResearch Laboratories) diluted in PBS containing 10% donkey serum for at least 10 minutes at 4°C. Remaining mouse epitopes were saturated with unconjugated AffiniPure Fab fragment rabbit anti-mouse IgG (1:10; Jackson ImmunoResearch Laboratories). Cells were divided in different aliquots and stained with 1 of the following primary mouse antibodies: anti-CD43–FITC (1G10; BD PharMingen), anti-CD44–FITC (J173; Coulter Immunotech, Krefeld, Germany), anti-CD50–FITC (TU41; BD PharMingen), anti-CD54–FITC (84H10; Coulter Immunotech), anti-CD53–FITC (HI29; BD PharMingen), anti-CD62L (FREG56; Coulter Immunotech), anti-CD63–FITC (H5C6; BD PharMingen), or anti-CD71 (YDJ1.2.2; Coulter Immunotech). These antibodies were counterstained using Cy2-conjugated secondary antibodies (1:100; goat anti-mouse IgG; Jackson ImmunoResearch Laboratories).

For the intracellular staining procedure, cultured and prefixed $CD34^+$ cells were fixed with 4% paraformaldehyde in PBS for 20 minutes at 4°C and permeabilized using 0.1% Triton X100 (Sigma-Aldrich Chemie) in PBS. After blocking in 10% donkey serum (Jackson ImmunoResearch Laboratories), cells were incubated with the anti-CD63 antibody (1:50; H5C5; BD PharMingen) for at least 30 minutes at room temperature and counterstained with Cy3-conjugated AffiniPure Fab fragment donkey anti-mouse IgG (1:100; Jackson ImmunoResearch Laboratories) diluted in PBS containing 10% donkey serum for another 30 minutes at room temperature. After saturating remaining mouse epitopes with unconjugated AffiniPure Fab fragment rabbit anti-mouse IgG (1:10; Jackson ImmunoResearch Laboratories), cells were stained with the anti-CD71 antibody (1:50; YDJ1.2.2; Coulter Immunotech) and counterstained with Cy2-conjugated secondary antibodies (1:400 goat anti-mouse IgG; Jackson ImmunoResearch Laboratories).

Labeled cells were mounted in 75% glycerin containing propylgallat (50 mg/mL) and DAPI (200 ng/mL; Roche, Mannheim, Germany) and observed with an Axioplan 2 fluorescence microscope (Carl Zeiss, Goettingen, Germany) using a Zeiss Plan-Neofluar 100× objective lens (1.3 NA O). Pictures were taken with an Axiocam digital camera and processed using Axiovision 4.5 Software (Carl Zeiss).

Functional assays

For the long-term culture-initiating cell (LTC-IC) assays, approximately 6000 sorted cells were cocultured in a limiting dilution with the irradiated murine fetal liver stroma cell line AFT024 in IMDM (Invitrogen) supplemented with 12.5% FCS, 12.5% horse serum (Cell Systems, St. Katharinen, Germany), 2 mM L-glutamine (Invitrogen), 1000 U/mL penicillin, 100 U/mL streptomycin (Invitrogen), and 10^{-6} M hydrocortisone as extensively described previously.[14,24] Briefly, cultures were maintained for 5 weeks in a humidified atmosphere at 37°C and 5% CO_2 and fed once a week. At week 5, all wells were overlaid with clonogenic methylcellulose medium (Methylcel MC; Fluka, Sigma-Aldrich Chemie) in a final concentration of 1.2% containing IMDM, supplemented with 30% FCS for colony-forming cells (CFCs), 5 U/mL erythropoietin (Cell Systems), and supernatant of the bladder carcinoma cell line 5637 (10%). Wells were scored for the occurrence of secondary CFCs after an additional 10 days.

Statistics

Experimental results from different experiments were reported as standard deviation of the mean. Significance analyses were performed with the paired Student *t* test. LTC-IC frequencies were calculated as the reciprocal of the concentration of test cells that gives 37% negative cultures using Poisson statistics and the weighted mean method.

Results

Proliferation kinetics of cultured $CD34^+$ cells

Recently, we have shown that human $CD34^+$ cells grown for 5 days in the presence of early- or late-acting cytokines in suspension cultures segregate into $CD34^+CD133^+$ and $CD34^+CD133^{low/-}$ subfractions. Furthermore, we realized that early-acting cytokines

stimulate proliferation of CD34$^+$ cells more homogeneously than late-acting cytokines.[17] Since we aimed to study the subcellular distribution of antigens in dividing human CB–derived primitive hematopoietic cells and had the experimental requirement to obtain sufficient mitotic cells numbers, we first estimated the proliferation kinetics of CD34$^+$ cells labeled with the fluorescence dye PKH2 and subsequently cultured in the presence of early-acting cytokines. Cells were harvested at different time points, counted, and the expression of PKH2, CD133, and CD34 was analyzed by flow cytometry. According to the PKH2 staining (Figure 1) and in agreement with our previous studies,[23] only a few CD34$^+$ cells undergo cell division within the first 48 hours of cultivation. The proportions of both CD133$^+$ cells (Figure 1) and CD34$^+$ cells (data not shown) were not altered during this period. Analysis of the PKH2 staining at later time points revealed that most of the CD34$^+$ cells in vitro undergo their first cell division between day 2 and day 3 in culture, and subsequent divisions during the next few days (Figure 1). In agreement with our previous report,[17] the content of CD34$^+$ cells does not change during the first 5 days of culture (data not shown). However, with the onset of cell division, the proportion of CD133$^+$ cells decreases between day 2 and 5 in culture (Figure 1). This corresponds to the maximum expansion period of CD34$^+$ cells between days 3 and 4 seen in 3 different CB-derived CD34$^+$ cell samples (expansion rate, 2.3 ± 0.4 times).

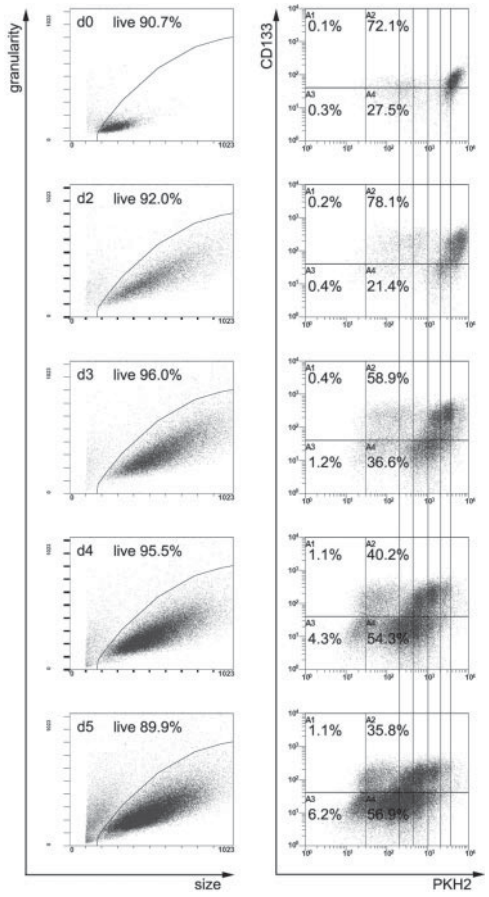

Figure 1. Flow cytometric analyses of PKH2-stained CD34$^+$-enriched cells. PKH2-stained CD34$^+$-enriched cells, either noncultivated (d0) or cultivated in the presence of early-acting cytokines for 2, 3, 4, or 5 days (d2, d3, d4, d5), were measured after labeling with anti-CD34 and anti-CD133 antibodies. The size and the granularity of all cells is plotted in the panels of the first column, and the PKH2 and anti-CD133 staining of the cells located in the live gates (shown in the first column) in the panels of the second column. Quadrants are adjusted according to corresponding isotype controls. Upon cultivation, CD34$^+$ cell increase in size and slightly up-regulate CD133 on their cell surface (compare d0 with d2 plots). Starting at day 3, the content of CD133$^+$ cells and the intensity of the PKH2 staining diminishes over time. Since PKH2 is a plasma membrane intercalating dye, its staining gets diluted with each cell division; the PKH2 intensity therefore reflects the number of cell divisions a given cell has performed during cultivation. The perpendicular lines should help to cluster cells regarding the number of cell divisions they had performed. The amount of cells depicted in all plots is normalized to the cell numbers of day 0; therefore, plots can be compared semiquantitatively. Note the small population with the weaker PKH2 staining follows the same kinetics as the large brightly stained population, demonstrating the reliability of the PKH2 experiment.

Because upon stimulation with late-acting cytokines CD133 expression was associated with the more primitive, slowly dividing CD34$^+$ cell fraction,[17] we assumed and verified (fourth paragraph of Results section) that cultivated CD34$^+$CD133$^+$ cells are more primitive than CD34$^+$CD133$^{low/-}$ cells, and decided to preferentially analyze CD34$^+$CD133$^+$ cells in the course of this project. Since the content of CD34$^+$CD133$^+$ cells was significant higher at culture day 3 compared with days 4 and 5 (day 3, 57.5% ± 1.9%; day 4, 44.7% ± 1.6%; day 5, 33.0% ± 5.2%; $P_{day3/day4} < .003$; $P_{day3/day5} < .02$; n = 3), we mainly used day-3 CB-derived CD34$^+$ cells for our further analyses.

Distribution of uropod markers in dividing CD34$^+$ cells

We have recently shown that several surface molecules, and especially CD133, become distributed in a localized fashion in cultivated primitive hematopoietic cells.[23] Now, we have studied their distribution in dividing CD34$^+$ cells. To minimize extrinsic effects on the distribution of these molecules, we generally cultured the cells under stroma-free, nonadherent culture conditions before staining. We analyzed in total 2409 mitotic CD34$^+$ cells from 14 different CB samples that were cultured for 3 or 4 days, respectively. A total of 1379 mitotic cells represented late mitotic stages (telophase), in which the 2 cellular poles can clearly be discriminated (Figure 2). Of the latter, 899 (65.2%) were found to be positive for CD133, a ratio consistent with the content of CD133$^+$ cells within the fraction of CD34$^+$ cells at day 3 of culture. In 892 of these mitotic cells, CD133 was distributed in a symmetrical fashion, displaying its highest concentration at the cleavage furrow or at the midbody, respectively (Figure 2). Only 7 (0.8%) late mitotic cells were found in which the anti-CD133 staining was not symmetrically distributed to the 2 prospective daughter cells; however, according to the appearance of these cells, the nonsymmetric distribution was nonspecific rather than specific.

Furthermore, we analyzed the distribution of other uropod markers in late mitotic CD34$^+$ cells (CD43, CD44, ICAM-1, and ICAM-3). All of these proteins were highly enriched at the cleavage furrow or midbody of the stained cells studied (Table 1; Figure 2). In none of the latter cells we did find any evidence for an asymmetric distribution of these proteins. Together with the results presented in paragraph 6 of the Results section, we assume that under the conditions used here, CD133 and the other uropod markers become highly enriched at the cleavage furrow and at the midbody of all dividing CD34$^+$CD133$^+$ cells, and thus do not identify putative asymmetric cell divisions.

Phenotypical characterization of the CD34$^+$CD133$^+$ versus the CD34$^+$CD133$^{low/-}$ cell fraction

Although our data argues against the possibility that CD133 segregates asymmetrically in dividing CD34$^+$CD133$^+$ cells, the kinetics of the cultured CD34$^+$ cells are principally compatible with a model in which asymmetric cell divisions give rise to more primitive cells that will maintain the CD34$^+$CD133$^+$ phenotype, and to committed cells that will reduce their CD133 surface

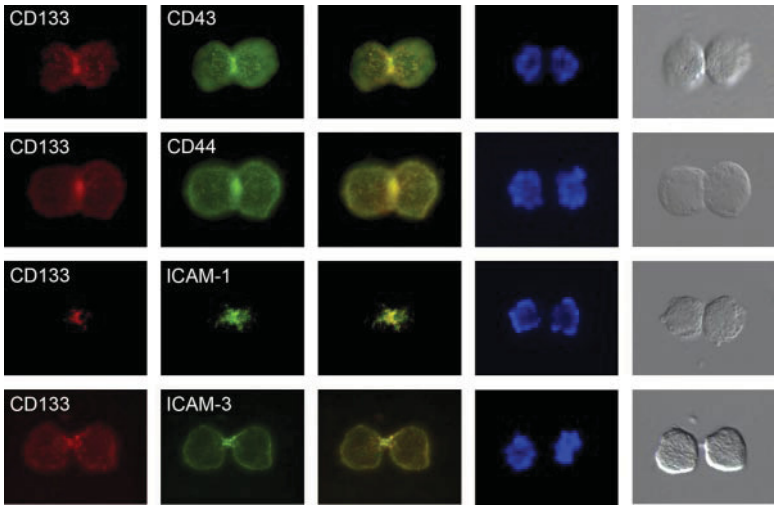

Figure 2. Cell-surface distribution of uropod markers in late mitotic CB-derived CD34$^+$CD133$^+$ cells. Before double labeling with anti-CD133 (red staining) and either anti-CD43, anti-CD44, anti–ICAM-1, or anti–ICAM-3 antibodies (green staining), cells were cultured for 3 days in serum-containing medium supplemented with early-acting cytokines. Note that CD133 as well as the other uropod markers are highly enriched at the cleavage furrow or midbody of dividing CD34$^+$CD133$^+$ cells. Column 1 shows anti-CD133 staining; column 2, anti-CD43, anti-CD44, anti–ICAM-1, and anti–ICAM-3 staining of cultivated CD34$^+$ cells; column 3, merge of columns 1 and 2; column 4, DAPI staining; and column 5, light microscopy images of the stained cells.

expression postmitotically. At this point we hypothesized that if CD34$^+$CD133$^+$ cells indeed can divide asymmetrically to give rise to CD34$^+$CD133$^+$ and CD34$^+$CD133$^{low/-}$ cells, any protein that is expressed differentially among these populations might be a candidate for a protein that segregates differentially in asymmetrically dividing CD34$^+$CD133$^+$ cells.

Thus, to challenge this hypothesis, we next screened for proteins that are expressed differentially on both populations. For the screening procedure, we cultured CB-derived MNCs in the presence of early-acting cytokines for 3 days. Then, cells were stained with anti-CD133–PE and anti-CD34–PCy5 antibodies as well as with 1 of 58 different FITC-conjugated antibodies that recognize different surface antigens. The expression levels of the corresponding antigens were measured by flow cytometry. Using a gating strategy on CD34$^+$ cells, the expression of the different antigens on CD34$^+$CD133$^+$ cells as well as on CD34$^+$CD133$^{low/-}$ cells was analyzed and compared with each other (Figure 3). According to our results, 39 of these antigens were judged to be expressed on cultivated CD34$^+$ cells, with 19 of them uncovering differences between the CD34$^+$CD133$^+$ and CD34$^+$CD133$^{low/-}$ subpopulations (data not shown).

Following this initial screening procedure, we chose a panel of 11 different antibodies and studied the expression of the corresponding antigens on 2 additional CB-derived MNC fractions. While CD47 and CD59 were expressed homogeneously on CD34$^+$ cells, CD13, CD31, CD53, CD62L, CD63, CD71, CD74, and CD105 were expressed in different amounts on CD34$^+$CD133$^+$ cells compared with CD34$^+$CD133$^{low/-}$ cells in all samples. The expression levels of CD164 on these subpopulations were not consistent among the different samples (data not shown). It should be mentioned that in comparative analyses, we have studied the expression of these proteins on MNCs of 2 BM-derived and 2 PB-derived MNC fractions as well and obtained comparable results (data not shown).

According to our results, the expression levels of CD53, CD62L, CD63, and CD71 displayed the highest contrast between CD34$^+$CD133$^+$ and CD34$^+$CD133$^{low/-}$ cells of the MNC fractions (Figure 3). To exclude any influence of CD34$^-$ MNCs on the expression levels of these antigens, we analyzed the expression of CD53, CD62L, CD63, and CD71 on purified CB-derived CD34$^+$ cells that were cultured for 3 days in the presence of early-acting cytokines and obtained comparable results (Figure S1).

Table 1. Analyses of the uropod marker distribution in mitotic CD34$^+$ cells

	n	No. stained telophases	Content of CD133$^+$ telophases, %
CD43	3	95	74.7
CD44	3	195	87.2
ICAM-1	3	124	95.2
ICAM-3	4	135	80.7

n indicates number of CB samples analyzed. The distribution of different antigens was studied in late mitotic cells counterstained with CD133. In all of the late mitotic cells analyzed, antigens were distributed in a symmetric fashion.

Functional characterization of the newly identified CD34$^+$ subpopulations

To functionally characterize the newly identified CD34$^+$ subfractions, we have purified CD133$^+$ and CD133$^{low/-}$ fractions in combination

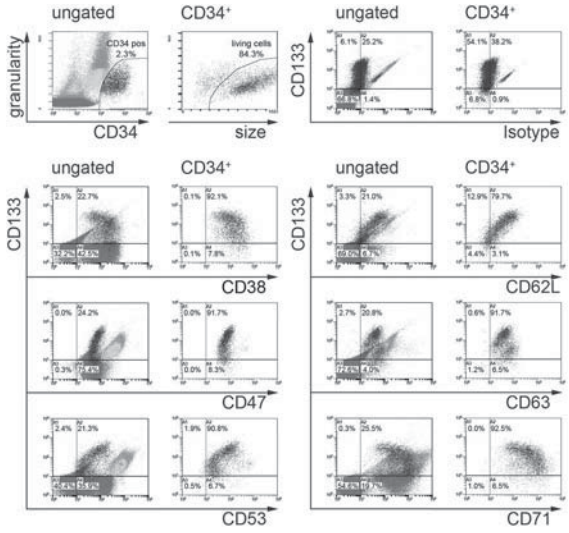

Figure 3. Flow cytometric analyses of CB-derived MNCs that have been cultivated for 3 days in the presence of early-acting cytokines. Plots represent MNCs that are ungated or gated on CD34$^+$ cells. The CD34$^+$ gate used is shown in the first plot of the first row. The size of these cells plotted against their granularity is shown in the second plot of row 1. The remaining plots represent the intensity of CD133 staining against the intensity of the isotype control, an anti-CD38, anti-CD47, anti-CD53, anti-CD62L, anti-CD63, or anti-CD71 staining, respectively. Quadrants are adjusted according to isotype controls of CD34 negative cells. Note that CD34$^+$CD133$^+$ cells contain different levels of CD53, CD63, CD62L, and CD71 than CD34$^+$CD133$^{low/-}$ cells.

with CD38, CD53, CD62L, CD63, or CD71 by fluorescent cell sorting (Figure S1B) and analyzed their primitive myeloid developmental capacity, measured as LTC-ICs. $CD34^+$ cells of the same samples were purified in parallel and analyzed as controls. According to our results, the LTC-IC frequency within the purified $CD34^+CD133^+$ cell fractions was significantly higher than in their $CD34^+CD133^{low/-}$ counterparts or in the total $CD34^+$ cell fractions (Table 2). Compared with the subfraction of cultivated $CD133^+CD38^{low/-}$ and $CD133^+CD71^{low}$ cells, cells of the $CD133^+CD53^+$, $CD133^+CD62L^+$, and $CD133^+CD63^{low}$ subfractions can be recognized as distinct cell populations (Figures 3, S1). Therefore, CD53, CD62L, and CD63 provide markers, which can be used in combination with CD133 to objectively identify potentially more primitive cells within the fraction of cultivated $CD34^+$ cells.

Subcellular distribution of identified antigens in polarized $CD34^+CD133^+$ cells

To subcellularly localize the identified antigens on polarized $CD34^+$ cells, we stained $CD34^+$ cells cultured for 3 days with antibodies against these markers and an anti-CD133 antibody. CD53 and CD63 were highly concentrated in vesicular-like structures at the base of the uropod. CD71 was distributed over the cell surface, including the leading edge of $CD34^+$ cells; in addition, it was highly concentrated in vesicular-like structures at the base of the uropod. CD62L was highly concentrated at the tip of the uropod, where it seemed to colocalize with CD133; in addition, faint staining was sometimes found at the base of the uropod (Figure 4). It should be mentioned that compared with the staining with the other antibodies, the anti-CD62L antibody staining is generally very weak on fixed cells.

CD53, CD62L, CD63, and CD71 segregation during mitosis of $CD34^+CD133^+$ cells

Hence, the proteins identified in our screen are candidates that might segregate differently during mitosis. Therefore, we have analyzed the distribution of CD53, CD62L, CD63, and CD71 on $CD34^+CD133^+$ cells of late mitotic stages (telophase). On approximately 20% of the mitotic cells studied, $CD53^+$ (19.6%), $CD63^+$ (20.5%), and $CD71^+$ (22.1%) vesicular structures were found preferentially in 1 of the prospective daughter cells, suggesting that these structures segregate differentially (Table 3, Figure 5). We also found late telophase $CD34^+CD133^+$ cells that displayed an asymmetric distribution of the CD62L antigen (15.2%). However, due to the weak anti-CD62L antibody staining of fixed cells, the number of asymmetrically dividing $CD133^+CD62L^+$ cells might be underestimated.

Intracellular distribution of CD63 and CD71 in late mitotic $CD34^+$ cells

Since CD53, CD63, and CD71 are expressed on vesicular-like structures and have been reported to be associated with the endosomal traffic,[25-28] the vesicular-like structures might correspond to budding endosomes. To exclude the possibility the asymmetric distribution of these structures is connected to a very dynamic process, which might frequently switch among the daughter cells, we decided to study the intracellular distribution of the identified antigens. Due to an incompatibility between the anti-CD53 antibody and the intracellular staining procedure, we double-stained cultured $CD34^+$ cells with anti-CD63 and anti-CD71 antibodies. In all cases studied, the anti-CD63 and the anti-CD71 staining colocalized (Figure 5B). In support of the data presented in the previous paragraph, we found an asymmetric distribution of the anti-CD63– and anti-CD71–stained structures in approximately 20% of the mitotic cells (Table 3, Figure 5B).

Discussion

Challenging the hypothesis of asymmetric cell division within the primitive hematopoietic cell compartment, we demonstrate here for the first time that primitive human hematopoietic cells indeed contain capabilities to divide asymmetrically. Furthermore, we report the identification of cell surface proteins that, in combination with CD133, can be used to define more primitive hematopoietic cells within the $CD34^+$ cell fraction. In addition, these proteins led to the discovery of a potentially new subcellular plasma-membrane domain on migrating $CD34^+$ cells in which endosomes seem to be formed to bud into the interior of the cell.

Asymmetric cell division of primitive hematopoietic cells

It has been suggested that HSCs can divide asymmetrically to give rise to 1 cell maintaining stem cell fate and to a daughter that is committed to differentiate. In agreement with this hypothesis, the findings of several groups, including our own, have demonstrated that primitive hematopoietic cells give rise to daughter cells adopting different cell fates or realizing different proliferation kinetics, respectively.[10-15,17] Following a definition in which a cell division is defined as asymmetric or symmetric according to the cell fates of its daughter cells,[29] these results would clearly demonstrate that primitive hematopoietic cells divide asymmetrically. However, if a more restrictive definition is used, in which asymmetrically dividing cells

Table 2. Functional analyses of sorted $CD34^+$ sub-fractions in LTC-IC assays

LTC-IC frequency	n	CD34′, %	$CD133^+$, %	$CD133^{low/-}$, %	*P* $CD133^+$ to $CD133^{low/-}$	*P* $CD133^+$ to $CD34^+$
CD38	3	4.2 ± 3.5	$CD38^{low}$, 13.4 ± 1.8	$CD38^+$, 0.3 ± 0.4	< .01	< .02
CD53	5	3.4 ± 2.7	$CD53^+$, 7.9 ± 4.2	$CD53^{low/-}$, 1.1 ± 1.0	< .03	< .03
CD62L	5	3.4 ± 2.7	$CD62L^+$, 8.9 ± 3.9	$CD62L^{low/-}$, 0.3 ± 0.1	< .01	< .01
CD63	5	5.3 ± 2.8	$CD63^{low/-}$, 11.4 ± 3.0	$CD63^+$, 0.3 ± 0.2	< .01	< .01
CD71	5	3.4 ± 2.7	$CD71^{low}$, 12.7 ± 10.0	$CD71^+$, 1.0 ± 0.8	< .06	< .05

n indicates number of experiments; $CD34^+$, LTC-IC frequency of $CD34^+$ cells purified at culture day 3 (note: identical CB- samples for CD53, CD62L, and CD71 analyses were used); $CD133^+$, LTC-IC frequency of purified, cultured $CD34^+$ $CD133^+$ cell fractions which are $CD38^{low}$, $CD53^+$, $CD62L^+$, $CD63^{low/-}$, or $CD71^{low}$, respectively; $CD133^{low}$, LTC-IC frequency of purified, cultured $CD34^+$ $CD133^{low/-}$ cell fractions which are $CD38^+$, $CD53^{low/-}$, $CD62L^{low/-}$, $CD63^+$, or $CD71^+$, respectively; *P* $CD133^+$ to $CD133^{low/-}$, *P* values of significance analyses of the LTC-IC frequency of $CD34^+CD133^+$ cell fractions compared with that of corresponding $CD34^+CD133^{low/-}$ cell fractions; *P* $CD133^+$ to $CD34^+$, *P* values of significance analyses of the LTC-IC frequency of $CD34^+CD133^+$ cell fractions compared with that of corresponding $CD34^+$ cell fractions.

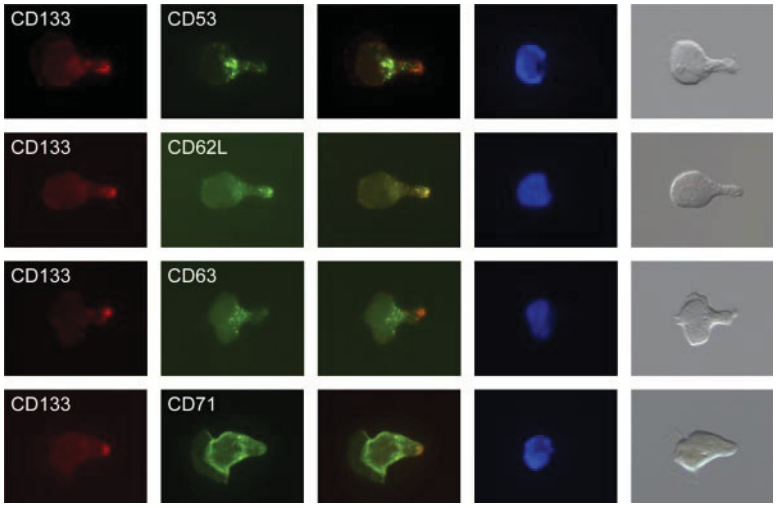

Figure 4. Localization of CD53, CD62L, CD63, and CD71 in polarized CD34$^+$CD133$^+$ cells. CD53, CD63, and CD71 are localized in vesicular-like structures at the base of the uropod. In addition, CD71 is expressed all over the cell surface, including the leading edge (left side of the cell shown in column 2). CD62L is highly localized at the tip of the uropod and colocalizes with CD133. Column 1 shows anti-CD133 staining; column 2, anti-CD53, anti-CD62L, anti-CD63, and anti-CD71 staining of CD34$^+$ cells; column 3, merge of columns 1 and 2; column 4, DAPI staining; and column 5, light microscopy images of the stained cells.

are defined as cells that by the different segregation of certain molecules become qualitatively different, these results are not sufficient to demonstrate asymmetric cell divisions within the primitive human hematopoietic cell compartment. The observed differences in the cell fate or the proliferation kinetics could theoretically be a result of extrinsic mechanisms that act postmitotically and alter the developmental capacities of initially identical daughter cells. A well-analyzed process in which cells with identical developmental capacities become different is the process of lateral inhibition, sometimes also referred as mutual inhibition or lateral specification. In this process, cells with identical developmental capacities mutually influence each others cell fate to become different.[20,21] Since this process is mediated by the Notch signaling pathway, which plays important roles during early and late hematopoiesis,[30] its action is one of several other predictable, postmitotically acting mechanisms which theoretically could account for the observed differences.

However, by the identification of marker proteins that segregate differently in approximately 20% of the mitotic, CB-derived CD34$^+$CD133$^+$ cells, it now becomes evident that primitive hematopoietic cells can indeed give rise to qualitatively different daughter cells and thus divide asymmetrically. Since we raised the cells in stroma-free suspension cultures, and the cells grew nonadherently, we suppose that the asymmetric distribution of the proteins in mitotic cells is assigned intrinsically rather than induced by extrinsic signals that might directly affect the subcellular localization of the identified proteins. This assumption is further enforced by the findings that (1) the ratio of late mitotic cells with asymmetric protein distributions fits into the same range with which primitive human hematopoietic cells deposited as single cells in suspension cultures generate daughter cells realizing different cell fates and different proliferation kinetics, and (2) that the latter rate was not influenced by the different cytokine conditions used to raise these cells in vitro.[14,16]

Although we cannot exclude that daughter cells inheriting different levels of the identified marker proteins can compensate for these differences and adopt identical developmental potentials, this congruency suggests that there is a high correlation between the marker distribution and the acquired cell fates of the daughter cells, which is supported by the fact that CD133 and the expression of the marker proteins we describe here correlates very well with the primitive state of CD34$^+$ cells. More primitive CD34$^+$CD133$^+$ cells express higher levels of CD53 and CD62L as well as lower levels of CD63 and CD71 than the more mature CD34$^+$CD133$^{low/-}$ cells. In this context, it should be noted that, in combination with CD133 and CD62L, CD53 or CD63 more objectively defined subpopulations of CD34$^+$ cells can be recognized and purified than with the CD38 antigen, which is commonly used to discriminate more primitive human HPCs (CD34$^+$CD38$^{low/-}$) from more mature ones (CD34$^+$CD38$^+$).[31,32] According to our findings, we postulate that asymmetrically dividing CD34$^+$CD133$^+$ cells obtaining more CD53 or CD62L or less CD63 are more primitive than their sister cells. As CD71 is distributed along the whole plasma membrane, we suggest that the daughter cells inheriting more of the CD71-stained vesicular-like structures will express higher levels of CD71 than their sister cells. Since CD34$^+$CD133$^+$CD71^{low} cells are more primitive than CD34$^+$CD133^{low}CD71$^+$ cells, we assume that the daughter cells inheriting more of the CD71$^+$ vesicular-like structures are more mature than their sister cells.

Table 3. Distribution of CD53, CD62L, CD63, and CD71 in late mitotic CD34$^+$ cells

Antigen	n	Total no. telophases	Total no. asym telophases	Content of asym telophases, %	Average rate of asym telophases per CB, %
CD53/CD133	3	97	19	19.6	18.9 ± 9.4
CD62L/CD133	4	112	17	15.2	17.8 ± 13.7
CD63/CD133	5	146	30	20.5	23.6 ± 6.5
CD71/CD133	4	131	29	22.1	29.9 ± 16.3
CD63/CD71	4	221	40	18.1	20.3 ± 6.5

The distribution of different antigens was studied in late mitotic cells counterstained with CD133 or in cells that were intracellularly stained with CD63 and CD71.
n indicates number of CB samples analyzed; asym, asymmetric.
*Data shows telophases.

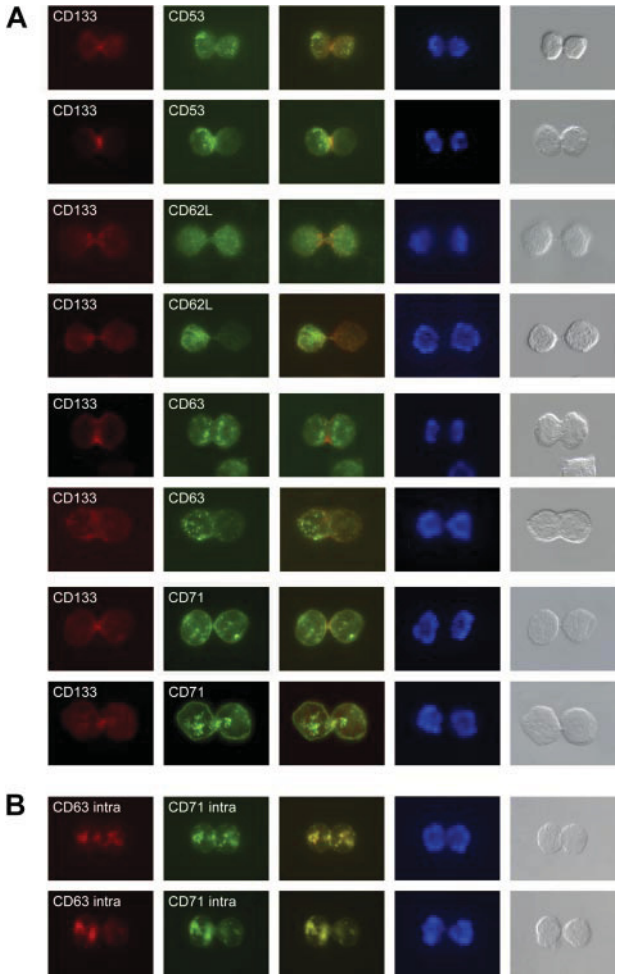

Figure 5. Localization of CD53, CD62L, CD63 and CD71 in dividing CD34$^+$CD133$^+$ cells. (A) Cell-surface distribution of CD53, CD62L, CD63, and CD71 on late mitotic CD34$^+$CD133$^+$ cells. For each of these markers, 1 mitotic cell is shown containing a symmetric distribution of the given antigen (top row), and 1 containing an asymmetric distribution (bottom row; green staining). Cells are counterstained with an anti-CD133 antibody (red staining) and DAPI (blue staining). Light microscopy images of the stained cells are presented in the fifth column. (B) Intracellular distribution of CD63 (red staining) and CD71 (green staining). The overlay of the 2 is given in the third column.

This view is supported by the result of our intracellular staining procedure, in which CD63$^+$ vesicular-like structures, which are supposed to label more mature cells, cosegregate with the CD71-stained structures. In addition, and consistent with our functional data, it was reported several years ago that CD34$^+$CD71^{low} cells are more primitive than CD34$^+$CD71$^+$ cells.[33,34] Similarly, previous evidence showed that CD62L expressing CD34$^+$ cells are more primitive than CD62L$^-$ CD34$^+$ cells.[35,36] To our knowledge, neither CD53 nor CD63 have been associated with the fate of CD34$^+$ cells. Therefore, we have qualified these as new markers to discriminate primitive cultured CD34$^+$ cells from more mature cells.

Tetraspanins

Both CD53 and CD63 encode members of the evolutionary conserved tetraspanin family, a large superfamily of small cell-surface membrane proteins characterized by 4 transmembrane and 2 extracellular domains. At present, 28 members of this family have been documented in humans, many of them expressed on multiple cell types. They seem to organize novel types of cell-surface membrane microdomains, the tetraspanin-enriched microdomains (TEMs), novel signaling platforms which are distinct from lipid rafts.[37,38] However, little is known about their function, though tetraspanins seem to take part in regulating the activation, motility, and antigen presentation of different leukocytes.[37,38] Interestingly, it has been shown that, in addition to the cell surface, many tetraspanins, including CD53 and CD63, are localized on the internal vesicles of multivesicular endosomes and on exosomes.[26] Due to the interaction between CD63 and subunits of AP-2 and AP-3 complexes, it is linked to clathrin-dependent endocytotic pathways and seems to play a role in the recycling of plasma membrane components and their transport to appropriate intracellular compartments.[25,27,39-42]

Since the transferrin receptor (CD71) also cycles between the plasma membrane and the endosomal compartment and can be secreted on exosomes,[28,39] 3 of the 4 identified proteins that frequently segregate asymmetrically in dividing CD34$^+$CD133$^+$ cells are linked to the endosomal/exosomal compartment. This, together with the fact that anti-CD53, anti-CD63, and anti-CD71 staining is highly enriched in vesicular-like structures in polarized as well as in mitotic CD34$^+$CD133$^+$ cells, suggest that the vesicular-like structures correspond to budding endosomes. This assumption is further supported by our finding that in living CD34$^+$ cells, antibodies against CD63 and CD71 become internalized within the region that is highly enriched for these vesicular-like structures (data not shown). Since these presumptive budding endosomes are highly enriched in a region at the base of the uropod, they define a membrane domain that to our knowledge has not been previously described in polarized CD34$^+$ cells. Furthermore, these results reveal a link between the endosomal compartment and mechanisms governing the asymmetric cell division of primitive human hematopoietic cells. It will, in the future, be interesting to determine the similarities between this asymmetric cell division in human HPCs and the role of the endosomal compartment and mechanisms governing asymmetric cell divisions that have been described in *Drosophila*.[43]

Acknowledgments

The authors thank Dr Michael Punzel, Dr Andreas Wodarz, and Dr Verdon Taylor for general discussion and critiques on the manuscript; and Svenja Jünger, Jan Spanholtz, and Gregor von Levetzow for general experimental support. Umbilical cord blood samples were kindly provided by Gesine Kögler of our institute (Institute for Transplantation Diagnostics and Cellular Therapeutics).

This work was supported by grants from the Deutsche Forschungsgemeinschaft (SPP1109 GI 336/1-4 to B.G. and P.W.) and from the Forschungskommission of the HHU-Duesseldorf (B.G.).

Authorship

Contribution: J.B. helped to design the study, performed experiments and assisted in the writing; S.S. performed experiments; P.W. provided intellectual input by discussing the data; J.C.F.

provided essential experimental support; and B.G. designed the study, performed experiments, and wrote the manuscript.

Conflict-of-interest disclosure: The authors declare no competing financial interests.

Correspondence: Bernd Giebel, Institute for Transplantation Diagnostics and Cell Therapeutics, Heinrich-Heine-University Duesseldorf, D-40225 Duesseldorf, Germany; e-mail: giebel@itz.uni-duesseldorf.de.

References

1. Iscove NN, Nawa K. Hematopoietic stem cells expand during serial transplantation in vivo without apparent exhaustion. Curr Biol. 1997;7:805-808.
2. Moore KA, Ema H, Lemischka IR. In vitro maintenance of highly purified, transplantable hematopoietic stem cells. Blood. 1997;89:4337-4347.
3. Nolta JA, Thiemann FT, Arakawa-Hoyt J, et al. The AFT024 stromal cell line supports long-term ex vivo maintenance of engrafting multipotent human hematopoietic progenitors. Leukemia. 2002;16:352-361.
4. Punzel M, Moore KA, Lemischka IR, Verfaillie CM. The type of stromal feeder used in limiting dilution assays influences frequency and maintenance assessment of human long-term culture initiating cells. Leukemia. 1999;13:92-97.
5. Thiemann FT, Moore KA, Smogorzewska EM, Lemischka IR, Crooks GM. The murine stromal cell line AFT024 acts specifically on human CD34+CD38- progenitors to maintain primitive function and immunophenotype in vitro. Exp Hematol. 1998;26:612-619.
6. Schofield R. The relationship between the spleen colony-forming cell and the haemopoietic stem cell. Blood Cells. 1978;4:7-25.
7. Calvi LM, Adams GB, Weibrecht KW, et al. Osteoblastic cells regulate the haematopoietic stem cell niche. Nature. 2003;425:841-846.
8. Kiel MJ, Yilmaz OH, Iwashita T, Terhorst C, Morrison SJ. SLAM family receptors distinguish hematopoietic stem and progenitor cells and reveal endothelial niches for stem cells. Cell. 2005;121:1109-1121.
9. Zhang J, Niu C, Ye L, et al. Identification of the haematopoietic stem cell niche and control of the niche size. Nature. 2003;425:836-841.
10. Suda T, Suda J, Ogawa M. Disparate differentiation in mouse hemopoietic colonies derived from paired progenitors. Proc Natl Acad Sci U S A. 1984;81:2520-2524.
11. Suda J, Suda T, Ogawa M. Analysis of differentiation of mouse hemopoietic stem cells in culture by sequential replating of paired progenitors. Blood. 1984;64:393-399.
12. Leary AG, Strauss LC, Civin CI, Ogawa M. Disparate differentiation in hemopoietic colonies derived from human paired progenitors. Blood. 1985;66:327-332.
13. Mayani H, Dragowska W, Lansdorp PM. Lineage commitment in human hemopoiesis involves asymmetric cell division of multipotent progenitors and does not appear to be influenced by cytokines. J Cell Physiol. 1993;157:579-586.
14. Punzel M, Zhang T, Liu D, Eckstein V, Ho AD. Functional analysis of initial cell divisions defines the subsequent fate of individual human CD34(+)CD38(-) cells. Exp Hematol. 2002;30:464-472.
15. Brummendorf TH, Dragowska W, Zijlmans J, Thornbury G, Lansdorp PM. Asymmetric cell divisions sustain long-term hematopoiesis from single-sorted human fetal liver cells. J Exp Med. 1998;188:1117-1124.
16. Huang S, Law P, Francis K, Palsson BO, Ho AD. Symmetry of initial cell divisions among primitive hematopoietic progenitors is independent of ontogenic age and regulatory molecules. Blood. 1999;94:2595-2604.
17. Giebel B, Zhang T, Beckmann J, Spanholtz J, Wernet P, Ho AD, Punzel M. Primitive human hematopoietic cells give rise to differentially specified daughter cells upon their initial cell division. Blood. 2006;107:2146-2152.
18. Ema H, Takano H, Sudo K, Nakauchi H. In vitro self-renewal division of hematopoietic stem cells. J Exp Med. 2000;192:1281-1288.
19. Takano H, Ema H, Sudo K, Nakauchi H. Asymmetric division and lineage commitment at the level of hematopoietic stem cells: inference from differentiation in daughter cell and granddaughter cell pairs. J Exp Med. 2004;199:295-302.
20. Giebel B. The notch signaling pathway is required to specify muscle progenitor cells in Drosophila. Mech Dev. 1999;86:137-145.
21. Martinez Arias A, Zecchini V, Brennan K. CSL-independent Notch signalling: a checkpoint in cell fate decisions during development? Curr Opin Genet Dev. 2002;12:524-533.
22. Betschinger J, Knoblich JA. Dare to be different: asymmetric cell division in Drosophila, C. elegans and vertebrates. Curr Biol. 2004;14:R674-R685.
23. Giebel B, Corbeil D, Beckmann J, et al. Segregation of lipid raft markers including CD133 in polarized human hematopoietic stem and progenitor cells. Blood. 2004;104:2332-2338.
24. Punzel M, Wissink SD, Miller JS, Moore KA, Lemischka IR, Verfaillie CM. The myeloid-lymphoid initiating cell (ML-IC) assay assesses the fate of multipotent human progenitors in vitro. Blood. 1999;93:3750-3756.
25. Arribas M, Cutler DF. Weibel-Palade body membrane proteins exhibit differential trafficking after exocytosis in endothelial cells. Traffic. 2000;1:783-793.
26. Escola JM, Kleijmeer MJ, Stoorvogel W, Griffith JM, Yoshie O, Geuze HJ. Selective enrichment of tetraspan proteins on the internal vesicles of multivesicular endosomes and on exosomes secreted by human B-lymphocytes. J Biol Chem. 1998;273:20121-20127.
27. Kobayashi T, Vischer UM, Rosnoblet C, et al. The tetraspanin CD63/lamp3 cycles between endocytic and secretory compartments in human endothelial cells. Mol Biol Cell. 2000;11:1829-1843.
28. Qian ZM, Li H, Sun H, Ho K. Targeted drug delivery via the transferrin receptor-mediated endocytosis pathway. Pharmacol Rev. 2002;54:561-587.
29. Morrison SJ, Kimble J. Asymmetric and symmetric stem-cell divisions in development and cancer. Nature. 2006;441:1068-1074.
30. Suzuki T, Chiba S. Notch signaling in hematopoietic stem cells. Int J Hematol. 2005;82:285-294.
31. Hao QL, Shah AJ, Thiemann FT, Smogorzewska EM, Crooks GM. A functional comparison of CD34+ CD38- cells in cord blood and bone marrow. Blood. 1995;86:3745-3753.
32. Bhatia M, Wang JC, Kapp U, Bonnet D, Dick JE. Purification of primitive human hematopoietic cells capable of repopulating immune-deficient mice. Proc Natl Acad Sci U S A. 1997;94:5320-5325.
33. Lansdorp PM, Dragowska W. Long-term erythropoiesis from constant numbers of CD34+ cells in serum-free cultures initiated with highly purified progenitor cells from human bone marrow. J Exp Med. 1992;175:1501-1509.
34. Mayani H, Dragowska W, Lansdorp PM. Cytokine-induced selective expansion and maturation of erythroid versus myeloid progenitors from purified cord blood precursor cells. Blood. 1993;81:3252-3258.
35. Mohle R, Murea S, Kirsch M, Haas R. Differential expression of L-selectin, VLA-4, and LFA-1 on CD34+ progenitor cells from bone marrow and peripheral blood during G-CSF-enhanced recovery. Exp Hematol. 1995;23:1535-1542.
36. Koenig JM, Baron S, Luo D, Benson NA, Deisseroth AB. L-selectin expression enhances clonogenesis of CD34+ cord blood progenitors. Pediatr Res. 1999;45:867-870.
37. Hemler ME. Tetraspanin functions and associated microdomains. Nat Rev Mol Cell Biol. 2005;6:801-811.
38. Tarrant JM, Robb L, van Spriel AB, Wright MD. Tetraspanins: molecular organisers of the leukocyte surface. Trends Immunol. 2003;24:610-617.
39. de Gassart A, Geminard C, Hoekstra D, Vidal M. Exosome secretion: the art of reutilizing nonrecycled proteins? Traffic. 2004;5:896-903.
40. Duffield A, Kamsteeg EJ, Brown AN, Pagel P, Caplan MJ. The tetraspanin CD63 enhances the internalization of the H, K-ATPase beta-subunit. Proc Natl Acad Sci U S A. 2003;100:15560-15565.
41. Mantegazza AR, Barrio MM, Moutel S, et al. CD63 tetraspanin slows down cell migration and translocates to the endosomal-lysosomal-MIICs route after extracellular stimuli in human immature dendritic cells. Blood. 2004;104:1183-1190.
42. Janvier K, Bonifacino JS. Role of the endocytic machinery in the sorting of lysosome-associated membrane proteins. Mol Biol Cell. 2005;16:4231-4242.
43. Shen Q, Temple S. Creating asymmetric cell divisions by skewing endocytosis. Sci STKE. 2002;2002:PE52.

STEM CELLS AND DEVELOPMENT 15:278–285 (2006)

Technical Report

Nucleofection, an Efficient Nonviral Method to Transfer Genes into Human Hematopoietic Stem and Progenitor Cells

GREGOR VON LEVETZOW,[1,2] JAN SPANHOLTZ,[1,2] JULIA BECKMANN,[1] JOHANNES FISCHER,[1] GESINE KÖGLER,[1] PETER WERNET,[1] MICHAEL PUNZEL,[1] and BERND GIEBEL[1]

ABSTRACT

The targeted manipulation of the genetic program of single cells as well as of complete organisms has strongly enhanced our understanding of cellular and developmental processes and should also help to increase our knowledge of primary human stem cells, e.g., hematopoietic stem cells (HSCs), within the next few years. An essential requirement for such genetic approaches is the existence of a reliable and efficient method to introduce genetic elements into living cells. Retro- and lentiviral techniques are efficient in transducing primary human HSCs, but remain labor and time consuming and require special safety conditions, which do not exist in many laboratories. In our study, we have optimized the nucleofection technology, a modified electroporation strategy, to introduce plasmid DNA into freshly isolated human HSC-enriched $CD34^+$ cells. Using enhanced green fluorescent protein (eGFP)-encoding plasmids, we obtained transfection efficiencies of approximately 80% and a mean survival rate of 50%. Performing functional assays using GFU-GEMM and long-term culture initiating cells (LTC-IC), we demonstrate that apart from a reduction in the survival rate the nucleofection method itself does not recognizably change the short- or long-term cell fate of primitive hematopoietic cells. Therefore, we conclude, the nucleofection method is a reliable and efficient method to manipulate primitive hematopoietic cells genetically.

INTRODUCTION

FOR MORE THAN 30 YEARS, hematopoietic stem cells (HSCs) have been successfully used in a various number of clinical applications (1). However, the current understanding about the molecular and cellular mechanisms governing the biology of these cells remains limited. In a variety of different organisms (e.g., *Drosophila* and *Caenorhabditis elegans*) or cellular systems, the understanding of different cellular processes was fundamentally improved by genetic approaches (2). In this regard over- or ectopic-expression studies, as well as inhibition of expression by RNA interference, revealed important results, similar to naturally occurring mutations. Therefore, an effective method to manipulate human HSCs or hematopoietic progenitor cells (HPCs) genetically should help to increase the current understanding of the basic mechanisms governing the biology of human HSCs and HPCs. Additionally, an effective transfection method might help to improve HSC/HPC applications in clinical trials.

In principle, there are different strategies to manipulate human HSCs/HPCs genetically, i.e., techniques based on viral or nonviral gene transfer. Although viral strategies are highly efficient to transfer genes into primary cells (up to 90%) (3), they are time consuming and require special safety precautions to minimize the risk of

[1]Institute for Transplantation Diagnostics and Cell Therapeutics, Heinrich-Heine-University Düsseldorf, D-40225 Düsseldorf, Germany.

[2]Both authors contributed equally to this work.

exposure to biohazards (4), most nonviral techniques, e.g. electroporation, require a prestimulation of the corresponding cells and result in a maximal, regularly nonpermanent transfection efficiency of 30% (5,6).

Recently, a new and highly efficient nonviral method called nucleofection technology was described. This modified electroporation strategy, which delivers the transfected nucleic acids directly into the nuclei of most cell types investigated so far, permits transient transfection of primary cells without any prestimulation (7–10). Indeed, we and others have successfully applied this technique to transfect freshly isolated human $CD34^+$ cells and have obtained transfection efficiency rates of up to 80% when using green fluorescent protein (GFP)-encoding plasmids (11,12). Because the survival rate of transfected cells dropped significantly with decreasing cell numbers used in a single nucleofection reaction, we now have optimized the technology to transfect as little as 2×10^5 freshly isolated $CD34^+$ cells.

For many experiments, especially those involving immature cell types, it is required that the cell fate of treated cells is not significantly altered by the transfection method itself. Therefore, we have also assessed whether the optimized nucleofection technology has any influence on the developmental potential of human HSCs/HPCs.

MATERIALS AND METHODS

Cell preparation

Umbilical cord blood (CB) samples were obtained from donors after informed consent according to the Declaration of Helsinki. Mononuclear cells were isolated from individual samples by Ficoll (Biocoll Separating Solution, Biochrom AG, Berlin Germany) density gradient centrifugation. Remaining red blood cells were lysed at 4°C in 0.83% ammonium chloride with 0.1% potassium hydrogen carbonate, followed by a phosphate-buffered saline (PBS) washing step. $CD34^+$ cells were isolated by magnetic cell separation using the MidiMacs technique according to the manufacturer's instructions (Miltenyi Biotec, Bergisch Gladbach, Germany), yielding $CD34^+$ cells of 80.2 ± 8.6 % purity ($n = 19$).

Transfection of $CD34^+$ cells

The pEGFP-N1 vector (BD Clontech, Heidelberg, Germany) was amplified in *Escherichia coli* strain DH12S (Invitrogen GmbH, Karlsruhe, Germany) and purified using an Endofree-Plasmid-Maxi-preparation kit (Qiagen,Hilden, Germany) according to the manufacturer's instructions.

$CD34^+$-enriched cells were divided into aliquots of equal size ($2–5 \times 10^5$ cells per aliquot) and were either not transfected, transfected without DNA (mock), or transfected with 5 μg of the vector pEGFP-N1 as described in the text. By rinsing the transfection cuvettes two times with 1 ml of I20 [Iscove's modified Dulbecco's medium (Invitrogen GmbH) supplemented with 20% fetal calf serum (FCS; Biochrom, Berlin, Germany)] transfected cells were transferred into a 15-ml plastic tube and washed in a total volume of 10 ml of I20. Pelleted cells were incubated for 15 min in a humidified atmosphere at 37°C and 5% CO_2, then they were resuspended in 1 ml of Myleocult H5100 (Stem Cell Technologies Inc, Vancouver, Canada) supplemented with early-acting cytokines (fetal liver tyrosine kinase-3 ligand [FLT3L], stem cell factor [SCF], thrombopoietin [TPO], each at 10 ng/ml final concentration [all PeproTech, Inc., Rocky Hill, NJ]). Cells were cultured at a density of $\approx 1 \times 10^5$ cells/ml, either in the presence or absence of the general caspase inhibitor Z-VAD-FMK (BD Biosciences, Heidelberg, Germany) in a humidified atmosphere at 37°C and 5% CO_2.

Flow cytometry and cell sorting

After 2 days, cultivated mock- and GFP-transfected cells, as well as nontransfected cells, were stained with an anti-CD34-PeCy5 antibody (clone 581; BD Pharmingen, Heidelberg, Germany). $CD34^+$ cells of the controls and successfully transfected $CD34^+GFP^+$ cells were highly purified using a Coulter EPICS Elite ESP fluorescence cell-sorting system equipped with the Expo32 software (Beckman Coulter, Krefeld, Germany). For functional assays, defined numbers of appropriate cells were immediately sorted into corresponding media. Flow cytometric analyses were performed on a Cytomics FC 500 flowcytometer equipped with the RXP software (Beckman Coulter).

Functional assays

Primitive hematopoietic progenitors were assessed as long-term culture initiating cells (LTC-IC) as described before (13). Briefly, 5,000 cells were sorted into LTBMC medium consisting of Iscove's modified Dulbecco medium (IMDM; Invitrogen GmbH) containing 12.5% horse serum, 12.5% FCS for human myeloid LTC (both Stem Cell Technologies Inc), 2 mM L-glutamine, 100 U/ml penicillin, and 100 U/ml streptomycin (all Invitrogen GmbH). The cells were transfered into 96-well tissue culture plates (Costar, Corning Incorporated, New York) containing irradiated stroma cells of the murine fetal liver cell line AFT024 (14) in limiting dilutions (LDA; 22 replicates per concentration: 150, 50, 15, 5 cells/well). Half-medium exchanges were performed once a week. After 5 weeks of culture in a humidified atmosphere at 37°C and 5% CO_2, all medium was replaced by secondary clonogenic methylcellulose medium consisting of 1,12% methylcellulose (Sigma-Aldrich Chemie GmbH, Steinheim, Germany) in IMDM (Invitro-

gen GmbH) containing 30% FCS for human myeloid CFC (Stem Cell Technologies, Inc.), 2 U/ml erythropoietin (EPO; NeoRecormon; Roche Diagnostics GmbH, Mannheim, Germany), and 10% supernatant of the human bladder carcinoma cell line 5637 (13,15). Cells were cultured for another 2 weeks before individual wells were scored for the presence or absence of secondary colony-forming units (CFU). Using Poisson statistics and the weighted mean method, the frequencies of LTC-IC were calculated (15,16).

To perform CFU-GEMM assays, 250 cells were sorted into MethoCult GF H4434 containing recombinant human SCF, interleukin-3 (IL-3), granulocyte/macrophage colony-stimulating factor (GM-CSF), and EPO (Stem Cell Technologies Inc). The cells were incubated in a humidified atmosphere at 37°C and 5% CO_2. Hematopoietic colonies were scored after 10–14 days as described before (13,15).

Stromal feeders for LTC-IC assays

The murine fetal liver cell line AFT024 was used as a stromal feeder layer to support hematopoietic growth in LTC-IC assays. The cell line was maintained at 33°C in Dulbecco's modified Eagle's medium (DMEM; Invitrogen GmbH) containing 20% FCS (Biochrom AG) and 160 μM 2-mercaptoethanol (Invitrogen GmbH). The 96-well plates (Costar, Corning Incorporated) used for the LTC-IC assays were coated with 0.1% gelatin (Stem Cell Technologies, Inc.) and seeded with AFT024 cells. Cells were grown to confluence and irradiated with 2,000˘rad. One day after irradiation, all medium was replaced by LTBMC medium.

Immunofluorescence and microscopy

Analyses of living cells were performed at 37°C in a humidified, 5% CO_2 atmosphere using a DMIRB inverse fluorescence microscope (Leica, Bensheim, Germany). Pictures were taken with an Axiocam digital camera and processed using Axiovision Software (Carl Zeiss, Goettingen, Germany).

Statistics

Experimental results from different experiments were reported as mean ± standard deviation of the mean (SD). Significance analyses were performed with the paired Student's *t*-test.

RESULTS

Optimization of the nucleofection technology to transfect primitive hematopoietic cells

As described recently, we have successfully applied the nucleofection technology to transfect freshly isolated $CD34^+$ cells with different GFP-encoding plasmids (12). When following the manufacturer's instructions (especially using the nucleofection program U08) and using more than 5×10^5 $CD34^+$-enriched cells, we obtained satisfying transfection and survival rates. However, when using less than 5×10^5 $CD34^+$-enriched cells in a single transfection reaction, the survival rate decreased dramatically, and transfection buffer-derived floe-like structures arose within the concomitant cell culture. To overcome these difficulties when transfecting as little as 2×10^5 $CD34^+$-enriched cells, we tested different nucleofection programs and obtained the best results using the nucleofection program U01. However, even a large proportion of the transfected cells were still viable at day 1 post transfection (p.t.), most of them died within two days p.t. (data not shown). In accordance with the original protocol, we initially cultured transfected $CD34^+$ cells in the presence of the transfection buffer. When the transfection buffer was removed immediately after the transfection procedure, the survival rate of cultivated, transfected cells was obviously increased (data not shown).

Electroporation processes create minipores in cell membranes that selectively enable the passage of small ions, resulting in a colloidal osmotic swelling that kills cells (18,19). Because the postpulse pelleting procedure, i.e., the immediate precipitation and incubation of pelleted, transfected cells for 15 min at 37°C, was reported to suppress this swelling in human primary hematopoietic stem cells (19,20), we adapted this procedure to our protocol. Using our improved protocol and 5 μg of Endofree-preparted plasmid DNA (pEGFP-N1), we now obtain survival rates at day 2 p.t. of 52.9% ± 18.9% (n = 19) with a mean transfection efficiency of 79.8% ± 14.1% (n = 19). Upon usage of higher amounts of plasmid DNA (10 μg), the viability of transfected cells dropped down (data not shown).

Effects of apoptosis inhibitor Z-VAD-FMK on cell survival

Recently, it was shown that the electrotransfection-induced DNA uptake resulted in the induction of large-scale apoptosis in $CD34^+$ cells isolated from peripheral blood, and that this apoptotic effect was clearly reduced when caspase inhibitors, e.g., Z-VAD-FMK, were added to the postpulse culture media (20). To analyze whether inhibition of caspases also increase the survival rate of nucleofected $CD34^+$ cells, we compared the survival rate of nontransfected, mock-transfected, and GFP-transfected $CD34^+$ cells that were cultured in the presence or absence of Z-VAD-FMK (20 μM or 120 μM) for 2 days (n = 6). As depicted in Table 1, we did not find any significant impact of Z-VAD-FMK on the survival rate of GFP transfected $CD34^+$ cells; a slight increase was observed when added at a final concentration of 120 μM (Table 1).

TABLE 1. MEAN SURVIVAL RATE OF CULTURED NONTRANSFECTED AND TRANSFECTED CELLS 2 DAYS POST TRANSFECTION

	Untreated	*20 μM Z-VAD-FMK*	*120 μM Z-VAD-FMK*
Control	84.5% ± 4.8%	76.3% ± 12.4%	78.9% ± 11.0%
		$p = 0.061$	$p = 0.171$
Mock	76.7% ± 10.5%	76.3% ± 10.7%	76.1% ± 6.2%
		$p = 0.246$	$p = 0.045$
GFP	49.5% ± 19.0%	52.8% ± 16.3%	60.4% ± 7.6%
		$p = 0.130$	$p = 0.044$

Content of $CD34^+$ cells, 78.8% ± 11.6%; GFP transfection rate, 85.1% ± 5.0%; $n = 6$; p Values are given in relation to corresponding untreated cell fractions.

Effects of the nucleofection procedure on the cell growth of $CD34^+$ cells

As we have described recently, upon cultivation $CD34^+$ cells increase in size and acquire a dynamic, polarized cell morphology, forming a leading edge at the front and an uropod at the rear pole (12). To analyze whether the nucleofection procedure has any morphological effect on $CD34^+$ cells, we compared GFP-transfected, mock-transfected, and nontransfected cells. We realized that most cultivated mock- or GFP-transfected $CD34^+$ cells acquire a polarized cell shape similar to that of nontransfected cells (Fig. 1). However, whereas nontransfected $CD34^+$ cells reach their final size at culture day 2, transfected $CD34^+$ cells seem to be delayed in their cell growth. This difference vanishes largely until day 3 post-transfection (Fig. 2A). It should be mentioned that we observed an additional reduction in cell growth upon treating transfected cells with Z-VAD-FMK (data not shown).

To analyze whether the transfection procedure has any obvious influence on the expression of stem cell-associated surface marker, we compared the content of CD34 and CD133 expression of nontransfected as well as of GFP-transfected cells over time. Under the con-

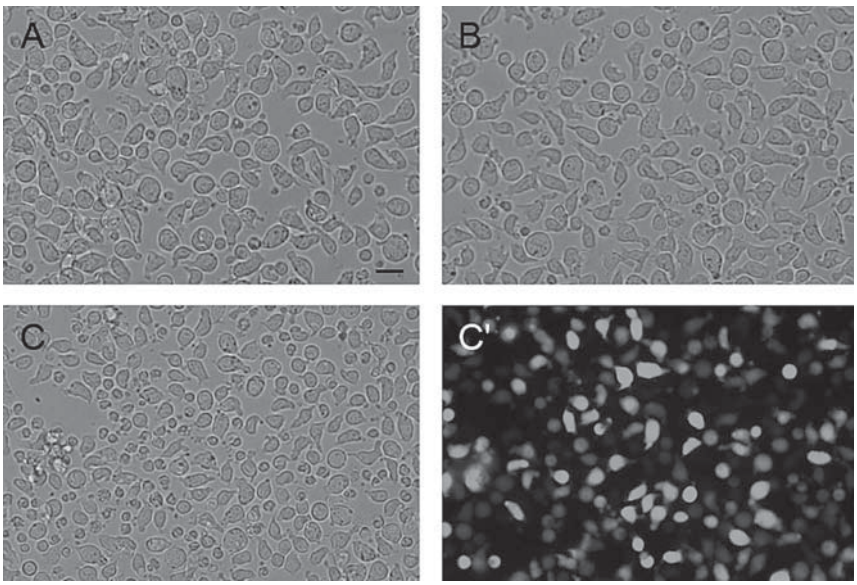

FIG. 1. Upon cultivation, nontransfected as well as transfected $CD34^+$ cells acquire a polarized cell shape. (**A**) Nontransfected $CD34^+$ cells. **(B)** Mock-transfected $CD34^+$ cells. **(C,C′)** GFP-transfected $CD34^+$ cells. All depicted cells were derived from the same $CD34^+$ preparation. Apart from the nucleofection reaction, cells were treated the same. Photos were taken at day 2 post transfection. GFP-transfected cells are clearly smaller than non- or mock-transfected cells (compare **C** to **A** or **B**, respectively). Note that most cells, even the GFP-transfected cells, acquired a polarized cell shape.

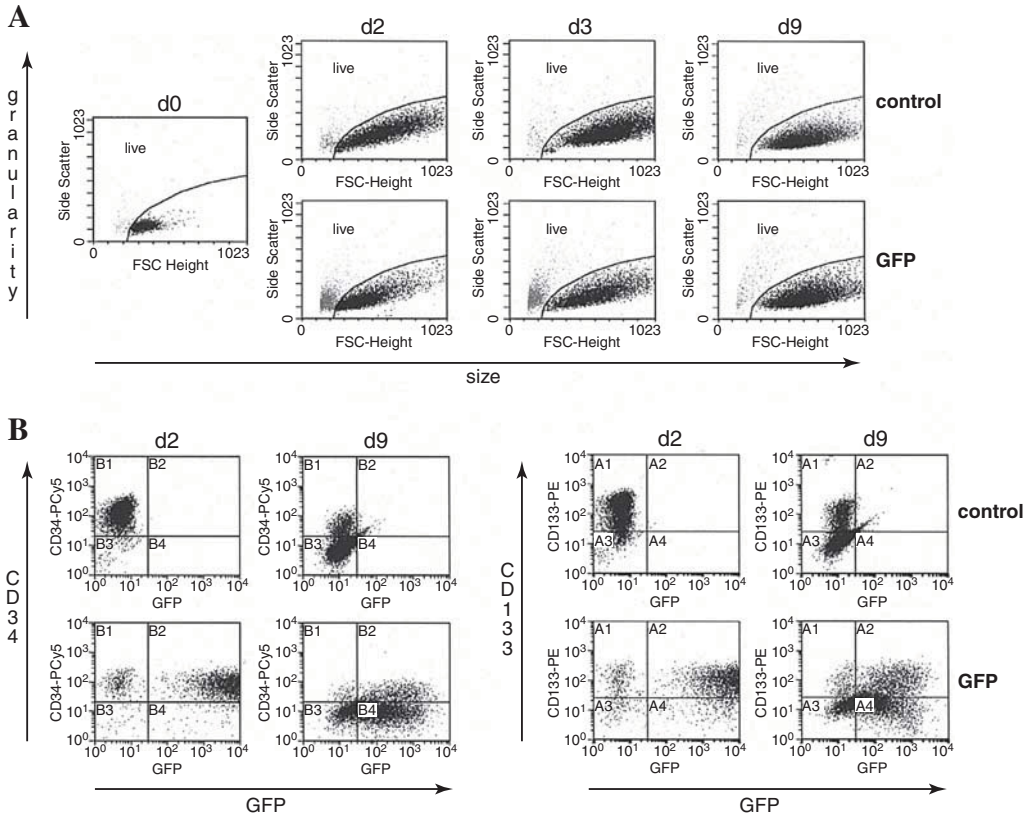

FIG. 2. Flow cytometric analysis of nontransfected and GFP-transfected cells. **(A)** Comparison of the size (FSC-height) and granularity (side scatter) of freshly isolated $CD34^+$ (day 0) and GFP-transfected cells (GFP) versus nontransfected cells $CD34^+$ cells at day 2, day 3, or day 9 past transfection. Upon cultivation, cultured cells increase in size and granularity. While cultivated control cells reach their final size after 2 days, the growth of GFP-transfected cells is delayed approximately 1 day. The "live" gate includes the living and excludes the dead cells. **(B)** Expression of CD34 and CD133 in GFP-transfected or nontransfected control cells that were cultured for 2 or 9 days in the presence of early-acting cytokines. Note that GFP-transfected cells express comparable levels of CD34 and CD133 expression than non-transfected cells. Only cells within the live gate (shown in **A**) are plotted.

ditions used, we observed similar dynamics of CD133 and CD34 expression in cultivated nontransfected or GFP-transfected $CD34^+$ cells, respectively (Fig. 2B). Starting from culture day 3, CD133 and CD34 expression declines over time leaving approximately 20% $CD133^+CD34^+$ cells at day 9 p.t. (Fig. 2B). In this context, it is worth mentioning that although the strength of GFP expression decreases more than 20-fold, approximately 50% of the cultured offspring of originally GFP-transfected cells still express GFP after 9 days (Fig. 2B).

Colony-forming potential of GFP-nucleofected $CD34^+$ cells

To identify potential effects of the nucleofection procedure on the colony-forming potential of $CD34^+$ cells, we performed CFU-GEMM assays of either transfected or nontransfected $CD34^+$ cells. To allow transfected cells to recover from the transfection procedure and to express the *trans*-gene, they were cultured for 2 days in the presence of early-acting cytokines. Then, viable GFP^+ $CD34^+$ cells or $CD34^+$ cells of the controls were purified by cell sorting and transferred in discrete numbers into the CFU-GEMM assay.

According to our data, GFP transfected $CD34^+$ cells form fewer colonies than non- and mock-transfected control cells do. However, we did not find any significant alteration in the ratio of erythroid to myeloid to mixed colonies in our assays (Table 2). The addition of the caspase inhibitor Z-VAD-FMK to the cultures of the 2-day lasting recovery phase did not reveal any positive effect on the frequency of colony formation of transfected or nontransfected cells (data not shown).

TABLE 2. MEAN COLONY FORMATION OF NONTRANSFECTED AND TRANSFECTED CELLS AND RATE OF WHITE TO RED TO MIXED COLONIES OF COLONIES FORMED

	Survival rate	*Colonies per 250 CD34$^+$ cells*	*Rate of red colonies*	*Rate of white colonies*	*Rate of mixed colonies*
Control	82.3% ± 6.0%	119.6% ± 64.7%	18.2% ± 11.3%	62.8% ± 14.2%	19.0% ± 11.6%
Mock	74.2% ± 9.7%	108.6 ± 56.0	15.3% ± 12.1%	64.0% ± 16.9%	20.8% ± 12.8%
	$p = 0.007$	$p = 0.331$	$p = 0.206$	$p = 0.440$	$p = 0.386$
GFP	50.5% ± 17.5%	86.3 ± 76.2	16.0% ± 10.5%	60.3% ± 15.8%	23.7% ± 20.8%
	$p < 0.001$	$p = 0.097$	$p = 0.288$	$p = 0.245$	$p = 0.177$

Content of CD34$^+$ cells, 78.8% ± 10.0%; GFP transfection rate, 79.6% ± 15.6%, $n = 10$, p values are given in relation to corresponding control cell fractions.

LTC-IC content of GFP-nucleofected CD34$^+$ cells

To test if more primitive hematopoietic cells within the CD34$^+$ cell fraction can be transfected without losing their primitive cell fate, we performed LTC-IC assays of successfully transfected CD34$^+$ cells in comparison to CD34$^+$ cells of the controls. Again, to allow the cells to recover from the transfection procedure, we cultured them for 2 days in the presence of early-acting cytokines, before, either in the presence or in the absence of Z-VAD-FMK.

According to our results, we detected a slight reduction in the LTC-IC frequency of transfected versus nontransfected cells (Table 3). A beneficial effect of the caspase inhibitor was not observed (data not shown).

DISCUSSION

In addition to their clinical relevance, primary human HSCs provide an attractive and challenging system to study certain biological processes, e.g., the process regulating the decision whether a stem cell is maintained as a stem cell or becomes committed to differentiate. To analyze such processes genetically, it is extremely helpful to have a reliable and highly efficient method to genetically manipulate these cells without altering their cell fate just by the method itself. As we and others have published recently, the nucleofection technology is very efficient method to transfect human HSC-enriched CD34$^+$ cells transiently (11,12). Herein we report the optimization of the nucleofection protocol to transfect transiently as little as 2×10^5 freshly isolated, human HSC-enriched CD34$^+$ cells and the effects of the transfection procedure on the short-term as well as on the long-term cell fate of these cells.

Using our optimized conditions and an enhanced (e) GFP-encoding plasmid, we obtained transfection efficiencies of 80.2% ± 8.6% ($n = 19$) and survival rates of 52.9% ± 18.9% at day 2 post transfection. This rate is higher than that reported of the manufacturers, in which precultured human CD34$^+$ cells were transfected with an efficiency of ~70% and a mean survival rate of less than 40% at day 2 post transfection (11). Optimized classical electroporation procedures of human CD34$^+$ cells result in transfection efficiencies of around 30% and survival rates up to 77%, but require a precultivation of transfected cells (5,6), which frequently alters the cell fate of primitive hematopoietic cells (21,22). In several studies, freshly isolated CD34$^+$ cells were electroporated with only low transfection efficiencies (6.9% and 12%) (5,23). Comparable to classical electroporation procedures, transfection rates obtained with liposome-based technologies remain far below the efficiency obtained with the nucleofection technology (24).

Compared to nontransfected control cells (82.3% ± 6.0%; $n = 10$), the cell survival rate of mock-transfected cells is only slightly decreased (74.2% ± 9.7%; $n = 10$) whereas many of the GFP-transfected cells die within the first 48 h post transfection (survival rate, 50.0% ± 17.5%; $n = 10$). These results clearly demonstrate that the lethality observed in our experiments is more related to the presence of the DNA or to the strong GFP expression than to the nucleofection procedure itself. In-

TABLE 3. MEAN LTC-IC RATE OF NONTRANSFECTED AND TRANSFECTED CELLS

	Survival rate	*LTC-IC in surviving cells*
Control	79.7% ± 7.5%	5.1% ± 1.5%
Mock	74.9% ± 14.3%	4.9% ± 0.5%
	$p = 0.183$	$p = 0.353$
GFP	53.0% ± 23.8%	3.4% ± 1.3%
	$p = 0.028$	$p = 0.059$

Content of CD34$^+$ cells, 79.1% ± 3.3%; GFP transfection rate, 66.7% ± 18.7%, $n = 4$, p Values are given in relation to corresponding control cell fractions.

deed the occurrence of DNA-induced cell death in electroporation experiments and the induction of apoptosis by high levels of GFP expression have been reported before (19,20,25–27).

Consistent with these observations, we realized a reduced colony-forming frequency of isolated GFP^+CD34^+ cells in CFU-GEMM and LTC-IC assays compared to that of isolated $CD34^+$ cells of the mock-transfected or nontransfected controls (Tables 2 and 3). Because the ratio of erythroid to myeloid to mixed colonies formed by GFP^+CD34^+ cells was largely the same as that of the $CD34^+$ control cells, we assume that the DNA and/or GFP-induced cell death is rather unspecific than specific for any of the $CD34^+$ cell subtypes. In summary, these results suggest that DNA transfer into freshly isolated human $CD34^+$ cells by the nucleofection procedure reduces the overall survival rate but has no major impact on the cell fate of surviving cells. Therefore, the nucleofection method is indeed a highly efficient and reliable method to manipulate primitive hematopoietic cells genetically.

Although we observed that approximately 50% of the offspring of the initially transfected cells still express low levels of GFP after 9 days, it was not our aim to analyze whether these cells were stably transfected or whether GFP-encoding plasmids remained transiently in those cells. As mentioned before, culture conditions have a major impact on the fate of HSCs and HPCs; under most stroma-free culture conditions, the majority of primitive cells become committed within the first few days of culture (21,22).

Thus, the nucleofection method is a useful technique to manipulate and dissect the genetic programs that regulate the maintenance or early commitment of HSCs or HPCs. As shown here, by performing CFU-GEMM or LTC-IC assays, it can easily be analyzed whether expression of certain genes modifies the colony-forming frequency or the ratio of erythroid to myeloid to mixed colonies in progenitor assays. As the morphology of cultivated transfected $CD34^+$ cells is not recognizably altered in comparison to cultivated control cells, this method is also very applicable to study the subcellular distribution of introduced GFP-fusion proteins (12). According to the high transfection efficiency, the method might also be helpful for in vivo applications of transfected HSCs/HPCs in scientific or clinical approaches.

ACKNOWLEDGMENTS

The authors thank Dr. Kay Giesen and Dr. Oliver Gresch for initial experimental support and Daniel Moik for a critical reading of the manuscript. This work was funded by grants from the Deutsche Forschungsgemeinschaft (SPP1109 GI 336/1–2 to B.G. and P.W.) as well as from the Forschungskommission of the HHU-Düsseldorf.

REFERENCES

1. Weissman IL. (2000). Translating stem and progenitor cell biology to the clinic: barriers and opportunities. Science 287:1442–1446.
2. Anderson KV and PW Ingham. (2003). The transformation of the model organism: a decade of developmental genetics. Nature Genet 33(Suppl):285–293.
3. Leurs C, M Jansen, KE Pollok, M Heinkelein, M Schmidt, M Wissler, D Lindemann, C Von Kalle, A Rethwilm, DA Williams and H Hanenberg. (2003). Comparison of three retroviral vector systems for transduction of nonobese diabetic/severe combined immunodeficiency mice repopulating human $CD34^+$ cord blood cells. Hum Gene Ther 14:509–519.
4. Baum C, J Dullmann, Z Li, B Fehse, J Meyer, DA Williams and C von Kalle. (2003). Side effects of retroviral gene transfer into hematopoietic stem cells. Blood 101:2099–2114.
5. Van Tendeloo VF, R Willems, P Ponsaerts, M Lenjou, G Nijs, M Vanhove, P Muylaert, P Van Cauwelaert, C Van Broeckhoven, DR Van Bockstaele and ZN Berneman. (2000). High-level transgene expression in primary human T lymphocytes and adult bone marrow $CD34^+$ cells via electroporation-mediated gene delivery. Gene Ther 7:1431–1437.
6. Wu MH, SL Smith and ME Dolan. (2001). High efficiency electroporation of human umbilical cord blood $CD34^+$ hematopoietic precursor cells. Stem Cells 19:492–499.
7. Hamm A, N Krott, I Breibach, R Blindt and AK Bosserhoff. (2002). Efficient transfection method for primary cells. Tissue Eng 8:235–245.
8. Harriague J and G Bismuth. (2002). Imaging antigen-induced PI3K activation in T cells. Nature Immunol 3:1090–1096.
9. Trompeter HI, S Weinhold, C Thiel, P Wernet and M Uhrberg. (2003). Rapid and highly efficient gene transfer into natural killer cells by nucleofection. J Immunol Methods 274:245–256.
10. Lakshmipathy U, B Pelacho, K Sudo, JL Linehan, E Coucouvanis, DS Kaufman and CM Verfaillie. (2004). Efficient transfection of embryonic and adult stem cells. Stem Cells 22:531–543.
11. Gresch O, FB Engel, D Nesic, TT Tran, HM England, ES Hickman, I Korner, L Gan, S Chen, S Castro-Obregon, R Hammermann, J Wolf, H Muller-Hartmann, M Nix, G Siebenkotten, G Kraus and K Lun. (2004). New non-viral method for gene transfer into primary cells. Methods 33:151–163.
12. Giebel B, D Corbeil, J Beckmann, J Hohn, D Freund, K Giesen, J Fischer, G Kogler and P Wernet. (2004). Segregation of lipid raft markers including CD133 in polarized human hematopoietic stem and progenitor cells. Blood 104:2332–2338.
13. Punzel M, SD Wissink, JS Miller, KA Moore, IR Lemischka and CM Verfaillie. (1999). The myeloid-lymphoid initiating cell (ML-IC) assay assesses the fate of multipotent human progenitors in vitro. Blood 93:3750–3756.
14. Moore KA, H Ema and IR Lemischka. (1997). In vitro maintenance of highly purified, transplantable hematopoietic stem cells. Blood 89:4337–4347.

15. Verfaillie C and P McGlave. (1991). Leukemia inhibitory factor/human interleukin for DA cells: a growth factor that stimulates the in vitro development of multipotential human hematopoietic progenitors. Blood 77:263–270.
16. Porter EH and RJ Berry. (1963). The efficient design of transplantable tumour assays. Br J Cancer 17:583–595.
17. Taswell C. (1981). Limiting dilution assays for the determination of immunocompetent cell frequencies. I. Data analysis. J Immunol 126:1614–1619.
18. Watanabe M, Y Shirayoshi, U Koshimizu, S Hashimoto, S Yonehara, Y Eguchi, Y Tsujimoto and N Nakatsuji. (1997). Gene transfection of mouse primordial germ cells in vitro and analysis of their survival and growth control. Exp Cell Res 230:76–83.
19. Li LH, P Ross and SW Hui. (1999). Improving electrotransfection efficiency by post-pulse centrifugation. Gene Ther 6:364–372.
20. Li LH, P McCarthy and SW Hui. (2001). High-efficiency electrotransfection of human primary hematopoietic stem cells. Faseb J 15:586–588.
21. Sorrentino BP. (2004). Clinical strategies for expansion of haematopoietic stem cells. Nature Rev Immunol 4:878–888.
22. Sauvageau G, NN Iscove and RK Humphries. (2004). In vitro and in vivo expansion of hematopoietic stem cells. Oncogene 23:7223–7232.
23. Weissinger F, P Reimer, T Waessa, S Buchhofer, T Schertlin, V Kunzmann and M Wilhelm. (2003). Gene transfer in purified human hematopoietic peripheral-blood stem cells by means of electroporation without prestimulation. J Lab Clin Med 141:138–149.
24. Floch V, G Le Bolc'h, MP Audrezet, JJ Yaouanc, JC Clement, H des Abbayes, B Mercier, JF Abgrall and C Ferec. (1997). Cationic phosphonolipids as non viral vectors for DNA transfection in hematopoietic cell lines and $CD34^{+}$ cells. Blood Cells Mol Dis 23:69–87.
25. Stacey KJ, IL Ross and DA Hume. (1993). Electroporation and DNA-dependent cell death in murine macrophages. Immunol Cell Biol 71(Pt 2):75–85.
26. Shimokawa T, K Okumura and C Ra. (2000). DNA induces apoptosis in electroporated human promonocytic cell line U937. Biochem Biophys Res Commun 270:94–99.
27. Liu HS, MS Jan, CK Chou, PH Chen and NJ Ke. (1999). Is green fluorescent protein toxic to the living cells? Biochem Biophys Res Commun 260:712–717.

Address reprint requests to:
Dr. Bernd Giebel
Institute for Transplantation Diagnostics
and Cell Therapeutics
Heinrich-Heine-University Düsseldorf
Moorenstrasse 5, Geb. 14.80
40225 Düsseldorf, Germany

E-mail: Giebel@itz.uni-duesseldorf.de

Received November 3, 2005; accepted February 2, 2006.

Journal of Pathology
J Pathol 2004; **204**: 538–545
Published online in Wiley InterScience (www.interscience.wiley.com). **DOI:** 10.1002/path.1664

Original Paper

The early transcription factor GATA-2 is expressed in classical Hodgkin's lymphoma

Eva-Maria Schneider,[1†,‡] Emina Torlakovic,[2‡] Albert Stühler,[1†] Volker Diehl,[1] Hans Tesch[1] and Bernd Giebel[1§*]
[1]*Department of Internal Medicine I, University of Cologne, D-50924 Cologne, Germany*
[2]*Department of Pathology, The Norwegian Radium Hospital, NO-0310 Oslo, Norway*

**Correspondence to: Bernd Giebel, Institute for Transplantation Diagnostics and Cell Therapeutics, Heinrich-Heine University Düsseldorf, Moorenstrasse 5, Building 14.80, D-40225 Düsseldorf, Germany. E-mail: Giebel@itz.uni-duesseldorf.de*

†*Current address: Paul-Ehrlich Institut, D-63225 Langen, Germany.*

‡*These authors contributed equally to this work.*

§*Current address: Institute for Transplantation Diagnostics and Cell Therapeutics, Heinrich Heine University Düsseldorf, D-40225 Düsseldorf, Germany.*

Received: 7 May 2004
Revised: 14 July 2004
Accepted: 27 July 2004

Abstract

Hodgkin/Reed–Sternberg (HRS) cells of classical Hodgkin's lymphoma (cHL) are thought to be derived from germinal centre B-cells in almost all cases. However, expression profiling has revealed that HRS cells do not show a germinal centre B-cell-like phenotype. Although the nature of this aberrant phenotype and the underlying molecular mechanisms remain largely unknown, it has been reported that the activity of NOTCH1 plays an important role in the growth and survival of HRS cells. In some leukaemic cell lines, the effect of Notch signalling is mediated by the early transcription factor GATA-2. This and the fact that HRS cells lack expression of PU.1, which can repress *Gata-2*, led to an investigation of GATA-2 expression in HRS cells. GATA-2 expression was found in all the cHL-derived cell lines studied, but not in a Burkitt lymphoma-derived cell line. In addition, 50% of biopsies from patients with cHL contained GATA-2-expressing HRS cells. In contrast, neither normal germinal centre B-cells nor malignant cells of nodular lymphocyte-predominant Hodgkin's lymphoma, Burkitt lymphoma or diffuse large B-cell lymphoma expressed GATA-2. Thus, GATA-2 expression was found specifically in HRS cells of cHL, suggesting that GATA-2 is important in establishing the abnormal B-cell phenotype of HRS cells.

Keywords: Hodgkin's disease; Hodgkin's lymphoma, HRS; Gata-2; Pu.1; Notch1

Introduction

Classical Hodgkin's lymphoma (cHL) is a lymphoproliferative malignancy caused by malignant Hodgkin and Reed–Sternberg (HRS) cells. In most of the cases studied, clonally related HRS cells contain non-functional immunoglobulin genes with somatic mutations in their V-region genes, suggesting that they are malignant derivatives of germinal centre (GC) B-cells that have escaped the normal negative selection programme of apoptosis [1–4]. In addition, HRS cells are characterized by an unusual immunophenotype; they lack a number of B-cell lineage markers [5–7] and specific transcription factors, eg PU.1 [8–11], possibly resulting in a general defect in B-cell lineage gene expression, as described recently [12]. However, HRS cells express transcription factors such as Pax-5, which is essential for B-cell commitment in fetal liver and progression of B-cell development beyond an early stage in the adult bone marrow [13–16], providing more evidence for a frequent B-cell origin of HRS cells.

One important transforming factor in the course of Hodgkin's disease could be NOTCH1. It has been reported that NOTCH1 is highly expressed on the surface of B-cell-derived HRS cells and activation of the Notch signalling pathway plays an important role in the growth and survival of HRS cells [17]. As in many other developmental processes, the Notch pathway plays an important role during cell fate specification in normal haematopoiesis, for example maintaining haematopoietic stem cell fate [18,19] and governing several lineage decision processes, such as B-cell versus T-cell development [20]. Furthermore, members of the Notch signalling pathway can be involved in malignant diseases. For example, the human Notch allele Tan-1, which encodes a constitutive active form of human NOTCH1, is a major oncogene in acute lymphocytic leukaemia [21]. *In vitro* experiments revealed that constitutive active forms of NOTCH are able to suppress differentiation programmes effectively by regulating the expression of certain transcription factors [22,23]; one of these transcription factors is GATA-2, the expression of which is sustained in a NOTCH-dependent manner in myeloid progenitor and erythroleukaemia cells [24].

GATA-2 belongs to the GATA family of transcription factors which contain a two-zinc-finger domain

structure and share a consensus binding sequence, WGATAR [25]. GATA 1–3 are important transcription factors in haematopoietic cells [25,26]. Beside its high expression in enriched haematopoietic stem and progenitor populations [27], GATA-2 is normally expressed in early erythroid cells, mast cells, and megakaryocytes [28–31]. While the loss of GATA-2 function is dispensable for erythroid and myeloid differentiation, GATA-2 is required for both proliferation and survival of haematopoietic stem and progenitor cells and for the formation of mast cells [32,33]. Overexpression experiments revealed that enforced expression of GATA-2 increases the number of immature haematopoietic cells [34] and inhibits the terminal differentiation of erythroid progenitors into erythrocytes by promoting their differentiation into the megakaryocyte lineage [31,34,35].

Interestingly, PU.1, which directs the differentiation of haematopoietic progenitors into macrophages, neutrophils, and B lymphocytes [36,37], interacts with GATA proteins; that is, they antagonize each other's activities by direct protein–protein interactions. In addition, PU.1 inhibits the expression of genes that encode GATA factors [38–42]. In view of the observation that PU.1 is aberrantly not expressed in HRS cells, and NOTCH1 is an important transforming factor in HD, together with the fact that both proteins regulate GATA-2 expression, we wondered if GATA-2 might be involved in HD. We have therefore analysed GATA-2 expression in different lymphoproliferative malignancies at transcriptional and protein levels.

Materials and methods

Cell lines

We used the cHL-derived cell lines L428, L1236, HDLM-2, KM-H2, and L591; the Burkitt lymphoma-derived cell line BL41; and the T-cell lymphoma-derived Jurkat cell line, grown in RPMI 1640 supplemented with 10% fetal calf serum and 100 U/ml penicillin/streptomycin (Sigma-Aldrich Chemie GmbH, Taufkirchen, Germany) in a humidified atmosphere at 37 °C and 5% CO_2.

Biopsy samples

Formalin-fixed and paraffin wax-embedded lymph node biopsies were collected from the archives of the Department of Pathology, The Norwegian Radium Hospital, Oslo, Norway and used in an anonymized fashion. This procedure is in agreement with the guidelines for the use of human biopsy material for research purposes issued by the Ethics Committee of the Norwegian Radium Hospital. The study included 50 cases of cHL, ten cases of nodular lymphocyte-predominant HL, 30 cases of diffuse large B-cell lymphomas (DLBCLs), ten cases of Burkitt lymphoma (BL), and five lymph nodes and five tonsils with follicular hyperplasia. All of the cases included were re-evaluated according to the WHO classification. Only those BLs with cytogenetically proven *c-myc* rearrangement were included in the study.

Reverse transcription-polymerase chain reaction (RT-PCR)

Total RNA was extracted from cultured cell lines using TRI-Reagent (Sigma-Aldrich Chemie GmbH) followed by DNAse I treatment (1 U DNAse/1 μg RNA, RNAse-free DNAse, Promega GmbH, Mannheim, Germany). cDNA was synthesized from total RNA (5 μg RNA/1 μl oligo$(dT)_{20}$ primers) using the ThermoScript™ RT-PCR System (Invitrogen GmbH, Karlsruhe, Germany) with oligo(dT) primers. PCRs were routinely performed by using the PCR Reagent System (Invitrogen GmbH) according to the manufacturer's instructions. By using human *Gata-2* [43] or human β-actin primers (Eurogentec sa, Seraing, Belgium), cDNA was amplified for 40 (*Gata-2*) or 30 (β-actin) cycles using annealing temperatures of 61 °C (*Gata-2*) or 58 °C (β-actin). Products were analysed by agarose gel electrophoresis.

Western blot analysis

For western blotting, whole-cell protein extracts of 1×10^5 cells per lane were separated on a discontinuous SDS-PAGE and blotted onto nitrocellulose filters (Hybond C extra, Amersham-Pharmacia Biotech, Freiburg, Germany). Expression of GATA-2 was analysed by using a monoclonal mouse anti-GATA-2 antibody (1 : 100; sc267) or a goat polyclonal anti-GATA-2 antibody (1 : 250; sc1235, both from Santa Cruz Biotechnology, Santa Cruz, USA). For control purposes, the expression of β-actin was analysed using a monoclonal mouse anti-β-actin antibody (1 : 10 000; Chemicon International, Temecula, CA, USA). Specifically bound primary antibodies were detected using a horseradish peroxidase (HRP)-conjugated secondary goat anti-mouse antibody (1 : 2000) or a rabbit anti-goat antibody (1 : 1000; both from DakoCytomation GmbH, Hamburg, Germany) and visualized by enhanced chemoluminescence (Amersham Biosciences Europe GmbH).

Flow cytometry

For flow cytometric analysis, cell aliquots of 1×10^5 cells were processed with FIX&PERM® (An der Grub GmbH, Kaumberg, Austria) according to the manufacturer's instructions. Cells were stained with a monoclonal mouse anti-GATA-2 antibody (1 : 25; sc-267) or a goat polyclonal anti-GATA-2 serum (1 : 25; sc-1235; both from Santa Cruz Biotechnology), followed by fluorescein isothiocyanate (FITC)-conjugated goat anti-mouse antibody or rabbit anti-goat antibody, respectively (1 : 200; both DakoCytomation GmbH). Flow cytometric analyses were performed using a FACSCalibur flow cytometry system with Cell Quest software (BD Bioscience, Heidelberg, Germany). Dot-plots

were generated with WinMDI Version 2.8 (Joseph Trotter).

Immunohistochemistry

Immunostaining was performed on formalin-fixed, paraffin wax-embedded tissue sections as described previously [10]. Goat polyclonal anti-GATA-2 serum (1 : 500 dilution; sc-1235) was used as the primary antibody and mouse anti-goat as the secondary antibody (1 : 100 dilution; both from Santa Cruz Biotechnology). Scoring of the intensity of the immunostaining was performed semi-quantitatively (no staining, weak expression = 10–30% HRS cells positive; strong expression = >30% HRS cells positive). Only nuclear expression of GATA-2 was recorded.

In situ hybridization for small EBER RNAs from Epstein–Barr virus (EBV) was performed as described previously [44].

Results

Expression of *Gata-2* transcripts in cHL-derived cell lines

To analyse *Gata-2* mRNA expression by cHL-derived cell lines, we initially performed RT-PCRs using DNAse-treated RNA isolated from both the cHL-derived cell lines L428, L1236, HDLM-2, KM-H2, and L591, and the Burkitt lymphoma-derived cell line BL41; the Jurkat cell line was used as a positive control [according to Santa Cruz Biotechnology (Santa Cruz, USA), Jurkat cells express GATA-2]. A band corresponding to the expected size of 242 bp was obtained for all the cHL-derived cell lines tested, but not for the Burkitt lymphoma cell line BL41 (Figure 1). Using β-actin-specific control PCRs, we detected specific bands of equal intensity for all the cell lines; this served as a loading control (data not shown). These data therefore indicate that *Gata-2* mRNA is expressed in all the cHL-derived cell lines analysed, but not in the Burkitt lymphoma-derived cell line BL41.

GATA-2 protein is expressed in cHL-derived cell lines

To analyse protein expression, we performed western blot analysis using commercially available anti-GATA-2 antibodies or a monoclonal mouse anti-β-actin antibody as a loading control. Using the β-actin antibody, we obtained bands of the expected size for all the cell lines (data not shown). Both the goat polyclonal anti-GATA-2 antibody (Figure 2) and the mouse anti-GATA-2 monoclonal antibody (data not shown) recognized a specific band of approximately 47 kD in whole-cell protein extracts of the cHL-derived cell lines (L428, L1236, HDLM-2, KM-H2, and L591) and of the Jurkat cell line, which was used as a positive control. Since GATA-2 has a predicted size of 47 kD [28], we concluded that GATA-2 protein is expressed in all the cHL-derived cell lines tested.

Although the results obtained by RT-PCR and western blot analysis show that GATA-2 is expressed in all the cHL-derived cell lines studied, it cannot be concluded that all cells of a cHL-derived cell

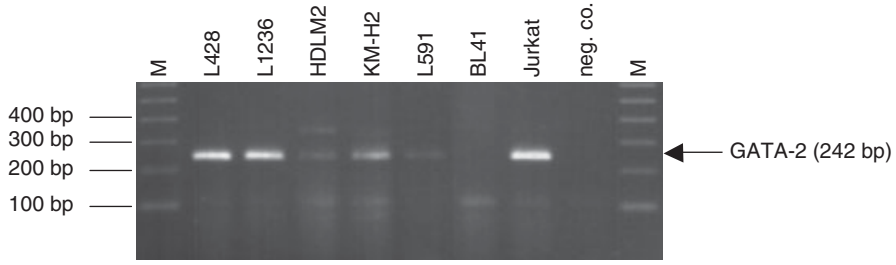

Figure 1. *Gata-2* mRNA is expressed in cHL-derived cell lines. Electrophoretic gel showing positive signal for GATA-2 in cHL-derived cell line samples (L428, L1236, HDML2, KM-H2, and L591) and in a Jurkat sample (242 bp). No signal is observed in the Burkitt lymphoma cell line BL41 sample or in the negative control (water; neg. co.). M = 100 bp DNA ladder

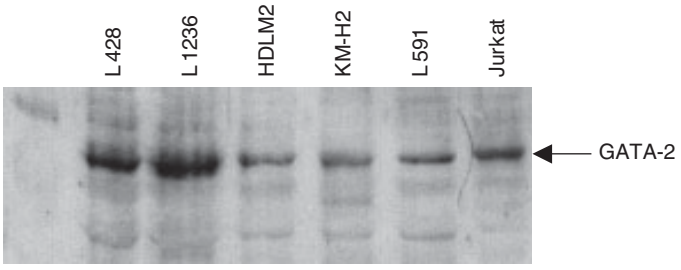

Figure 2. Western blot analysis of GATA-2 protein in cHL-derived cell lines. Whole-cell protein extracts were analysed using a specific polyclonal anti-GATA-2 antibody. A specific protein band of approximately 47 kD, which is found in all the cHL-derived cell lines tested as well as in the Jurkat positive control, is indicated by an arrow

line actually express GATA-2. Therefore, to generate more information about the number of GATA-2-expressing cHL-derived cell line cells and, in particular, to discriminate GATA-2 expression by mononucleated Hodgkin cells from that of polynucleated Reed–Sternberg cells — which are both found in the five cHL-derived cell lines tested — we analysed GATA-2 expression by flow cytometry. We used both the mouse monoclonal and the goat polyclonal anti-GATA-2 antibodies for intracellular staining of L428, L1236, HDLM-2, KM-H2, and L591 cells; in addition, Jurkat and BL41 cells were stained with these anti-GATA-2 antibodies as a positive or negative control, respectively. Furthermore, we performed corresponding isotype controls of all the cell lines used. In all cases, we obtained similar results with the polyclonal (Figure 3) and the monoclonal (data not shown) anti-GATA-2 antibodies. As shown in Figure 3, all the cHL-derived cell line cells and Jurkat cells are positive for GATA-2, while BL41 cells are negative. We therefore conclude that all Hodgkin cells and all Reed–Sternberg cells of the cHL-derived cell lines tested express GATA-2.

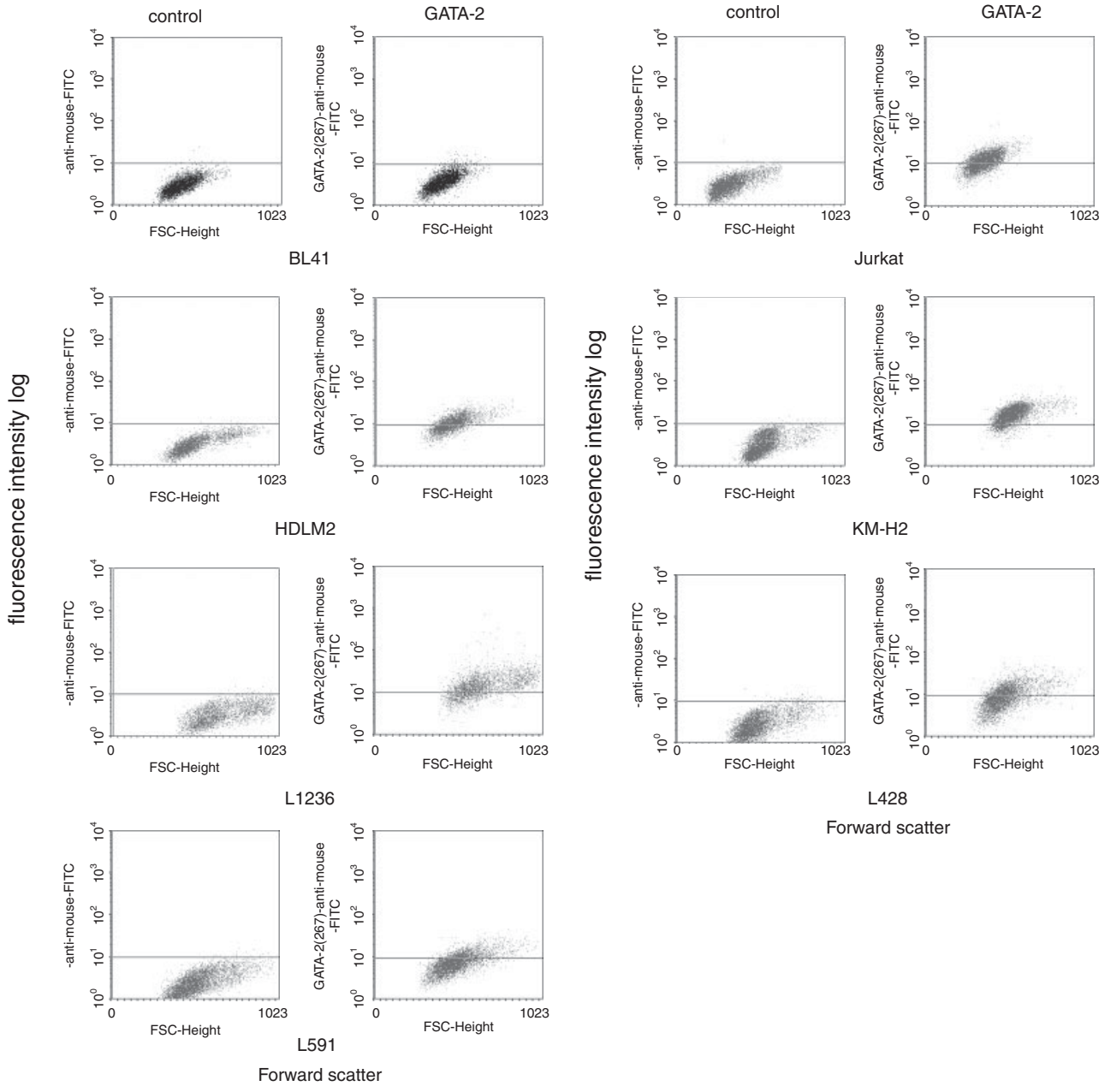

Figure 3. Flow cytometry of GATA-2 protein in cHL-derived cell lines. After fixation and permeabilization, cell lines were stained with either a mouse anti-GATA-2 antibody or a corresponding isotype IgG, followed by counterstaining with a FITC-conjugated goat anti-mouse antibody. The *X*-axes indicate the relative size and the *Y*-axes the logarithm of the relative intensity of green fluorescence of individual cells. The left panel of each individual cell line indicates the background fluorescence and the right panel the GATA-2-specific fluorescence. While cells of the Burkitt lymphoma-derived cell line BL41 do not express GATA-2, all the tested cHL-derived cell line cells (HDML-2, KM-H2, L1236, L428, and L591) as well as the cells of the Jurkat T-cell lymphoma cell line express GATA-2; Jurkat cells were used as a positive control

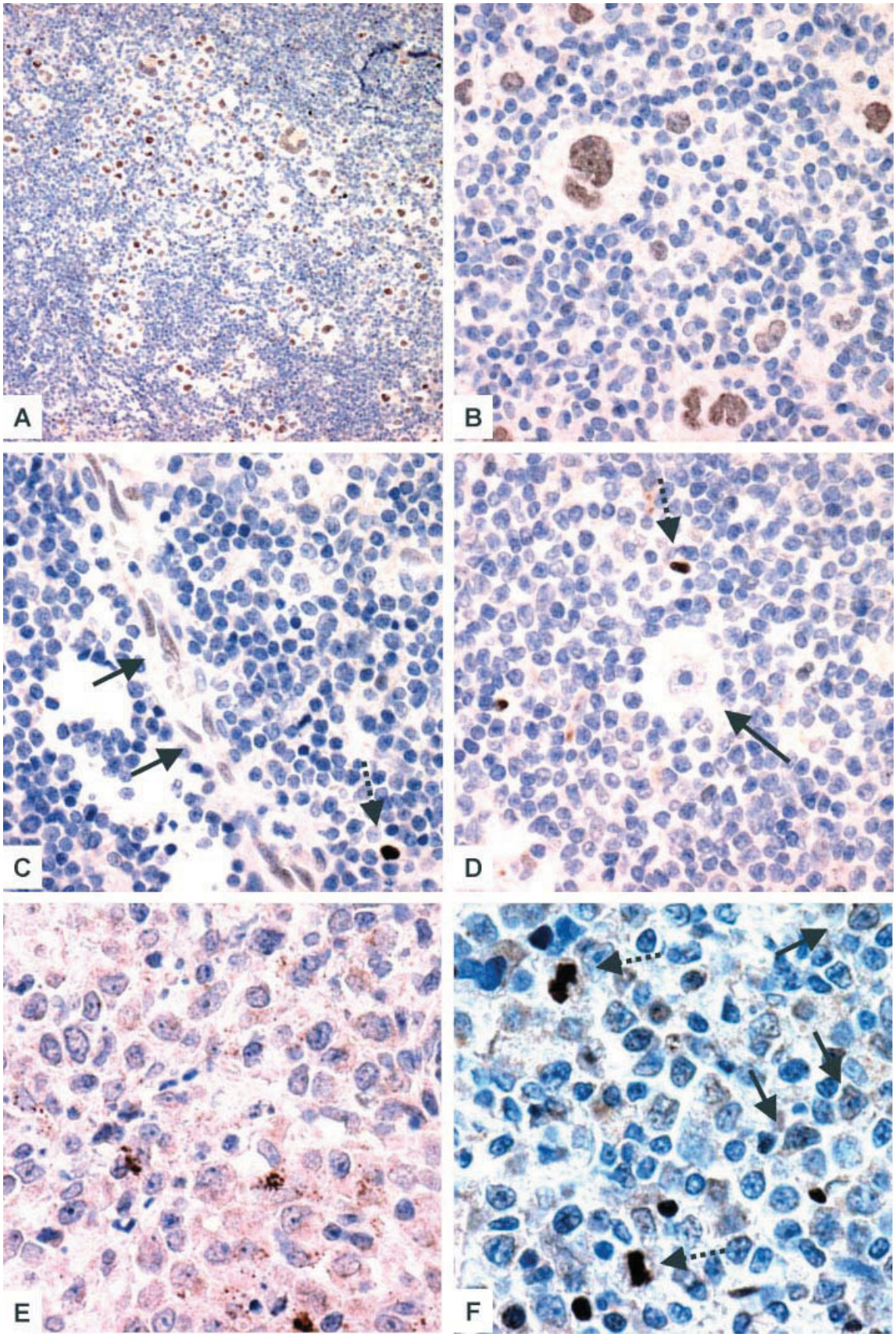

Figure 4. Immunohistochemical detection of GATA-2 expression (EnVision+®, DAB chromogen). Reed–Sternberg cells in classical Hodgkin's lymphoma express nuclear GATA-2 (A and B). Endothelial cells were also positive (C) (arrows). Rare small lymphoid cells show strong expression of GATA-2 (dotted arrows in C and D; ×200 magnification). About half of the cHLs did not express GATA-2 (D). DLBCLs were generally negative (E), but one case expressed weak nuclear GATA-2 in 3% of the malignant cells (full arrows). Expression appeared to be strong in mitotically active cells (dotted arrows) (F)

GATA-2 expression in primary HRS cells in classical Hodgkin lymphoma

To analyse if GATA-2 is expressed in primary HRS cells, we performed anti-GATA-2 antibody staining on formalin-fixed and paraffin wax-embedded lymph node biopsies from patients with cHL, 25 cases of nodular sclerosis, 20 of mixed cellularity, and five cHLs not otherwise specified. All 50 samples of cHL used in our study were positive for Pax-5 and CD30. Eighty-two per cent of the cases studied were positive for CD15 and none expressed nuclear PU.1. In cHL of nodular sclerosis subtype, only 4/25 harboured EBV in malignant cells. In contrast, 17/20 cases of the mixed cellularity cHL subtype and 3/5 remaining cases were associated with EBV ($p < 0.0001$, Fisher's exact test). An age histogram showed a bimodal distribution with peaks at about 20–30 years and about 60–70 years (data not shown).

Using these samples, we found nuclear GATA-2 expression in HRS cells in 50% of cHLs (Figures 4A and 4B). No differences were found between the nodular sclerosis and mixed cellularity subtypes. The level of expression varied, with about half of the positive cases displaying weak expression (10–30% positive HRS cells) and half strong (>30% HRS cells). GATA-2 expression was not associated with either patient sex or age. Since 50% of the cHLs studied express GATA-2 and 50% are EBV-associated, we tested whether there might be a correlation between GATA-2 expression and EBV status. According to our results, there was a random distribution (Table 1), suggesting that there is no relationship between GATA-2 expression and EBV status.

As a control, we stained human reactive lymph nodes and tonsils with the polyclonal anti-GATA-2 antibody. No expression was found in either B- or T-zones of reactive lymph nodes or tonsils. Very strong expression was observed in rare cells with morphological features of small lymphocytes (Figures 4C and 4D). The distribution of these cells appeared to be random and they were also present in the reactive background of cHL cases. We analysed TdT expression in five cHL cases and five reactive lymph nodes which contained the largest number of small GATA-2-positive lymphoid cells. In these samples, we found TdT-positive small lymphoid cells in similar numbers and distribution to the GATA-2-positive cells (data not shown). We therefore believe that these cells are the same as the small GATA-2-positive cells. It is possible that these cells correspond to lymphoid progenitors which were readily identified in tonsils from children and adults and rarely in reactive lymph nodes [45].

In addition, weak expression of GATA-2 was also regularly noted in endothelial cells (Figure 4C) which are known to be positive for GATA-2 [28,46].

To generate some information regarding whether GATA-2 is expressed in malignant cells of other lymphoma entities, we also studied GATA-2 expression in ten cases of nodular lymphocyte-predominant Hodgkin lymphoma (NLPHL), 30 cases of diffuse large B-cell lymphoma (DLBCL), and ten cases of Burkitt lymphoma (BL). While we did not find any GATA-2 expression in NLPHL (Figure 4E) and BL, one of the 30 DLBCLs contained 3% of malignant cells with weak expression of GATA-2 (Figure 4F and Table 2).

Table 1. GATA-2 expression and EBV status in cHL

	EBV-negative	EBV-positive	Total
GATA-2-negative	12	13	25
GATA-2-positive	14	11	25
Total	26	24	50

Table 2. GATA-2 expression in malignant lymphoma

Diagnosis	GATA-2 expression	Comment
cHL	25/50	Variable nuclear expression of GATA-2. Nuclear PU.1 was not expressed in any of the 50 cases
NLPHL	0/10	All cases expressed nuclear PU.1
DLBCL	1/30	Weak nuclear expression in 3% of malignant cells
Burkitt lymphoma	0/10	Weak to moderate cytoplasmic expression in one case

cHL = classical Hodgkin lymphoma; NLPHL = nodular lymphocyte-predominant Hodgkin lymphoma; DLBCL = diffuse large B-cell lymphoma.

Discussion

It is generally thought that HRS cells derive from GC B-cells. However, complex gene expression analysis revealed that HRS cells not only have lost the typical GC B-cell phenotype, but are also characterized by a comprehensive defect in the B-cell lineage [47]. The nature of this aberrant phenotype and the underlying molecular mechanisms remain largely unknown.

In our study, we have shown that the early transcription factor GATA-2 is expressed in all cells of cHL-derived cell lines investigated, but not in a Burkitt lymphoma-derived cell line. Furthermore, we found that in 50% of all the cases studied, lymph nodes of patients with cHL contain GATA-2-expressing HRS cells, while nodular lymphocyte-predominant Hodgkin lymphoma, Burkitt lymphoma, and diffuse large B-cell lymphoma did not express GATA-2.

In summary, our data suggest that, among different B-cell lymphomas, GATA-2 seems to be specifically expressed in HRS cells of cHL. Since we did not find any GATA-2 staining apart from endothelial cells which are known to express GATA-2 [28,46] and small lymphoid cells which were found in benign areas of malignant lymph nodes, and in benign lymph nodes and tonsils, we further conclude that GATA-2 is generally not expressed in GC B-cells. In agreement with our data, serial analysis of gene expression (SAGE) profiles of different B-cell stages [48,49]

did not reveal any GATA-2 expression in mature B-cells including GC B-cells, even though GATA-2 is expressed in pre-B-cells (M Müschen, personal communication). We have therefore identified GATA-2 as a new factor that is aberrantly expressed in HRS cells of cHL.

The observation that, in comparison to primary HRS cells, all cells of cHL-derived cell lines express GATA-2 might be connected to the fact that primary Hodgkin lymphomas do not grow well in culture. Since there are only a few Hodgkin cell lines available, it seems most likely that only a rare subset of primary HRS cells are able to proliferate *in vitro* over several passages. As all HRS cell lines studied express GATA-2, one might speculate that GATA-2 activity is required in such primary cells. Alternatively, it might be that some of the Hodgkin cell lines tested might be derivatives of originally GATA-2-negative HRS cells and express GATA-2 due to secondary effects.

The function of GATA-2 is normally required to maintain haematopoietic stem and early progenitor cells in an undifferentiated state [34,50]. Since we have found GATA-2 expression in HRS cells, we speculate whether GATA-2 activity leads to dedifferentiation of affected GC cells which have already acquired somatic hypermutation, giving rise to cells that re-acquire certain aspects of undifferentiated progenitor cells. In this context, it is worth mentioning that cHL-derived cell line cells were found to proliferate in a SCF (stem cell factor or c-kit ligand)-dependent manner comparable to other undifferentiated cells, eg haematopoietic progenitors, melanocyte precursors, and primordial germ cells [51], highlighting some further primitive features of HRS cells.

Since we found GATA-2 expression not in all but in 50% of the cHLs studied, it will be interesting to see if other GATA factors are expressed in GATA-2-negative cHLs, for example GATA-3, which is aberrantly expressed in three of the four cHL-derived cell lines [47], and if there is a link between the expression of GATA family members and the malignant phenotype of cHL, as has been described for acute myeloid leukaemia (AML) [52–54]. In general, it may be possible that only a certain number of cHLs are associated with the expression of GATA factors. A situation like that has been described for EBV status in cHL, as there is some indirect evidence that EBV is a causal agent in up to 50% of cHLs in Caucasian patients [55]. However, we found a random distribution between GATA-2 expression and the EBV status of cHL, suggesting that GATA-2 expression does not correlate with the EBV status of cHL.

Acknowledgements

We thank Grete L Mykkelbost and Maria Weber for excellent technical assistance and Markus Müschen, Michael Punzel, and Peter Wernet for critical discussion. This work was supported by grants from the Deutsche Forschungsgemeinschaft (SFB502).

References

1. Braeuninger A, Kuppers R, Strickler JG, Wacker HH, Rajewsky K, Hansmann ML. Hodgkin and Reed–Sternberg cells in lymphocyte predominant Hodgkin disease represent clonal populations of germinal center-derived tumor B cells. *Proc Natl Acad Sci U S A* 1997; **94**: 9337–9342.
2. Kanzler H, Kuppers R, Hansmann ML, Rajewsky K. Hodgkin and Reed–Sternberg cells in Hodgkin's disease represent the outgrowth of a dominant tumor clone derived from (crippled) germinal center B cells. *J Exp Med* 1996; **184**: 1495–1505.
3. Marafioti T, Hummel M, Anagnostopoulos I, *et al*. Origin of nodular lymphocyte-predominant Hodgkin's disease from a clonal expansion of highly mutated germinal-center B cells. *N Engl J Med* 1997; **337**: 453–458.
4. Marafioti T, Hummel M, Foss HD, *et al*. Hodgkin and Reed–Sternberg cells represent an expansion of a single clone originating from a germinal center B-cell with functional immunoglobulin gene rearrangements but defective immunoglobulin transcription. *Blood* 2000; **95**: 1443–1450.
5. Drexler HG. Recent results on the biology of Hodgkin and Reed–Sternberg cells. I. Biopsy material. *Leuk Lymphoma* 1992; **8**: 283–313.
6. Kuzu I, Delsol G, Jones M, Gatter KC, Mason DY. Expression of the Ig-associated heterodimer (mb-1 and B29) in Hodgkin's disease. *Histopathology* 1993; **22**: 141–144.
7. Watanabe K, Yamashita Y, Nakayama A, *et al*. Varied B-cell immunophenotypes of Hodgkin/Reed–Sternberg cells in classic Hodgkin's disease. *Histopathology* 2000; **36**: 353–361.
8. Re D, Muschen M, Ahmadi T, *et al*. Oct-2 and Bob-1 deficiency in Hodgkin and Reed Sternberg cells. *Cancer Res* 2001; **61**: 2080–2084.
9. Stein H, Marafioti T, Foss HD, *et al*. Down-regulation of BOB.1/OBF.1 and Oct2 in classical Hodgkin disease but not in lymphocyte predominant Hodgkin disease correlates with immunoglobulin transcription. *Blood* 2001; **97**: 496–501.
10. Torlakovic E, Tierens A, Dang HD, Delabie J. The transcription factor PU.1, necessary for B-cell development, is expressed in lymphocyte predominance, but not classical Hodgkin's disease. *Am J Pathol* 2001; **159**: 1807–1814.
11. Jundt F, Kley K, Anagnostopoulos I, *et al*. Loss of PU.1 expression is associated with defective immunoglobulin transcription in Hodgkin and Reed–Sternberg cells of classical Hodgkin disease. *Blood* 2002; **99**: 3060–3062.
12. Schwering I, Brauninger A, Klein U, *et al*. Loss of the B-lineage-specific gene expression program in Hodgkin and Reed–Sternberg cells of Hodgkin lymphoma. *Blood* 2003; **101**: 1505–1512.
13. Barberis A, Widenhorn K, Vitelli L, Busslinger M. A novel B-cell lineage-specific transcription factor present at early but not late stages of differentiation. *Genes Dev* 1990; **4**: 849–859.
14. Nutt SL, Thevenin C, Busslinger M. Essential functions of Pax-5 (BSAP) in pro-B cell development. *Immunobiology* 1997; **198**: 227–235.
15. Foss HD, Reusch R, Demel G, *et al*. Frequent expression of the B-cell-specific activator protein in Reed–Sternberg cells of classical Hodgkin's disease provides further evidence for its B-cell origin. *Blood* 1999; **94**: 3108–3113.
16. Torlakovic E, Torlakovic G, Nguyen PL, Brunning RD, Delabie J. The value of anti-pax-5 immunostaining in routinely fixed and paraffin-embedded sections: a novel pan pre-B and B-cell marker. *Am J Surg Pathol* 2002; **26**: 1343–1350.
17. Jundt F, Anagnostopoulos I, Forster R, Mathas S, Stein H, Dorken B. Activated Notch1 signaling promotes tumor cell proliferation and survival in Hodgkin and anaplastic large cell lymphoma. *Blood* 2002; **99**: 3398–3403.
18. Varnum-Finney B, Xu L, Brashem-Stein C, *et al*. Pluripotent, cytokine-dependent, hematopoietic stem cells are immortalized by constitutive Notch1 signaling. *Nature Med* 2000; **6**: 1278–1281.
19. Stier S, Cheng T, Dombkowski D, Carlesso N, Scadden DT. Notch1 activation increases hematopoietic stem cell self-renewal *in vivo* and favors lymphoid over myeloid lineage outcome. *Blood* 2002; **99**: 2369–2378.

20. Pui JC, Allman D, Xu L, *et al*. Notch1 expression in early lymphopoiesis influences B versus T lineage determination. *Immunity* 1999; **11**: 299–308.
21. Ellisen LW, Bird J, West DC, *et al*. TAN-1, the human homolog of the *Drosophila* notch gene, is broken by chromosomal translocations in T lymphoblastic neoplasms. *Cell* 1991; **66**: 649–661.
22. Milner LA, Bigas A. Notch as a mediator of cell fate determination in hematopoiesis: evidence and speculation. *Blood* 1999; **93**: 2431–2448.
23. Kojika S, Griffin JD. Notch receptors and hematopoiesis. *Exp Hematol* 2001; **29**: 1041–1052.
24. Kumano K, Chiba S, Shimizu K, *et al*. Notch1 inhibits differentiation of hematopoietic cells by sustaining GATA-2 expression. *Blood* 2001; **98**: 3283–3289.
25. Orkin SH. GATA-binding transcription factors in hematopoietic cells. *Blood* 1992; **80**: 575–581.
26. Weiss MJ, Orkin SH. Transcription factor GATA-1 permits survival and maturation of erythroid precursors by preventing apoptosis. *Proc Natl Acad Sci U S A* 1995; **92**: 9623–9627.
27. Orlic D, Anderson S, Biesecker LG, Sorrentino BP, Bodine DM. Pluripotent hematopoietic stem cells contain high levels of mRNA for c-kit, GATA-2, p45 NF-E2, and c-myb and low levels or no mRNA for c-fms and the receptors for granulocyte colony-stimulating factor and interleukins 5 and 7. *Proc Natl Acad Sci U S A* 1995; **92**: 4601–4605.
28. Dorfman DM, Wilson DB, Bruns GA, Orkin SH. Human transcription factor GATA-2. Evidence for regulation of preproendothelin-1 gene expression in endothelial cells. *J Biol Chem* 1992; **267**: 1279–1285.
29. Leonard M, Brice M, Engel JD, Papayannopoulou T. Dynamics of GATA transcription factor expression during erythroid differentiation. *Blood* 1993; **82**: 1071–1079.
30. Mouthon MA, Bernard O, Mitjavila MT, Romeo PH, Vainchenker W, Mathieu-Mahul D. Expression of tal-1 and GATA-binding proteins during human hematopoiesis. *Blood* 1993; **81**: 647–655.
31. Visvader J, Adams JM. Megakaryocytic differentiation induced in 416B myeloid cells by GATA-2 and GATA-3 transgenes or 5-azacytidine is tightly coupled to GATA-1 expression. *Blood* 1993; **82**: 1493–1501.
32. Tsai FY, Keller G, Kuo FC, *et al*. An early haematopoietic defect in mice lacking the transcription factor GATA-2. *Nature* 1994; **371**: 221–226.
33. Tsai FY, Orkin SH. Transcription factor GATA-2 is required for proliferation/survival of early hematopoietic cells and mast cell formation, but not for erythroid and myeloid terminal differentiation. *Blood* 1997; **89**: 3636–3643.
34. Kitajima K, Masuhara M, Era T, Enver T, Nakano T. GATA-2 and GATA-2/ER display opposing activities in the development and differentiation of blood progenitors. *EMBO J* 2002; **21**: 3060–3069.
35. Ikonomi P, Rivera CE, Riordan M, Washington G, Schechter AN, Noguchi CT. Overexpression of GATA-2 inhibits erythroid and promotes megakaryocyte differentiation. *Exp Hematol* 2000; **28**: 1423–1431.
36. DeKoter RP, Walsh JC, Singh H. PU.1 regulates both cytokine-dependent proliferation and differentiation of granulocyte/macrophage progenitors. *EMBO J* 1998; **17**: 4456–4468.
37. DeKoter RP, Singh H. Regulation of B lymphocyte and macrophage development by graded expression of PU.1. *Science* 2000; **288**: 1439–1441.
38. Rekhtman N, Radparvar F, Evans T, Skoultchi AI. Direct interaction of hematopoietic transcription factors PU.1 and GATA-1: functional antagonism in erythroid cells. *Genes Dev* 1999; **13**: 1398–1411.
39. Zhang P, Behre G, Pan J, *et al*. Negative cross-talk between hematopoietic regulators: GATA proteins repress PU.1. *Proc Natl Acad Sci U S A* 1999; **96**: 8705–8710.
40. Zhang P, Zhang X, Iwama A, *et al*. PU.1 inhibits GATA-1 function and erythroid differentiation by blocking GATA-1 DNA binding. *Blood* 2000; **96**: 2641–2648.
41. Nerlov C, Querfurth E, Kulessa H, Graf T. GATA-1 interacts with the myeloid PU.1 transcription factor and represses PU.1-dependent transcription. *Blood* 2000; **95**: 2543–2551.
42. Walsh JC, DeKoter RP, Lee HJ, *et al*. Cooperative and antagonistic interplay between PU.1 and GATA-2 in the specification of myeloid cell fates. *Immunity* 2002; **17**: 665–676.
43. Kaufman DS, Hanson ET, Lewis RL, Auerbach R, Thomson JA. Hematopoietic colony-forming cells derived from human embryonic stem cells. *Proc Natl Acad Sci U S A* 2001; **98**: 10 716–10 721.
44. Torlakovic G, Snover DC, Torlakovic E. Simultaneous EBV-positive lymphoepithelioma-like carcinoma and EBV-negative intestinal-type adenocarcinoma in a patient with *Helicobacter pylori*-associated chronic gastritis. *Am J Clin Pathol* 2004; **121**: 237–243.
45. Strauchen JA, Miller LK. Lymphoid progenitor cells in human tonsils. *Int J Surg Pathol* 2003; **11**: 21–24.
46. Lee ME, Temizer DH, Clifford JA, Quertermous T. Cloning of the GATA-binding protein that regulates endothelin-1 gene expression in endothelial cells. *J Biol Chem* 1991; **266**: 16 188–16 192.
47. Kuppers R, Klein U, Schwering I, *et al*. Identification of Hodgkin and Reed–Sternberg cell-specific genes by gene expression profiling. *J Clin Invest* 2003; **111**: 529–537.
48. Feldhahn N, Schwering I, Lee S, *et al*. Silencing of B cell receptor signals in human naïve B cells. *J Exp Med* 2002; **196**: 1291–1305.
49. Muschen M, Lee S, Zhou G, *et al*. Molecular portraits of B cell lineage commitment. *Proc Natl Acad Sci U S A* 2002; **99**: 10 014–10 019.
50. Persons DA, Allay JA, Allay ER, *et al*. Enforced expression of the GATA-2 transcription factor blocks normal hematopoiesis. *Blood* 1999; **93**: 488–499.
51. Aldinucci D, Poletto D, Nanni P, *et al*. Hodgkin and Reed–Sternberg cells express functional c-kit receptors and interact with primary fibroblasts from Hodgkin's disease-involved lymph nodes through soluble and membrane-bound stem cell factor. *Br J Haematol* 2002; **118**: 1055–1064.
52. Ohyashiki K, Ohyashiki JH, Shimamoto T, Toyama K. Pattern of expression and their clinical implications of the GATA family, stem cell leukemia gene, and EVI1 in leukemia and myelodysplastic syndromes. *Leuk Lymphoma* 1996; **23**: 431–436.
53. Wang L, Dong L, Liu G, *et al*. [GATA-2 gene expression in leukemia patients and its significance]. *Zhonghua Xue Ye Xue Za Zhi* 2001; **22**: 27–29.
54. Shimamoto T, Ohyashiki K, Ohyashiki JH, *et al*. The expression pattern of erythrocyte/megakaryocyte-related transcription factors GATA-1 and the stem cell leukemia gene correlates with hematopoietic differentiation and is associated with outcome of acute myeloid leukemia. *Blood* 1995; **86**: 3173–3180.
55. Glaser SL, Lin RJ, Stewart SL, *et al*. Epstein–Barr virus-associated Hodgkin's disease: epidemiologic characteristics in international data. *Int J Cancer* 1997; **70**: 375–382.

STEM CELLS®
TISSUE-SPECIFIC STEM CELLS

Stringent Regulation of DNA Repair During Human Hematopoietic Differentiation: A Gene Expression and Functional Analysis

TOMKE U. BRACKER,[a] BERND GIEBEL,[c] JAN SPANHOLTZ,[c] URSULA R. SORG,[b] LUDGER KLEIN-HITPASS,[a] THOMAS MORITZ,[b] JÜRGEN THOMALE[a]

[a]Institut für Zellbiologie and [b]Innere Klinik (Tumorforschung), Universitätsklinikum Essen, Essen, Germany; [c]Institut für Transplantationsdiagnostik und Zelltherapeutika, Universitätsklinikum Düsseldorf, Düsseldorf, Germany

Key Words. Comet assay • Ethylnitrosourea • EtNU • Melphalan • Nucleotide excision repair Base excision repair • Hematotoxicity

ABSTRACT

For the lymphohematopoietic system, maturation-dependent alterations in DNA repair function have been demonstrated. Because little information is available on the regulatory mechanisms underlying these changes, we have correlated the expression of DNA damage response genes and the functional repair capacity of cells at distinct stages of human hematopoietic differentiation. Comparing fractions of mature ($CD34^-$), progenitor ($CD34^+38^+$), and stem cells ($CD34^+38^-$) isolated from umbilical cord blood, we observed: 1) stringently regulated differentiation-dependent shifts in both the cellular processing of DNA lesions and the expression profiles of related genes and 2) considerable interindividual variability of DNA repair at transcriptional and functional levels. The respective repair phenotype was found to be constitutively regulated and not dominated by adaptive response to acute DNA damage. During blood cell development, the removal of DNA adducts, the resealing of repair gaps, the resistance to DNA-reactive drugs clearly increased in stem or mature compared with progenitor cells of the same individual. On the other hand, the vast majority of differentially expressed repair genes was consistently upregulated in the progenitor fraction. A positive correlation of repair function and transcript levels was found for a small number of genes such as *RAD23* or *ATM*, which may serve as key regulators for DNA damage processing via specific pathways. These data indicate that the organism might aim to protect the small number of valuable slow dividing stem cells by extensive DNA repair, whereas fast-proliferating progenitor cells, once damaged, are rather eliminated by apoptosis. STEM CELLS *2006;24:722–730*

INTRODUCTION

The cellular capacity to remove drug-induced lesions from the nuclear DNA strongly determines the sensitivity of normal and malignant hematopoietic cells to DNA-reactive agents, such as alkylator-type antineoplastic drugs [1–3]. Here, on the molecular level, a network of distinct and evolutionary, highly conserved pathways has been identified, that allows cells to repair their DNA when damaged by adducts, crosslinks, or strand breaks [4, 5]. Studies in animals defective for specific repair functions have underscored the role of the DNA repair machinery in the response of mammalian hematopoietic cells to DNA damage [6–8], and this notion is further supported by genetic or pharmacological manipulation of DNA repair function in primary blood cells [9–14]. However, little information is available on the regulation of this network, the exact role of individual pathways, or crosstalk between pathways in the lympho-hematopoietic system and other primary tissues.

In human leukocytes generated from peripheral blood or umbilical cord blood samples, a broad spectrum of individual DNA repair phenotypes has been observed regarding overall repair capacity and distinct repair functions [15–18]. These variations could be ascribed, at least partly, to polymorphisms [19] or other genetic variances in the corresponding structural or regulatory gene sequences [20]. In addition to the individual repair phenotype, we and others have demonstrated distinct shifts in functional DNA repair when comparing defined subpopulations in the lymphohematopoietic differentiation process such as $CD34^+$ progenitor or mature $CD34^-$ cells [18, 21, 22]. The functional impairment of progenitor cells to process DNA

Correspondence: Jürgen Thomale, Ph.D., Institute of Cell Biology, University of Duisburg-Essen Medical School, Essen, Germany. Telephone: 49-201-723-4230; Fax: 49-201-723-3104; e-mail: juergen.thomale@uni-essen.de. Received May 18, 2005; accepted for publication September 9, 2005; first published online in STEM CELLS *EXPRESS* September 29, 2005. 1066-5099/2006/$20.00/0 doi: 10.1634/stemcells.2005-0227

alkylation damage was not restricted to a specific function or component of the multipathway network [22] (Fig. 1), implying some sort of differentiation-dependent regulation of the complex DNA repair machinery during hematopoiesis. At present it is not known, however, whether the repair capacity of primary human cells is mainly determined by transcriptional regulation, for example, of rate-limiting gene products along a given pathway, or at subsequent steps like protein modification or cellular localization of critical components. Therefore, we have analyzed the expression profiles of DNA damage response genes at different stages of maturation in primary human hematopoietic cells, with a specific focus on genes directly involved in major repair pathways [23]. Additionally, we have correlated their regulatory pattern to the kinetics of DNA damage processing in these cells.

MATERIALS AND METHODS

Preparation of Cells

Umbilical cord blood was obtained from individual donors after informed consent according to the Declaration of Helsinki. Mononuclear cells were isolated by Ficoll gradient centrifugation and resuspended in prewarmed Roswell Park Memorial Institute (RPMI) medium supplemented with 10% fetal calf serum (FCS; PAA Laboratories, Linz, Austria, http://www.paa.at). $CD34^+$ cells were purified by immunomagnetic isolation using the indirect MidiMACS technique (Miltenyi Biotech, Bergisch Gladbach, Germany, http://www.miltenyibiotec.com). The purity of $CD34^+$ fractions was controlled by flow cytometry and averaged 78% in samples for functional assays and 85% for gene expression analysis. $CD34^-$ cells were taken from the column flow-through.

For functional analysis the primitive, stem cell-enriched fraction of $CD34^+38^{low}$ cells and the progenitor-enriched $CD34^+38^+$ cell fraction were isolated from preselected $CD34^+$ cells by fluorescence-activated cell sorting (FACS). After incubation with CD34-fluorescein isothiocyanate (FITC), CD38-PE, and CD45-PerCP-Cy5.5 antibodies (BD Pharmingen, San Diego, http://www.bdbiosciences.com/pharmingen; 15 minutes in phosphate-buffered saline (PBS)/1% FCS), cells were washed in PBS and sorted by using a FACSVantage (BD Biosciences). The purity of $CD34^+38^{low}$ and $CD34^+38^+$ fractions was >95%. During and after drug exposure, cells were kept in supplemented RPMI medium at 37°C in a humidified atmosphere containing 5% CO_2.

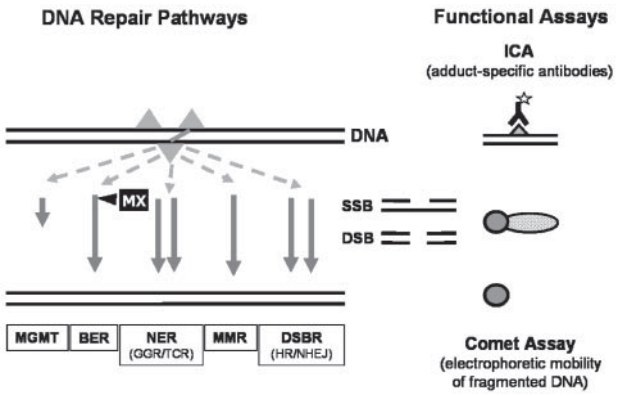

Figure 1. Schematic outline of major DNA damage repair pathways and functional assays. Primary adducts are detected by the immunocytological assay (ICA) and secondary lesions by the comet assay. Abbreviations: BER, base excision repair; NER, nucleotide excision repair; GGR, global genomic repair; TCR, transcription coupled repair; MMR, mismatch repair; DSBR, double-strand break repair; HR, homologous recombination; NHEJ, nonhomologous end joining; SSB, single-strand break; DSB, double-strand break; MX, methoxyamine (a specific inhibitor of early BER).

For comparative microarray expression analysis of primitive and progenitor cells, $CD34^+38^{low}$ and $CD34^+38^+$ cells were isolated from the $CD34^+$-enriched fraction by immunostaining with CD3-FITC, CD14-FITC, CD16-FITC, CD19-FITC, CD20-FITC, and CD56-FITC (lin1 antibody cocktail; BD Biosciences), as well as glycophorin A (GA)-FITC, CD38-PE, and CD34-PeCy5 antibodies (BD Pharmingen). $lin1^-GA^-CD34^+CD38^{low}$ and $lin1^-GA^-CD34^+CD38^+$ cells were highly purified using a Coulter EPICS Elite ESP fluorescence cell-sorting system equipped with the Expo32 software (Beckmann Coulter) with $lin1^-GA^-CD34^+CD38^{low}$ comprising one-sixth of total $lin1^-GA^-CD34^+$ cells. Separated cell fractions were frozen in TRIzol (Invitrogen, Carlsbad, CA, http://www.invitrogen.com) and stored at −80°C until RNA was prepared.

Exposure to Drugs and Apoptosis Assay

For the measurement of repair kinetics, cells were exposed to *N*-ethylnitrosourea (EtNU; Sigma, 100 μg/ml) for 30 minutes or to melphalan (Alkeran; 10 μg/ml; GlaxoSmithKline, Research Triangle Park, NC, http://www.gsk.com) in RPMI medium (10% FCS, 5 mM HEPES) for 2 hours at 37°C. Thereafter, cells were washed in PBS, resuspended in prewarmed RPMI, and incubated at 37°C. Cell aliquots were taken prior and at different time points after drug treatment. For expression profile analysis, EtNU-exposed cells were postincubated for 2 hours prior to RNA isolation. For repair inhibition studies, cells were preincubated with 1 mM methoxyamine (MX; Sigma) for 1 hour prior to EtNU exposure and throughout the experiment. Drug-induced apoptosis in cells was measured 24 hours after the addition of cisplatin (Platinex; Bristol-Meyers Squibb, New York, http://www.bms.com), EtNU, or melphalan to the medium. The fraction of apoptotic cells was determined by annexin V-FITC staining (Annexin V Detection Kit I; BD Pharmingen) and FACS analysis.

Comet Assay

DNA strand breaks in individual nuclei of small cell fractions were measured by single-cell gel electrophoresis ("comet assay") modified according to McNamee et al. [24]. In brief, from 8-well cell culture chamber slides (BD Falcon, Franklin Lakes, NJ, http://www.bdbiosciences.com) the glass bottom was removed and replaced by GelBond film (Cambrex, Walkersville, MD, http://www.cambrex.com; Biozym, Hess, Oldendorf, Germany, http://www.biozym.com). Aliquots of 10^4 cells were suspended in 45 μl of low-melting point agarose (0.75% in PBS, prewarmed at 42°C; Metaphor; Biozym) and cast into the wells. After coagulation the frames were removed, and the gels on the film were soaked overnight at 4°C in lysis buffer (2.5 M NaCl, 100 mM EDTA, 10 mM Tris, 10% dimethyl sulfoxide, 1% Triton X-100, 1% *n*-laurylsarcosinate, pH 10). Nuclear DNA was denatured by alkaline treatment (300 mM NaOH, 1 mM EDTA, 10 mM Tris-HCl, pH 12.7) for 15 minutes, and GelBond

films were subjected to alkaline electrophoresis in the same buffer (20 minutes, 4°C, 1.5 V/cm). After neutralization (30 minutes, 400 mM Tris-HCl, pH 7.5), gels were dehydrated in absolute ethanol (1 h) and air-dried. Before evaluation of comet formation, gel films were rehydrated, and the nuclear DNA was stained with SYBR-Green (dilution 1:10,000; Roche Diagnostics, Basel Switzerland, http://www.roche-applied-science.com).

Immunocytological Assay

Immunoanalytical measurement of melphalan-induced adducts in the nuclear DNA of individual cells was performed as described [22] with minor modifications: 10^4 cells/sample were applied to precoated microscopic slides (ImmunoSelect; Squarix, Marl, Germany, http://www.squarix.de) and immunostained for melphalan-DNA adducts with rat monoclonal antibody Amp 4–42 (kindly provided by Dr. M. J. Tilby, University of Newcastle upon Tyne, Newcastle upon Tyne, U.K.). Binding of primary antibody was visualized by consecutive staining with rabbit anti-(rat Ig) and goat anti-(rabbit Ig), both labeled with Cy3 (Dianova).

Quantitative Image Analysis and Statistics

Comet assay and immunocytological assay (ICA) were evaluated by quantification of fluorescence signals using a photomicroscope (Axioplan; Zeiss, Jena, Germany, http://www.zeiss.de) and a multiparameter image analysis system (ACAS; Ahrens Electronics, Bargteheide, Germany). Melphalan adduct levels of individual cell nuclei were calculated by normalizing the antibody-derived fluorescence signals for the DNA content of the same cell. The relative amount of DNA strand breaks (comet assay) was determined using the olive tail moment [OTM = (migrated DNA) × (distance between the head and center of gravity of DNA in the tail)] [25]. Mean signal values (±SEM) were calculated from >100 individual cells per sample. Data of corresponding cell pairs from the same donor were analyzed by paired *t* test.

RNA Preparation

Cells were homogenized using a QIAShredder column (Qiagen, Hilden, Germany, http://www1.qiagen.com), and total RNA was isolated according to the manufacturer's instructions. RNA concentrations were measured by fluorescence staining (Ribo-Green Kit; Molecular Probes) using a microplate reader, and RNA quality was verified by electrophoresis in 1% agarose gels. Due to the small number of cells in the $CD34^+38^{low}$ fraction, isolated RNA from four individual cord blood samples was pooled and compared with pooled RNA from the $CD34^+38^+$ fractions of the same four donors.

RNA Amplification

To obtain sufficient amounts of labeled material for the GeneChip hybridization, RNA samples from individual $CD34^+$ or $CD34^-$ cell fractions were subjected to a two-round amplification procedure according to Baugh et al. [26] with modifications. Briefly, total RNA (300 ng) was converted into cDNA using 0.5 μg of an oligodeoxythymidine primer containing the T7 RNA polymerase binding site (5′-GCATTAGCGGCCGC-GAAATTAATACGACTCACTATAGGGAGA-$(dT)_{21}$V-3′) (MWG Biotech, Ebersberg, Germany, http://www.mwg-biotech.com) for first-strand synthesis in a total volume of 15 μl of (1× First Strand Buffer [Invitrogen], 0.5 mM dNTPs, 10 mM dithiothreitol [DTT], 200 U of SuperScript II [Invitrogen], 0.5 μg of T4gp32 [GE Healthcare, Piscataway, NJ, http://www1.amershambiosciences.com], 30 U of RNasin [Promega, Mannheim, Germany, http://www.promega.com]) for 45 minutes at 42°C, 10 minutes at 45°C, and 10 minutes at 48°C. After heat inactivation for 15 minutes at 65°C, second-strand synthesis in 100-μl reactions [1× Second-strand buffer (Invitrogen), 0.2 mM dNTPs, 1 U of RNase H (Takara, Otsu, Japan, http://www.takara.co.jp), 20 U of *Escherichia coli* DNA polymerase I (Invitrogen), 6 U of *E. coli* DNA ligase (Takara)] was performed for 2 hours at 16°C. Subsequently, 8 U of T4 DNA polymerase (Invitrogen) was added, and incubation continued for 15 minutes at 16°C. Double-stranded cDNA was purified on spin columns (Microarray purification kit; Roche Diagnostics), precipitated with glycoblue (Ambion, Austin, TX, http://www.ambion.com) and transcribed in 40 μl of [1× T7 RNA polymerase buffer (Takara), 4 mM NTPs, 10 mM $MgCl_2$, 1% polyethylene glycol 20000, 6.25 mM DTT, 40 U of pyrophosphatase (USB), 40 U of RNasin (Promega), 1.5 μg of T7 RNA polymerase] for 16 hours at 37°C. Reactions were treated with 2 U of RNase-free DNase I (Ambion) for 30 minutes at 37°C before purification on spin columns (Roche) and quantitated by optical density measurement. For second-round cDNA synthesis, 500 ng of first-round amplification products was used in all cases. Reverse transcription with SuperScript II was performed with 0.5 μg of random hexamer primer (Stratagene) in 15-μl reactions without T4gp32 as described above. Following heat inactivation, RNA templates were removed by digestion with 2 U of RNase H for 30 minutes at 37°C. After annealing of T7-dT_{21}V primer (100 ng) at 42°C for 5 minutes, reactions were snap-cooled in ice water. Second-strand cDNA synthesis was performed in a final volume of 100-μl reactions (1× Second-strand buffer, 0.2 mM dNTPs, 1 U of RNase H, 20 U of *E. coli* DNA polymerase I) for 2 hours at 16°C and trimmed with 10 U of T4 DNA polymerase for another 15 minutes at 16°C. CDNA was purified, precipitated, and transcribed with T7 RNA polymerase as described above, except that ribonucleotide concentrations were 4 mM each for GTP and ATP, 1.4 mM each for CTP and UTP, and 0.6 mM each for biotin-11-CTP and biotin-11-UTP (PerkinElmer Life and Analytical Sciences, Boston, http://www.perkinelmer.com). Pooled samples of $lin^-CD34^+38^+$ or $lin^-CD34^+38^{low}$-derived RNA (500 ng) were amplified by one round of cDNA synthesis using the MessageAmp II aRNA kit (Ambion) and in vitro transcription in the presence of biotinylated NTPs as described above.

Oligonucleotide Microarray Analysis

Biotin-labeled cRNA was purified on RNeasy columns (Qiagen), fragmented, and hybridized to HG-U133A GeneChips (Affymetrix, Santa Clara, CA, http://www.affymetrix.com) following the Affymetrix standard protocol. The arrays were washed and stained according to the manufacturer's recommendation and finally scanned in a GeneArray scanner 2500 (Agilent, Palo Alto, CA, http://www.home.agilent.com). Array images were processed to determine signals and detection calls (present, absent, and marginal) for each probe set using the Affymetrix Microarray Suite 5.0 software. Scaling across all probe sets of a given array to an average intensity of 1,000 was

performed to compensate for variations in the amount and quality of the cRNA samples and other experimental variables of nonbiological origin.

Analysis of Microarray Data

For unsupervised hierarchical clustering, signals of individual probe sets were normalized to the mean probe set signal of all included arrays and log transformed. Log transformed ratios were subjected to UPGMA clustering using correlation as similarity measure (Spotfire DecisionSite for functional genomics). As additional criteria we used the present calls in ≥30% of the samples and a ratio of means of ≥1.5 or ≤0.67. To compare corresponding pairs of $CD34^+/CD34^-$ or $CD34^+38^+/CD34^+38^{low}$ cells from the same donor for the magnitude and direction of change, we employed the signal log ratio (SLR) algorithm giving the differences as binary logarithmic values.

Quantitative Reverse Transcription-Polymerase Chain Reaction

For real-time polymerase chain reaction (PCR) analyses, total RNA was reverse-transcribed using random primers (High Capacity cDNA Archive Kit; Applied Biosystems). PCR was carried out in duplicate 20-μl reactions containing cDNA corresponding to 5 ng of total RNA, 1 μl of Taqman-based assay, and 1× master mix reagents (Applied Biosystems). PCR was performed on an ABI Prism 7900HT system as recommended by the manufacturer using the glyceraldehyde-3-phosphate dehydrogenase assay (Hs99999905_m1) as the endogenous reference and ATM (Hs00175892_m1), RAD23A (Hs00192541_m1), and RAD50 (Hs00194871_m1) as target assays. Differential expression was estimated by the comparative C_t method (ABI Prism 7700 Sequence Detection System User Bulletin #2: Relative Quantification of Gene Expression [P/N 4303859]).

RESULTS

Expression of Damage Response Genes in $CD34^+$ and $CD34^-$ Cells

To assess the transcriptional activity of genes involved in DNA damage response at different stages of lymphohematopoietic differentiation, $CD34^+$ progenitor cells and their mature $CD34^-$ counterparts were prepared from seven individual cord blood samples. Total RNA was isolated, and gene expression profiles were determined using Affymetrix HG_U133A GeneChips. Hybridization signals from 1418 probe sets, representing a total of 803 DNA damage response genes, were evaluated. By our criteria (present calls in ≥30% of the samples), transcripts for 633 (79%) of these genes were detected. This set comprised 296 of 366 genes related to cell-cycle control, 254 of 330 genes related to apoptosis, and 153 of 189 genes related to DNA repair functions with some genes listed in more than one subgroup. Pronounced interindividual variances in specific transcript levels of DNA repair genes were observed at both stages of differentiation. For instance, the amount of mRNA transcribed from the mismatch repair gene *MSH2* varied at a maximum range of 7.5-fold (fluorescence signals: 286–2,145) among $CD34^+$ and 4.6-fold (signals: 190–882) among $CD34^-$ cell samples. The corresponding values for *RAD23A*, a gene involved in nucleotide excision repair, were 6.7-fold (signals: 764–5,142) and 4.1-fold (signals: 2,909–12,024), respectively. For the majority of genes, interindividual variations were found in a 2.5- to 3.5-fold range, with a tendency to broader variations in progenitor cells. On the other hand, a small number of genes was expressed more constantly, showing less than 2-fold interindividual variations within either of the cell fractions. One member of this group was the *XPA* gene coding for a key component of both sub-pathways of nucleotide excision repair (NER), that is global genomic (GGR) and transcription-coupled repair (TCR).

Despite the pronounced interindividual variation at the level of specific transcripts, stringently regulated, differentiation-dependent shifts in gene expression profiles were observed. Unsupervised hierarchical cluster analyses employing the whole set of damage response genes revealed a clear-cut separation between progenitor and mature blood cells (Fig. 2A). A similar

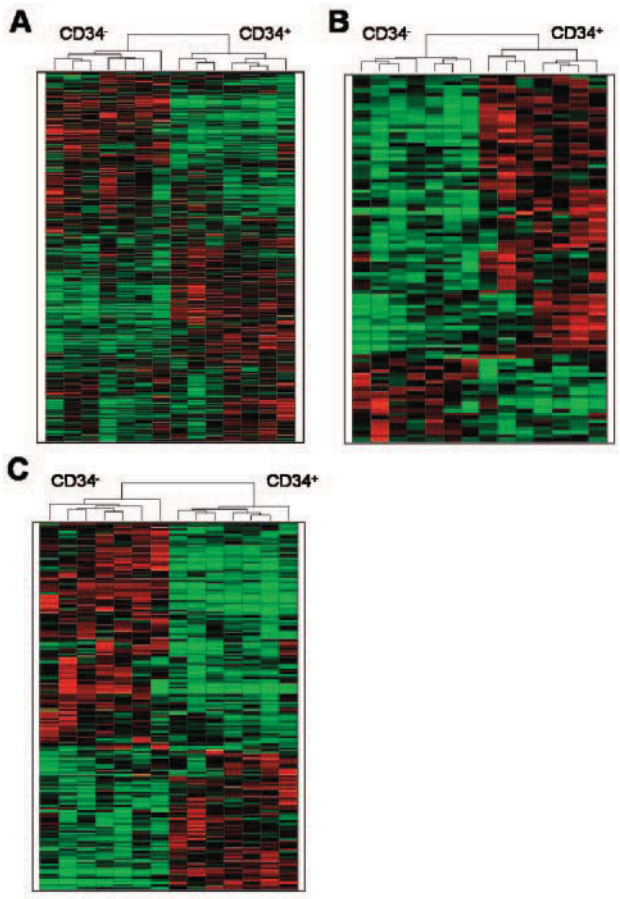

Figure 2. Expression profiles of DNA damage response genes separate mature ($CD34^-$) and progenitor ($CD34^+$) cord blood cells. Fourteen RNA samples from seven corresponding pairs of hematopoietic cells were subjected to GeneChip analysis. Signals from individual probe sets were normalized to the mean and log-transformed, and ratios were analyzed by unsupervised hierarchical clustering (see Materials and Methods; relative expression: red [significantly higher], green [significantly lower], or black [mean]). The dendrograms and matrices represent the clustering of 962 probe sets (DNA damage response) **(A)**, 102 probe sets (DNA repair) **(B)**, and 219 probe sets (apoptosis) **(C)**. Criteria for the depicted probe sets in **(A):** present call in ≥30% of the $CD34^+$ or the $CD34^-$ samples; additional in **(B)**, and **(C):** ratio of means ≥1.5 or ≤0.667.

pattern was found when focusing on genes associated with DNA repair functions or apoptosis (Fig. 2B, 2C), indicating that these genes are stringently regulated during hematopoietic cell development and that this regulation dominates interindividual variability in gene expression.

When transcript levels of individual pairs of $CD34^+$ and $CD34^-$ cells from the same donor were compared using the SLR algorithm, 37% (291/803) of the DNA damage response genes were found to be significantly up- or downregulated (cut-off: p values of SLRs ≤ 0.005 or ≥ 0.995 for at least four of seven cell pairs). More than half (175) of these genes displayed higher mRNA levels in the corresponding progenitor cell fraction. Among the genes related to DNA repair mechanisms, 58 of 153 detectable gene products were up- and 10 were downregulated in $CD34^+$ cells. When focusing on 97 genes coding for constituents of major DNA repair pathways [23] (see Fig. 1), 37 of 83 detectable genes were differentially expressed, namely 10/28 in base excision repair (BER), 13/38 in NER, 7/16 in mismatch repair (MMR), and 12/33 in double-strand-break repair (DSBR; Fig. 3). Most of these genes showed significantly higher transcript levels (mean, 2.6-fold) in the corresponding progenitor cell fraction. Only two genes (*ATM* and *RAD23A*) were identified as clearly downregulated in the progenitor fraction of all seven samples. These genes are employed in DSBR or NER functions, respectively.

The array data were validated by real-time reverse transcription (RT)-PCR reanalysis of RNA from five $CD34^+$/$CD34^-$ cell pairs and three different transcripts (ATM, RAD23A, and RAD50). In each single case the same magnitude and direction of regulation was measured by both assays (mean SLRs: ATM, −1.78 and −1.65; RAD23A, −2.05 and −1.64; and RAD50, 0.75 and 0.98 for RT-PCR and microarray analysis, respectively).

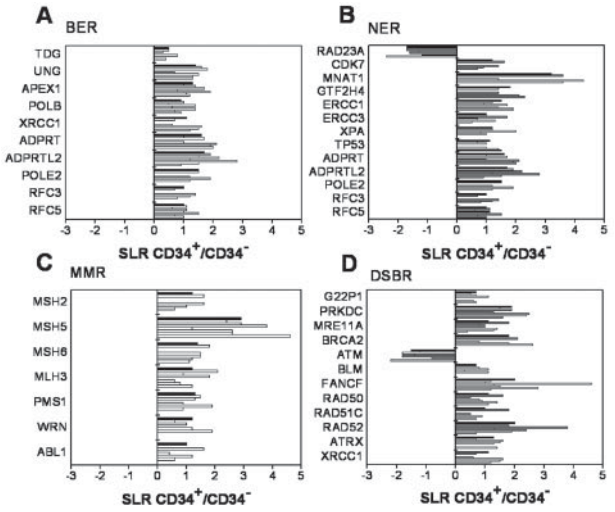

Figure 3. Most differentially expressed genes contributing to major DNA repair pathways are consistently upregulated in progenitor compared with mature cells. SLRs of 37 differentially expressed genes with function in one or more of the major repair pathways: BER **(A)**, NER **(B)**, MMR **(C)**, and DSBR **(D)**. White bars show the SLRs of individual $CD34^+$/$CD34^-$ cell pairs from the same donor; black bars represent the mean SLRs of all seven samples (criterion for significant up- or downregulation: $p \leq .005$ or $\geq .995$ for at least 4/7 $CD34^+$/$CD34^-$ cell pairs). Abbreviations: SLR, single log ratio; BER, base excision repair; NER, nucleotide excision repair; MMR, mismatch repair; DSBR, double-strand break repair.

Functional Analysis of Cellular DNA Repair and Correlation with Gene Expression Profiles

The overall capacity of hematopoietic cells to process DNA damage was measured by single-cell gel electrophoresis ("comet assay"), which determines repair-induced DNA strand breaks in individual cell nuclei and by ICA allowing the direct measurement of drug-induced DNA adducts (Fig. 1). To induce a set of structurally defined DNA adducts, $CD34^+$ or $CD34^-$ cell fractions in liquid holding were exposed to a short pulse of EtNU, a fast-reacting monofunctional alkylator ($t_{1/2}$ in cells: 7 minutes), which is not subject to active drug transportation. EtNU interacts with the cellular DNA to form about a dozen different ethylation products (among them 15% N^7-guanine, 9% O^6-guanine, 9% O^2-/O^4-thymine, 4% N^3-adenine, and 3% O^2-cytidine) [27], which simultaneously trigger repair responses via various pathways such as NER, BER, and MMR or direct removal by the alkyl-DNA alkyltransferase O^6-methylguanine-DNA methyltransferase (MGMT).

For quantitative evaluation of the repair kinetics by the comet assay, two parameters were utilized: 1) the amount of

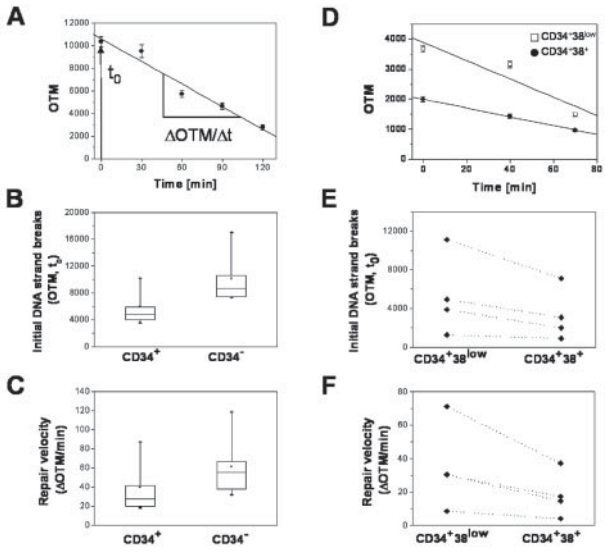

Figure 4. Processing of DNA lesions in hematopoietic cells shows high interindividual variation and is impaired in progenitor compared with stem and mature cells. Following exposure to *N*-ethylnitrosourea (EtNU; 100 μg/ml; 30 minutes), the kinetics of repair-induced DNA strand breaks were determined by the comet assay (measurement of OTM) in $CD34^+$ or $CD34^-$ cells isolated from eight cord blood samples, as well as in $CD34^+38^{low}$ or $CD34^+38^+$ cells from four individual samples. **(A):** Two parameters for the cellular repair capacity, the efficiency of initial strand incision (OTM, t_0), and the velocity of repair gap resealing (ΔOTM/minutes) were determined. **(B, C):** Both parameters were significantly lower in the related $CD34^+$ cell fractions (paired t test: $p = 0.004$ and 0.018, respectively). Statistical evaluation is given in the box (25–75 percentile) and whisker (5–95 percentile) plots. **(D):** Kinetics for $CD34^+38^{low}$ and $CD34^+38^+$ cell fractions from an individual donor. **(E, F):** In addition to pronounced differences between four individual samples, the frequency of initial DNA strand breaks and repair velocity were consistently higher in the stem cell fraction. Abbreviation: OTM, olive tail moment.

DNA strand breaks present directly after a 30-minutes period of drug exposure (OTM, t_0: representing the efficiency of initial repair incision) and 2) the slope of the repair curve (ΔOTM/Δt: depicting the efficiency of gap filling in religation steps) (Fig. 4A). Although analysis of both parameters confirmed the high interindividual variance in the DNA repair capacity of hematopoietic cells at the functional level, repair kinetics between mature and progenitor cells from the same donor differed markedly, too (Fig. 4B, 4C). Fewer early incisions into adducted DNA (8/8 samples, $p = .004$) and slower religation of repair gaps (7/8 samples, $p = .018$) both indicate less efficient repair processing of EtNU-induced DNA lesions in $CD34^+$ progenitor cells.

To corroborate these findings for a different set of DNA lesions, corresponding pairs of isolated cell fractions were challenged with the alkylating anticancer drug melphalan (10 μg/ml), which initially forms mono-adducts and, subsequently, interstrand crosslinks, preferentially at the N^7-position of guanine. The level of primary DNA adducts, as measured 2 hours after drug exposure by quantitative immunocytological analysis, was significantly higher in progenitor compared with mature cells (mean, 1.7-fold, $n = 3$, $p < .05$ [paired t test]). Together with the simultaneously lower frequencies of repair-induced strand breaks in melphalan-exposed $CD34^+$ cells (mean, 0.66-fold), these data again reflect the limited capacity of progenitor cells to deal with damaged DNA. A possible bias of these data by differential drug uptake or efflux was excluded by chromatographic analysis of extracts from exposed $CD34^+$ or $CD34^-$ cells and demonstration of similar intracellular levels of melphalan and its metabolites in both cell fractions.

To link the removal of primary and secondary DNA lesions to chemosensitivity, the onset of apoptosis after exposure to EtNU, melphalan, or cisplatin was investigated (Table 1). A consistently higher apoptotic response in progenitor versus mature cells was observed, thus backing up our earlier observation of accelerated induced cell death after treatment with DNA-damaging agents in progenitor cells [22].

As both repair functions and drug sensitivity are very likely affected by DNA replication, we have determined the cycle distribution in the progenitor cell fraction immediately after isolation. DNA histograms (FACS analysis) of 4,6-diamidino-2-phenylindole-stained cells confirmed observations of other groups that nearly all (>98%) $CD34^+$ cord blood cells are in G_0/G_1 [28].

Table 1. Higher frequencies of apoptosis in progenitor versus mature cord blood cells following ex vivo exposure to DNA-reactive drugs

Drug	Apoptotic cells (%)[a]		Factor
	$CD34^+$	$CD34^-$	$CD34^+/CD34^-$
EtNU (200 μg/ml, $n = 1$)	31	7	4.6
Melphalan (20 μg/ml, $n = 2$)[b]	16	4	4.3
Cisplatin (50 μg/ml, $n = 3$)[b]	36	10	3.6

[a] Positive staining for annexin V 24 hours after exposure, fluorescence-activated cell sorting measurement.
[b] Mean values; $p < .05$ (paired t test).
Abbreviation: EtNU, *N*-ethylnitrosourea.

To address the relative contribution of individual pathways to the overall repair activity, the pharmacological inhibitor MX was employed, which prevents the strand incision as an early step along the BER pathway [15] (Fig. 1). Thus, the proportion by which MX reduces the frequency of DNA strand breaks after drug treatment estimates the contribution of BER to the overall repair capacity of a cell. When comparing $CD34^+$ and $CD34^-$ cell pairs after exposure to EtNU alone or combined with MX, the relative contribution of BER was consistently (4/4 samples) higher in the $CD34^+$ subset than in mature cells (mean ± SEM: 51 ± 7% and 21 ± 12%, respectively). This observation is in agreement with the augmented mRNA levels of all (10/10) differentially expressed BER genes in the progenitor cell compartment (Fig. 3A).

No Immediate Transcriptional Response to EtNU-Induced DNA Damage

It has been shown that exposure of human cell lines to DNA-damaging agents can induce a significant shift in the expression profile of DNA damage response genes [29]. Therefore, the functional differences in repair capacity, which we observed between $CD34^+$ and $CD34^-$ cells, could be due to cell type-specific rapid up- or downregulation of DNA damage-related genes shortly after drug exposure. To investigate this possibility, we have compared gene expression profiles in both cell fractions prior to and 2 h after exposure to EtNU. However, no major shifts in mRNA levels upon initial DNA damage were observed either in mature or in progenitor cells (Fig. 5A, 5B). The changes induced by EtNU treatment were by far less pronounced than those observed between cells of different maturation status (Fig. 5C).

Functional Repair Analysis and Expression Profiles in Primitive $CD34^+38^{low}$ Cells

To analyze DNA repair capacity and DNA damage response in very early stages of hematopoietic differentiation $CD34^+38^{low}$

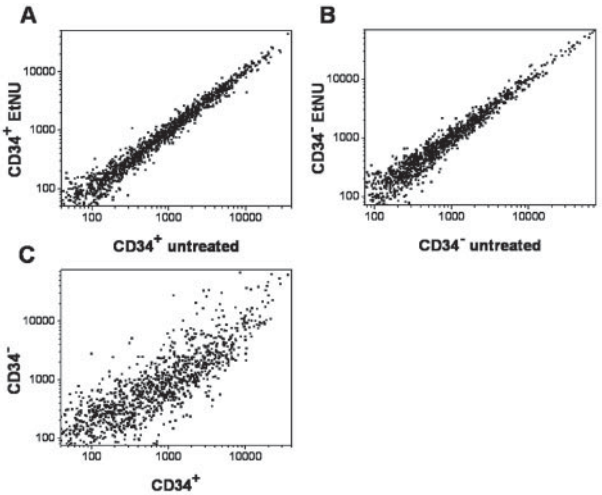

Figure 5. Lack of transcriptional response in mature and progenitor hematopoietic cells early after DNA alkylation stress. Scatter plots of the hybridization signals from 1,418 probe sets (representing 803 DNA damage response genes); comparison of cord blood–derived cells prior to and 2 hours after ex vivo exposure to EtNU (100 μg/ml) $CD34^+$ **(A)**; $CD34^-$ **(B)**; and $CD34^+$ versus $CD34^-$, both untreated **(C)**. Abbreviation: EtNU, *N*-ethylnitrosourea.

cells were utilized. Repair kinetics after challenge with EtNU revealed consistently (4/4 samples) higher frequencies of initial strand breaks and faster resealing of repair gaps in primitive $CD34^+38^{low}$ cells compared with the related progenitor cells (Fig. 4D–4F). To reconcile functional analysis and gene expression profiles, mRNA from $lin1^-CD34^+38^{low}$ cells was subjected to microarray analysis. Due to the low cell number in this fraction, RNA from four individual cord blood samples was pooled. Analyzing the set of the 803 DNA damage response genes or the 189 genes related to DNA repair, 157 (20%) or 47 (25%) of them were differentially expressed in $CD34^+38^{low}$ versus $CD34^+38^+$ cells. Among the 97 genes contributing to the major DNA repair pathways, 19 were significantly up- or downregulated. Interestingly, and in contrast to the higher repair capacity of primitive $CD34^+38^{low}$ cells, the vast majority of those genes (16/19) had reduced transcript levels in the stem cell fraction (Fig. 6). Again, *ATM* was among the few genes for which transcript levels were positively correlated to the overall repair capacity. This unique regulatory status was confirmed by RT-PCR analysis in three independent individual pairs of $CD34^+38^+$/$CD34^+38^{low}$ cells (SLRs for ATM: −1.84, −0.79, and −2.28 by RT-PCR vs. −0.3 by array analysis of pooled RNA).

DISCUSSION

Although pharmacotherapy with DNA-reactive agents has represented a cornerstone of systemic antineoplastic therapies for more than half a century, crucial steps of the molecular mechanisms determining the therapeutic potential, but also the side effects of these drugs, have remained ill-defined. We and others have recently introduced the cellular DNA repair capacity as an important modulator of drug susceptibility within the lymphohematopoietic system. In these studies, accentuated hematotoxicity and increased apoptotic response were associated with a consistently lower DNA repair capacity in human $CD34^+$ progenitor cells compared with their mature $CD34^-$ counterparts [18, 22].

We now have employed gene array technology to allow a correlation of functional and gene expression analysis and have extended our studies to the hematopoietic stem cell compartment. We show that the differentiation-dependent alterations in DNA repair function and apoptotic response are accompanied by characteristic and consistent shifts in the expression profiles of related genes. Although genome-wide transcriptional signatures have been described for distinct stages of lymphohematopoietic differentiation [30, 31], very limited information is available on the regulation of the DNA repair machinery. For a small number of repair genes, such as *XPG*, *XPD*, *MSH2*, *KU80*, *LIG3*, or *RAD23A*, higher expression in bone marrow stem cells compared with terminally differentiated cells has been reported in mice [29, 30]. However, no comparable data are available on distinct developmental stages in the human system. The study presented here now reveals a strict differentiation-dependent regulation within the DNA damage response network of human hematopoietic cells. The uniform shift in transcript levels of regulated genes, up or down, in all seven cord blood specimens investigated implies a high biological relevance for this observation.

Despite this stringent regulation during development, intriguingly high interindividual differences were observed in repair gene expression, as well as functional repair capacity. Similar individual variations were detected for the induction of apoptosis following cytotoxic drug exposure (Table 1) or toxicity of chloroethylnitrosourea- or triazine-type alkylating agents for human clonogenic progenitor cells (personal observation). It can be speculated also that the substantial differences in antineoplastic response or hematotoxic side-effects observed with DNA-damaging agents in the clinical situation may be related to the individual DNA repair capacity of malignant or physiologic cells, respectively. Thus, dosage based on prior assessment of DNA repair capacity in tumor cells, as well as normal tissue, may represent a way to individualize antineoplastic therapy and improve results.

Rather surprising results were obtained when functional and expression profiling data were compared. Despite their significantly lower capacity to remove DNA adducts and secondary strand breaks, progenitor cells contained higher mRNA levels than their maturated progeny for 35/37 differentially expressed pathway-related repair genes. Comparing the progenitor and stem cell fractions, a similar discrepancy was noted. Here, reduced expression for 16/19 pathway-related genes in primitive cells was associated with higher repair efficiency. A possible explanation for this observation could be the impact of post-transcriptional control instances on the performance of the repair system such as ubiquitination-triggered protein turnover [32–34], stability modulation of protein complexes [35, 36], or intracellular/intranuclear localization of key components [37, 38]. In addition, low abundant gene products not detectable by oligonucleotide arrays may represent rate-limiting "bottleneck" positions along a given repair pathway and significantly determine its functional activity. Thus, important regulatory functions might be associated with the substantial number of repair

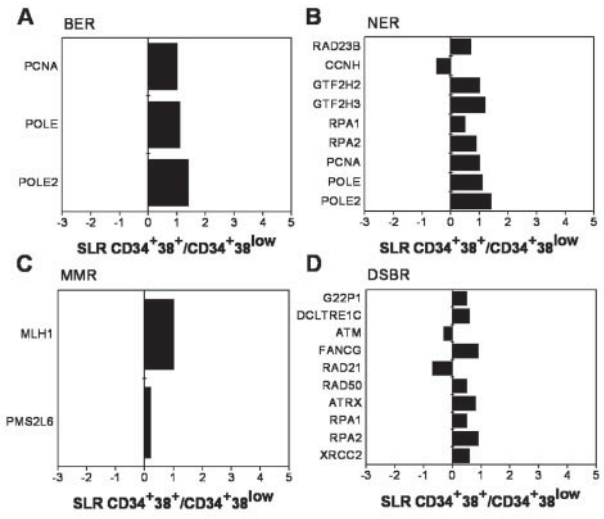

Figure 6. Genes for major DNA repair functions are differentially expressed in primitive $CD34^+38^{low}$ and $CD34^+38^+$ progenitor cells. Up- or downregulation of transcripts (single log ratio [SLR]; see Fig. 3) as measured in pooled RNA samples from four cord blood specimens (criterion for significance: p values of SLRs $\leq .005$ or $\geq .995$). Abbreviations: BER, base excision repair; NER, nucleotide excision repair; MMR, mismatch repair; DSBR, double-strand break repair.

genes not qualifying for present calls in our analyses (14/97 in mature vs. progenitor cell analysis, 21/97 in progenitor vs. stem cells).

On the other hand, the few pathway-related genes with shifts in transcript levels being conform to the alterations in functional repair may be essential for fine-tuning the cellular response to DNA damage. One of these genes encodes for ATM, a protein kinase that senses and signals the presence of DNA lesions, in particular double-strand breaks, to essential checkpoints and initiates rejoining [39]. Mammalian cells deficient for this protein are sensitive to radiation but also to DNA alkylation damage [40], most likely due to an essential role of ATM in stabilization and nuclear localization of mismatch repair complexes [41]. Recently, functional ATM was shown to be involved in counteracting oxidative stress in mouse bone marrow cells. In this model, ATM represented a crucial factor for the self-renewal capacity of hematopoietic stem cells but was less important for their differentiation into progenitor cells [42].

The other gene with significantly diminished transcript levels in progenitor versus mature cells is *RAD23A*. The RAD23 proteins are involved in the regulation protein turnover via the ubiquitin/proteasome pathway [43, 44] and recently were found to stabilize the XPC protein, which is the core damage recognition factor initiating global repair via the NER pathway [35]. Thereby, they are ideal candidates to regulate the NER activity by controlling the influx into the pathway without disrupting the balance of the complex interaction of the other components. Based on these findings, the RAD23 proteins have been suggested to play a central role in a novel, newly emerging DNA damage-dependent regulatory mechanism for DNA repair in mammalian cells [45]. Interestingly, *RAD23A* is among the repair genes with the broadest interindividual variation of transcript levels in the cord blood samples analyzed and thus may be a key factor in controlling the individual repair capacity. Its relevance for the handling of DNA alkylation products is further strengthened by our observation that human XPC-RAD23 complexes can recognize EtNU-induced adducts in DNA and are essential for their NER-mediated excision in human lymphoid cells (unpublished data). Also in line with the downregulation of *RAD23A* and the reduced NER activity in progenitor cells is the higher relative contribution of BER (no downregulated constituents) to their overall repair capacity.

Thus, in contrast to expression levels of the majority of genes involved, the least efficient DNA repair during hematopoietic differentiation resides within the progenitor cell compartment, whereas increased capacity is observed in more mature as well as more primitive cells. At first sight this may appear surprising, as an organism can be expected to equip its pool of particularly proliferation-competent cells with protective mechanisms to counteract DNA damage and the emergence of mutated daughter cells. From the perspective of the organism, however, eliminating damaged cells via apoptosis rather than attempting to restore their genomic integrity also represents an efficient defense mechanism against genotoxic stress in critical cell compartments. A well-known example of this principle is intrathymic T-cell development, where cells expressing nonfunctional T-cell receptors are eliminated via apoptosis [46]. Along a similar line, experiments with murine embryonic stem (ES) cells have revealed their limited capacity to remove UV photolesions from the genome [47, 48]. Interestingly, the relative repair deficiency of ES compared with fully differentiated cells was not accompanied by an increased mutation rate, and this was due to an effective induction of cell death programs even at low levels of DNA damage. These data suggest that apoptosis in stem cells is triggered preferentially by global genomic damage, whereas transcription-blocking lesions in active genes may represent the critical signals in maturated cells. The model is in agreement with our observations in the human lymphohematopoietic system, where the proliferation-competent progenitor cells exhibit reduced efficiency of global repair and increased apoptotic response upon exposure to DNA-damaging agents. Thus, this might be a general way to protect somatic "cell replenishment compartments" from the accumulation of genetic damage and thereby avoiding the expansion of mutated cells and their potential malignant transformation.

ACKNOWLEDGMENTS

We thank S. Niesert (Elisabeth-Krankenhaus, Essen, Germany) and G. Kögler and P. Wernet (Universitätsklinikum Düsseldorf) for providing cord blood samples; M. J. Tilby (University of Newcastle upon Tyne) for the generous gift of anti-(melphalan-DNA adduct) antibodies; R. A. Hilger and M. Grubert (Universitätsklinikum Duisburg-Essen, Essen, Germany) for the measurement of intracellular melphalan levels; and A. Feldmann and M. Möllmann (Innere Klinik [Tumorforschung]) for excellent technical assistance. Research was supported by Wilhelm Sander-Stiftung Grant 1999.082.1 and in part by Bundesministerium für Bildung und Forschung-Nationales Genomforshungsnetz Grant KR S06T06 and Mildred Scheel-Stiftung Grant 10-2039 to J.T. and T.M.

DISCLOSURES

The authors indicate no potential conflicts of interest.

REFERENCES

1 Müller MR, Buschfort C, Thomale J et al. DNA repair and cellular resistance to alkylating agents in chronic lymphocytic leukemia. Clin Cancer Res 1997;3:2055–2061.

2 Gerson SL. MGMT: Its role in cancer aetiology and cancer therapeutics. Nat Rev Cancer 2004;4:296–307.

3 Spanswick VJ, Craddock C, Sekhar M et al. Repair of DNA interstrand crosslinks as a mechanism of clinical resistance to melphalan in multiple myeloma. Blood 2002;100:224–229.

4 Christmann M, Tomicic MT, Roos WP et al. Mechanisms of human DNA repair: An update. Toxicology 2003;193:3–34.

5 Sancar A, Lindsey-Boltz LA, Unsal-Kacmaz K et al. Molecular mechanisms of mammalian DNA repair and the DNA damage checkpoints. Annu Rev Biochem 2004;73:39–85.

6 Shiraishi A, Sakumi K, Sekiguchi M. Increased susceptibility to chemotherapeutic alkylating agents of mice deficient in DNA repair methyltransferase. Carcinogenesis 2000;21:1879–1883.

7 Reese JS, Liu L, Gerson SL. Repopulating defect of mismatch repair-deficient hematopoietic stem cells. Blood 2003;102:1626–1633.

8 Essers J, van Steeg H, de Wit J et al. Homologous and non-homologous recombination differentially affect DNA damage repair in mice. EMBO J 2000;19:1703–1710.

9 Pollok KE, Hartwell JR, Braber A et al. In vivo selection of human hematopoietic cells in a xenograft model using combined pharmacologic and genetic manipulations. Hum Gene Ther 2003;14:1703–1714.

10 Kobune M, Xu Y, Baum C et al. Retrovirus-mediated expression of the base excision repair proteins, formamidopyrimidine DNA glycosylase or human oxoguanine DNA glycosylase, protects hematopoietic cells from *N*,*N*′,*N*″-triethylenethiophosphoramide (thioTEPA)-induced toxicity in vitro and in vivo. Cancer Res 2001;61:5116–5125.

11 Sawai N, Zhou S, Vanin EF et al. Protection and in vivo selection of hematopoietic stem cells using temozolomide, O^6-benzylguanine, and an alkyltransferase-expressing retroviral vector. Mol Ther 2001;3:78–87.

12 Zielske SP, Reese JS, Lingas KT et al. *In vivo* selection of MGMT(P140K) lentivirus-transduced human NOD/SCID repopulating cells without pretransplant irradiation conditioning. J Clin Invest 2003; 112:1561–1570.

13 Ragg S, Xu-Welliver M, Bailey J et al. Direct reversal of DNA damage by mutant methyltransferase protein protects mice against dose-intensified chemotherapy and leads to in vivo selection of hematopoietic stem cells. Cancer Res 2000;60:5187–5195.

14 Jansen M, Sorg UR, Ragg S et al. Hematoprotection and enrichment of transduced cells in vivo after gene transfer of MGMT(P140K) into hematopoietic stem cells. Cancer Gene Ther 2002;9:737–746.

15 Buschfort C, Müller MR, Seeber S et al. DNA excision repair profiles of normal and leukemic human lymphocytes: Functional analysis at the single-cell level. Cancer Res 1997;57:651–658.

16 Boffetta P, Nyberg F, Mukeria A et al. O^6-Alkylguanine-DNA-alkyltransferase activity in peripheral leukocytes, smoking and risk of lung cancer. Cancer Lett 2002;180:33–39.

17 Vodicka P, Kumar R, Stetina R et al. Genetic polymorphisms in DNA repair genes and possible links with DNA repair rates, chromosomal aberrations and single-strand breaks in DNA. Carcinogenesis 2004;25: 757–763.

18 Gerson SL, Phillips W, Kastan M et al. Human CD34+ hematopoietic progenitors have low, cytokine-unresponsive O^6-alkylguanine-DNA alkyltransferase and are sensitive to O^6-benzylguanine plus BCNU. Blood 1996;88:1649–1655.

19 Terry MB, Gammon MD, Zhang FF et al. Polymorphism in the DNA repair gene XPD, polycyclic aromatic hydrocarbon-DNA adducts, cigarette smoking, and breast cancer risk. Cancer Epidemiol Biomarkers Prev 2004;13:2053–2058.

20 Butkiewicz D, Popanda O, Risch A et al. Association between the risk for lung adenocarcinoma and a (−4) G-to-A polymorphism in the XPA gene. Cancer Epidemiol Biomarkers Prev 2004;13:2242–2246.

21 Myllyperkio MH, Vilpo JA. Increased DNA single-strand break joining activity in UV-irradiated CD34+ versus CD34− bone marrow cells. Mutat Res 1999;425:169–176.

22 Buschfort-Papewalis C, Moritz T, Liedert B et al. Down-regulation of DNA repair in human CD34(+) progenitor cells corresponds to increased drug sensitivity and apoptotic response. Blood 2002;100: 845–853.

23 Wood RD, Mitchell M, Sgouros J et al. Human DNA repair genes. Science 2001;291:1284–1289.

24 McNamee JP, McLean JR, Ferrarotto CL et al. Comet assay: Rapid processing of multiple samples. Mutat Res 2000;466:63–69.

25 Olive PL, Banath JP, Durand RE. Heterogeneity in radiation-induced DNA damage and repair in tumor and normal cells measured using the "comet" assay. Radiat Res 1990;122:86–94.

26 Baugh LR, Hill AA, Brown EL et al. Quantitative analysis of mRNA amplification by in vitro transcription. Nucleic Acids Res 2001;29:E29.

27 Beranek DT. Distribution of methyl and ethyl adducts following alkylation with monofunctional alkylating agents. Mutat Res 1990;231:11–30.

28 Summers YJ, Heyworth CM, De Wynter EA et al. Cord blood G_0 $CD34^+$ cells have a thousand-fold higher capacity for generating progenitors in vitro than G_1 $CD34^+$ cells. STEM CELLS 2001;19:505–513.

29 Rieger KE, Chu G. Portrait of transcriptional responses to ultraviolet and ionizing radiation in human cells. Nucleic Acids Res 2004;32:4786–4803.

30 Ramalho-Santos M, Yoon S, Matsuzaki Y et al. "Stemness": Transcriptional profiling of embryonic and adult stem cells. Science 2002;298: 597–600.

31 Ivanova NB, Dimos JT, Schaniel C et al. A stem cell molecular signature. Science 2002;298:601–604.

32 Ustrell V, Hoffman L, Pratt G et al. PA200, a nuclear proteasome activator involved in DNA repair. EMBO J 2002;21:3516–3525.

33 Krogan NJ, Lam MHY, Fillingham J et al. Proteasome involvement in the repair of DNA double-strand breaks. Mol Cell 2004;16:1027–1034.

34 Rechsteiner M, Hill CP. Mobilizing the proteolytic machine: Cell biological roles of proteasome activators and inhibitors. Trends Cell Biol 2005;15:27–33.

35 Okuda Y, Nishi R, Ng JM et al. Relative levels of the two mammalian Rad23 homologs determine composition and stability of the xeroderma pigmentosum group C protein complex. DNA Repair (Amst) 2004;3: 1285–1295.

36 Strom L, Lindroos HB, Shirahige K et al. Postreplicative recruitment of cohesin to double-strand breaks is required for DNA repair. Mol Cell 2004;16:1003–1015.

37 Jefford CE, Feki A, Harb J et al. Nuclear-cytoplasmic translocation of BARD1 is linked to its apoptotic activity. Oncogene 2004;23:3509–3520.

38 Gill G. SUMO and ubiquitin in the nucleus: Different functions, similar mechanisms? Genes Dev 2004;18:2046–2059.

39 McGowan CH, Russell P. The DNA damage response: Sensing and signaling. Curr Opin Cell Biol 2004;16:629–633.

40 Debiak M, Nikolova T, Kaina B. Loss of ATM sensitizes against O^6-methylguanine triggered apoptosis, SCEs and chromosomal aberrations. DNA Repair (Amst) 2004;3:359–368.

41 Luo Y, Lin FT, Lin WC. ATM-mediated stabilization of hMutL DNA mismatch repair proteins augments p53 activation during DNA damage. Mol Cell Biol 2004;24:6430–6444.

42 Ito K, Hirao A, Arai F et al. Regulation of oxidative stress by ATM is required for self-renewal of haematopoietic stem cells. Nature 2004;431: 997–1002.

43 Raasi S, Pickart CM. Rad23 ubiquitin-associated domains (UBA) inhibit 26 S proteasome-catalyzed proteolysis by sequestering lysine 48-linked polyubiquitin chains. J Biol Chem 2003;278:8951–8959.

44 Ortolan TG, Chen L, Tongaonkar P et al. Rad23 stabilizes Rad4 from degradation by the Ub/proteasome pathway. Nucleic Acids Res 2004; 32:6490–6500.

45 Ng JMY, Vermeulen W, van der Horst GTJ et al. A novel regulation mechanism of DNA repair by damage-induced and RAD23-dependent stabilization of xeroderma pigmentosum group C protein. Genes Dev 2003;17:1630–1645.

46 Strasser A, Bouillet P. The control of apoptosis in lymphocyte selection. Immunol Rev 2003;193:82–92.

47 Van Sloun PP, Jansen JG, Weeda G et al. The role of nucleotide excision repair in protecting embryonic stem cells from genotoxic effects of UV-induced DNA damage. Nucleic Acids Res 1999;27:3276–3282.

48 de Waard H, de Wit J, Gorgels TG et al. Cell type-specific hypersensitivity to oxidative damage in CSB and XPA mice. DNA Repair (Amst) 2003;2:13–25.

Activation-induced cytidine deaminase acts as a mutator in *BCR-ABL1*–transformed acute lymphoblastic leukemia cells

Niklas Feldhahn,[1,2] Nadine Henke,[1,3] Kai Melchior,[1,2] Cihangir Duy,[1,2] Bonaventure Ndikung Soh,[1,3] Florian Klein,[1,3] Gregor von Levetzow,[3] Bernd Giebel,[3] Aihong Li,[4] Wolf-Karsten Hofmann,[5] Hassan Jumaa,[6] and Markus Müschen[1,2]

[1]Leukemia Research Program, Childrens Hospital Los Angeles, [2]Leukemia and Lymphoma Program, Norris Comprehensive Cancer Center, University of Southern California, Los Angeles, CA 90027
[3]Biologisch Medizinisches Forschungszentrum, Heinrich-Heine-Universität Düsseldorf, 40225 Düsseldorf, Germany
[4]Department of Medical Biosciences, Pathology, Umea University, SE-901 87 Umea, Sweden
[5]Department of Hematology and Oncology, University Hospital Benjamin Franklin, 12200 Berlin, Germany
[6]Max-Planck Institute for Immunobiology, D-79108 Freiburg, Germany

The Philadelphia chromosome (Ph) encoding the oncogenic BCR-ABL1 kinase defines a subset of acute lymphoblastic leukemia (ALL) with a particularly unfavorable prognosis. ALL cells are derived from B cell precursors in most cases and typically carry rearranged immunoglobulin heavy chain (*IGH*) variable (V) region genes devoid of somatic mutations. Somatic hypermutation is restricted to mature germinal center B cells and depends on activation-induced cytidine deaminase (AID). Studying AID expression in 108 cases of ALL, we detected AID mRNA in 24 of 28 Ph$^+$ ALLs as compared with 6 of 80 Ph$^-$ ALLs. Forced expression of *BCR-ABL1* in Ph$^-$ ALL cells and inhibition of the BCR-ABL1 kinase showed that aberrant expression of AID depends on BCR-ABL1 kinase activity. Consistent with aberrant AID expression in Ph$^+$ ALL, *IGH* V region genes and *BCL6* were mutated in many Ph$^+$ but unmutated in most Ph$^-$ cases. In addition, AID introduced DNA single-strand breaks within the tumor suppressor gene *CDKN2B* in Ph$^+$ ALL cells, which was sensitive to BCR-ABL1 kinase inhibition and silencing of AID expression by RNA interference. These findings identify AID as a BCR-ABL1–induced mutator in Ph$^+$ ALL cells, which may be relevant with respect to the particularly unfavorable prognosis of this leukemia subset.

CORRESPONDENCE
Markus Müschen:
mmuschen@chla.usc.edu

Abbreviations used: Abelson-MuLV, Abelson murine leukemia virus; AID, activation-induced cytidine deaminase; ALL, acute lymphoblastic leukemia; CSR, class-switch recombination; DNA-SSB, DNA single-strand breaks; LBC, lymphoid blast crisis; LM-PCR, ligation-mediated PCR; Ph, Philadelphia chromosome; SHM, somatic hypermutation; siRNA, small interfering RNA; V, variable.

Somatic hypermutation (SHM) and class-switch recombination (CSR) represent physiological processes that modify variable (V) and constant regions of Ig genes in mature germinal center B cells (1). Both SHM and CSR critically depend on expression of activation-induced cytidine deaminase (AID), which introduces single-strand breaks into target DNA (2). AID-mediated DNA single-strand breaks (DNA-SSB) leading to SHM and CSR are specifically introduced into V or constant regions of Ig genes, respectively. At much lower frequency, however, AID can also target non-Ig genes in germinal center B cells (3, 4) and may even act as a genome-wide mutator (5). Such targeting errors carry the risk of oncogenic mutation leading to the transformation of a germinal center B cell, which may give rise to B cell lymphoma. For instance, aberrant SHM or CSR may lead to chromosomal translocation of protooncogenes, including *MYC*, *BCL2*, *BCL6*, and *CCND1*, and cause various types of B cell lymphoma (3). Therefore, tight regulation of AID expression in germinal center B cells and control of DNA strand breaks related to SHM and CSR are critical to prevent B cell malignancy. In fact, previous work demonstrated that *Myc-Igh* chromosome translocations as they occur in human Burkitt's lymphoma are caused by Aid (6). The emergence of *Myc-Igh* gene rearrangements is not only prevented by tight regulation of Aid expression; the activation of DNA damage–induced checkpoints during physiological AID-dependent CSR may eventually lead to the activation of the tumor suppressors ATM, NBS1, CDKN2D (INK4D,

The online version of this article contains supplemental material.

www.jem.org/cgi/doi/10.1084/jem.20062662

P19/ARF), and TP53 and is indeed critical to prevent oncogenic *Myc-Igh* gene rearrangements (7).

RESULTS

Aberrant AID expression correlates with the Philadelphia chromosome (Ph) in acute lymphoblastic leukemia (ALL)

ALL cells are typically derived from pro– or pre–B cells. These B cell precursors do not express AID (Table I and Fig. 1 A, left) and carry Ig genes that have neither undergone SHM nor CSR (8). Therefore, it was unexpected that AID is expressed in a subset of ALL cell lines (Table I and Fig. 1 A, right). Interestingly, AID expression correlates with the presence of t(9;22)(q34;q11), resulting in the so-called Philadelphia chromosome (Ph). Ph encodes the oncogenic BCR-ABL1 kinase and defines a subgroup of ALL with a particularly unfavorable prognosis (9). Studying AID mRNA expression in 108 cases of ALL, AID mRNA was detected in 24 of 28 cases of Ph^+ ALL, but only in 6 of 80 cases of Ph^- ALL (Table I). Compared with normal germinal center B cells, mRNA levels for AID are lower in most but similar in some Ph^+ ALL cell lines (Fig. 1 A, right).

SHM and CSR of Ig genes in Ph^+ ALL

This raises the possibility that Ig V region genes might aberrantly be targeted by SHM in Ph^+ ALL. Therefore, we analyzed the sequence of V_H region genes in 60 Ph^- and 46 Ph^+ cases of ALL. Among Ph^- ALL, 6 of 60 cases carry somatically mutated V_H region genes (Table I and Table S1, which is available at http://www.jem.org/cgi/content/full/jem.20062662/DC1). In contrast, 30 of 46 Ph^+ ALL cases harbor mutated V_H gene rearrangements (Table I and Table S2). Counting only Ph^+ and Ph^- leukemia cases, for which information on both AID expression and V_H region sequence was available, this correlation was even more conspicuous: 16 of 18 Ph^+ leukemia cases, all expressing AID, also carried mutated V_H region genes, whereas 10 Ph^- leukemia cases, all lacking AID expression, also all carried unmutated V_H gene rearrangements. The average mutation frequency was 34.5 ± 4 mutations/10^3 bp in Ph^+ and 4.9 ± 1 mutations/10^3 bp in Ph^- ALL among all sequences (means based on data from 70 and 76 sequences ± SEM, $P < 0.05$; Tables S1 and S2). Also among the six Ph^- cases carrying mutated V_H region genes, the mutation frequency was high, suggesting that in a small subset of Ph^- ALL, aberrant SHM may also be induced by other factors that are not related to BCR-ABL1.

Analyzing CSR of Ig C_H region genes in Ph^+ and Ph^- ALL, we identified switched Cγ1, Cγ2, Cγ3, and Cα2 transcripts in 4 of 21 Ph^+ but not in any of 10 Ph^- ALL cases (Table II). Based on the small number of cases studied, we cannot give an estimate of the overall frequency of CSR in Ph^+ ALL. Collectively, we conclude that Ig genes in Ph^+ ALLs can be targeted by SHM and in rare cases even undergo CSR, which is consistent with specific expression of AID in this ALL subset.

Aberrant SHM of non-Ig genes in Ph^+ ALL

Given that previous studies demonstrated that aberrant SHM also involves mutation of non-Ig genes (3, 4), we also studied known potential target regions of SHM within the *BCL6* and *MYC* genes (3, 4) in Ph^- and Ph^+ cases. 7 of 10 Ph^+ ALL cases and 1 of 5 Ph^- ALL cases harbored a mutated *BCL6* gene (Table I and Table S3). In both Ph^- and Ph^+ ALL, the average mutation frequency was above the error rate of the PFU DNA polymerase used in this experiment. Comparing Ph^+ and Ph^-

Table I. Aberrant SHM of Ig- and non-Ig genes in Ph^+ ALL cells

Cell type	*IGHV*[a]		*BCL6*		*MYC*		AID mRNA expression
	Mutated clones/cases	Mutations per 10^3 bp	Mutated clones/cases	Mutations per 10^3 bp	Mutated clones/cases	Mutations per 10^3 bp	
Pre–B cells (clones)	1/36	4.4 ± 4	n.d.		n.d.		No
Naive B cells (clones)	0/12	3.1 ± 1	1/21[b]	0.05[b]	7/179[c]	0.05[c]	No
Germinal center B cells (clones)	12/14	40.2 ± 12	5/15[b]	1.0[b]	n.d.		Yes
Memory B cells (clones)	52/54	45.2 ± 9	26/71[c]	1.38 ± 0.34[c]	9/178[c]	0.09[c]	No
Ph^- ALL (cases)	6/60	4.85 ± 1.23	1/5[d]	0.11 ± 0.11	1/5[c]	0.16 ± 0.11	6/80 cases
Ph^+ ALL (cases)	30/46	34.48 ± 4.42	7/10[d]	1.07 ± 0.23	3/9[d]	0.51 ± 0.15	24/28 cases
MYC-IGH Burkitt's lymphoma (cases)	12/12[b]	69[b]	11/30[b]	0.4 [b]	12/12[b]	1.9[b]	Yes

[a]For normal B cell subsets, rearranged V_H gene segments were amplified, cloned, and sequenced from bulk populations. For leukemia and lymphoma cells, individual cases were analyzed. Mutation frequencies are given as means (mutations per 10^3 bp) ± standard error of the mean. V_H gene rearrangements were amplified using Taq DNA polymerase. V_H gene rearrangements amplified from ALL cases were considered mutated if the average mutation frequency of all amplified sequences was significantly ($P < 0.01$) above the error rate of Taq DNA polymerase.

[b]Data from reference 3.

[c]Data from reference 4.

[d]*BCL6* and *MYC* alleles were amplified using PFU DNA polymerase and sequenced from both DNA strands. *BCL6* or *MYC* alleles amplified from ALL cases were considered mutated if at least two mutated sequences were amplified per case with an average mutation frequency of all amplified sequences significantly ($P < 0.01$) above the error rate of PFU DNA polymerase. Only mutations confirmed on both DNA strands were counted.

cases, the average mutation frequency was significantly higher in Ph^+ ALL (Table I and Table S3; $P < 0.05$). Likewise, *MYC* gene mutations were found in both Ph^- and Ph^+ ALL cells. In this case, however, the difference between Ph^+ and Ph^- cells was not significant (Table I; $P = 0.13$).

Besides rearranged *IGH* V region genes, $CD19^+$ B cell lineage ALL cells frequently carry *TCRB* (10) and *TCRG* (11) gene rearrangements. Consistent with these previous findings, we were able to amplify *TCRB* and *TCRG* gene rearrangements from four of eight (*TCRB*) and seven of seven (*TCRG*) cases of Ph^+ ALL (Table S3, available at http://www.jem.org/cgi/content/full/jem.20062662/DC1). Given that transgenic expression of Aid in murine T cell lymphomas also induces SHM of rearranged *TCRB* genes (12), we performed sequence analysis of *TCRB* and *TCRG* gene rearrangements in Ph^+ ALL, as well as normal peripheral blood T cells (Table S3). *TCRB* gene rearrangements amplified from Ph^+ ALL were somatically mutated in all four cases with an average

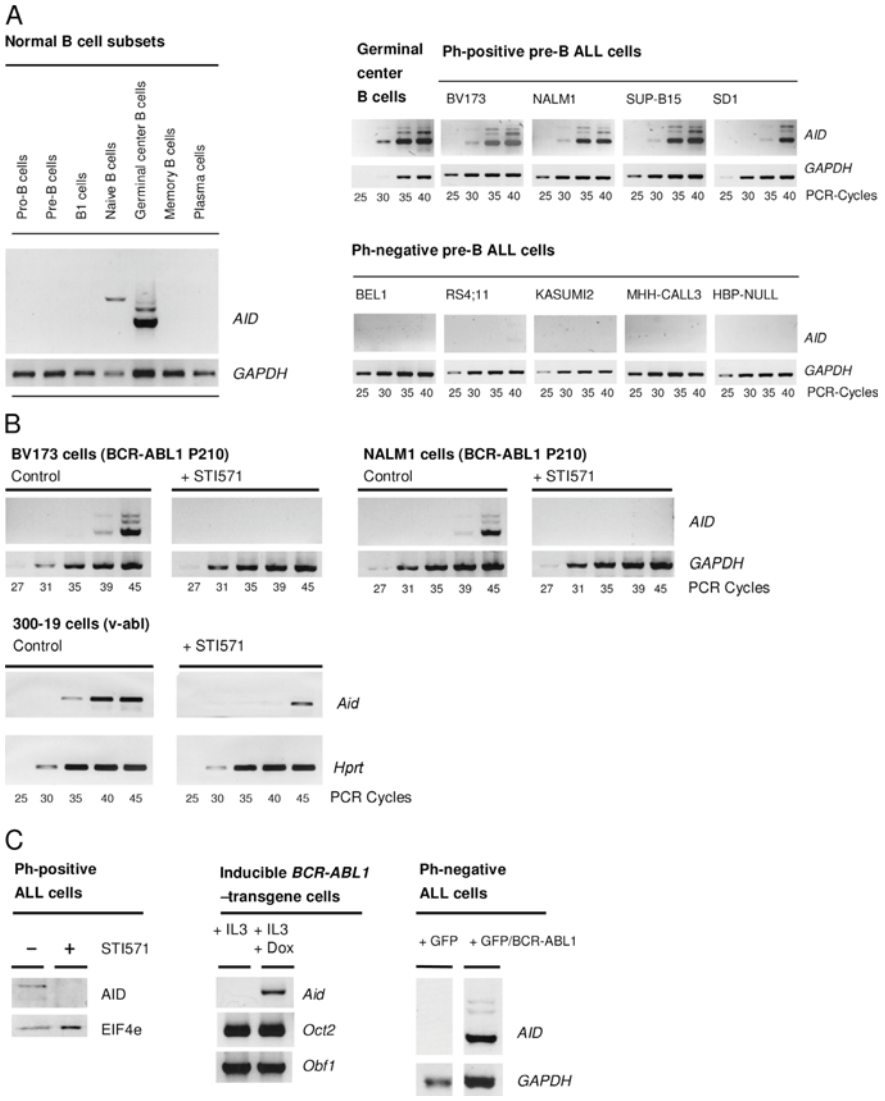

Figure 1. AID expression in Ph^+ ALL cells. mRNA expression of AID was measured in normal human pro–B, pre–B, B1, naive, germinal center, and memory B cells as well as plasma cells by RT-PCR (A). In a semiquantitative RT-PCR analysis, AID mRNA expression in Ph^+ ALL cells was compared with germinal center B cells and Ph^- ALL cells. GAPDH was used for normalization of cDNA amounts (A). Ph^+ ALL cell lines (BV173 and Nalm1; 10 μmol/l STI571) and v-abl–transformed mouse pre–B cells (300-19; 1 μmol/l STI571) were treated with or without STI571 for 24 h and subjected to semiquantitative RT-PCR analysis for human AID and GAPDH or murine Aid and Hprt mRNA expression (B). Protein lysates from STI571-treated or untreated Ph^+ ALL cells (BV173) were used for Western blotting (C) together with antibodies against AID and EIF4E (used as a loading control). IL-3–dependent murine pro–B cells carrying a doxycycline-inducible BCR-ABL1 transgene were incubated with or without 1 μg/ml doxycycline for 24 h and subjected to RT-PCR analysis of Aid, Oct2, and Obf1 mRNA expression (C). Ph^- ALL cells were transiently transfected with a pMIG vector encoding GFP and/or GFP and BCR-ABL1. After 24 h, GFP-expressing cells were sorted and subjected to RT-PCR analysis for AID expression (C).

Table II. CSR in Ph+ ALL cells

Case	V_H	D_H	J_H rearrangement	C_H region
LBCII (FACS-sort:	TATGTATTATTGTACGAAAGA	**GGGTTCAGCTATGG**	CCGACCTGAACTTCTGGGGCCAGGGAACCCTGGTCACCGTCTCCTCAG	**GGAGTGCATCCGCCCCAA** Cμ
$CD19^+$ $CD34^+$)	TATGTATTATTGTACGAAAGA	**GGGTTCAGCTATGG**	CCGACCTGAACTTCTGGGGCCAGGGAACCCTGGTCACCGTCTCCTCAG	CCTCCACCAAGGGCCCAT Cγ2
Case 22 in Table S2	–G–––––––C–––G–––––––	––A–A–––––––––	A–T––T–TG–––A––	
	V_H3-30	D_H5-5	J_H4	
LBCIII (FACS-sort:	GCCTTCTATTATTGTGCGCGA	**GGTGATACC** ACAGTCAGCGGGA	CCAACTGGCTCGCCCCCTGGGGCCAGGGAACCCTGGTCACCGTCTCCTCTG	**GGAGTGCATCCGCCCCAA** Cμ
$CD19^+$ $CD34^+$)	GCCTTCTATTATTGTGCGCGA	**GGTGATACC** ACAGTCAGCGGGA	CCAACTGGCTCGCCCCCTGGGGCCAGGGAACCCTGGTCACCGTCTCCTCTG	CCTCCACCAAGGGCCCAT Cγ2
Case 23 in Table S2	–––G–G–––––C––––––A––	––––––TG–	A–––––––T–––A–––––––––––––––––––––––––––––––––A––––––––––––––––––	
	V_H1-46	D_H2-21	J_H5	
Ph^+ cell line Nalm-1	AGTCTGAGAGCTGAGGACACC TGGGGG	**TACTTTGACT** ACTGGGGCC	AGGGAACCCTGGTCACCGTCTCCTCAG	**GGAGTGCATCCGCCCCAA** Cμ
	AGTCTGAGAGCTGAGGACACC TGGGGG	**TACTTTGACT** ACTGGGGCC	AGGGAACCCTGGTCACCGTCTCCTCAG	CTTCCACCAAGGGCCCAT Cγ3
	AGTCTGAGAGCTGAGGACACC TGGGGG	**TACTTTGACT** ACTGGGGCC	AGGGAACCCTGGTCACCGTCTCCTCAG	CATCCCCGACCAGCCCCA Cα2
	––––––––––A––––––––––	––T–––––––	–––	
	V_H3-43	D_H3-9	J_H5	
Ph^+ cell line SD1	GCTGTCTATTATTGTGTGAAA	**CCGATGGGAC** CCTACCGCGAG	GCTTTTGATATCTGGGGCCAAGGGACAGTGGTCACCGTCTCTTCAG	**GGAGTGCATCCGCCCCAA** Cμ
	GCTGTCTATTATTGTGTGAAA	**CCGATGGGAC** CCTACCGCGAG	GCTTTTGATATCTGGGGCCAAGGGACAGTGGTCACCGTCTCTTCAG	CCTCCACCAAGGGCCCAT Cγ1
	–––––G–––––C––––C––––	–A–C–––T––	––––––––––––––––––––––––––A–––––––––––––––––––––––––––––––––	
	V_H3-30	D_H3-9	J_H3	

Sequence alignments of the V_H and C_H region genes of four Ph^+ ALL cases (top) are compared to germline sequences (bottom). Constant regions are underscored. CSR was analyzed in 31 cases of ALL, including 10 cases of Ph^- ALL (0/10 Ph^- cases with CSR, all with Cμ) and 21 cases of Ph^+ ALL (4/21 Ph^+ cases with CSR: 1 Cγ1, 2 Cγ2, 1 Cγ3, 1 Cα2, in all 21 Ph^+ cases also co-amplification of Cμ).

mutation frequency of 6.2 mutations per 10^3 bp (±2.3 mutations per 10^3 bp, SEM), which was substantially above the mutation frequency of rearranged *TCRB* alleles amplified from normal T cells. Only 2 of 30 *TCRB* gene rearrangements amplified from normal T cells harbored a single mutation with an average mutation frequency of 0.2 ± 0.1 mutations per 10^3 bp ($P < 0.01$; Table S3). Likewise, five of seven *TCRG* gene rearrangements amplified from Ph^+ ALL cases carried somatic mutations with an average mutation frequency of 5.7 ± 1.0 mutations per 10^3 bp. In contrast, only 1 in 16 *TCRG* gene rearrangements amplified from normal T cells harbored a single point mutation (average mutation frequency: 0.2 ± 0.2 mutations per 10^3 bp, $P < 0.01$; Table S3). Collectively, these data indicate that besides rearranged Ig genes, non-Ig genes, namely *BCL6*, *TCRB*, and *TCRG*, can also be targeted by aberrant SHM in Ph^+ ALL, which is consistent with aberrant expression of AID in this leukemia subset.

BCR-ABL1–induced AID expression in Ph^+ ALL

We next investigated whether the Ph-encoded BCR-ABL1 kinase contributes to aberrant AID expression in Ph^+ ALL. As shown in Fig. 1, inhibition of BCR-ABL1 kinase activity by STI571 down-regulates AID expression in Ph^+ ALL at the mRNA (Fig. 1 B) and protein levels (Fig. 1 C, left). Activation of transgenic expression of *BCR-ABL1* in a murine pro–B cell line and forced transient expression of *BCR-ABL1* in a Ph^- ALL (Fig. 1 C, middle and right) induce de novo expression of AID in these cells. To validate the causative link between BCR-ABL1 kinase activity and aberrant AID expression also in patients suffering from Ph^+ ALL, we compared four matched sample pairs of Ph^+ ALL before the onset and during continued therapy with the BCR-ABL1 kinase inhibitor STI571 (Fig. 2). Confirming in vitro observations, primary patient–derived Ph^+ ALL cells down-regulate AID mRNA (Fig. 2 A) and protein (Fig. 2 B) levels under extended treatment with the BCR-ABL1 kinase inhibitor STI571. We conclude that BCR-ABL1 kinase activity is essential for aberrant AID expression in Ph^+ ALL cells.

Given that STI571 inhibits both oncogenic BCR-ABL1 as well as physiologic ABL1 kinase activity, we investigated whether ABL1 kinase activity contributes to AID expression in normal germinal center–derived B cells. To this end, we isolated splenic B cells from C57/BL6 mice and cultured them in the presence or absence of 10 μmol/l STI571 in the presence or absence of 1 ng/ml IL-4 and 25 μg/ml LPS, or both IL-4/LPS and STI571 (Fig. S1, available at http://www.jem.org/cgi/content/full/jem.20062662/DC1). To compare the effect of ABL1 kinase inhibition in normal B cells and BCR-ABL1–transformed B cells, splenocytes from *BCR-ABL1*–transgenic C57/BL6 litter mates were also cultured in the presence or absence of 10 μmol/l STI571. After 3 d, Aid mRNA levels were measured by real-time PCR as a ratio of Aid and Hprt mRNA levels. As described previously (13), activation of splenic B cells resulted in a dramatic increase of Aid mRNA expression. Aid mRNA levels in *BCR-ABL1*–transgenic B cells were also constitutively higher than in B cells isolated from wild-type littermates (Fig. S1). Interestingly, ABL1 kinase inhibition through STI571 not only diminished Aid mRNA levels in *BCR-ABL1*–transgenic B cells, but also effectively prevented the up-regulation of Aid in normal B cells upon stimulation by IL-4 and LPS. These findings are paralleled by the blastoid morphology and the formation of large cell aggregates of the Aid-expressing B cells. In the presence of STI571, however, IL-4 and LPS failed to induce a blastoid morphology and formation of cell aggregates (Fig. S1). Although we cannot exclude that the high concentrations of STI571 used in this experiment may inhibit other signaling molecules besides normal ABL1 in the splenic B cells, these

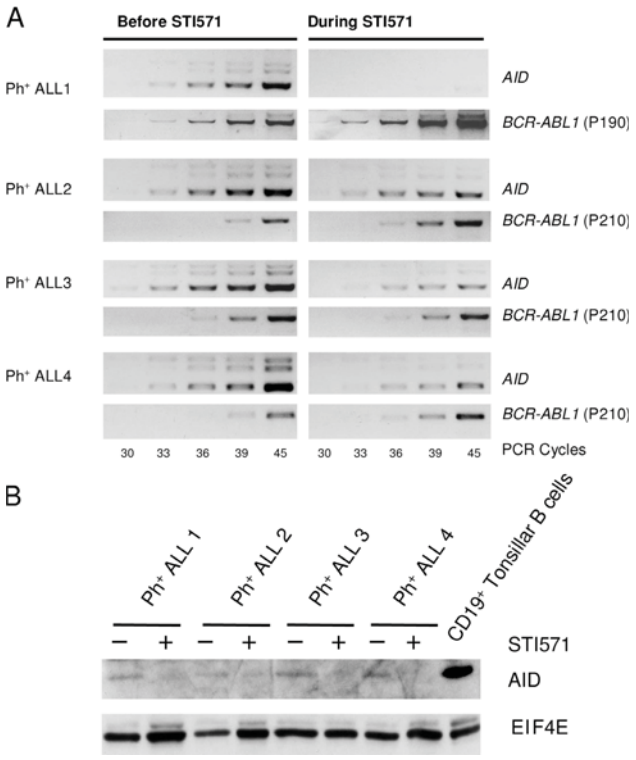

Figure 2. AID expression in patient-derived Ph+ ALL cells depends on BCR-ABL1 kinase activity in vivo. Matched sample pairs from four patients with Ph+ ALL before the onset and during continued treatment with the BCR-ABL1 kinase inhibitor STI571 were analyzed for AID mRNA levels by semiquantitative RT-PCR (A). The content of Ph+ ALL cells in all samples was normalized by BCR-ABL1 fusion transcripts (A), with "p190" and p210" indicating the two different breakpoints. Protein lysates from the same Ph+ ALL cases were also subjected to Western blot analysis for AID expression using EIF4E as a loading control (B). Protein lysates from CD19+ tonsillar B cells were used as a positive control.

findings suggest that Aid induction in normal B cells also requires ABL1 kinase activity. Further experiments that address this possibility are currently under way. Of note, the same concentration of STI571 had no significant effect on Aid mRNA levels in a number of B cell lymphoma cell lines that exhibit constitutive expression of Aid (Fig. S2).

Our finding that BCR-ABL1 induces aberrant AID expression in Ph+ ALL cells is in agreement with a recent study demonstrating that murine B cell precursors infected with the Abelson murine leukemia virus (Abelson-MuLV) also exhibit aberrant expression of Aid (14). The authors of this study attribute aberrant Aid expression induced by the Abelson-MuLV to retroviral infection and interpret aberrant Aid expression as an innate defense mechanism against the transforming retrovirus. Because both BCR-ABL1 and the transforming oncogene of the Abelson-MuLV, v-abl, share ABL1 kinase activity, the results we present here suggest that v-abl kinase activity may also contribute to aberrant expression of Aid in the murine B cell precursors infected by Abelson-MuLV. To test this hypothesis, we analyzed Aid expression in an Abelson-MuLV–transformed murine pre–B cell line (300-19) in the presence or absence of STI571, which inhibits both BCR-ABL1 and v-abl kinase activity (Fig. 1 B). In five repeat experiments, inhibition of v-abl kinase activity resulted in substantial down-regulation of Aid expression in the Abelson-MuLV–transformed 300-19 cells (Fig. 1 B). We conclude that v-abl kinase activity also contributes to Aid expression in Abelson-MuLV–transformed pre–B cells. However, inhibition of v-abl did not abolish Aid expression entirely, which indicates that other factors leading to the up-regulation of Aid (e.g., the antiretroviral host defense proposed; reference 16) may indeed contribute to Aid expression in these cells as well.

BCR-ABL1–induced up-regulation of AID involves repression of ID2, a negative regulator of AID

Previous studies demonstrated that AID expression is tightly regulated by the transcription factor pair PAX5 and E2A and the E2A inhibitor ID2 (15, 16). Interestingly, previous work showed that ID2 is among the genes that are transcriptionally activated by STI571-induced ABL kinase inhibition in murine Abelson-MuLV–transformed pre–B cells (17). We therefore investigated the relationship between BCR-ABL1 kinase activity, E2A/PAX5, and their inhibitor ID2 with respect to regulation of AID expression in Ph+ ALL. Analyzing Affymetrix U133A 2.0 microarray data on two Ph+ ALL cell lines (BV173 and SUP-B15; the full dataset is available through GEO accession no. GSE7182) that were cultured in the presence or absence of 10 μmol/l STI571 for 16 h, we confirmed that inhibition of BCR-ABL1 kinase activity by STI571 increased ID2 mRNA levels, whereas mRNA levels for PAX5 and E2A did not change significantly (Fig. 3 A). In addition, the two Ph+ ALL cell lines were treated with STI571 for 48 h, and AID and ID2 protein levels were measured in the surviving cells (annexin V^-, propidium $iodide^-$) by flow cytometry (Fig. 3 B). Although BCR-ABL1 kinase inhibition by STI571 decreased AID protein expression, levels of ID2 were clearly increased in the two Ph+ ALL cell lines (Fig. 3 B).

To test whether up-regulation of ID2 (as observed upon BCR-ABL1 kinase inhibition by STI571) leads to transcriptional repression of AID in Ph+ ALL cells, we transduced two AID-expressing Ph+ ALL cell lines with a lentiviral vector encoding ID2 and GFP or GFP alone as a control. GFP+ cells were sorted and analyzed for mRNA levels of ID2 and AID using GAPDH as a reference gene (Fig. 3 C). Lentiviral overexpression of ID2 indeed resulted in transcriptional inactivation of AID in both Ph+ ALL cell lines. These findings indicate that up-regulation of AID by BCR-ABL1 involves transcriptional repression of ID2, which would act as a negative regulator of AID in the absence of BCR-ABL1 kinase activity.

AID-induced DNA-SSB in Ph+ leukemia cells

Consistent with an active SHM mechanism, we detected footprints of ongoing subclonal diversification of V_H gene segments in 11 of 46 cases of Ph+ ALL (Table S2). Reflecting their clonal evolution, several early mutations are common

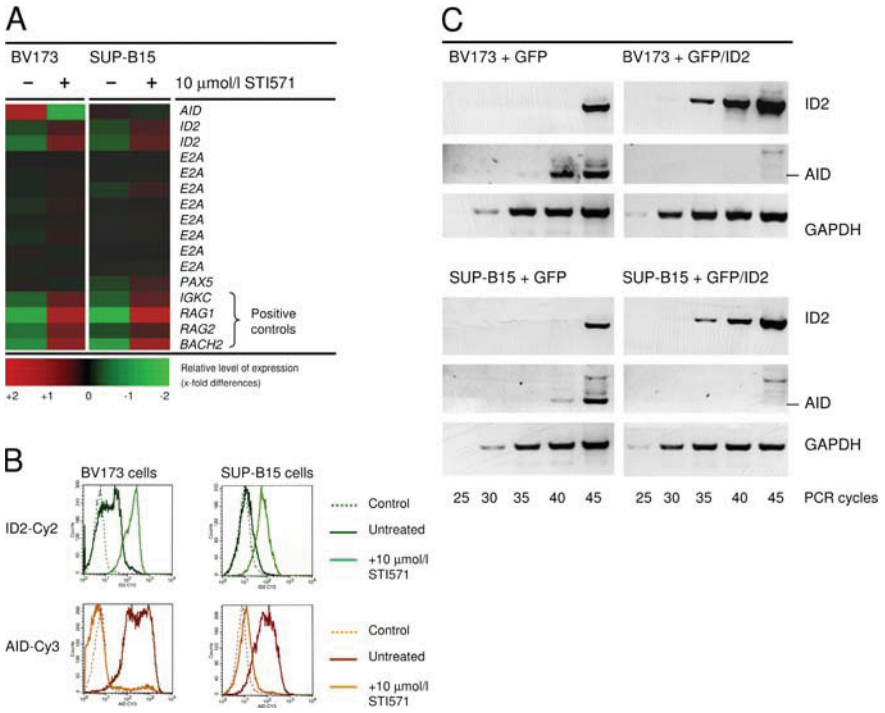

Figure 3. BCR-ABL1–mediated up-regulation of AID involves repression of ID2, a negative regulator of AID. Two Ph$^+$ ALL cell lines (BV173 and SUP-B15) were incubated in the presence or absence of 10 μmol/l STI571 for 16 h and subjected to microarray analysis using the Affymetrix U133A 2.0 platform as described in Materials and methods (A). mRNA levels of ID2 were compared with those of AID and its positive regulators E2A and PAX5. As controls, known STI571-inducible genes (*IGKC*, *RAG1*, *RAG2*, and *BACH2*) are shown. (B) The two Ph$^+$ ALL cell lines were cultured for 48 h in the presence or absence of STI571, and protein levels of ID2 (top) and AID (bottom) were measured by flow cytometry. (C) To test the functional relevance of BCR-ABL1–mediated down-regulation of ID2 in Ph$^+$ ALL cells, the effect of ID2 overexpression on AID mRNA levels was measured in Ph$^+$ ALL cells. Therefore, the two Ph$^+$ ALL cell lines were stably transduced with a vector encoding only GFP (left) or both GFP and ID2 (right). Overexpression of ID2 was monitored together with mRNA levels of AID. GAPDH mRNA levels were used for normalization of cDNA amounts.

among many subclones, which differ from each other by subsequently introduced diversifying mutations. As an example, genealogic trees for four V_H gene rearrangements amplified from Ph$^+$ ALL cell lines are shown in Fig. 4. To test whether AID expression and aberrant SHM are indeed causally linked in Ph$^+$ ALL, we studied DNA-SSB within rearranged Ig V_H genes and the tumor suppressor gene *CDKN2B* in the presence and absence of AID.

CDKN2B encodes the p15/INK4B tumor suppressor, which is frequently deleted in Ph$^+$ ALL and lymphoid blast crisis (LBC) of Ph$^+$ chronic myeloid leukemia (18, 19). Therefore, we silenced AID expression in three Ph$^+$ ALL cell lines by RNA interference (Fig. 5 A) and studied the effect of AID knockdown on DNA-SSB in rearranged V_H genes and the *CDKN2B* locus. AID targeting and nontargeting small interfering RNA (siRNA) duplexes were fluorochrome labeled and repeatedly transfected into Ph$^+$ ALL cells by nucleofection. At a transfection efficiency between 3 and 10%, fluorochrome-labeled cells were sorted by flow cytometry and subjected to further analysis. RNA interference substantially reduced AID mRNA levels in all three Ph$^+$ ALL cell lines (Fig. 5 A). Comparing Ph$^+$ ALL cells carrying nontargeting siRNAs with Ph$^+$ ALL cells carrying AID-specific siRNA duplexes, DNA-SSB were detected within rearranged V_H gene segments as well as within the *CDKN2B* gene in the former but not in the latter case (Fig. 5 B). Likewise, inhibition of BCR-ABL1 kinase activity by STI571, leading to down-regulation of AID (Fig. 1), largely reduced the frequency of DNA-SSB within V_H and *CDKN2B* genes (Fig. 5 B). We conclude that DNA-SSB introduced into both rearranged V_H region genes and the tumor suppressor gene *CDKN2B* require AID expression. To search for actual somatic mutations within the *CDKN2B* and the immediately adjacent *CDKN2A* genes, we attempted to amplify genomic fragments of these genes from multiple Ph$^+$ and Ph$^-$ leukemia cell lines. Consistent with previous findings, however (18, 19), we found that one or even both genes were already deleted in Ph$^+$ (BV173, K562, Nalm1, SUP-B15) and Ph$^-$ (REH, RS4;11) cell lines, which precluded a comprehensive sequence analysis (not depicted). *CDKN2A* (INK4A, P16) and *CDKN2B* (INK4B, P15) belong to a group of genes that encode the INK4 family of tumor suppressors. Interestingly, a recent study demonstrated that deletion of another member of these gene families, *CDKN2D* (INK4D, P19/ARF), was sufficient to render otherwise normal B cells highly susceptible to aberrant chromosomal rearrangements during

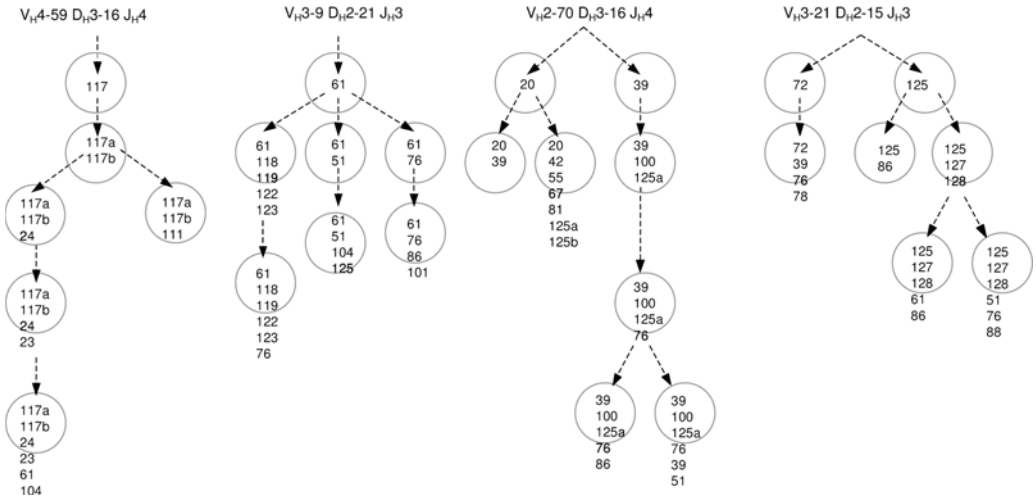

Figure 4. Tracing the clonal evolution of Ph$^+$ ALL cells by V_H region gene mutations. Genealogic trees of ongoing SHM of V_H gene segments amplified from the Ph$^+$ ALL cell lines NALM1 and BV173 are shown. Numbers indicate the mutated codons within the rearranged V region. Each circle represents one V_H sequence amplified from a leukemia subclone, and a and b denote distinct mutations within the same codon.

AID-mediated CSR (7). Therefore, the loss of one or more of these INK4 tumor suppressors in the context of aberrant AID expression in Ph$^+$ ALL may further enhance genetic instability in these leukemia cells.

DISCUSSION

In summary, these findings identify AID as a mutator within but also outside the Ig gene loci in Ph$^+$ ALL cells. Aberrant expression of AID leading to SHM of Ig and non-Ig genes is

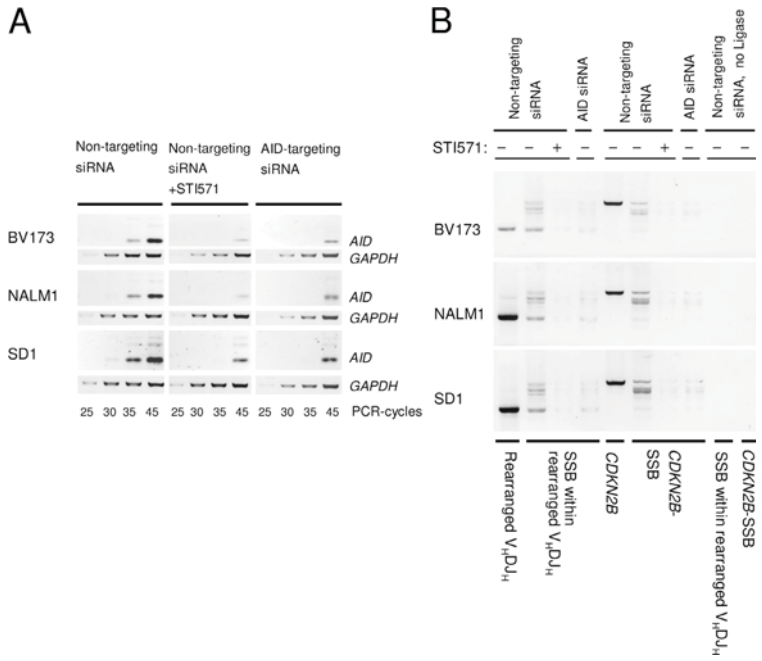

Figure 5. AID induces DNA-SSB in Ig and non-Ig genes. To establish a causative link between AID function and the occurrence of DNA-SSB, AID mRNA expression was silenced in three Ph$^+$ ALL cell lines by RNA interference using fluorochrome-labeled siRNAs against AID or nontargeting siRNA duplexes as a control. Fluorochrome-labeled cells were sorted and analyzed for silencing efficiency and specificity by RT-PCR (A), and for DNA-SSB within rearranged V_H gene segments and the *CDKN2B* gene by LM-PCR (B). For BV173, Nalm1, and SD1 cells, DNA-SSB intermediates in rearranged V_H3-21, V_H3-9, and V_H3-30 gene segments were amplified, respectively. As a loading control for genomic DNA, V_H gene rearrangements and a genomic fragment of the *CDKN2B* gene were amplified (B). The *CDKN2A* gene at chromosome 9p21 immediately adjacent to *CDKN2B* was partly or entirely deleted in BV173 and Nalm1 cells, precluding LM-PCR analysis of this locus in these cell lines (not depicted).

driven by oncogenic BCR-ABL1 kinase activity and likely contributes to the particularly unfavorable prognosis of Ph^+ leukemia (9). Ph^+ leukemias typically carry secondary genetic aberrations (Table S2) and develop resistance to chemotherapy and inhibition of BCR-ABL1 kinase activity within a short period of time (9). Further studies that address a specific role of AID in the acquisition of mutations leading to drug resistance in Ph^+ ALL are currently under way. Of note, a small fraction of cases of Ph^- pre–B ALL carry mutated V_H region genes (and presumably express AID) in the absence of BCR-ABL1. This indicates that other aberrations besides the Ph may likewise induce aberrant SHM in ALL cells. Given that BCR-ABL1–induced up-regulation of AID involves repression of ID2 and indirect activation of E2A, one would envision that other factors that influence the balance between ID2 and E2A may have a similar effect in Ph^- leukemia cells.

MATERIALS AND METHODS

Patient samples and cell lines. Normal pro–B cells ($CD19^+$ $CD34^+$ μ $chain^-$) and pre–B cells ($CD19^+$ $VpreB^+$ μ $chain^+$) were sorted from human bone marrow (from four healthy donors; Cambrex) by flow cytometry using antibodies from BD Biosciences and a FACSVantage SE cell sorter (BD Biosciences). B1 cells ($CD19^+$ $CD5^+$), naive B cells ($CD19^+$ $CD27^-$ IgD^+), and memory B cells ($CD19^+$ $CD27^+$ IgD^-) as well as plasma cells ($CD19^+$ $CD20^-$ $CD138^+$) were sorted from the peripheral blood of 12 healthy donors (buffy coats were obtained from the Institute for Blood Transfusion, Heinrich-Heine-Universität Düsseldorf) by flow cytometry using the same FACS sorter. Human germinal center B cells were isolated from tonsillar resectates provided by T. Hoffmann (Heinrich-Heine-Universität Düsseldorf). To this end, tonsillar B cells were preenriched by MACS using immunomagnetic beads against CD19 (Miltenyi Biotec). Thereafter, $CD20^+$ $CD38^+$ germinal center B cells were isolated by flow cytometry as described above using antibodies from BD Biosciences.

In total, 108 cases of ALL were analyzed for AID expression. 28 cases of Ph^+ leukemia, including seven cell lines (BV173, CMLT1, K562, NALM1, SD1, SUP-B15, and TOM1; DSMZ,) and 80 cases of Ph^- ALL, including eight cell lines (BEL1, HBP-NULL, KASUMI2, MHH-CALL3, NALM6, REH, RS4;11, and 697; DSMZ) were analyzed by RT-PCR (see below). Ph^+ leukemia also included five cases of LBC CML (cases 21–25 in Table S2). In these cases, $CD19^+$ $CD34^+$ B lymphoid leukemia cells were sorted by flow cytometry from leukemic bone marrow samples using antibodies from BD Biosciences.

V_H gene rearrangements were amplified and sequenced from 106 cases of ALL, including 46 Ph^+ and 60 Ph^- cases. For 28 cases (18 Ph^+, 10 Ph^-), information on both AID expression and V_H region gene sequence was available. Cytogenetic data on the patient samples and cell lines studied are given in Tables S1 and S2. Patient samples were provided from the Department of Hematology and Oncology, Universität Frankfurt (W.-K. Hofmann) and the Department of Medical Biosciences, Pathology, Umea University, Umea, Sweden (A. Li) in compliance with Institutional Review Board regulations. Murine Abelson-MuLV–transformed pre–B cells (300–19) were provided by M. Reth (Max-Planck-Institute for Immunobiology, Freiburg, Germany). Human Ph^+ ALL cells and v-abl–transformed mouse pre–B cells were cultured in the presence or absence of 10 μmol/l STI571 (human ALL) or 1 μmol/l STI571 (murine pre–B cells), respectively. STI571 was provided by Novartis. Germinal center–derived B cell lines (MHH-PREB1, MN60, Karpas-422, MC116, JEKO-1, and SJO) were obtained from DSMZ.

Induced expression of BCR-ABL1 and ID2. A murine IL-3–dependent pro–B cell line, TONB210, which carries an inducible *BCR-ABL1* transgene under the control of a doxycycline-dependent promoter (provided by G.Q. Daley, Harvard Medical School, Boston, MA), and Ph^- ALL cells transiently transfected with pMIG-GFP or pMIG-GFP/BCR-ABL1 vectors were studied in cell culture experiments as described previously (20). pMIG-GFP or pMIG-GFP/BCR-ABL1 vectors encode either GFP only or GFP and BCRABL1 and were transfected by electroporation (250 V and 950 μF). For both transfections, GFP^+ and GFP^- cells were sorted after 24 h and subjected to further analysis. BV173 and SUP-B15 cells were transduced with the lentiviral vector pCL1 (provided by H. Hanenberg, Heinrich-Heine-Universität Düsseldorf, Germany) encoding GFP or GFP and ID2 as described previously (21). The coding sequence of the ID2 cDNA (provided by E. Hara, Science University of Tokyo, Noda, Japan) was excised with BamHI and XhoI and subcloned into pIRESEGFP via BglII and XhoI. The expression cassette containing ID2-IRES-EGFP was digested with NheI and BsrGI and cloned into the lentiviral vector pCL1. 10 d after lentiviral transduction, GFP^+ cells were sorted by flow cytometry and further analyzed or kept under cell culture conditions.

Sequence analysis of V_H and C_H region genes and semiquantitative RT-PCR. To characterize the configuration of V_H and C_H region genes, two primer sets were used to amplify the V region alone (using V_H- and J_H-specific primers) or the V region together with the constant region (using V_H- and C_H-specific primers) of Ig heavy chain transcripts as described previously (22) in two rounds of PCR using the primers listed in Table S4, which is available at http://www.jem.org/cgi/content/full/jem.20062662/DC1. PCR products were then cloned and sequenced.

Mutation analysis of BCL6 and MYC genes. For mutation analysis of *BCL6* and *MYC* genes, genomic fragments were amplified and sequenced as described previously (3) using PFU DNA polymerase. For each PCR product, both DNA strands were sequenced and mutations were only counted if they were found both in the forward and reverse sequence. PCR primers used for amplification of *BCL6* and *MYC* fragments are listed in Table S4.

Mutation analysis of TCRB and TCRG V region genes. TCRB and TCRG gene rearrangements were amplified from multiple leukemia samples, including Ph^+ ALL cell lines, primary leukemia cells from Ph^+ LBC CML ($CD19^+$ $CD34^+$ B lymphoid cells were sorted from leukemic bone marrow samples), and Ph^- ALL cell lines. As controls, TCRB and TCRG gene rearrangements were amplified from normal $CD3^+$ T cells (purified by $CD3^+$ MACS from peripheral blood) using the primers listed in Table S4.

Affymetrix GeneChip analysis and semiquantitative RT-PCR. Total RNA from cells used for microarray or RT-PCR analysis was isolated by RNeasy (QIAGEN) purification. For microarray analysis, two human Ph^+ ALL cell lines (BV173, SUP-B15) were cultured for 16 h in the presence or absence of 10 μmol/l STI571 (Novartis). Double-strand cDNA was generated from 5 μg of total RNA using a poly(dT) oligonucleotide that contains a T7 RNA polymerase initiation site and the SuperScript III Reverse Transcriptase (Invitrogen). Biotinylated cRNA was generated and fragmented according to the Affymetrix protocol and hybridized to U133A 2.0 microarrays (Affymetrix). After scanning (scanner from Affymetrix), the expression values for the genes were determined using Affymetrix GeneChip software. For semiquantitative RT-PCR analysis of human *AID*, *ID2*, *GAPDH*, and *BCR-ABL1* and for RT-PCR analysis of murine *Aid*, *Oct2*, *Obf1*, and *Hprt* transcripts, PCR primers are listed in Table S4.

Western blotting and flow cytometry. For the detection of AID by Western blot, an antibody against human AID (L7E7; Cell Signaling Technology) was used together with the WesternBreeze immunodetection system (Invitrogen). Detection of EIF4e was used as a loading control (Santa Cruz Biotechnology, Inc.). For analysis of AID and ID2 expression by flow cytometry, antibodies against ID2 (rabbit anti–human ID2 IgG; C-20; Santa Cruz Biotechnology, Inc.) and AID (mouse anti–human AID IgG1; L7E7; Cell Signaling Technology) were used together with secondary antibodies

(goat anti–rabbit IgG Cy2 and goat anti–mouse IgG Cy3; Jackson ImmunoResearch Laboratories). Before staining, cells were fixed with 0.4% paraformaldehyde and incubated for 10 min in 90% methanol on ice.

Silencing of AID mRNA expression by RNA interference. For silencing of AID mRNA expression, one previously validated siRNA (23) and a nontargeting siRNA duplex were used. All siRNA duplexes (for sequences see Table S4) were labeled with fluorescein using an siRNA labeling kit (Ambion) according to the manufacturer's protocol. Fluorochrome-labeled siRNA duplexes were transfected into Ph^+ ALL cell lines (BV173, Nalm1, SD1) by nucleofection according to the manufacturer's protocol (Amaxa). Transfection was repeated after 48 h and transfected $fluorescein^+$ cells were sorted by FACS after 72 h as described previously (24). RNA interference–mediated knockdown of AID mRNA expression was verified by RT-PCR.

Ligation-mediated PCR (LM-PCR) for detection of DNA-SSB. Genomic DNA from 2.5×10^6 cells containing a nick on the lower strand was denatured for 10 min at 95°C. Thereafter, a gene-specific primer (Table S4) was hybridized and extended to the position of the nick as described previously (first strand extension; reference 25), leaving a blunt end using Vent DNA polymerase (New England Biolabs, Inc.). Next, a double-stranded linker was ligated to the newly created blunt end using T4 DNA ligase (Invitrogen) at 14°C overnight. The linker was constructed by annealing of the oligonucleotides 5′- TTTCTGCTCGAATTCAAGCTTCTAACGATGTACGGGGACATG 3′ and 3′ amino (C7)- GACGAGCTTAAGTTCGAAGATTGCTACATGCCCCT-5′, and protruding 3′ overhangs were removed by 3′→5′ exonuclease activity of the Klenow fragment of *Escherichia coli* DNA polymerase I (Invitrogen). LM-PCR (26) was performed with modifications as described previously (27). In two semi-nested rounds of amplification at an annealing temperature of 59°C, linker-ligated intermediates of DNA-SSB within various genes were amplified using gene-specific primers together with two linker-specific primers (Table S4).

Online supplemental material. Fig. S1 shows the morphology measurement of mRNA levels of Aid in normal mouse splenocytes that were stimulated with IL-4 and LPS and treated with or without STI571. Fig. S2 shows mRNA levels in human B cell lymphoma cells that constitutively express AID after treatment with or without STI571. Tables S1–S4 and Figs. S1 and S2 are available at http://www.jem.org/cgi/content/full/jem.20062662/DC1.

We would like to thank Nora Heisterkamp, John Groffen (Los Angeles, CA), Janet D. Rowley (Chicago, IL), and Michael Reth (Freiburg) for critical discussions; Nora Heisterkamp and John Groffen for provision of BCR-ABL1–transgenic mice; Shahab Asgharzadeh (Los Angeles, CA) for his support with quantitative RT-PCR; Kornelia Linnenbrinck and Gabi Tillmann (Düsseldorf, Germany) for help with sequencing; Christoph Göttlinger (Köln, Germany) for cell sorting; and Dr. Gernot Röder (Düsseldorf, Germany) for performing Affymetrix GeneChip hybridizations and analysis.

N. Feldhahn is supported by a fellowship award from the Deutsche José-Carreras-Leukemia Foundation. This work is supported by grants from the Stem Cell Network North-Rhine-Westphalia (to M. Müschen), the Deutsche Forschungsgemeinschaft (through *Emmy-Noether*-Program; to M. Müschen), the German José-Carreras-Leukemia Foundation (grant to M. Müschen), the Deutsche Krebshilfe (program project grant; to M. Müschen), and the T.J. Martell Foundation.

The authors have no conflicting financial interests.

Submitted: 19 December 2006
Accepted: 28 March 2007

REFERENCES

1. MacLennan, I.C., and D. Gray. 1986. Antigen-driven selection of virgin and memory B cells. *Immunol. Rev.* 91:61–85.
2. Muramatsu, M., K. Kinoshita, S. Fagarasan, S. Yamada, Y. Shinkai, and T. Honjo. 2000. Class switch recombination and hypermutation require activation-induced cytidine deaminase (AID), a potential RNA editing enzyme. *Cell.* 102:553–563.
3. Pasqualucci, L., P. Neumeister, T. Goossens, G. Nanjangud, R.S. Chaganti, R. Küppers, and R. Dalla-Favera. 2001. Hypermutation of multiple proto-oncogenes in B-cell diffuse large-cell lymphomas. *Nature.* 412:341–346.
4. Shen, H.M., N. Michael, N. Kim, and U. Storb. 2000. The TATA binding protein, c-Myc and survivin genes are not somatically hypermutated, while Ig and *BCL6* genes are hypermutated in human memory B cells. *Int. Immunol.* 12:1085–1093.
5. Wang, C.L., R.A. Harper, and M. Wabl. 2004. Genome-wide somatic hypermutation. *Proc. Natl. Acad. Sci. USA.* 101:7352–7356.
6. Ramiro, A.R., M. Jankovic, T. Eisenreich, S. Difilippantonio, S. Chen-Kiang, M. Muramatsu, T. Honjo, A. Nussenzweig, and M.C. Nussenzweig. 2004. AID is required for *c-Myc/Igh* chromosome translocations in vivo. *Cell.* 118:431–438.
7. Ramiro, A.R., M. Jankovic, E. Callen, S. Difilippantonio, H.T. Chen, K.M. McBride, T.R. Eisenreich, J. Chen, R.A. Dickins, S.W. Lowe, et al. 2006. Role of genomic instability and p53 in AID-induced *c-Myc-Igh* translocations. *Nature.* 440:105–109.
8. Bird, J., N. Galili, M. Link, D. Stites, and J. Sklar. 1988. Continuing rearrangement but absence of somatic hypermutation in immunoglobulin genes of human B cell precursor leukemia. *J. Exp. Med.* 168:229–245.
9. Arico, M., M.G. Valsecchi, B. Camitta, M. Schrappe, J. Chessells, A. Baruchel, P. Gaynon, L. Silverman, G. Janka-Schaub, W. Kamps, et al. 2000. Outcome of treatment in children with Philadelphia chromosome-positive acute lymphoblastic leukemia. *N. Engl. J. Med.* 342:998–1006.
10. Beishuizen, A., M.A. Verhoeven, E.R. van Wering, K. Hahlen, H. Hooijkaas, and J.J. van Dongen. 1994. Analysis of Ig and T-cell receptor genes in 40 childhood acute lymphoblastic leukemias at diagnosis and subsequent relapse: implications for the detection of minimal residual disease by polymerase chain reaction analysis. *Blood.* 83:2238–2247.
11. Brumpt, C., E. Delabesse, K. Beldjord, F. Davi, J.M. Cayuela, C. Millien, P. Villarese, P. Quartier, A. Buzyn, F. Valensi, and E. Macintyre. 2000. The incidence of clonal T-cell receptor rearrangements in B-cell precursor acute lymphoblastic leukemia varies with age and genotype. *Blood.* 96:2254–2261.
12. Okazaki, I.M., H. Hiai, N. Kakazu, S. Yamada, M. Muramatsu, K. Kinoshita, and T. Honjo. 2003. Constitutive expression of AID leads to tumorigenesis. *J. Exp. Med.* 197:1173–1181.
13. McBride, K.M., A. Gazumyan, E.M. Woo, V.M. Barreto, D.F. Robbiani, B.T. Chait, and M.C. Nussenzweig. 2006. Regulation of hypermutation by activation-induced cytidine deaminase phosphorylation. *Proc. Natl. Acad. Sci. USA.* 103:8798–8803.
14. Gourzi, P., T. Leonova, and F.N. Papavasiliou. 2006. A role for activation-induced cytidine deaminase in the host response against a transforming retrovirus. *Immunity.* 24:779–786.
15. Gonda, H., M. Sugai, Y. Nambu, T. Katakai, Y. Agata, K.J. Mori, Y. Yokota, and A. Shimizu. 2003. The balance between Pax5 and Id2 activities is the key to AID gene expression. *J. Exp. Med.* 198:1427–1437.
16. Sayegh, C.E., M.W. Quong, Y. Agata, and C. Murre. 2003. E-proteins directly regulate expression of activation-induced deaminase in mature B cells. *Nat. Immunol.* 4:586–593.
17. Muljo, S.A., and M.S. Schlissel. 2003. A small molecule Abl kinase inhibitor induces differentiation of Abelson virus-transformed pre-B cell lines. *Nat. Immunol.* 4:31–37.
18. Sill, H., J.M. Goldman, and N.C. Cross. 1995. Homozygous deletions of the p16 tumor-suppressor gene are associated with lymphoid transformation of CML. *Blood.* 85:2013–2016.
19. Haidar, M.A., X.B. Cao, T. Manshouri, L.L. Chan, A. Glassman, H.M. Kantarjian, M.J. Keating, M.S. Beran, and M. Albitar. 1995. p16INK4A and p15INK4B gene deletions in primary leukemias. *Blood.* 86:311–315.
20. Klein, F., N. Feldhahn, S. Herzog, M. Sprangers, J.L. Mooster, H. Jumaa, and M. Müschen. 2006. BCR-ABL1 induces aberrant splicing of IKAROS and lineage infidelity in pre-B lymphoblastic leukemia cells. *Oncogene.* 25:1118–1124.
21. Feldhahn, N., P. Rio, B.N. Soh, S. Liedtke, M. Sprangers, F. Klein, P. Wernet, H. Jumaa, W.K. Hofmann, H. Hanenberg, et al. 2005.

Deficiency of Bruton's tyrosine kinase in B cell precursor leukemia cells. *Proc. Natl. Acad. Sci. USA*. 102:13266–13271.
22. Klein, F., N. Feldhahn, L. Harder, H. Wang, M. Wartenberg, W.K. Hofmann, P. Wernet, R. Siebert, and M. Müschen. 2004. The BCR-ABL1 kinase bypasses selection for the expression of a pre–B cell receptor in pre–B acute lymphoblastic leukemia cells. *J. Exp. Med*. 199: 673–685.
23. Machida, K., K.T. Cheng, V.M. Sung, S. Shimodaira, K.L. Lindsay, A.M. Levine, M.Y. Lai, and M.M. Lai. 2004. Hepatitis C virus induces a mutator phenotype: enhanced mutations of immunoglobulin and proto-oncogenes. *Proc. Natl. Acad. Sci. USA*. 101:4262–4267.
24. Feldhahn, N., F. Klein, J.L. Mooster, P. Hadweh, M. Sprangers, M. Wartenberg, M.M. Bekhite, W.K. Hofmann, S. Herzog, H. Jumaa, et al. 2005. Mimicry of a constitutively active pre–B cell receptor in acute lymphoblastic leukemia cells. *J. Exp. Med*. 201:1837–1852.
25. Arudchandran, A., R.M. Bernstein, and E.E. Max. 2004. Single-stranded DNA breaks at cytosines occur during Ig gene class switch recombination. *J. Immunol*. 173:3223–3229.
26. Schlissel, M., A. Constantinescu, T. Morrow, M. Baxter, and A. Peng. 1993. Double-strand signal sequence breaks in V(D)J recombination are blunt, 5′-phosphorylated, RAG-dependent, and cell cycle regulated. *Genes Dev*. 7:2520–2532.
27. Klein, F., N. Feldhahn, S. Lee, H. Wang, F. Ciuffi, M. von Elstermann, M.L. Toribio, H. Sauer, M. Wartenberg, V.S. Barath, et al. 2003. T lymphoid differentiation in human bone marrow. *Proc. Natl. Acad. Sci. USA*. 100:6747–6752.